

Mechanisms of Ebolavirus Entry


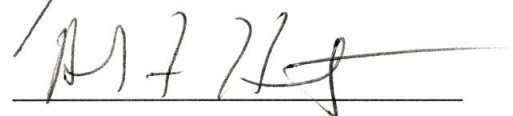
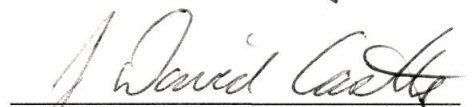
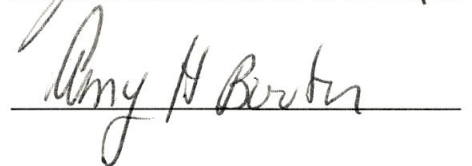
Charles Jason Shoemaker  
Charlottesville, Virginia

B.S., Loyola College in Maryland, 2005

A Dissertation presented to the Graduate Faculty  
of the University of Virginia in Candidacy for the  
Degree of Doctor of Philosophy

Department of Cell Biology

University of Virginia  
December, 2012

## **Abstract**

Ebola virus (EBOV) is an enveloped RNA virus belonging to the family Filoviridae. It occurs episodically in sub-Saharan Africa, and is noted for the severe and highly lethal hemorrhagic fever it causes in humans as well as non-human primates. There are currently no clinically approved therapies or vaccines, and many mysteries remain concerning its path of entry into the cell. After binding to and being internalized from the cell surface, it traffics to a late endocytic compartment, where the viral glycoprotein is proteolytically primed and triggered to fuse. Fusion enables genome egress to the cytoplasm and subsequent replication. While much has been learned in recent years about its method of entry into host cells, many mysteries remain about EBOV entry and fusion. To address some of these questions, I developed a novel preparation of filamentous virus-like-particles (VLPs) as surrogates for EBOV. These VLPs enabled me to dissect different steps of EBOV penetration into the host cell, particularly internalization from the cell surface and cytoplasmic entry. Using these multi-purpose VLPs, I found that EBOV VLP entry is slow relative to particle internalization. I further showed that this delayed entry was not the result of cathepsin priming of GP. Subsequently, we used this VLP system to characterize the method of action of several compounds that had been shown to inhibit EBOV infection. We showed that these compounds blocked a late stage of EBOV entry. In a concurrent study, we found that these drugs belonged to a chemical class known as cationic amphiphiles, and that they cause cholesterol accumulation in endosomes, a hallmark of Niemann-Pick C1 disease. All of the

robust EBOV entry inhibitors identified in this study also caused this phenotype, and furthermore appeared to be acting through an NPC1-dependent pathway distinct from that previously described by other groups. These studies have therefore revealed a possible additional critical role for NPC1 in supporting successful EBOV entry, and further validate NPC1 as a target for anti-EBOV therapy. Lastly, these studies have identified a large class of chemical compounds which may hold potential for combating filoviral, and especially ebolavirus infection.

## Table of Contents

<b>Abstract.....</b>	<b>i</b>
<b>Table of Contents.....</b>	<b>iii</b>
<b>List of Figures and Tables.....</b>	<b>vi</b>
<b>List of Publications .....</b>	<b>x</b>
<b>List of Abbreviations .....</b>	<b>xii</b>
<b>Acknowledgements.....</b>	<b>xvi</b>
<b>Chapter I. Introduction.....</b>	<b>1</b>
<b>Background on Virus Entry.....</b>	<b>2</b>
Viral Glycoproteins.....	4
Viral Receptor Binding.....	5
Viral Internalization.....	6
Viral Trafficking.....	15
Viral Fusion.....	16
<b>Ebolavirus Overview.....</b>	<b>22</b>
Emergence.....	23
Life Cycle.....	25
Structure.....	26
Replication and Assembly.....	32
Clinical Presentation and Pathogenesis.....	33
Vaccines and Therapeutics.....	37
<b>EBOV Entry Pathway.....</b>	<b>39</b>
EBOV Receptor Binding.....	39

EBOV Internalization.....	43
EBOV Trafficking.....	52
Cathepsin Remodeling and Fusion Triggering.....	53
Potential Triggering Conditions.....	55
Role of NPC1 in EBOV Entry.....	56
Research Goals and Significance.....	60
<b>Chapter II. Ebolavirus VLPs for Studies of Virus Entry.....</b>	<b>63</b>
Introduction.....	64
Materials and Methods.....	65
Results.....	68
Summary.....	76
<b>Chapter III. FDA Approved Selective Estrogen Receptor Modulators Inhibit Ebola Infection.....</b>	<b>88</b>
Abstract.....	89
Introduction.....	89
Materials and Methods.....	92
Results.....	101
Discussion.....	125
<b>Chapter IV. Multiple Cationic Amphiphiles that Induce a Niemann-Pick C Phenotype Inhibit Ebola Virus Entry and Infection.....</b>	<b>135</b>
Abstract.....	136
Introduction.....	137
Materials and Methods.....	139

<b>Results and Discussion.....</b>	<b>146</b>
<b>Chapter V. Summary and Future Directions.....</b>	<b>176</b>
<b>Literature Cited.....</b>	<b>194</b>
<b>Appendix. <math>\alpha 5\beta 1</math> Integrin Controls Ebolavirus Entry by Regulating</b>	
<b>Endosomal Cathepsins.....</b>	<b>212</b>

## List of Figures and Tables

### Chapter I

Table 1.1 Examples of the different types of molecules utilized by viruses as receptors.....	9
Figure 1.1 Endocytic mechanisms used by viruses.....	12
Figure 1.2 The conserved pathway of viral membrane fusion and the structure of the Ebola virus (EBOV) glycoprotein.....	19
Figure 1.3 Diversity of viral fusion proteins.....	21
Figure 1.4 Morphology and genome organization of EBOV.....	30
Figure 1.5 Model of EBOV pathogenesis.....	35
Figure 1.6 The life cycle of EBOV.....	41
Figure 1.7 Assessing macropinocytosis as the means of uptake of EBOV VLPs.....	49
Figure 1.8 Effects of inhibitors that block macropinocytosis (EIPA), CME (chlorpromazine), or dynamin-dependent endocytosis (dynasore) on EBOV GP-mediated infection.....	51
Figure 1.9 EBOV GP priming and triggering: possible roles of NPC1.....	59

### Chapter II

Figure 2.1 Optimization and characterization of multi-purpose VLPs.....	71
---	----

Figure 2.2 Multi-purpose VLPs for studies of EBOV internalization and entry.....	78
Figure 2.3 Multi-purpose VLPs are uniform in diameter but pleomorphic in shape.....	80
Figure 2.4 Validation of multi-purpose VLPs for studies of VLP internalization and entry.....	82
Figure 2.5 Time courses of EBOV VLP internalization and entry.....	84
Figure 2.6 Time courses of EBOV VLP internalization and entry in NPC1 -/+ cells.....	86

### Chapter III

Figure 3.1 Selective estrogen receptor (ER) modulators inhibit EBOV infection <i>in vitro</i> .....	104
Figure 3.2 <i>In vitro</i> 8-point dose response curves for clomiphene and toremifene.....	106
Figure 3.3 The activity of clomiphene and toremifene with native strains of filoviruses.....	108
Table 3.1 Summary of clomiphene and toremifene evaluation in the mouse EBOV infection model.....	111
Figure 3.4 Representative survival plots for clomiphene and toremifene in a mouse model of EBOV infection.....	113
Table 3.2 Estrogen receptor expression and infection status in cell lines.....	116

<b>Figure 3.5 Clomiphene inhibition of EBOV infection is not dependent on ER expression.....</b>	<b>118</b>
<b>Figure 3.6 Effects of clomiphene and toremiphene in EBOV VLP entry assay.....</b>	<b>122</b>
<b>Figure 3.7 Evaluation of clomiphene and toremifene on EBOV VLP-GP internalization and cathepsin processing.....</b>	<b>127</b>
<b>Figure 3.8 Clomiphene and toremifene do not affect the pH of endosomes.....</b>	<b>129</b>

#### **Chapter IV**

<b>Figure 4.1 Effects of sterol pathway inhibitors on EBOV infection.....</b>	<b>150</b>
<b>Figure 4.2 Effects of sterol pathway inhibitors on EBOV VLP entry.....</b>	<b>152</b>
<b>Figure 4.3 Ro 48-8071 inhibits EBOV entry at a post internalization step and does not inhibit endosome acidification or cathepsin activity levels.....</b>	<b>156</b>
<b>Figure 4.4 U18666A inhibits EBOV entry at a post internalization step and does not inhibit endosome acidification or cathepsin activity levels.....</b>	<b>158</b>
<b>Figure 4.5 CADs that strongly inhibit EBOV entry and infection cause cholesterol accumulation in LE/Lys.....</b>	<b>160</b>
<b>Figure 4.6 CADs inhibit EBOV GP-mediated infection in an NPC1-dependent manner.....</b>	<b>163</b>

<b>Figure 4.7 CADs do not disrupt the interaction of 19 kDa GP and NPC1.....</b>	<b>166</b>
<b>Figure 4.8 Models for how CADs may block EBOV entry.....</b>	<b>170</b>
<b>Table 4.1 Properties and effects of sterol synthesis pathway inhibitors on EBOV entry and infection and on cholesterol accumulation in LE/Lys.....</b>	<b>173</b>
<b>Figure 4.9 Structures of the eleven compounds analyzed in this study.....</b>	<b>175</b>

## **Chapter V**

<b>Table 5.1 Observations made by other groups studying interplay of ASMase and LBPA in NPC1-defective cells.....</b>	<b>187</b>
<b>Table 5.2 Summary: FDA-approved CADs that block EBOV entry and infection.....</b>	<b>192</b>

## List of Publications

(arranged chronologically)

- I. Schornberg, K. L., C. J. Shoemaker, D. Dube, M. Y. Abshire, S. E. Delos, A. H. Bouton, and J. M. White. 2009.  $\alpha 5 \beta 1$ -integrin controls ebolavirus entry by regulating endosomal cathepsins. *Proc Natl Acad Sci USA* 106:8003-8008.  
*(Contributed figure 3B, supplemental figures S1A, S1B, S4, and S5; see appendix)*
- II. Dube, D., K. L. Schornberg, C. J. Shoemaker, S. E. Delos, T. S. Stantchev, K. A. Clouse, C. C. Broder, and J. M. White. 2010. Cell adhesion-dependent membrane trafficking of a binding partner for the ebolavirus glycoprotein is a determinant of viral entry. *Proc Natl Acad Sci USA* 107:16637-16642.  
*(Contributed reagent and optimized assay used in figure 5D)*
- III. Johansen, L. M., Brannan, J.M., Delos, S.E., Shoemaker, C.J., Stossel, A., Lear, C., Hoffstrom, B.G., Schornberg, K.L., Scully, C., Lehar, J., Hensley, L.E., White, J.M., Olinger, G.G. 2012. FDA-Approved Selective Estrogen Receptor Modulators Inhibit Ebola Infection. In revision.

*(Contributed figures 6, 7A, 8 and insights for Discussion; see chapter III)*

- IV. Charles J. Shoemaker, Kathryn L. Schornberg, Sue E. Delos, Corinne Scully, Hassan Pajouhesh, Gene G. Olinger, Lisa M. Johansen, and Judith M. White. 2012. Multiple Cationic Amphiphiles that Induce a Niemann-Pick C Phenotype Inhibit Ebola Virus Entry and Infection. Submitted.

*(Contributed figures 2, 3, 4, 5, 6, 7, and 8. Wrote manuscript along with J.M. White; see chapter IV.)*

## List of Abbreviations

ASMase: acid sphingomyelinase

ATCC: American type culture collection

Blam: beta-lactamase

BMP: bis(monoacylglyceryl)phosphate

CAD: cationic amphiphilic drugs

Cat B/Cat L: cathepsins B and L

CCP: clathrin coated pit

CE: caveolar endocytosis

Chap: chapter

CHO: Chinese hamster ovary

CHOL: cholesterol

clogP: partition coefficient for n-octanol/water

CME: clathrin-mediated endocytosis

DIC: disseminated intravascular coagulation

DMEM: Dulbecco's modified Eagle medium

DMSO: dimethyl sulfoxide

E64d/EST: (2S,3S)-*trans*-Epoxy succinyl-L-leucylamido-3-methylbutane ethyl ester

EBOV: Zaire ebolavirus

EEA1: early endosome antigen 1

EGF: epidermal growth factor

eGFP/GFP: enhanced green fluorescent protein/green fluorescent protein

EIPA: 5-(N-Ethyl-N-isopropyl) amiloride

Env: envelope glycoprotein

ER: estrogen receptor

EMEM: Eagle's minimum essential medium

FBS: fetal bovine serum

Fig: figure

G: envelope glycoprotein (Vesicular Stomatitis virus)

GP: envelope glycoprotein (EBOV)

GP $\Delta$ : glycoprotein (EBOV) deleted for mucin domain

HCV: Hepatitis C virus

HA: hemagglutinin (influenza envelope glycoprotein)

HIV: Human immunodeficiency virus

HR: heptad region

IC<sub>50</sub>: half maximal inhibitory concentration

Ig: immunoglobulin

kDa: kilodaltons

L: RNA-polymerase (EBOV)

LAMP: Lysosomal-associated membrane protein

LBPA: lysobisphosphatidic acid

LCMV: Lymphocytic choriomeningitis virus

LCMV GP: LCMV glycoprotein

LE: late endosome

LE/Lys: late endosome/lysosome

Lys: lysosome

mAb: monoclonal antibody

M: matrix protein (VSV)

MARV: Lake Victoria Marburgvirus

MOI: multiplicity of infection

NHP: non-human primate

nm: nanometer

MW: molecular weight

NP: nucleoprotein (EBOV)

NPC1: Niemann-Pick C Type 1 protein

OMEM: Optimem I

PAK: p21 activated kinase

pKa: logarithm of the acid dissociation constant

PBS: phosphate buffered saline

PFU: plaque forming unit

PMA: phorbol-12-myristate-13-acetate

RBR/RBD: receptor binding region/receptor binding domain

RNP: ribonucleoprotein complex

SARS: severe acute respiratory syndrome coronavirus

SCS: supplemented calf serum

SDS-PAGE: sodium dodecyl sulfate-polyacrylamide gel electrophoresis

SERM: selective estrogen receptor modulator

SFV: Semliki Forest virus

sGP: soluble GP (EBOV)

SUDV: Sudan ebolavirus

TIM-1: T-cell Ig and mucin domain 1

TM: transmembrane

TMD: transmembrane domain

USAMRIID: United States army medical research institute of infectious disease

VHF: viral hemorrhagic fever

VLP: virus-like particle

VLP-GP/GP $\Delta$ /G/LCMV-GP: EBOV VLPs bearing indicated glycoproteins on surface

VP24: viral protein 24 kDa (EBOV)

VP30: viral protein 30 kDa (EBOV)

VP35: viral protein 35 kDa (EBOV)

VP40: viral protein 40 kDa (EBOV)

VRB: virus resuspension buffer

VSV: Vesicular Stomatitis virus

VSV-GP/GP $\Delta$ /G: recombinant VSV pseudotyped with indicated glycoproteins

19 kDa GP: cathepsin-primed form of EBOV GP, believed to be final “fusion-ready” state of protein

## Acknowledgements

Seven years is a long time. This has been quite a journey, and at times the outcome didn't always seem certain. As is often the case with major endeavors, however, I have not been alone in this journey.

First, I would like to thank my advisor Dr. Judith White. Judy has been my template for what it means to be a research scientist. She has always led by example, working long hours, and was a model of what I should aspire to be. More than encouraging healthy work habits though, Judy has helped me change the way I think about and approach problems; encouraging me to ask the most incisive questions and to rarely take things at face value. She has also been very patient in my development as a scientist. Being a PI is a stressful job, and yet I always knew that she had my best interests at heart when it came to my progression here. For all her wisdom and patience, I am truly grateful.

I would also like to take this time to thank the members of my committee, comprising Drs. Amy Bouton, Rick Horwitz, and David Castle for their helpful advice and guidance over the years. I'm especially grateful for the times they helped me to take a step back from my project(s) and reevaluate so as not to lose sight of the forest for the trees. These moments were very valuable, and benefited me greatly in the long run.

I am deeply obliged to all the members of the White lab, both past and present, for their help and their camaraderie over the years. In no particular order, I'd like to thank Matt Brecher, who always had a lot to say about the science at hand, as well as various political goings on in the world at large. Derek

Dube could always be counted on as a model of scientific efficiency as well as a master organizer of athletics, social events, and pretty much any distraction imaginable (especially including the hours lost to LandGrab). Kat Schornberg was always a great source of advice, both scientific and oenological. I have been truly blessed and considerably spoiled by the generous sharing of her artistic talent when it came time to design data figures and illustrations. I have been lucky to know two great laboratory technicians in my tenure here. Edward Park was hard-working and always had a great sense of humor (along with a tremendous opinion of his own athletic talent). Elizabeth Nelson, was equally hard-working, and yet also found time to educate me in the decadence of modern pop culture. Sue Delos, our recently retired associate researcher, was an invaluable sounding board for ideas and never hesitated in sharing her considerable wealth of technical knowledge...which more than made up for her resistance to music being played in lab.

I couldn't have done any of this without my friends, family, and teachers. My parents encouraged me in science from an early age. Whether it was looking at paramecium on a microscope or allowing me to grow bacteria on my own homemade culture plates (very smelly), they always encouraged me in my interests. I'd especially like to thank my Dad for stoking my imagination over the years with great science books (both fiction and non-fiction). I owe my choice of a Ph.D track to my undergraduate research advisor, Terry Bird. He gave me my first real taste of independent research, and helped me to confirm that I wanted to pursue a career in science.

I'd like to thank my wonderful wife, Sara. Without Sara's steadfast support, I never would have made it this far. My journey here involved a lot of late nights and working weekends. Through this whole process, her love and belief in me have been the essential ingredients to my success. Lastly, I would like to thank my young daughter, Ellie, who though she arrived rather late in this process, has indelibly put her stamp on it (along with random pen marks here and there). In science, it is all too often easy to blind ourselves to the "magic" of the very things that we investigate. With clear eyes, I can say that my daughter is by far the most amazing thing I have ever seen in this life, and the promise of watching her grow, learn about this world, and put her own mark on it, fills me with awe and a deep sense of happiness.

*Aut viam inveniam aut faciam*

## **Chapter I: Introduction**

## **Background on Virus Entry**

While viral diseases such as rabies and smallpox have been known to humans for millennia, the actual causative agents of these diseases remained unknown until the modern era. The rise of the germ theory of disease in the 19<sup>th</sup> century greatly advanced human knowledge and welfare by positing that infectious diseases were spread by microscopic agents. Although microorganisms such as bacteria and protozoa were soon shown to cause many infectious diseases (51), viruses were only identified as a cause of animal diseases starting at the turn of the 20<sup>th</sup> century. Moreover, it was shown by such early pioneers as Martinus Beijerinck, Friedrich Loeffler, and Peyton Rous that these infectious agents existed at a sub-cellular level. Slowly, over the ensuing decades, an awareness grew that viruses were obligate intracellular parasites that depended on prokaryotes and eukaryotes for their survival and proliferation. Put simply, in order to replicate, all viruses must hijack the host cell's biological machinery and repurpose it for its own ends.

For successful infection to occur, the viral genome must be delivered to a suitable replication site, either the nucleus (e.g., for DNA viruses, retroviruses, and some RNA viruses) or the cytoplasm (for most RNA viruses). All virus infections follow five general steps. Firstly, the virus must attach to the host cell surface. This is accomplished by specific or non-specific binding to a target molecule(s) on the cell surface. Secondly, it must penetrate to an appropriate intracellular milieu. The means of penetration as well as the ultimate destination of the virus genome will depend on many factors, including whether the virus is

enveloped. Thirdly, once this site is reached, transcription, translation, and replication of the viral genome will proceed. The fourth stage is virus assembly; the newly synthesized viral proteins and replicated genomes are packaged into a new viral particle. Lastly, the virus must egress from the cell. This is accomplished either by cellular lysis, exocytosis, or direct budding from the plasma membrane of the cell.

Animal viruses can broadly be divided into two groups: non-enveloped and enveloped. Both types contain a nucleocapsid, consisting of the packaged genome, structural proteins, and any accessory proteins required for replication or transcription. For non-enveloped particles such as adenoviruses, the capsid proteins mediate particle binding and penetration into the host cell. Enveloped viruses have a host derived membrane surrounding the nucleocapsid. In addition, enveloped viruses have glycoproteins anchored in their membranes that mediate viral entry into the host cell. Due to the presence of a viral membrane, the surface glycoprotein(s) must perform a function that is unique to enveloped viruses, namely fusion. Whether fusion occurs on the cell surface or in an internal compartment, these glycoproteins must drive the merger of the viral membrane with the target membrane, thus enabling the viral nucleocapsid to reach the cytoplasm. A dysfunction in this fusion mechanism results in failed viral entry, and terminates the infection cycle.

Viruses have evolved along different lines with regard to how they gain entry to host cells. Measles virus, for instance, fuses at the plasma membrane while viruses like influenza hijack a cell's natural endocytic machinery to reach a

late endosome, where fusion occurs. For viruses that exploit endocytosis, a series of consecutive events must occur: attachment, internalization, trafficking, and penetration. For enveloped viruses, all of these steps are mediated by glycoproteins.

### **Viral Glycoproteins**

All enveloped viruses depend on integral membrane glycoproteins on their surface to mediate their penetration into the host cell. Sometimes, as in the case of rhabdoviruses, a single glycoprotein is responsible for mediating all of the events involved in entry. Others such as herpesvirus, delegate various roles among up to 10 glycoproteins that participate in a carefully choreographed dance that eventually leads to viral entry. While they are involved in other roles as well, glycoproteins serve two primary roles during enveloped virus entry; attachment and fusion. Viruses that possess a single envelope glycoprotein such as the HIV Envelope protein (Env), typically have separate subunits tasked with surface attachment (gp120) and fusion (gp41).

Enveloped viruses can vary greatly in the molecules they bind to as well as their site of fusion. Most retroviruses and paramyxoviruses rely on their glycoproteins to effect both attachment and fusion at the plasma membrane. Orthomyxoviruses and rhabdoviruses, on the other hand, mediate these processes in discrete locations. Despite these differences, the glycoproteins of enveloped viruses share many structural and mechanistic similarities, particularly with regard to their roles in fusion.

## **Viral Receptor Binding**

Enveloped viruses have evolved to attach to different cell surface targets (Table 1.1). These targets can include both glycoproteins and glycolipids, and may involve engagement of a single cell surface target or multiple molecules. Cellular receptors can provide two functions, that of an attachment factor and/or entry receptor. The initial binding may be of only low affinity and specificity, simply relying on electrostatic interactions. In fact, some viruses exhibit a degree of promiscuity with regard to their attachment receptors. Hepatitis C virus, for example, can utilize both heparin sulfate and L-SIGN as initial attachment factors (13, 77), since both can act as charged molecules for the viral glycoprotein to bind with. Initial binding to a cell surface target molecule is not always sufficient for virus entry to proceed, and other receptors and sometimes co-receptors must also be recruited. The best studied case of this is with HIV entry. Initial attachment of the virion to the cell surface involves the gp120 receptor binding subunit of the HIV Envelope (Env) glycoprotein, and is likely mediated by various low-specificity attachment factors such as heparin sulfate and DC-SIGN (12, 178). Next, HIV typically binds (through gp120) to its primary receptor CD4, a member of the immunoglobulin superfamily (49, 144). In most HIV strains, it is essential for CD4 to interact with gp120 (279). This, however, is not sufficient for HIV fusion and entry to occur as a coreceptor is also required. This function is typically provided by either CXCR4 or CCR5, both members of the chemokine family of receptors (43, 66). In general, only when both CD4 and a coreceptor are present and engaged by HIV Env can structural changes be induced in the Env

fusion subunit gp41 (a class I fusion protein) that will eventually promote fusion at the cell surface. A minority of HIV-1 strains, however, do exhibit CD4 independence. It appears that these strains already have exposed co-receptor binding sites, enabling fusion to be solely co-receptor mediated, and rendering CD4 dispensable for fusion (105).

Many animal enveloped animal viruses do not, however, fuse directly at the cell surface. Instead they rely on the host cell's endocytic machinery to ferry the particle into the cell. In this scenario, engagement with an appropriate cell surface receptor (or coreceptor) is often a pre-requisite for subsequent internalization into the cell.

### **Viral Internalization**

After binding to the cell surface, viruses that are endocytosed can exploit several internalization mechanisms, many of which are still poorly understood. The discovery of these varied routes of virus entry has paralleled the emerging understanding of endocytosis at large, and has in many cases helped to elucidate the basic cellular processes. Endocytosis refers to a complex system of pathways, which exist to ferry cargoes into the cell. It is complemented by exocytosis, which transports cargoes to the outside of the cell. Endocytosis encompasses numerous distinct uptake routes (Fig. 1.1), almost all of which can be exploited by viruses.

Clathrin-mediated endocytosis (CME) was both the first endocytic pathway described as well as the first to be described in the context of virus entry (98,

163). Both Vesicular Stomatitis Virus (VSV) and Semliki Forest Virus exploit this pathway, which is dependent on engagement of a cell surface receptor such as the low-density lipoprotein receptor, which in turn signals the recruitment of the protein clathrin. Clathrin then self-polymerizes and drives the formation of a clathrin coated pit (CCP) (7, 196, 213). The formation of a CCP imposes curvature on the plasma membrane, which then engulfs the particle as it invaginates into the cell. Scission of this clathrin-coated vesicle from the cell surface is accomplished by the small GTPase dynamin (50, 99, 261). Caveolar endocytosis (CE) is a clathrin-independent form of endocytosis involving lipid raft-associated invaginations that are enriched with the protein caveolin. Like CME, caveolae require dynamin to complete scission of the vesicle from the cell surface. These structures are normally responsible for the uptake of cargoes such as GPI-linked proteins and folate. Viruses proven to enter through caveolae include the non-enveloped small DNA viruses polyomavirus and SV40 (143, 197). To date, no conclusive evidence has been presented showing caveolar endocytosis as a viable route for an enveloped virus.

Both CME and CE involve fairly small membrane-enclosed carriers. The average diameter of a CCP or vesicle is only ~100-200 nm.(48, 150, 218). Caveoli are even smaller being only ~ 50-80 nm (150).

Such structures are not likely to be amenable to larger enveloped viruses such as mimivirus (750 nm diameter) and vaccinia virus (200 nm diameter x 300 nm length). Mimivirus was shown to enter macrophages via a CME/CE independent route that was highly dependent on rearrangement of the actin

**Table 1.1. Examples of the different types of molecules utilized by viruses**

**as receptors.** Almost all of these molecules are thought to engage their respective viruses on the cell surface. Some virus particles use a single-receptor species; others can use alternative molecules, either of which is sufficient, whereas other viruses require a specific combination of receptors. Examples from each category are given and illustrate the diversity of receptors. All viruses except SV40, Reovirus, and Adenovirus are enveloped viruses. ACE, angiotensin-converting enzyme; CAR, coxsackie B virus and adenovirus receptor; DAF, decay-accelerating factor; DC-SIGN, Dendritic Cell-Specific Intercellular adhesion molecule-3-Grabbing Non-integrin; HAVCR1, Hepatitis A virus cellular receptor 1; HBGA, histoblood group antigen; HVEM, herpesvirus entry mediator; JAM, junctional adhesion molecule; NPC1, Niemann-Pick C1; PSGL-1, P-selectin glycoprotein ligand-1; SLAM, signaling lymphocyte-activation molecule; TIM-1 (T-cell Ig and mucin domain 1). \*TIM-1 was recently identified as a surface binding part for ebolavirus in some, but not all cell lines. \*\*A novel exception to virus-receptor binding on the cell surface occurs during ebolavirus entry. After binding to as yet incompletely-defined surface attachment factors and receptors, ebolavirus is internalized into the endocytic pathway where GP is proteolytically primed; this primed GP then interacts with the intracellular protein Niemann-Pick C1 (NPC1), presumably in late endosomes/lysosomes. Adapted from “The cell biology of receptor-mediated virus entry” by Grove and Marsh, 2011. (91)

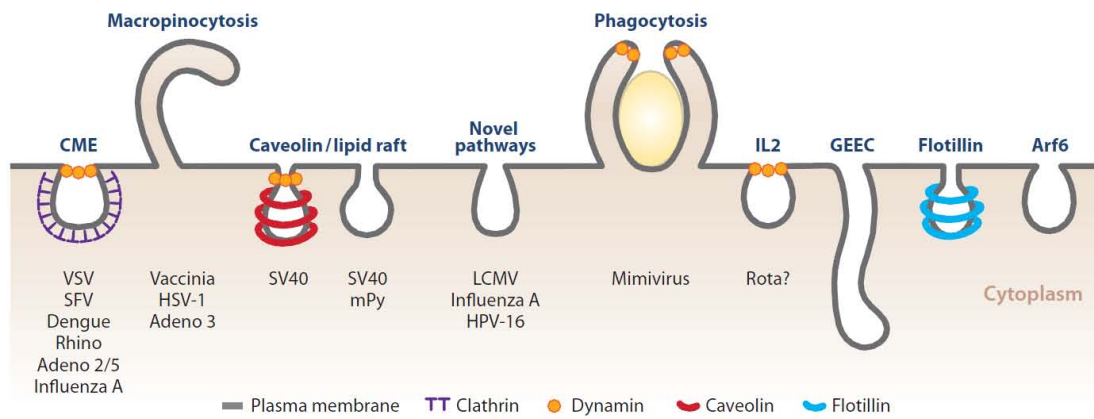
<b>Virus</b>	<b>Family</b>	<b>Receptors</b>	<b>Reference(s)</b>
Old World arenaviruses	Arenaviridae	$\alpha$ -Dystroglycan	Cao et al., 1998
Influenza A	Orthomyxoviridae	Sialic acid	Matlin et al., 1981
Henipavirus	Paramyxoviridae	Ephrin B2	Negrete et al., 2005
Bunyavirus	Phleboviridae	DC-SIGN	Lozach et al., 2011
Hepatitis A virus	Picomaviridae	HAVCRI (TIM-1)	Kaplan et al., 1996
SV40 polyomavirus	Polyomaviridae	GM1	Tsai et al., 2003
Reovirus	Reoviridae	JAM	Barton et al., 2001
SARS coronavirus	Coronaviridae	ACE 2	Li et al., 2003
HSV 1/2	Herpesviridae	Nectin-1/2 or HVEM	Montgomery et al., 1996; Geraghty et al., 1998; Krummenacher et al., 1998
Measles virus	Paramyxoviridae	SLAM or Nectin- 4	Tatsuo et al., 2000; Noyce et al., 2011
Adenovirus 2	Adenoviridae	CAR and $\alpha$ v integrins	Wickham et al., 1993; Bergelson et al., 1997; Tomko et al., 1997
Ebolavirus	Filoviridae	TIM-1* and NPC1**	Kondratowicz et al., 2011; Carette et al., 2011; Côté et al., 2011;
HCV	Flaviviridae	CD81 and SR- B1	Pileri et al., 1998; Scarselli et al., 2002; Evans et al., 2007; Ploss et al., 2009
HIV	Retroviridae	CD4 and CCR5 or CXCR4	Dalglish et al., 1984; Klatzmann et al., 1984; Choe et al., 1996; Deng et al., 1996; Dragic et al., 1996; Feng et al., 1996

cytoskeleton as well as dynamin II; both of which are hallmarks of phagocytosis (85).

This was further verified by EM ultrastructural analysis, which showed “tightly-fitted” smooth endosomal structures containing mimivirus that were consistent with phagosomes. Phagocytosis is an actin-dependent process that results in engulfment of a cargo on the cell surface. The process is localized in nature and is often driven by engagement of the cargo by Fc receptors. Phagocytosis is thus one means by which the innate immune system targets foreign particles for uptake and destruction. The Fc receptors engage antibodies that have opsonized onto foreign objects (i.e. pathogens). Mimivirus, and perhaps other enveloped viruses like Herpes Simplex virus-1 have simply evolved to exploit this pre-existing mechanism for internalizing large particles (44), albeit with the caveat that this internalization route is largely confined to professional phagocytic cells like neutrophils, dendritic cells, and macrophages.

Macropinocytosis is also an actin-dependent pathway that can mediate the internalization of large enveloped viruses. In recent years, the poxvirus vaccinia has been shown to exploit the macropinocytic pathway. This would seem to be an appropriate uptake mechanism since macropinocytosis promotes the internalization of large extracellular volumes, and potentially large cargoes. It is driven by large scale rearrangements of the cortical actin network near the cell surface. This generates ruffling of the plasma membrane, which can sometimes “erupt” outwards, engulf a particle and then collapse back inward forming an invagination into the cell. These ruffles can vary in nature depending on cell type

**Figure 1.1. Endocytic mechanisms used by viruses.** Viruses can exploit many different endocytic mechanisms for entering animal cells. Classical pathways like clathrin-mediated endocytosis and caveolar endocytosis involve dynamin-2 for scission from the plasma membrane as indicated by the beads around the necks of the membrane invaginations, while others operate independently of it. Large particles are taken up by phagocytosis, a process limited to a few specialized cell types, and also by macropinocytosis, which can be transiently stimulated in numerous cell types. In addition, there are numerous poorly understood pathways such as that for IL-2, the GEEC pathway, and the flotillin- and ADP-ribosylation factor 6 (Arf6)-dependent pathways that carry specific cellular cargoes into cells, but have not yet been described as pathways for virus entry. Abbreviations: Adeno 2/5, adenovirus 2/5; Adeno 3, adenovirus 3; CME, clathrin-mediated endocytosis; HPV-16, human papillomavirus 16; HSV-1, herpes simplex virus 1; LCMV, lymphocytic choriomeningitis virus; mPy, mouse polyomavirus; SFV, Semliki Forest virus; SV40, simian virus 40; VSV, vesicular stomatis virus. Figure obtained with permission from: Mercer, et al. "Virus Entry by Endocytosis." *Annu. Rev. Biochem.* 2010. 79:803–33. (169)



and the activation mechanism being utilized by the virus for inducing macropinocytosis (166). The membrane protrusions induced by viruses have been described as lamellopodial ruffles (Ebola virus and adenovirus 35), circular ruffles (HIV-1), filopodial protrusions (Nipah virus), and blebs (vaccinia virus). The resultant macropinosome will then be severed from the cell surface by a scission factor. A macropinosome is thus a large, uncoated, irregularly-shaped, and fluid filled compartment. Unlike in CME, CE, or phagocytosis; dynamin does not appear to be required for the closure of either lamellopodial ruffles or blebs. In its place, the C-terminal binding protein (CtBP1/BARS) seems to function as the relevant scission factor. The circular ruffles associated with viruses such as HIV-1 have, however, been reported to require dynamin for macropinosome formation. Macropinocytosis is a highly dynamic process that occurs over a time-scale of seconds. Macropinosomes are immense (500 nm-10  $\mu$ m) compared to other endocytic structures (168). Unlike phagocytosis, macropinocytosis is usually a rather non-specific, transient mechanism that can only be triggered for a relatively short period of time. It seems to be the result of cell-wide signaling changes affecting the actin cytoskeleton. These changes can be instigated by a number of cell surface receptors that can, in turn, initiate signaling cascades that lead to actin rearrangement. Examples of such signaling factors are receptor tyrosine kinases, integrins, and phosphatidylserine receptors. The last of these was shown to be involved in the entry of vaccinia virus, which can induce macropinocytosis in non-professional phagocytic host cells (167). A single particle was capable of inducing macropinosomes to form over the entire cell

surface, suggesting a global signaling cascade. In addition to demonstrating macropinocytosis by direct imaging of actin-enriched structures, vaccinia virus was also shown to boost the uptake of dextran, a polysaccharide commonly used as a fluid-phase marker of macropinocytosis, by more than 3 fold. Moreover, many of the signaling molecules (e.g. PI3K, PKC, Pak1, Cdc42/Rac1) commonly associated with macropinocytosis were shown to be required to support successful vaccinia virus entry. The actual triggering mechanism for vaccinia's macropinocytotic uptake was shown to be engagement of phosphatidylserine in the viral membrane with phosphatidylserine receptors on the host cell. These receptors are known to be involved in apoptotic clearance of cellular debris. In effect, vaccinia and potentially other viruses like cytomegalovirus (97), use a form of "apoptotic mimicry" to trigger a latent macropinocytic-driven debris clearance response in host cells as means of gaining entry.

Additionally, there exist several poorly understood internalization mechanisms that are distinct from CME, CE, phagocytosis, and macropinocytosis. One of these is known as the CLIC/GEEC pathway, which is associated with uptake of GPI-anchored proteins. It is distinguished by tubular invaginations that are independent of clathrin, caveolin, dynamin, and actin polymerization, but are dependent on the small GTPases Cdc42 or Arf6 (164). The non-enveloped virus adeno-associated virus 2 is known to enter via this mechanism, but no enveloped viruses have yet been associated with a CLIC/GEEC uptake pathway. The most distinguishing characteristic of this pathway is that it rapidly delivers cargoes to the late endosome. Lastly, there are

likely other (undiscovered) endocytic routes of internalization available for viruses to exploit. For example, the arenavirus LCMV is not known to enter through any of the previously described pathways (207).

### **Viral Trafficking**

Regardless of their internalization mechanism, viruses that are brought into the cell must interface with the intracellular network of endocytic vesicles. This consists of a collection of vesicular compartments that are responsible for sorting and delivering internalized cargoes to their final destinations. Early endosomes (EEs) frequently act as the initial acceptor compartment. EEs are peripherally located compartments with a combination of vacuoles and tubular structures. EEs are also distinguished by the presence of the GTPase Rab5 and by PI(3)P; they have a luminal pH of 6.5-6.0. The EE has an important early sorting function, with cargoes diverted to either the recycling endosome (where cargoes like the iron transporter transferrin will be delivered back to the cell surface) or sent further into the endocytic pathway. Sorting into the late endocytic pathway involves maturation of the early endosome, first into a multi-vesicular body (MVB), then into a late endosome (LE), and finally to a lysosome (Lys) (150). This maturation involves recruitment of the GTPase Rab7, which eventually replaces Rab5, a drop in pH (pH 6.0-5.0 in LEs, pH 5.0-4.5 in Lys), replacement of PI(3)P with PI(3,5)P<sub>2</sub>, and eventual recruitment of lysosomal hydrolases during the terminal stages. Progressive loss of tubules is another hallmark of the transition from early to late endosomes; tubules are completely absent by the mature LE/Lys stage. In addition, these later stage compartments

engage the microtubule network more avidly, and as a consequence they tend to have a more perinuclear distribution.

Some viruses like Semliki Forest virus have evolved to fuse in the relatively mildly acidic milieu of the early endosome, while others like influenza virus must transit to the late endosome because of the lower pH requirement of its fusion protein (136, 237, 272, 273). Modern imaging techniques have enabled the tracking of viruses as they pass through different endocytic compartments, as denoted by colocalization with markers such as Rab 5 and Rab 7.

### **Viral Fusion**

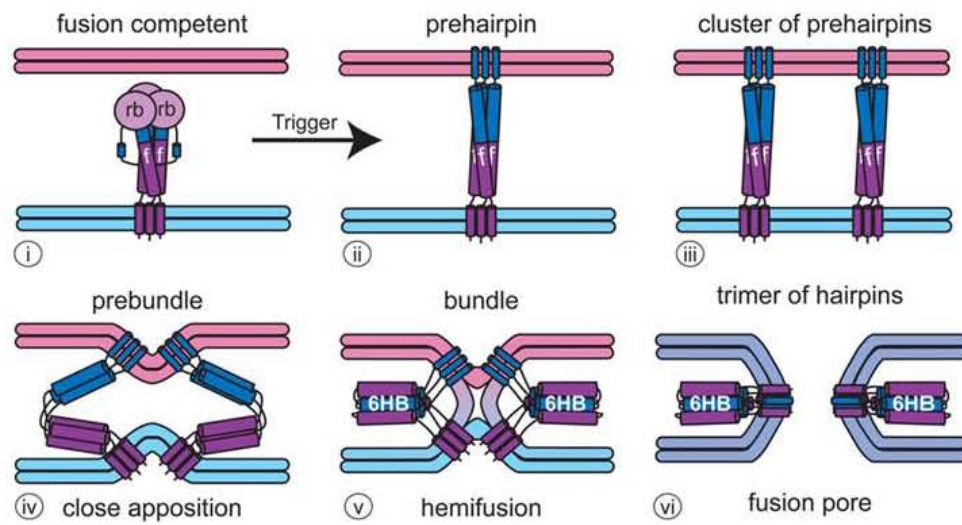
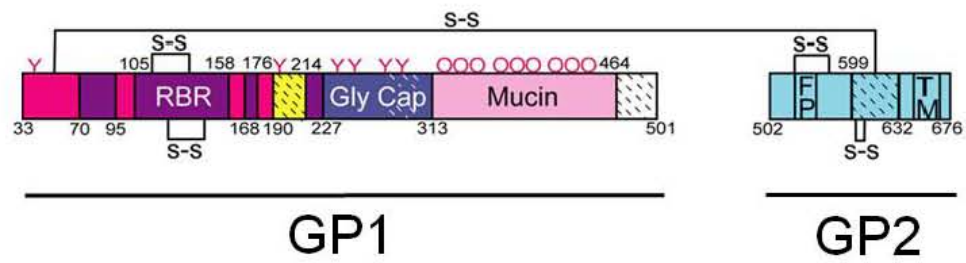
Once it reaches its entry site, an enveloped virus must fuse, with either the plasma membrane or the limiting membrane of the compartment it is contained in, in order to escape into the cytoplasm. Failure to do so would result in aborted virus entry and a termination of infection. Whether at the cell surface or in an endosome, fusion is brought about by viral glycoproteins, specifically the fusion subunit of one of these proteins. Normally, fusion proteins exist in a metastable state on the virion surface. Upon exposure to certain triggering conditions, however, the fusion proteins undergo a series of related structural changes whose end result is merging of the viral membrane with the target membrane.

The viral glycoprotein(s) associated with membrane fusion can be subdivided into three main classes based on their structural characteristics. Class I fusion proteins exist as trimers both pre and post fusion, and have a fusion subunit that is rich in  $\alpha$ -helices (Fig. 1.2B). Class II fusion proteins exist as dimers pre-fusion, but transition to trimers post fusion, and have a  $\beta$ -strand rich

fusion subunit. Lastly, class III fusion proteins are trimeric in their pre and post fusion states and possess a fusion subunit that has both high  $\alpha$ -helical and  $\beta$ -sheet content. The central paradigm for fusion mediated by all viral fusion proteins is the formation of a “trimer of hairpins”, which drives the merging of the viral and host membranes (Fig. 1.2A) (275). The process starts when the fusion competent glycoprotein transitions to a membrane embedded pre-hairpin state (34). It continues as the pre-hairpin converts to a trimer of hairpins. Following this conversion in glycoprotein structure, a fusion pore is created and expands to a size large enough for the viral nucleocapsid to traverse into the cytoplasm.

Prior to fusion it is essential for the fusion glycoprotein to be in a fusion competent state. Attaining this state generally involves proteolytic priming of either the fusion glycoprotein or a companion protein(s). Many class I fusion proteins, including the prototypical influenza hemagglutinin (HA), require proteolytic processing during viral assembly in order for newly budded virions to be fusion competent, and therefore infectious. For influenza, newly synthesized HA precursor protein (HA<sub>0</sub>) is cleaved by trypsin-like host cell proteases (the identity of which can depend on both the virus strain as well as the infected tissue type) into HA<sub>1</sub> (the receptor binding subunit) and HA<sub>2</sub> (the fusion subunit). Others such as the class III fusion proteins VSV-G and HSV-1 gB do not exhibit a requirement for proteolytic priming. Once a fusion glycoprotein has been proteolytically modified (if necessary), it is considered to be in a fusion competent state, which is usually but not always metastable. At this point all fusion glycoproteins require an external trigger (or triggers) in order to initiate the fusion

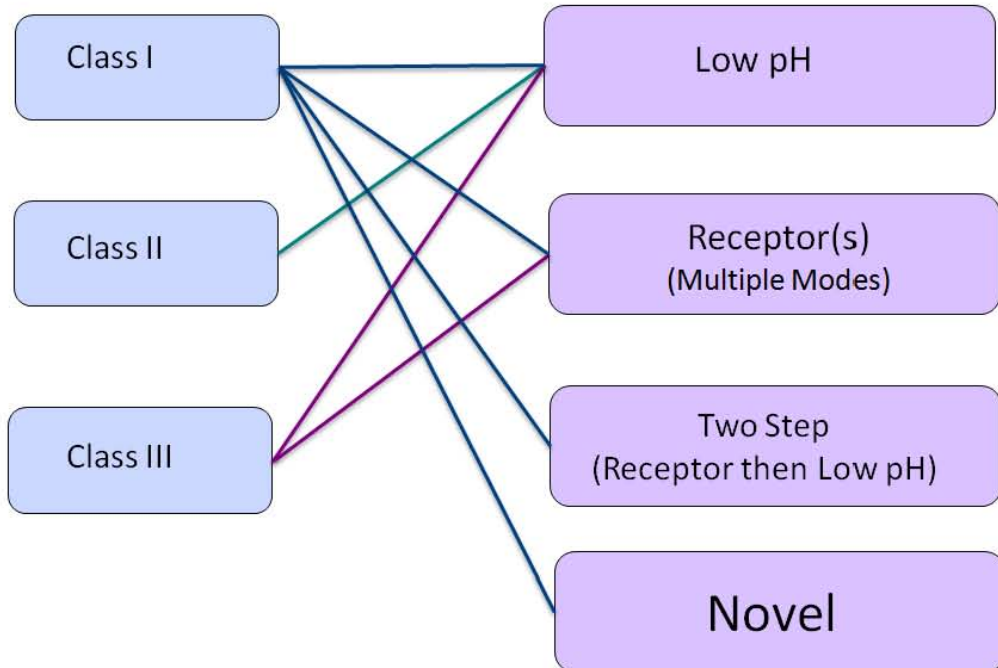
**Figure 1.2. The conserved pathway of viral membrane fusion and the structure of the Ebola virus (EBOV) glycoprotein.** (A) The model depicts a Class I fusion protein, but related structures (e.g., prehairpins and trimers-of-hairpins) form for Class II and III proteins, and also promote membrane merger through the same (indicated) stages. The illustration shows a fusion protein that does not require any other viral surface proteins for fusion (e.g., influenza HA); it contains both a receptor binding subunit (labeled rb in image i) and a fusion subunit (labeled f in images i to iii). The target cellular and viral membranes are at the top and bottom of the image, respectively. (B) Schematic of GP1 and GP2 subunits of the EBOV glycoprotein (a class I fusion protein) along with their respective sub-domains. From N-terminus to C-terminus (left to right) for GP1 subunit are the: signal peptide (not shown), base (hot pink), head group containing the receptor binding region (RBR, purple), linker region (yellow), glycan cap (Gly Cap, dark blue), mucin-like domain (pink), and the C-terminal domain (white). From N-terminus to C-terminus for GP2 subunit (light blue) are the: fusion peptide (FP) and the transmembrane domain (TM). Red Ys and red Os represent sites of N- and O-glycosylation, respectively. Inter- and intra-subunit disulfide bonds are indicated. Fig. 1.2A modified (by Kathryn Schornberg) from White, et al. 2008. See publication for further details. (275). Fig. 1.2B created by Kathryn Schornberg. Used with permission from her thesis dissertation (Fig. 1.4). Schornberg, K.L. 2008. Ebolavirus Entry. University of Virginia, Charlottesville, VA. (226)

**A.****B.**

**Figure 1.3. Diversity of viral fusion proteins.** The major differences among viral fusion proteins are their structural class (*left*) and mode of fusion triggering (*right*). See White, et al. 2008 for further details. Figure modified (by Kathryn Schornberg) from White, et al. 2008. (275)

## Structural Class

## Fusion Trigger



process. These triggers can vary (Fig. 1.3), but common ones include receptor binding (e.g. HIV Env, paramyxovirus F), low pH (e.g. influenza HA, VSV G), or a combination of the two (ASLV Env). Whatever the trigger, the next step involves formation of the pre-hairpin intermediate, which embeds into the target membrane via apolar regions (fusion peptides or fusion loops) found in the fusion subunit. For all glycoproteins, the prehairpin intermediate exists as a homotrimer of the fusion subunit. This is followed by clustering of several of these pre-hairpin homotrimers. The prehairpins in these clusters then undergo dramatic fold-back steps forming trimers of hairpins. The result is close apposition of the viral and host membranes, eventually resulting in hemifusion and finally in fusion pore formation (Fig. 1.2A). The driving force behind these fold back steps derives from the fact that the trimer of hairpins conformation is the most energetically stable state for the triggered glycoprotein. Once the fusion pore has been stably established, the lumen of the virus is continuous with the host cell cytoplasm, and nucleocapsid delivery can proceed, thus completing the virus entry process.

### **Ebolavirus Overview**

Ebolaviruses are the causative agents of Ebola hemorrhagic fever, a highly lethal viral disease. The viruses are infectious to humans, non-human primates (NHPs), and other mammalian species. Ebolavirus is one of only two genera in the family *Filoviridae* in the order *Mononegavirales*, the other being Marburgvirus (MARV). Ebolaviruses are enveloped, single-strand, negative-sense RNA viruses. They were first given the name Ebola (later, ebolavirus),

after the Ebola river, which runs through the area of the Democratic Republic of Congo where the disease first emerged. To date the genus consists of 5 species: Zaire ebolavirus (EBOV), Sudan ebolavirus (SUDV), Reston ebolavirus (RESTV), Taï Forest ebolavirus (formerly Côte d'Ivoire ebolavirus) (TAFV), and Bundibugyo ebolavirus (BDBV) (132). These species vary in their lethality in humans, but EBOV is considered the deadliest with a lethality range of 60-90% over all recorded outbreaks (71).

### **Emergence**

The first recorded occurrence of ebolavirus was an EBOV outbreak in the Yambuku area of Zaire (now the Democratic Republic of Congo) in August 1976 (277). An adult male with gastrointestinal bleeding presented himself at a local hospital. He died within 2 weeks of admission. Within a short time span, several other patients at the same hospital developed similar symptoms. Within 2 months of the index case, there were 318 confirmed or suspected cases within the area, eventually resulting in 280 deaths (88% fatality rate). Since this initial outbreak, there have been more than 20 ebolavirus outbreaks, with 2764 human infections resulting in 1900 deaths (90). Due to the poor health surveillance networks in the affected areas, these numbers most likely underestimate the true numbers of people affected. All human outbreaks of the disease have been confined to the equatorial region of sub-Saharan Africa. SUDV first emerged in a separate large-scale outbreak in 1976 in the Nzara and Maridi areas of Sudan. The third strain identified, RESTV, is non-pathogenic in humans but is deadly in NHPs. It is the only ebolavirus strain to have been observed in outbreaks outside of Africa.

These NHP outbreaks occurred in the United States in 1989, Italy in 1992-1993, and the Philippines in 1996 and 2008 (173, 174). Until recently, RESTV outbreaks have occurred in animal research support facilities and were linked to the handling and/or importation of infected Macaque monkeys. In 2008, however, there was an outbreak among domestic pigs in the Philippines. A disturbing characteristic of both the 1996 and 2008 outbreaks is that there was some evidence of seroconversion (albeit non-pathogenic and inefficient) in humans who worked in close proximity to the pigs, raising the possibility of monkey to human and pig to human zoonotic transmission. In 1994 a fourth ebolavirus species, TAFV, was identified in a woman who had performed an autopsy on a wild chimpanzee in Côte d'Ivoire, Africa. A fifth species of ebolavirus, named BDBV, broke out in Uganda in December 2007, infecting 149 people, and killing 39. Lastly, a sixth, distantly-related ebolavirus species, provisionally named Lloviu virus (LLOV), may exist that has been attributed as the causal agent of mass die-offs of fruit bats in Spain (185). Preliminary genetic analysis suggests that this filovirus is more similar to ebolavirus than marburgvirus, although more characterization is needed.

Immediately after the twin EBOV and SUDV outbreaks of 1976, MARV was initially suspected. Also a filovirus, MARV generates acute hemorrhagic fever in infected humans. First identified in 1967 in an infected researcher (who later died) in Germany, the first major MARV outbreak occurred in 1975. Upon examination, however, it was determined that while clinically similar to MARV, these newer outbreaks were immunologically distinct. Due to their deadly nature,

studies regarding ebolavirus and MARV infections have been stymied by the requirement for Biosafety Level 4 facilities in order to study live, native virus.

### **Life Cycle**

Neither humans nor NHPs are natural reservoirs for ebolavirus, as it is highly lethal to both groups. In fact, recent human outbreaks of the disease have been paralleled by severe ebolavirus outbreaks amongst NHPs, particularly among the great ape (i.e. gorilla and chimpanzee) populations of tropical Africa, which have been decimated in consequence. The concurrence of these outbreaks is likely not coincidental and probably occurs within the same epidemiological event; perhaps in an analogous manner to that observed in MARV outbreaks (5, 280). By and large, humans serve as epidemiological dead ends for the virus as they exhibit an extremely rapid mortality profile, thus rendering outbreaks in human populations inherently self-limiting, the so called “burn-out” effect.

Like all other ebolavirus strains, EBOV is a zoonotic infectious agent. Since its initial discovery, the native reservoir has remained elusive. However, recent survey data collected on small vertebrates during the 2001 and 2003 EBOV outbreaks in Gabon and the Democratic Republic of Congo have provided evidence of apparent asymptomatic infection in three species of fruit bats (139). Combined with earlier evidence of EBOV replication in otherwise healthy bats (248) and circumstantial evidence detailing the presence of some index human patients at sites where bats are found (e.g. caves, mines) prior to them acquiring

the disease (89), this suggests that some species of fruit and insectivorous bats may serve as natural reservoirs for EBOV.

### **Structure**

*Particle Morphology.* Like all enveloped viruses, EBOV has a nucleocapsid surrounded by a host-derived lipid envelope. Filoviruses such as EBOV are among some of the largest known viruses. From a morphological standpoint, they appear filamentous albeit highly pleomorphic. They are commonly described as being filamentous, six (or shepherd's crook)-shaped, or circular. While EBOV has a consistent diameter of ~80 nm, the lengths of particles can vary dramatically with particles in excess of 20  $\mu\text{m}$  having been observed (17, 83). Recent electron microscopic studies have revealed an underlying organizational logic behind this apparent length pleomorphism. Four basic particle types have been observed; empty particles containing no genome, single particles containing one genome, continuous virions with genomes packed end-to-end, and linked particles that contain multiple genomes, but unlike continuous genomes are separated from each other by short stretches of empty envelope. An EM-based statistical study of EBOV particles revealed that single genome particles constitute ~53% of particles observed and that they are approximately 1 micron in length (17). Continuous and linked particles made up most of the remaining particles. These can account for the larger particles previously described in the literature. The presence of polyploidy in a typical EBOV population may enhance the virus' infectivity as has been observed for infectious bursal disease virus (152).

*Particle Organization.* The EBOV structural proteins are the nucleoprotein (NP), virion proteins (VP) 24, 30, 35, 40, the viral membrane-anchored glycoprotein (GP), and an RNA-dependent RNA polymerase (L). In addition, due to a transcriptional editing event (see below), a non-structural form of GP called soluble GP (sGP) is produced. The viral core is composed of NP, VP24, VP30, VP35, L, and the viral RNA. The overall organization of the nucleocapsid is helical in appearance (17). It is now thought that the nucleocapsid has an inner core made up of RNA, VP30, and NP, which is in turn stabilized by an outer layer of VP24-VP35 bridges. These peripheral bridges may also link the nucleocapsid to the viral matrix. The matrix is composed almost entirely of VP40, which is arranged in a lattice-like framework of VP40 oligomers. This scaffolding connects the nucleocapsid to the host-derived viral envelope, which is densely studded with trimeric GP spikes (Fig. 1.4A).

*Matrix Protein VP40.* VP40 is the major EBOV matrix protein and is by far the most abundant structural protein of the viral particle. The matrix proteins of other enveloped viruses such as VSV-M and HIV-Gag serve as bridges between the viral envelope and the viral nucleocapsid and are critical in mediating particle assembly. VP40 has been shown to oligomerize with itself and form ring-like structures, which associate with lipid-raft domains at the plasma membrane (194, 253). Harty, et al. showed that VP40 expression in host cells was sufficient to cause association with the plasma membrane and subsequent release into the supernatant (96). Furthermore, this group showed that budding was highly

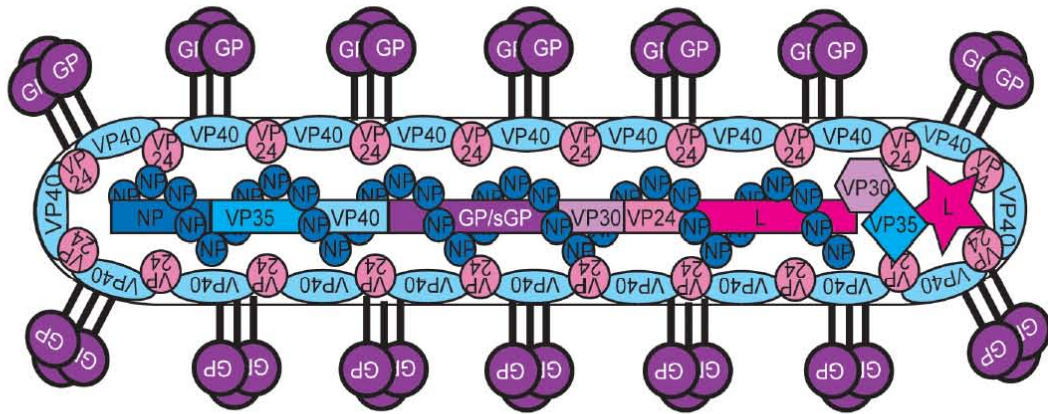
dependent on a conserved PPxY motif in a late-budding domain in the N-terminus of VP40. This motif is responsible for interacting with the ubiquitin ligase Nedd4, resulting in multiubiquitination of VP40. Perturbation of this ubiquitination effectively blocks ebolavirus VLP budding (190). The role of ubiquitination in ebolavirus release likely has to do with the known function of ubiquitination in the ESCRT pathway (23, 95, 190). At this time, many groups have shown that expression of VP40 alone causes the formation and budding of EBOV virus-like-particles (VLPs) from the cell surface, and that GP can be readily co-incorporated into these particles (188, 254).

*GP.* The glycoprotein, GP, exists as a trimer protruding from the viral envelope and is the only protein exposed on the virion surface. Consequently, GP is the sole mediator of virus entry into cells (39, 267). These surface spikes protrude ~5-10 nm from the viral envelope (83). Each GP monomer consists of two subunits, GP1 (the receptor binding subunit) and GP2 (the fusion subunit), which are linked by a disulfide bond (Fig. 1.2B). Much of the C-terminal region of GP1 consists of the heavily N and O glycosylated mucin-like domain, whose *in vivo* function has yet to be clearly defined. However, the mucin domain is dispensable for infection, at least *in vitro* (112). The remainder of GP1 contains a receptor-binding domain (58, 133, 158). GP2 is a class I fusion protein and consists of a coiled-coil domain adjoining the fusion peptide, which ultimately forms a trimer of hairpins during fusion (156).

GP is encoded in two different reading frames. Transcriptional editing by the EBOV RNA polymerase inserts an adenosine and bypasses a default stop

**Figure 1.4. Morphology and genome organization of EBOV.** (A) The structure of an EBOV virion. The ribonucleoprotein complex (RNP) is comprised of the genomic RNA (colored rectangles in (A) and (B)) as well as the nucleoprotein (NP), viral proteins 30 and 35 (VP30, VP35), and the RNA-dependent RNA polymerase (L). Viral protein 24 (VP24) and VP35 form a layer of heterodimeric “bridges” which act to both stabilize the nucleocapsid and connect it to the viral matrix. The viral matrix is comprised predominantly of a lattice-like network of VP40 oligomers. The matrix underlies the viral membrane, whose sole surface protein is the trimeric glycoprotein (GP). (B) The genome organization of the negative sense RNA is represented by colored rectangles. Due to a transcriptional editing event, both a truncated, soluble form (sGP) of GP is expressed along with the full length, membrane-anchored form. Figure created by Kathryn Schornberg. Used with permission from her thesis dissertation (Fig. 1.1). Schornberg, K.L. 2008. Ebolavirus Entry. University of Virginia, Charlottesville, VA. (226)

A.



B.



codon resulting in the production of two different forms of GP (221). Transcripts failing to bypass the default stop codon yield a smaller nonstructural form of the protein (291 amino acids before processing) called sGP, which is then secreted in abundance from infected cells. The role of sGP in EBOV pathogenesis remains unclear, but proposed functions include suppressing the inflammatory response in endothelial cells and inhibiting neutrophil activation (265, 283). In addition, it has been demonstrated that antibodies in sera from human survivors preferentially recognize sGP (160). This suggests that sGP may act as a decoy against the host antibody-mediated immune response, scavenging antibodies that might otherwise target circulating virus (which has full length GP) (111). Production of this secreted form occurs in approximately 80% of GP transcription events. In the remaining 20% of transcripts, an adenosine insertion shifts translation into the second reading frame, resulting in the full length (676 amino acids before processing) form of GP that integrates into the virion surface (221, 264). The N-terminal signal sequence of GP is removed by signal peptidase, followed by N-linked glycosylation and trimerization in the ER. Maturation of N-glycans and O-glycosylation occurs in the Golgi apparatus, followed by furin cleavage of GP into GP1 and GP2 (73). These subunits remain covalently linked by a disulfide bond between Cys53 of GP1 and Cys609 of GP2 (112). While this furin cleavage is similar to that which takes place with influenza HA<sub>0</sub>, it is not necessary for infection in the case of EBOV (187, 282).

## **Replication and Assembly**

EBOV has a non-segmented 18.9-kb negative-sense single-stranded RNA genome with seven genes encoding 7 structural proteins: NP, VP24, VP30, VP35, VP40, GP, and L (Fig. 1.4B). EBOV only has to reach the host cell cytoplasm in order to initiate replication. Following intracellular fusion, the ribonucleoprotein (RNP) complex is released into the cytoplasm. The RNP consists of the RNA genome, NP, VP30, VP35, and L, and is sufficient for supporting viral RNA transcription and replication (181). Once in the cytoplasm, the polymerase complex (L protein and the cofactor VP35) initiate transcription of the negative sense template into positive-sense mRNA. The L protein caps and polyadenylates these new monocistronic mRNAs, which are subsequently translated by the host cell machinery. The minor nucleoprotein VP30 is thought to act as a transcription activating factor during these processes (269). In addition to transcribing mRNAs, the RNA polymerase complex also drives the synthesis of complementary anti-genomes (positive sense templates). These serve as templates for the L protein to replicate progeny genomes. The switch from transcription to replication seems dependent on the active translation of the NP protein, which is then recruited along with L, VP35, and VP30 to the anti-genomes to form replicative complexes. The negative sense progeny genomes from these sites are then packaged into new nucleocapsids, which in turn are recruited to lipid raft microdomains at the plasma membrane where they coalesce with the matrix proteins VP24 and VP40. VP40 then drives the viral

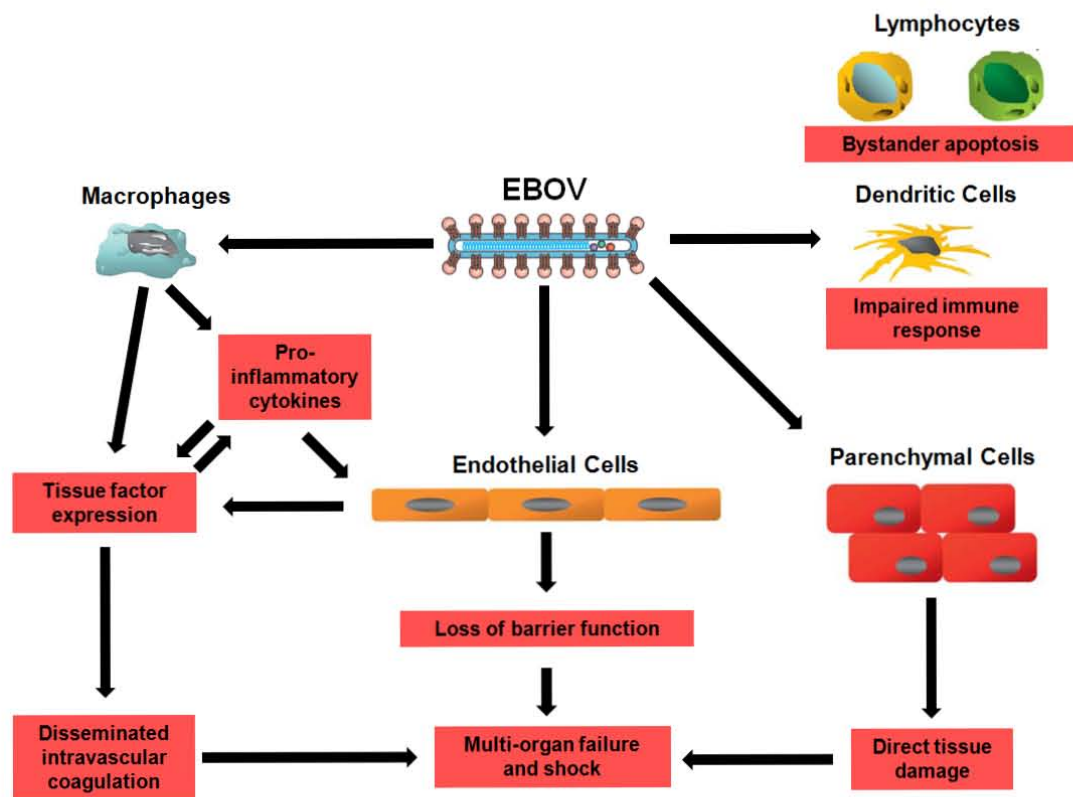
budding, in the process sheathing the virus in a host cell-derived membrane studded with GP (220, 276).

### **Clinical Presentation and Pathogenesis**

Transmission of the disease generally results from contact with bodily fluids from patients or infected animals (e.g. NHPs) (72). Transmission of EBOV through mucosal exposure also occurs experimentally in NHPs and, although it has never been shown in humans, it is thought that contact between contaminated hands and the mucosa of the eye can result in infection. While there is some evidence that airborne transmission is possible (210), this does not seem to be a primary route of transmission, as all outbreaks to date have been contained without the use of airborne-specific protocols.

The disease is characterized by rapid onset, high viremia, vascular dysfunction, and system-wide organ failure (Fig. 1.5) (81, 104). Following an incubation of 4-10 days (113), a high fever develops followed by a constellation of non-specific symptoms including nausea and vomiting. Impaired coagulation is universally observed as the disease progresses leading to extensive hemorrhaging, bruising, and the presence of blood in bodily secretions. By the terminal stages of the disease, very high viral loads are observed ( $>1 \times 10^8$  genome copies per ml of blood), which contributes to intravascular coagulopathy (245, 257). The endothelium is a major target of EBOV infection and contributes to the hemorrhagic character of the disease state. Extensive, disseminated damage to the microvascular endothelium contributes to a crisis-state in the vascular system. This is likely caused by a combination of direct damage

**Figure 1.5. Model of EBOV pathogenesis.** EBOV initially infects macrophages and dendritic cells, and impairs their function. Afterwards, it infects endothelial and parenchymal cells causing direct tissue damage. Furthermore, proinflammatory cytokines are released by infected macrophages, which together with direct infection damage, leads to a loss of endothelial barrier function. Tissue factor is expressed by both infected macrophages and endothelial cells leading to disseminated intravascular coagulation. The combination of widespread endothelial dysfunction, direct tissue damage, and disseminated intravascular coagulation results in multiple organ failure, and ultimately leads to a clinical profile resembling septic shock. Figure adapted from Groseth, et al. *Filoviruses: Ebola, Marburg and Disease*. 2011. John Wiley & Sons, Ltd. (90)



caused by infection as well as an activated inflammatory response in the endothelium. One major pro-inflammatory response pathway that seems to be activated involves TNF- $\alpha$ , which is secreted from infected macrophages/monocytes. Exposure to this cytokine can cause a loss of barrier function in the endothelium. It can also stimulate the release of Tissue Factor (TF), which in turn leads to disseminated intravascular coagulation (DIC). DIC causes an apparent contradiction, a sharp decrease in clotting factors at large in the body combined with a rise in clots forming in the microvasculature (90). Death usually occurs 6-16 days after the onset of symptoms and typically results from shock induced by multiple organ dysfunction syndrome and hypotension (31, 220, 245).

EBOV infection is characterized by its broad cellular tropism (104, 111). Indeed, by the terminal stage of infection, some amount of virus can be detected in almost every tissue type in the body, with the notable exception of B and T lymphocytes and immature monocytes. Macrophages and dendritic cells are usually thought of as early targets of infection. In addition to these, numerous types of parenchymal cell types (e.g. hepatocytes) are directly targeted for infection, causing major tissue damage contributing to eventual organ failure.

EBOV also exhibits an ability to dampen the host immune response. Innate immunity is likely down-regulated due to the fact that innate immune cells, including macrophages and dendritic cells, are among the first cells to be infected *in vivo* (82, 215). In addition, studies have shown that two ebolavirus structural proteins: VP24 and VP35 impair the host interferon response (15). Due

to the extremely rapid progression of the disease, it is commonly thought that most infected subjects are unable to mount an adequate adaptive immune response. Moreover, the aforementioned targeting of dendritic cells, which are crucial for adaptive immunity, likely also dampens the humoral immune response. While not susceptible to direct infection, B and T lymphocytes along with immature monocytes, are subject to “bystander apoptosis” during progression of the disease (26).

### **Vaccines and Therapeutics**

There are currently no approved vaccines or antiviral treatments for EBOV infections. At present, treatment is limited to supportive therapies, primarily attempting to maintain blood volume, respiration, and body temperature as the disease progresses (90). There are, however, multiple ongoing studies examining potential EBOV therapies, including vaccines and antiviral pharmaceuticals.

The first vaccine approach demonstrated to have some protective effect in an NHP model was a combined DNA/recombinant adenoviral regimen, wherein the animal was first directly injected with cDNAs encoding EBOV GP and NP, and then boosted with replication-deficient adenovirus expressing the same proteins (70). While safe and immunogenic in NHPs, this combination vaccine must be administered 32 weeks before challenge to have an effect. Phase I clinical trials have been completed for the DNA component. Interestingly, it was found that when the adenoviral component was solely administered, it could confer total immunity if administered only 4 weeks before challenge. Pre-existing

immunity against the adenoviral component among human populations in Africa, however, may preclude use of this approach. Perhaps, the most promising current vaccine candidate is a replication-competent VSV expressing EBOV GP, which can provide significant protection both pre and post-virus challenge (78-80). Because of this, it was chosen as an emergency intervention for a scientist accidentally exposed to EBOV, who subsequently survived (260).

A promising passive immunotherapy approach has recently been reported, wherein NHPs that had been challenged with EBOV 24 hours previously were subsequently administered a cocktail of three tissue-culture derived monoclonal antibodies that were each neutralizing against EBOV (205). This IgG therapy offered complete survival benefit to all NHPs treated with it. In addition, the therapy could still offer some protection (50%) when administered 2 days post infection.

At present, there is also an absence of approved pharmacological approaches for combating EBOV infection. Treatments such as Ribavirin, interferon- $\alpha$ , heparin, and anti-EBOV immunoglobulins have all shown little if any effect in combating infection (244). One therapy that has shown some efficacy in NHP trials involves the use of the recombinant nematode anticoagulant protein c2, which is believed to work by reducing DIC and the accompanying inflammatory response in infected animals (104). A recent study has also indicated that pre-treatment of target cells with a drug cocktail containing the kinase inhibitors genistein and tyrphostin AG1478 inhibits EBOV infection *in vitro*; although at present the mechanism of inhibition is not understood (125).

Additionally, Abl-specific kinase inhibitors such as nilotinib have been reported to inhibit productive EBOV replication by blocking the egress of particles from infected cells (76). In spite of this research, however, there are still no clinically available antiviral agents that directly block EBOV infection.

### **EBOV Entry Pathway**

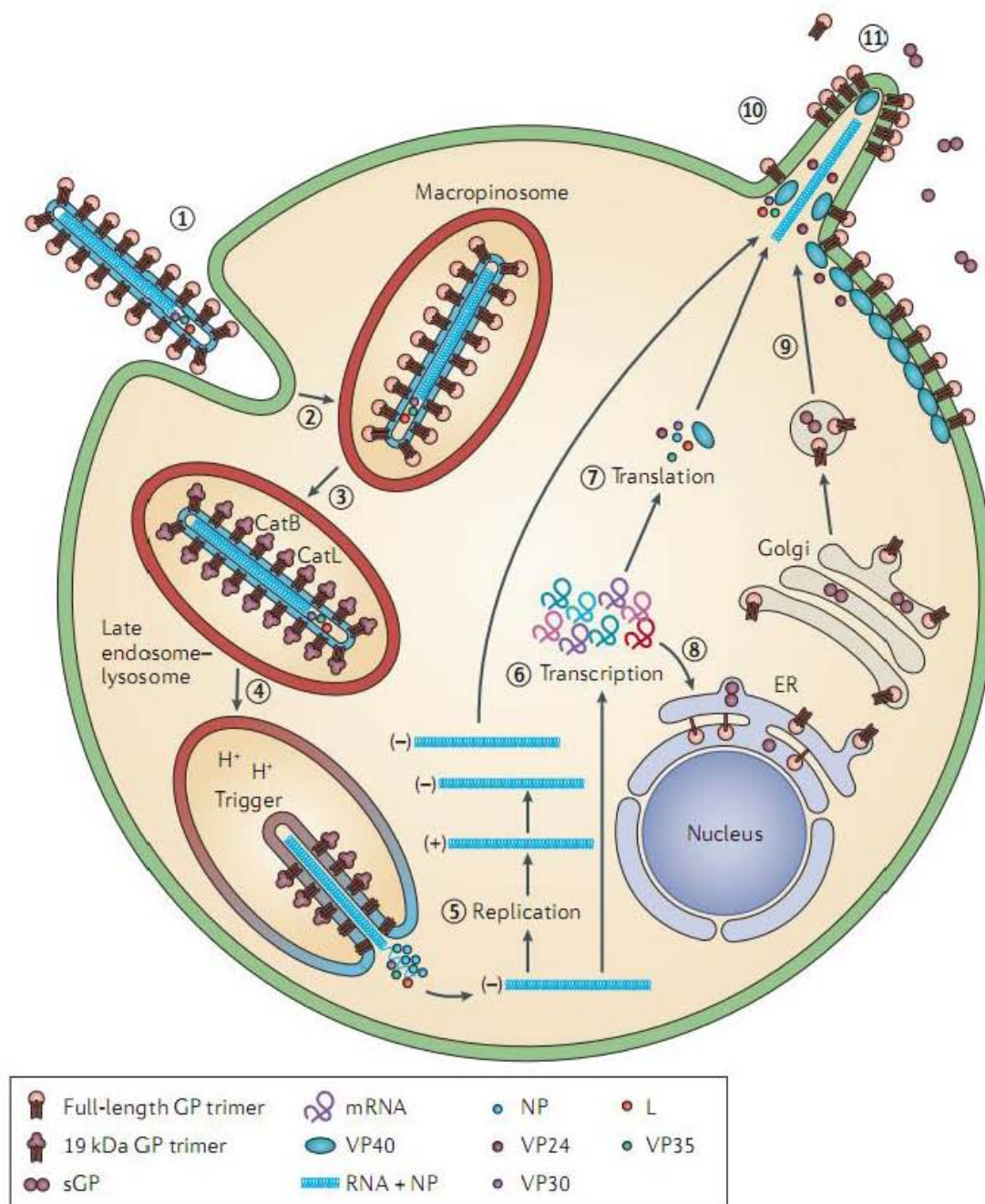
The entry of EBOV into the cytoplasm can be divided into five steps: 1) particle binding to the cell surface, 2) particle internalization into the endocytic pathway, 3) particle trafficking to the fusion compartment, 4) glycoprotein remodeling and fusion triggering, 5) Membrane fusion followed by delivery of the nucleocapsid to the host cell cytoplasm. Once in the cytoplasm, transcription, translation, genome replication, and particle assembly can commence. Figure 1.6 provides an overview of what is currently known about EBOV entry.

### **EBOV Receptor Binding**

Although several cell surface molecules such as DC-SIGN, folate receptor alpha and the tyrosine kinase receptor Axl have been reported to be EBOV entry cofactors (4, 65, 234, 286), none of these factors has been shown to be a universal receptor whose presence is an absolute requirement for virus binding and subsequent infection. Rather, they appear to enhance virus infection.

Significant work has been done by our lab and others to define the region of EBOV GP that is responsible for receptor binding. This is known as the receptor binding region or domain (RBR/RBD) and is located near the N-terminal portion of GP1 (58, 133, 158). Dube, et al. described a highly conserved region between

**Figure 1.6. The life cycle of EBOV.** EBOV binds to attachment factors and receptors on the cell surface (step 1), is internalized via a macropinocytosis-like process (step 2), and is subsequently trafficked to a late endosome/lysosome containing cathepsins B (CatB) and CatL (step 3). These proteases digest GP to a “primed” 19 kDa form, which is then triggered to form a fusion pore between the viral and endosomal membranes (step 4). Following fusion, the viral nucleocapsid is released through the fusion pore into the cytoplasm, where genome replication occurs (step 5). Viral genes are then transcribed (step 6) with the aid of the viral proteins NP, VP35, VP30 and L, and viral mRNAs are then translated (step 7). mRNAs encoding GP are brought to the endoplasmic reticulum (ER) (step 8), where GP is synthesized, modified, and trimerized. GP is further modified in the Golgi and transported to the plasma membrane in secretory vesicles (step 9). At the plasma membrane the RNP and associated viral proteins assemble with the membrane-associated viral proteins (VP24 and VP40, and GP), and new virions bud from the cell surface (step 10). A soluble form of GP (sGP) is also secreted (step 11). Figure obtained with permission from: White, et al. “A new player in the puzzle of filovirus entry”. 2012. *Nat Rev Microbiol* **10**:317-322. (276)



residues 90-149 that consists of a two-stranded  $\beta$ -sheet, the two intra- GP1 disulfide bonds, and four critical Lys residues. Much of this work was accomplished through the use of soluble ectodomain proteins containing the EBOV RBR. In follow-up studies, they used these soluble RBRs to probe cells and learn more about the nature of its putative receptor. They concluded that the RBR receptor is proteinaceous and is up-regulated on the cell surface following cell adhesion (59, 60). They also determined that trafficking of the RBR receptor was bidirectional as loss of adherence resulted in the putative receptor being down-regulated from the cell surface. This trafficking was independent of protein synthesis, and depended on the actin cytoskeleton for receptor internalization from the cell surface, and on microtubules for trafficking to the cell surface. Furthermore, this EBOV RBR binding partner was found to be highly enriched in an intracellular vesicle located near the microtubule organizing center (59). Perhaps most surprising, Dube observed that B and T lymphocytes, which were long thought to be refractory for EBOV infection due to the absence of a receptor, also had this intracellular pool of “receptor” (although they lacked RBR receptor on the cell surface, presumably due to their non-adherent phenotype). Furthermore, lymphocyte cell lines that had been transformed, and therefore had adopted an adherent phenotype, exhibited both RBR binding on the surface and acquired permissivity for EBOV entry and infection ((59), Dube, et al. data not shown). Unfortunately, subsequent efforts to elucidate the identity of this binding partner have not been successful. While the precise identity of this EBOV binding partner remains unknown, the results are nonetheless intriguing.

Recently, T-cell Ig and mucin domain 1 (TIM-1) has been reported as a surface receptor for EBOV in some epithelial cell lines (128). It is present in a number of epithelial cells permissive for EBOV infection, and its depletion correlated with a decrease in infection. Likewise, ectopic expression of TIM-1 increased infectivity in poorly EBOV permissive cell lines. Most importantly, pseudovirions bearing EBOV GP were shown to bind to TIM-1. Inhibitory antibodies against TIM-1 were also shown to block EBOV infection *in vitro*. Intriguingly, potential *in vivo* relevance for TIM-1 in EBOV infection was suggested by the fact that it is expressed on the surface of epithelial cells found in human mucosal surfaces (e.g. trachea, eye conjunctiva). TIM-1 may therefore serve as a receptor for EBOV infection via mucosal routes. Nevertheless, its absence in many other cell types permissive for EBOV infection (e.g. macrophages, dendritic cells) strongly suggests the existence of alternate receptors in other cell types.

### **EBOV Internalization**

The means utilized by EBOV for internalization into host cells has been a subject of controversy, and numerous recent publications have presented conflicting lines of evidence. My own work has also highlighted that much work remains to clarify this aspect of EBOV entry.

An early report suggested caveolae as a possible EBOV internalization route based on the sensitivity of pseudovirion infection and entry, as well as live virus infection, to various cholesterol perturbing agents (16, 65, 286) such as nystatin and  $\beta$ -cyclodextrin, which are known to disrupt the cholesterol-enriched

lipid rafts associated with caveolae formation. In addition, one of these studies reported colocalization of EBOV pseudovirions with caveolin-1, a marker of caveolae (65). A separate study, however, failed to see an increase in EBOV pseudovirion infectivity when caveolin-1 was exogenously expressed in a cell line devoid of the protein (238). A major weakness of these studies was their reliance on infection as a readout; the applied perturbations might reflect post-internalization effects. Disruption of caveolin might also affect lipid rafts, which have been implicated in other endocytic pathways such as clathrin-mediated endocytosis (CME) (161). Yonezawa, et al. reported that EBOV pseudovirion entry into the cytoplasm (using a specific cytoplasmic entry assay; see Chap. II) was also sensitive to actin filament-disrupting agents. The actin cytoskeleton is involved in multiple internalization pathways, but especially in macropinocytosis.

Several recent studies have presented a strong case for macropinocytosis as a major route of EBOV internalization. These studies have used a combination of chemical perturbants, dominant-negative constructs, targeted siRNA, and particle imaging to reach this conclusion (182, 183, 216, 217). Notably, live EBOV infection and VLP internalization/entry were found to be susceptible to 5-(N-Ethyl-N-isopropyl) amiloride (EIPA; an amiloride derivative known to inhibit the membrane ruffling associated with macropinocytosis). Furthermore, key signaling proteins (Rac1, PAK1, Arf6, Arp2) associated with regulation and remodeling of the actin cytoskeleton, and macropinocytosis in particular, were implicated in EBOV entry. In addition, EBOV virus-like particles (VLPs) were shown to colocalize with dextran, a fluid phase marker of

macropinocytosis, during particle entry (182, 216), and were capable of stimulating dextran uptake over basal levels (182, 216). This stimulation appeared independent of the mucin domain of GP, arguing that other regions of the glycoprotein are responsible for mediating this process (182). Nanbo et al. presented the most convincing visual-based evidence for a macropinocytic-like process when they imaged actin-enriched ruffles engulfing fluorescently tagged live EBOV virus. They also claimed that entry of EBOV via a macropinocytic route is dictated by the EBOV glycoprotein since similar entry dynamics were observed when visualizing entry of VSV pseudovirions bearing EBOV GP (Nanbo 2010). Similar to this, Mulherkar et al. used thin-section EM to observe VSV pseudovirions bearing EBOV GP $\Delta$ mucin engaged with MP-like ruffles in Vero cells. Saeed, et al. reported that EBOV entry was dynamin-independent (216). This is not surprising as classical macropinocytosis is described as being dynamin independent. Furthermore, they claimed that the EBOV entry was dependent on the C-terminal binding protein CtBp1. CtBp1 has been proposed to fulfill a scission role for macropinosomes analogous to that played by dynamin in other endocytic processes (142).

I have also obtained some results supporting macropinocytosis as a route of EBOV entry. Specifically, I found that EBOV VLP internalization is inhibited by EIPA and knockdown of PAK1 (Fig. 2.4D and Fig. 1.7A respectively). However, I have also made some observations that are at odds with the conclusion that EBOV enters cells by a classical macropinocytosis pathway. First, I have not observed significant stimulation of dextran uptake by exposure of cells to either

EBOV VLPs or VSV pseudovirus bearing EBOV GP on their surface (Fig. 1.7B). This was despite observing the expected stimulation by both the phorbol ester PMA and human EGF in the same experiments. It should be noted that the groups that reported stimulation of dextran uptake by EBOV reported a low stimulation (<2 fold). This contrasts with the stimulation reported for vaccinia virus (~3 x fold over background) and adenovirus type 3 (~4 x fold) (6, 167). This may suggest that the macropinocytic response induced by EBOV is not as robust as that caused by other viruses. Additionally, in my experiments, siRNA against PAK1 perturbed the internalization and entry of VLPs bearing VSV-G as well as EBOV GPΔ (Fig. 1.7A). Since VSV G-mediated endocytosis is thought to occur through CME (114), this may suggest that some macropinocytosis perturbants also affect other endocytic pathways, perhaps due to the wide ranging dependence of these processes on the actin cytoskeleton. Alternatively, it is possible that both of these VLPs are internalized through macropinocytosis and that the particle itself, as well as the glycoprotein, is involved in the selection of macropinocytosis for EBOV internalization.

To date, two groups have presented evidence ruling out major contributions to EBOV entry by either CME or CE or any dynamin-dependent process (183, 216). Recently, however, other groups and my own work have illustrated this may not be entirely accurate, and that multiple endocytic pathways may be involved and/or an unorthodox form of macropinocytosis may be at play in EBOV entry. Firstly, various perturbants of CME, including chlorpromazine and dominant-negative Eps15, severely block EBOV infection as well as EBOV

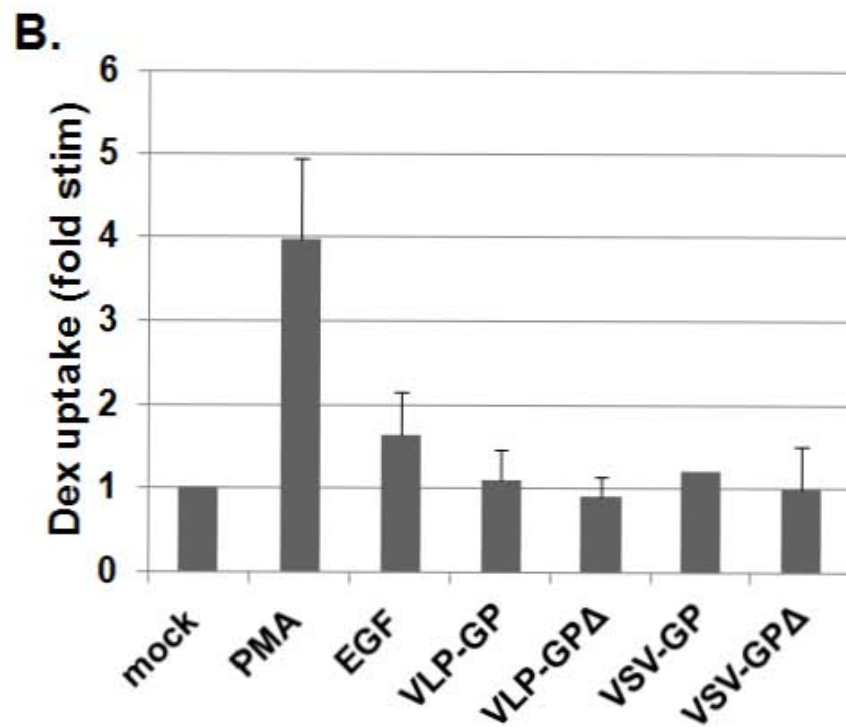
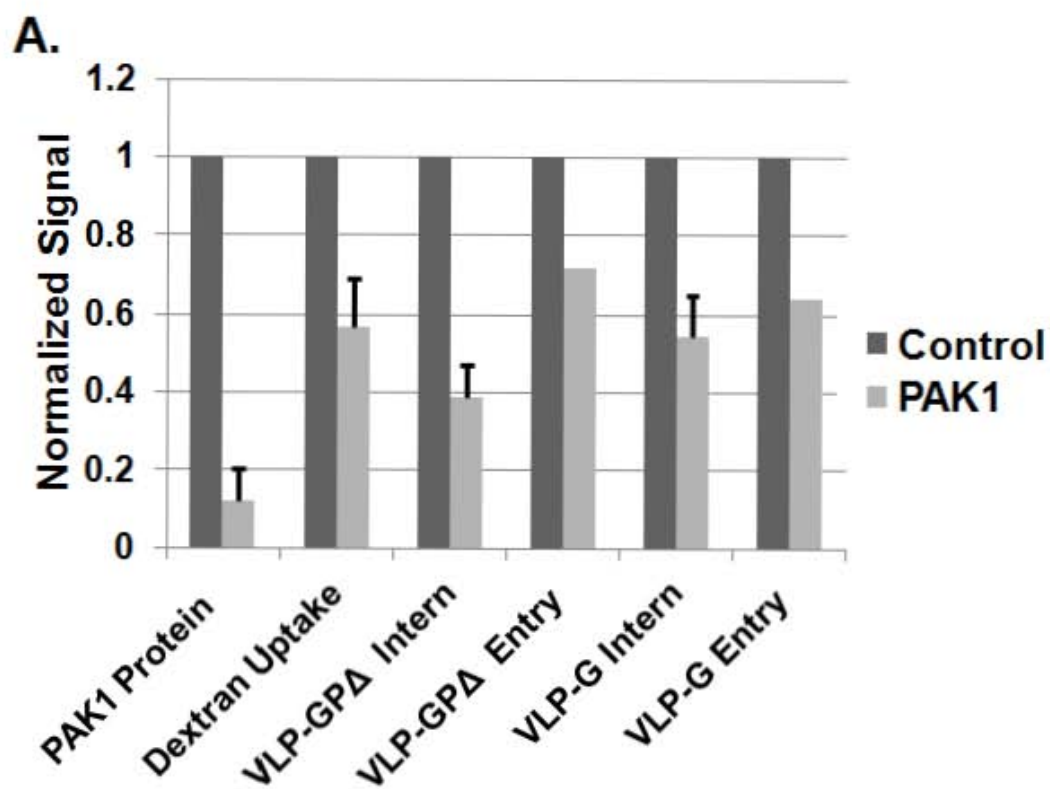
pseudovirion infection (19, 107, 219) (Fig. 1.8). Moreover, I and others have found that EBOV entry is also sensitive to inhibitors of dynamin, including the GTPase inhibitor dynasore (107, 182) (Fig. 1.8).

Hunt, et al. observed that EBOV entry could involve clathrin-mediated endocytosis, caveolar endocytosis, and macropinocytosis, all operating concurrently in the same cell type (107). Of particular interest was their observation that the macropinocytosis associated with EBOV entry was partially dependent on the tyrosine-kinase receptor Axl. Specifically, they observed that macropinocytosis-dependent EBOV entry was dependent on Axl in those cell types possessing Axl on their surface (SNB19, Hff). Axl-independent cells (Vero E6, HEK 293) were still capable of supporting macropinocytosis, but did so independently of Axl. Furthermore, the macropinocytosis supported by Axl appeared distinct from classical macropinocytosis in that it was dynamin dependent. They postulated that the ability to utilize multiple internalization pathways expands the range of cell types that EBOV can enter and infect.

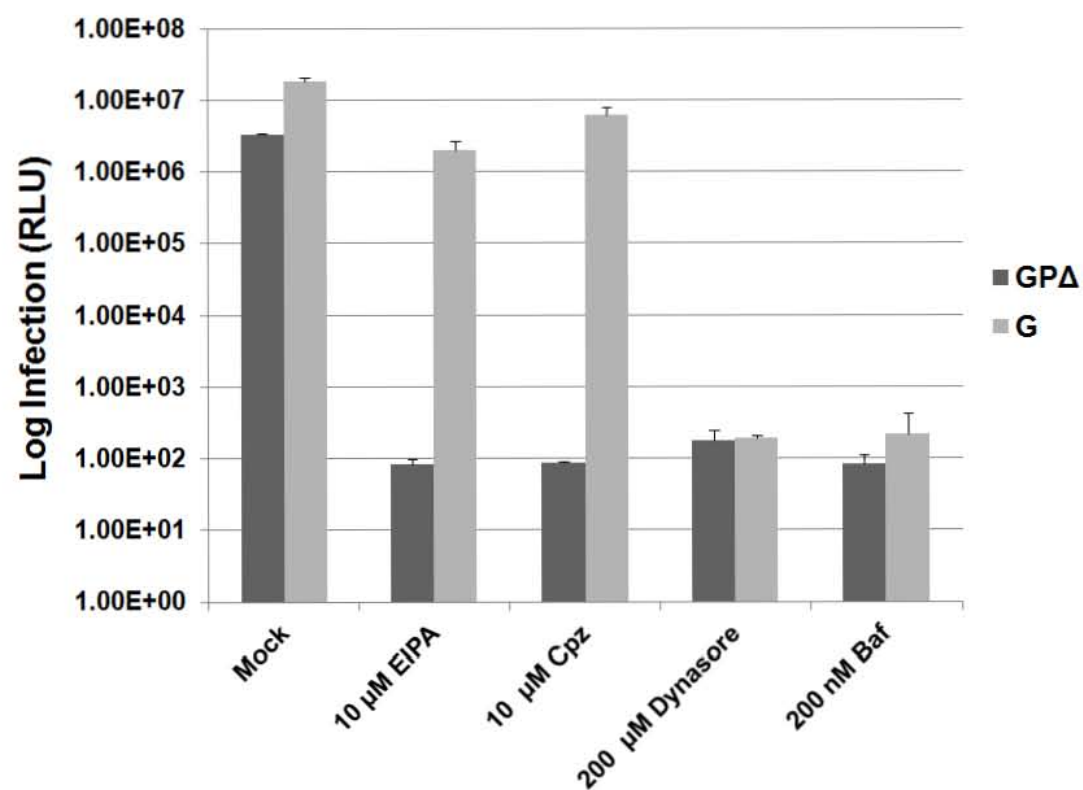
Considering all of the evidence collected to date, it seems likely that EBOV uses multiple internalization strategies, with macropinocytosis or a macropinocytic-like mechanism at play in many cell types. If this is indeed the case, much work remains to be done to understand the intersecting endocytic pathways that may drive EBOV internalization. In addition, the relative contributions of the EBOV GP (and perhaps other elements of the EBOV particle) to internalization needs to be further elucidated.

**Figure 1.7. Assessing macropinocytosis as the means of uptake of EBOV**

**VLPs.** (A) PAK1 levels were knocked down in 293AD cells by transfections with 100 nM anti-PAK1 siRNA at 24 and 48 hr following plating in 60 mm plates. 72 hr after plating, cells were re-plated into 12 well (for western blot) or 48 well plates (for internalization and entry assays). 96 hr post original plating, cells were either lysed for western blot analysis of PAK1 protein expression, pulsed with 10 kDa rhodamine-dextran, or assessed for VLP-GP $\Delta$  and VLP-G internalization and entry (see methods in Chap. II). All values are normalized to control samples (cells treated with non-targeting siRNA) and are averaged across the following number of experiments, each performed in triplicate: PAK1 knockdown (n=5), Dextran uptake (n=6), VLP-GP $\Delta$  intern (n=5), VLP-GP $\Delta$  entry (n=1), VLP-G intern (n=2), and VLP-G entry (n=1). Error bars represent standard deviation. (B) Effects of known stimulants of macropinocytosis and different EBOV VLP and pseudovirion types on dextran uptake were assessed in SNB19 cells that had been serum starved overnight. Cells were warmed at 37°C for 20 min in presence of 400 nM PMA, 200 ng/ml human EGF, or pre-bound VLP/VSV particles. Cells were then pulsed for 10 min with 0.5 mg/ml 10 kDa FITC-dextran. Cells were then stripped of surface dextran for 10 min at 4°C in acid buffer (.05 M NaCl, 0.1 M NaOAc, pH 5.5), lifted, fixed, and analyzed by flow cytometry. Data are normalized to mock (DMSO)-treated cells and are averaged across the following number of experiments, each performed in triplicate: PMA (n=7), EGF (n=4), VLP-GP (n=6), VLP-GP $\Delta$  (n=4), VSV-GP (n=1), VSV-GP $\Delta$  (n=2). Error bars represent standard deviation.



**Figure 1.8. Effects of inhibitors that block macropinocytosis (EIPA), CME (chlorpromazine), or dynamin-dependent endocytosis (dynasore) on EBOV GP-mediated infection.** PCI13 cells (human head and neck carcinoma) were pretreated with indicated amounts of inhibitor in serum free media or mock treated with DMSO for 1 hr prior to infection with VSV-GP $\Delta$  or VSV-G pseudovirions (encoding *Renilla* luciferase). Cells were infected for 8 hr, and then lysed, and analyzed for luciferase activity. Results are from one experiment performed in triplicate. Error bars represent standard deviation. Abbreviations: EIPA, 5-(N-Ethyl-N-isopropyl)amiloride; Cpz, chlorpromazine; Baf, bafilomycin. RLU: relative light units.



## **EBOV Trafficking**

Following initial internalization, EBOV must travel deep into the endocytic pathway. Due to its dependence on low pH and cysteine proteases for successful entry, it is commonly thought that EBOV must transit to a late endosome/lysosome (LE/Lys) for penetration. Dependence on both Rab5 and Rab7 GTPase indicates that the virus likely traffics through the early endosome and is then delivered to a late endosome, if not further (165, 216). Additional evidence for delivery to a LE/Lys comes from the sensitivity of EBOV pseudovirus infection to microtubule destabilizing agents (286), which are critical for transport of maturing endosomes from the cellular periphery to the perinuclear region (92, 137). Direct imaging of labeled EBOV and EBOV VLP/pseudovirus transport showed its initial colocalization with the early endosome marker (EEA1), and later colocalization with the late endosome marker (Rab7) (183, 216). These results suggest that EBOV utilizes a classical early to late endosome transport route in reaching its fusion compartment. Nanbo, et al. argues that the initial acceptor compartment for EBOV is the macropinosome (marked by the sorting nexin SNX5) (183). Macropinosome maturation is thought to parallel endosome maturation in many respects, and can even sequentially acquire some of the same early (EEA1, Rab5) markers, as well as the later marker Rab7 (166). While their terminal fate remains a matter of debate, there is evidence to suggest that they can eventually fuse with late endosomes and lysosomes, thus providing a route for EBOV to reach its probable fusion compartment(s). Since so many of these endosomal markers are shared by both maturing endosomes and

macropinosomes, considerable ambiguity remains concerning the trafficking pathways that are at play in EBOV entry. It may be that the trafficking pathway depends on the internalization mechanism that the virus exploits, as is the case with the arenavirus LCMV (207). Since the evidence suggests that the virus exploits multiple internalization routes, it would follow that it can also follow multiple endocytic routes to reach its final destination.

### **Cathepsin Remodeling and Fusion Triggering**

Due to its sensitivity to lysomotropic agents, low pH has been established as a requirement for ebolavirus infection (249), indicating that the virus must be endocytosed to an intracellular compartment before fusion can occur. It has since been shown, however, that low pH alone is insufficient to cause EBOV GP-mediated fusion. The EBOV GP is unusual among viral glycoproteins in that it requires post-biosynthetic proteolytic modifications in order for cytoplasmic entry and infection to occur. Such post-biosynthetic proteolytic modification has also been identified as a prerequisite for reovirus penetration and infection, but had never been documented for an enveloped virus before (62). Our lab and others showed that GP triggering requires sequential processing by the endosomal cysteine proteases, cathepsins B and L (40, 227, 281). EBOV GP starts off as a 130 kDa protein and its priming appears to occur in two discrete steps (Fig. 1.9A). First, cathepsin L removes the mucin domain and glycan cap, leaving a 20 kDa intermediate. Next, cathepsin B further reduces the protein to 19 kDa. Optimal enzymatic activity of these cysteine proteases is, therefore, critical for the proper priming of EBOV GP, and subsequent fusion and infection.

Intriguingly, this enzymatic activity appears to be dependent on the presence of  $\alpha 5\beta 1$  integrin on the cell surface (228). Cells lacking this integrin were not permissive to infection by EBOV pseudovirions ((228), (see Appendix).

Subsequent analyses, that I participated in, revealed that this defect in infection was not due to impaired particle binding or internalization, but was linked to lower cathepsin B/L activity. This defect was not due to mistrafficking of cathepsin protein to late endosomes and lysosomes, but rather was a consequence of impaired processing of the cathepsins to their enzymatically-active double chain forms. This defect, in turn, led to impaired GP priming and a block in the entry of EBOV pseudovirions. This entry block could be overcome by *in vitro* pre-priming of GP on the pseudovirions to the 19 kDa form. Likewise, exogenous expression of  $\alpha 5\beta 1$  in cells lacking this integrin also restored both cathepsin activity and EBOV-mediated entry and infection.

Our lab previously proposed that 19 kDa GP is the fusion-competent form of GP (227). In support of this model, recent evidence collected by our lab indicates that the 19 kDa form can be triggered to engage target membrane and induce fusion ((28), White lab, unpublished data). Although low pH alone is not sufficient to trigger the fusion activity of 19 kDa GP, it supports fusion triggering in at least two ways: 1) by maintaining optimal cathepsin B and L activities, and 2) apparently by inducing changes in 19 kDa GP that renders it sensitive to a fusion trigger.

## Potential Triggering Conditions

Our lab previously tested a number of potential physiological EBOV triggering factors by using an *in vitro* liposome binding assay with a 19 kDa-primed soluble form of EBOV GP (28). This assay recapitulates the initial membrane embedding step associated with the early stages of fusion. Additional cleavage by cathepsin L, earlier theorized as a potential trigger (40), failed to produce liposome binding. Changes in calcium levels, thought to be involved in the penetration of rotavirus (41), also failed to trigger liposome binding. The effect of target membrane lipid composition was also tested. Lysobisphosphatidic acid (LBPA) is an anionic lipid found in late endosomes, that was shown to be critical for the fusion of Dengue virus (287); however, no effect on EBOV GP binding to membrane was observed. The only condition tested in which liposome association was seen at 37°C was a combination of low pH and a low level of a disulfide-bond reducing agent (28). The combination of low pH and reducing conditions also inactivated EBOV pseudovirions for subsequent infection, presumably by irreversibly triggering GP. Preliminary data, that I helped obtain, also suggests that the combined action of low pH and reduction suffice for 19 kDa GP to mediate fusion with liposomes and with the plasma membrane of target cells (White lab, unpublished data). The exact *in vivo* relevance of these findings remains to be established. Potential cellular factors providing endosomal reductive capacity include thiol isomerases and/or the reducing potential of the LE/Lys itself (9, 199). Alternatively, reduction might not be the *bona fide* trigger, and may only be mimicking the effects of the physiological trigger(s).

### **Role of NPC1 in EBOV Entry**

The Niemann-Pick C1 protein (NPC1) was recently discovered to be indispensable for EBOV entry (35, 46, 94). This was achieved from a human genome-wide screen of a mutagenized haploid cell line that was infected with replication-competent VSV bearing the EBOV GP (instead of its own G protein). All subunits of the HOPS complex, a group of proteins required for endosomal transport were also identified as critical factors for EBOV GP-mediated infection. NPC1, however, was the most significant factor identified. NPC1 is a 13 transmembrane domain containing integral membrane protein found in the limiting membranes of late endosomes and lysosomes (LE/Lys). NPC1 has three large loops (A, C, I) that protrude into the endosomal lumen. It is associated with cholesterol transport from the LE/lys to other cellular membranes (e.g. plasma membrane and ER), and together with its partner protein, NPC2, is vital for maintaining cellular cholesterol homeostasis (109). NPC1 may also be involved in the transport of other lipids (e.g. sphingolipids), as well as lipid derivatives (e.g. sphingosine) (147, 148, 231). Interestingly, both Cote, et al. and Carette, et al. found that the NPC1 requirement for EBOV infection was independent of the role of NPC1 in cholesterol transport; NPC1 proteins with mutations known to cause a defect in cholesterol egress from LE/Lys were, nonetheless, able to support EBOV infection. Similarly, loss of NPC2 did not inhibit EBOV pseudovirion infection, emphasizing the primacy of a cholesterol-independent role for NPC1. The essential importance of NPC1 for EBOV infection was further highlighted by its ability to confer infection to a reptilian cell line that is completely refractory to

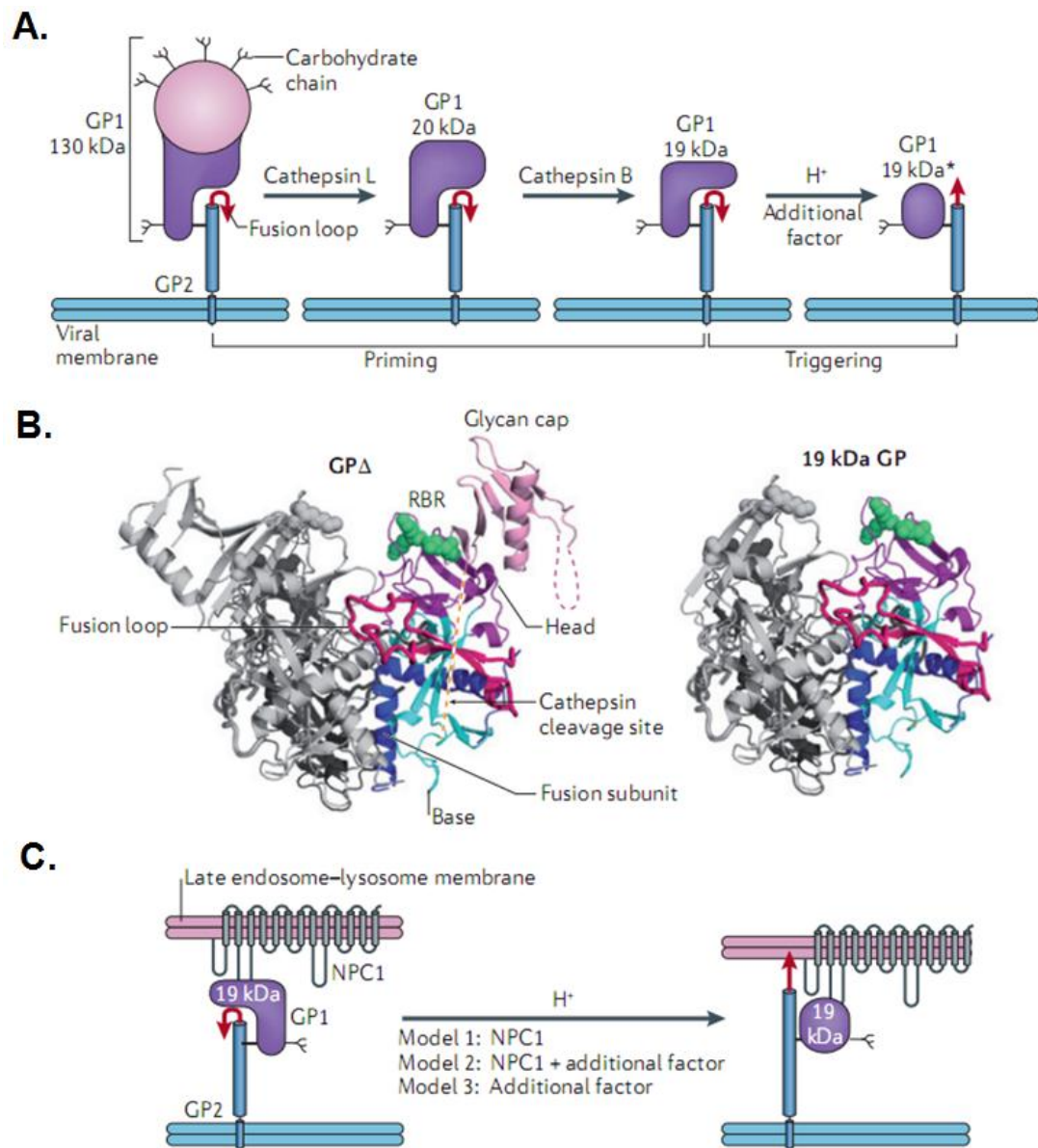
filovirus infection (and infection by all filoviruses) (171), suggesting that NPC1 may play a key role in determining the tropism of EBOV infection.

NPC1 was shown to cause a block in the entry of EBOV pseudovirions, suggesting a failure of GP fusion triggering (35). Furthermore, pseudovirions that had been pre-cleaved *in vitro* to the primed form were also incapable of infecting NPC1 null cells (35). NPC1 was shown to bind to the primed form of GP, but not the uncleaved form of GP. This interaction is critical for supporting EBOV entry, and its blockage by certain piperazine compounds was shown to robustly block EBOV entry and infection (46). The region of NPC1 critical for binding to primed GP is the second luminal, or C, loop. In fact, a soluble form of the C-loop was shown to bind to primed EBOV GP (171). Additionally, a membrane-bound form of the C-loop conferred infection to an NPC1 deficient cell line, albeit with considerably less efficiency than the full length NPC1 protein. The GP site critical for binding to NPC1 appears to lie within the EBOV RBR (171). Since the RBR is exposed upon removal of the mucin domain and glycan cap during cathepsin-driven priming, the RBR would represent a reasonable site for NPC1 to bind (Fig. 1.9B). Numerous residues that our lab and others previously identified as severely deleterious for EBOV GP-mediated infection were subsequently shown to be of critical importance for interacting with NPC1. Additionally, the impaired infectivity caused by these mutations could be largely overcome by wildtype NPC1 overexpression. Taken together, these results make a strong argument for a key role for NPC1 in mediating EBOV entry into the host cytoplasm.

Miller et al., however, also noted (data not shown) that pre-cleaved EBOV

**Figure 1.9. EBOV GP priming and triggering: possible roles of NPC1. (A)**

Cathepsin L cleaves EBOV glycoprotein 1 (GP1), removing the mucin-like domain and glycan cap (pink) and generating 20 kDa GP, which is subsequently cleaved to the primed 19 kDa state by cathepsin B. Primed 19 kDa GP requires low pH and an unknown additional factor to trigger rearrangements (indicated by an asterisk) to begin the fusion cascade. (B) Ribbon diagram of GP $\Delta$  (GP lacking the mucin-like domain) and a model for 19 kDa GP (right). The model for cathepsin-primed GP (right) assumes that no conformational changes occur post cathepsin-cleavage. A monomer of each trimer is shown in color, while the other two are in grey. Green spheres depict important lysine residues in the receptor-binding region (RBR); mutations at these sites impair binding of primed GP to the C-loop of Niemann–Pick C1 (NPC1) and GP-mediated infection. (C) We propose three possible roles for NPC1 (following its binding to primed GP) in triggering EBOV fusion. Model 1; NPC1 is the additional factor, which together with low pH can trigger the conformational changes that enable membrane fusion. Model 2; while NPC1 binding to primed GP is required, it is not sufficient to trigger GP and one or more additional factors is required. Model 3; NPC1 binds primed GP, bringing the virus close to the limiting endosomal membrane, but cannot induce conformational changes in GP, necessitating the involvement of additional factors to trigger fusion. See White, et al. 2012 (White 2012) for further details. Figure obtained with permission from: White, et al. “A new player in the puzzle of filovirus entry”. 2012. *Nat Rev Microbiol* **10**:317-322. (276)



pseudovirions could not be triggered to fuse directly to the plasma membrane of cells displaying the C-loop of NPC1 on the surface, even upon exposure to low pH (171). We have also found that low pH does not suffice to induce fusion of VLPs bound to cells overexpressing NPC1 on their surface (White lab, unpublished data). These findings argue that low pH and NPC1 binding are not sufficient to activate primed GP for fusion. There must, therefore, be an additional triggering factor(s) at play (Fig. 1.9C).

### **Research Goals and Significance**

The primary goals of my thesis research were to further clarify late stage events during EBOV entry into the cell, and to identify inhibitors that block EBOV entry. To this end, I first developed a multi-purpose EBOV VLP system that enabled me to interrogate both the internalization of these particles as well as their cytoplasmic delivery (Chap.II). In addition to being morphologically similar to EBOV, these particles recapitulated all of the known entry requirements for EBOV that have been identified to date, thus confirming their fitness as EBOV surrogates. These multi-purpose VLPs enabled me to characterize the kinetics of EBOV VLP internalization and cytoplasmic entry, and to determine if various perturbants were acting at the level of internalization or were inhibiting EBOV entry further downstream. Most recently, we have used these multi-purpose VLPs in direct fusion studies interrogating the triggering requirements of EBOV GP (White lab, unpublished data).

In chapter III, I contributed to a study screening for potential pharmacological inhibitors of EBOV entry and infection. I used my multi-purpose

VLP system to identify and elucidate the mechanism of action for two compounds, clomiphene and toremiphene. I determined that these compounds were acting at a post internalization step and were blocking EBOV GP-mediated cytoplasmic entry without affecting either endosomal acidification or cathepsin activity levels in LE/Lys. While both of these drugs are canonically known as selective estrogen receptor modulators (SERMs), we showed that their mechanism of action against EBOV was independent of the estrogen receptor.

In a concurrent study, I further attempted to probe the mechanism by which one of these drugs, clomiphene, was acting against EBOV entry. Since clomiphene is also known as an inhibitor of sterol synthesis, I interrogated a set of sterol synthesis inhibitors to see if sterol biosynthesis is required for EBOV entry (Chap. IV). All members of this set of inhibitors had been shown to block infection by Hepatitis C virus (HCV). Interestingly, and unlike the situation for HCV replication, only a subset of these compounds blocked EBOV infection, suggesting a mechanism of action independent of cholesterol synthesis. Furthermore, I found that several of these compounds blocked EBOV infection at a point prior to cytoplasmic entry. Moreover, all the compounds that did robustly block EBOV entry were structurally similar cationic amphiphiles. Significantly, these cationic amphiphiles all induced cholesterol accumulation in LE/Lys, a hallmark of Niemann Pick C1 disease. Furthermore, the efficacy of these cationic amphiphiles against EBOV GP-mediated infection was significantly weakened by overexpression of NPC1, suggesting that these cationic amphiphiles are acting through an NPC1-dependent pathway. While the binding of NPC1 with cathepsin

primed EBOV GP is known to be a requirement for successful EBOV entry, these compounds did not interfere with this interaction. These latter results suggest an additional role for NPC1 in EBOV entry beyond binding to primed GP.

Two of the compounds focused on in chapter III, clomiphene and toremiphene, showed efficacy against live EBOV infection in a mouse model. These drugs are currently being tested for their effectiveness in NHPs. Beyond this however, we have identified cationic amphiphiles as a promising class of drugs for further testing as therapeutic tools for combating EBOV infection. Since many of these drugs are already FDA-approved and well tolerated in humans, their potential for clinical repurposing is high. More work is needed, however, to see if these drugs or similar ones represent viable clinical tools to combat EBOV infection.

Overall, much remains unknown about EBOV entry, particularly with regards to the triggering events that happen to the primed GP immediately prior to the onset of fusion. My thesis work has expanded on the role of NPC1 in EBOV entry and strongly suggests that NPC1 plays at least two roles in EBOV entry, and that an additional endosomal factor(s), beyond low pH, cathepsins, and NPC1 is required to trigger EBOV fusion. Lastly, I have helped to validate a class of small molecules as potential EBOV therapeutics; the shared chemical properties of these inhibitors should be useful as a guide for future EBOV and filovirus antiviral drug design.

## **Chapter II: Ebolavirus VLPs for Studies of Virus Entry**

## Introduction

To aid studies of EBOV entry, I developed an EBOV virus-like particle (VLP) system capable of monitoring all stages of EBOV entry: binding, internalization, trafficking, fusion, and entry into the cytoplasm of the target cell. I have focused on using these “multi-purpose VLPs” to study particle internalization and cytoplasmic delivery. My scheme is an extension of an established method (116, 188) of co-transfecting producer cells with plasmids encoding the matrix protein (VP40) and the glycoprotein (GP) from EBOV. By supplementing the transfection mixture with EBOV VP40 tagged with  $\beta$ -lactamase (157, 259), Rong and coworkers developed EBOV VLPs that can be used to quantitate particle entry into the cytoplasm. If the particles fuse (with an endosomal membrane),  $\beta$ -lactamase-VP40 enters the cytoplasm where it can cleave a  $\beta$ -lactamase substrate (36). I developed an additional tagged version of VP40, with mCherry fused to its N-terminus. I added this mCherry VP40 plasmid to the transfection mixture, thus producing dually-tagged VLPs that can be used to monitor specific steps of VLP entry. For example, I developed an assay to measure VLP internalization from the cell surface (based on mCherry-VP40) and entry into the cytoplasm (based on  $\beta$  lactamase-VP40). Both assays are quantitated by flow cytometry. I have made EBOV VLPs with full length GP, GP $\Delta$ mucin (GP $\Delta$ ), and a pre-primed form of GP, 19 kDa GP. In addition, I have produced VLPs with foreign glycoproteins, such as VSV-G and LCMV GP to serve as controls. Here, I demonstrate the validity of using these particles as surrogates for studying EBOV entry.

## Materials and Methods

**Cells.** 293T HEK cells were maintained as described in chapters III and IV. BSC-1 cells (ATTC CCL-26) were maintained in DMEM (Gibco Invitrogen) supplemented with 10% fetal bovine serum (FBS, Gibco Invitrogen), 1% antibiotic/antimycotic, 1% L-Glutamine, and 1% sodium pyruvate. SNB19 human glioblastoma cells (ATCC: CRL-2219) were maintained in DMEM supplemented with 10% FBS, 1% antibiotic/ antimycotic, 1% L-Glutamine, and 1% Sodium Pyruvate. The parental CHO cell line 25RA and CT43, a mutant 25RA line with defective, truncated NPC1, were maintained as previously described (47). VLP internalization and entry experiments were conducted as described below, except that samples were only incubated at 37°C for indicated time points.

**Virus-like particle (VLP) preparation.** VLPs were generated by transfecting 293T cells with plasmids encoding  $\beta$ -lactamase-VP40, mCherry-VP40, VP40, and a viral glycoprotein (EBOV GP $\Delta$  [Zaire-Mayinga], VSV-G, or LCMV GP) at a ratio of 9:9:4:6 respectively using Polyethylenimine (PolySciences Inc). Following transfection, VLPs were harvested at 24 hr and 48 hr, cleared of debris twice at 1500 x g, 4°C, and then pelleted in an SW28 tube through 20% sucrose-virus resuspension buffer (VRB; 130 mM NaCl, 20 mM HEPES, pH 7.4) at 112,398 x g (25,000 rpm) at 4°C. VLPs were resuspended in 10% sucrose-VRB overnight, and frozen at -80°C for long term storage. For examination by immunofluorescence, VLPs were adsorbed to poly-L lysine coated coverslips, fixed with 4% paraformaldehyde, probed with an anti-GP monoclonal antibody (gift of Lisa Hensley, USAMRIID), followed by an anti-mouse AlexaFluor 488

antibody (Molecular Probes), and then imaged on a Nikon Eclipse TE2000 laser-scanning confocal fluorescent microscope, equipped with 488 and 543 nm lasers and appropriate filters. Negative stain electron microscopy was conducted with the assistance of the UVA Advanced Microscopy Core; VLPs were adsorbed to FormVar/carbon coated grids, stained with 2% PTA (pH 7.0), and imaged on a JEOL 1230 transmission electron microscope. Note that aside from figure 2.5B, all VLP analysis and experimentation done in this and subsequent chapters was done with VLPs that had undergone a single pellet through 20% sucrose-VRB.

**EBOV entry and internalization assays.** The day before each experiment, 100,000 SNB19 cells were seeded in 48-well plates. All internalization and entry assays were conducted in serum-free Optimem I media (Gibco Invitrogen). For inhibitor studies, SNB19 cells were pretreated with either DMSO (mock) or the indicated concentration of inhibitor for 1 hr at 37°C, and inhibitors were maintained in all following steps. Cells were then pre-chilled to 4°C for 15 min and VLPs were bound to cells by spinfection at 250 x g for 1 hr at 4°C. Following 2 washes (with inhibitor where appropriate), cells were warmed to 37°C for 1 or 3 hr for internalization and entry assays, respectively. Cells were then returned to 4°C. Internalization samples were treated with 0.5% Trypsin-EDTA (Gibco Invitrogen) for 30 min at 4°C to strip surface associated particles. Cells were then lifted by pipetting, washed, and fixed for flow cytometry on an LSR Fortessa cytometer (Becton Dickinson). Data are presented as percent of population with mCherry fluorescent signal. Cells exposed to VLPs, but not removed from cold block served as baseline for compensation gating. Entry samples were

processed as in internalization assay, but were incubated for 3 hr at 37°C following the spinfection. After this incubation, entry samples were washed once with loading buffer (phenol red free DMEM supplemented with 2 mM L-glutamine, 2.5  $\mu$ M probenecid, 25 mM HEPES, and 200 nM Bafilomycin). Cells were then incubated in the dark for 1 hr in loading buffer supplemented with 1  $\mu$ M of the  $\beta$ -lactamase substrate CCF2-AM (Invitrogen). After incubation, cells were washed once more with loading buffer before being incubated in 10% FBS-loading buffer overnight. The following day, cells were lifted with trypsin, fixed, and analyzed on a FACSCaliber flow cytometer. Cells were monitored for blue (447 nm) fluorescence. Cells treated with only CCF2-AM substrate were used as a baseline for compensation gating. All flow cytometric data was analyzed with FlowJo software.

**Purification of VLP-GPA for thermolysin cleavage.** VLPs were prepared and pelleted through sucrose as described above. VLPs were further purified on a 7-step nycodenz gradient prepared in an SW55 tube with the following steps: 2.5%, 5%, 7.5%, 10%, 15%, 20%, and 30% (270). All gradient steps were 490  $\mu$ l except the 30% layer, which was 730  $\mu$ l. All nycodenz steps were made with VRB. 490  $\mu$ l of VLPs were then layered on top of this gradient and centrifuged to equilibrium for 13 min at 24,271 x g (16,000 rpm) at 4°C. 1.5 ml fractions were then harvested by hand from the top of each gradient, with the second fraction (containing filamentous particles) being kept for further processing. The pooled second fractions were then re-pelleted at 96,808 x g (28,000 rpm) for 2 hr at 4°C

in an SW41 rotor. Final pellets were resuspended O/N in 250  $\mu$ l 10% sucrose-VRB. This procedure was designed to enrich for filamentous VLPs.

**Thermolysin cleavage of VLP-GP $\Delta$  to VLP-19 kDa GP.** Nycodenz-purified VLPs were then cleaved with 0.1 mg/ml thermolysin for 1 hr at 37°C in HEPES-MES buffer (130 mM NaCl, 20 mM HEPES, 20 mM MES, 4 mM CaCl<sub>2</sub>; pH 7.4). Mock-cleaved samples were exposed to the same conditions, but without thermolysin. Protease activity was quenched with 500  $\mu$ M phosphoramidon and samples were stored at 4°C until the experiment 3 days later. GP $\Delta$  cleavage was assessed by SDS-PAGE and western blotting with a mouse mAb against EBOV GP (191).

## Results

**Preparation and characterization of EBOV VLPs.** To develop these multi-purpose VLPs, I tested transfections using twelve different ratios of cDNA encoding unlabeled VP40,  $\beta$ -lactamase-VP40 (Blam-VP40), mCherry-VP40, and EBOV GP (full length and  $\Delta$ mucin; Fig. 2.1A). First, the particles were characterized by western blotting for VP40 and GP. As seen in figure 2.1B, both VP40 and GP $\Delta$  incorporated well into particles. Full length GP does not appear to incorporate as well as the mucin domain deleted form, although this might be due (in part) to full length GP not being as reactive with our GP antibody. Since both Blam-VP40 and mCherry-VP40 are approximately 69 kDa, they run close together on the western blot. Next, I assessed the entry fitness of these VLPs by the  $\beta$ -lactamase entry assay (Fig. 2.1C). Consistent with the observations from the western blots and on studies with VSV pseudovirions (White lab, unpublished

data), particles with full length GP on their surface showed less entry signal than particles with GPΔ. Overall, the best ratio of producer plasmids appeared to be 9:9:4:6 (mCherry- VP40: Blam-VP40: VP40: glycoprotein (GP, GPΔ for foreign GP), and this is what I elected to use for the VLP preparations used for the experiments detailed in this thesis.

Particles were also tested by fluorescence microscopy for the degree to which the mCherry-VP40 labeled particles incorporated EBOV GPΔ. There was a high degree of colocalization of VP40 and GP, the latter being detected by indirect immuno-fluorescence with a mAb to GP (Fig. 2.1D, 2.1E, and 2.2A). These EBOV GPΔ VLPs were also examined by negative-stain electron microscopy to assess their morphology. As seen in figures 2.2B and 2.3, these particles were filamentous, albeit pleomorphic. Although their diameters were a relatively consistent ~70 nm (~50 nm nucleocapsid with 10 nm projecting GP spikes on both sides) their lengths were highly variable, ranging from 290 to 2429 nm. From a sample population of 32 particles, the mean length was 972 +/- 538 nm, and the median length was 833 nm. These observations are consistent with studies made on EBOV and EBOV VLPs prepared with only VP40 and GP (17, 116). In studies made on fixed EBOV samples, Beniac, et al. observed a pleomorphic population with approximately half of the particles being 1 μm in length (17).

I continued my characterization of dually-tagged EBOV VLPs using ones bearing EBOV GPΔ, due to the better incorporation/detection of GPΔ in particles, higher entry efficiency of the resultant particles, and because the mucin domain

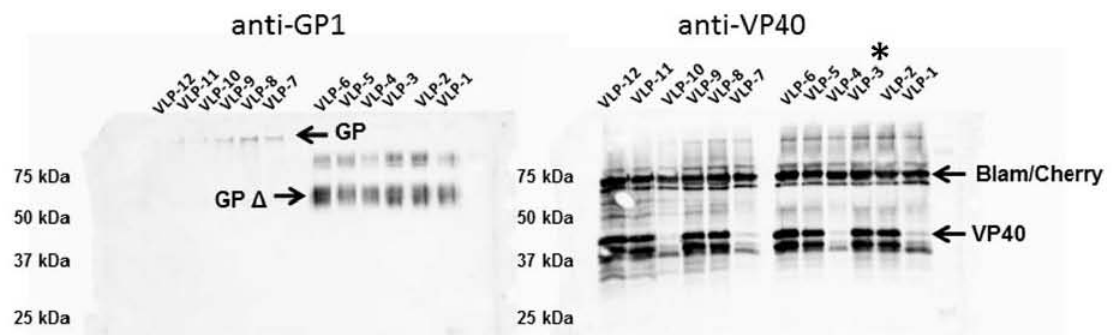
**Figure 2.1. Optimization and characterization of multi-purpose VLPs.** (A) Different VLP formulations tested. (B) Western blot of VLPs probed with anti-GP and anti-VP40 antibodies. Blam-VP40 and mCherry-VP40 have the same approximate molecular weight (and therefore migrate together). VP40 (tagged or untagged) runs as a doublet. (C) VLP entry tested on BSC-1 cells. (D) VLP-GP $\Delta$  particles (red) were adsorbed to poly-lysine-coated coverslips, fixed, and then stained for GP with an anti-GP monoclonal antibody followed by an anti-mouse IgG antibody (green). Particles were imaged on a confocal laser microscope at 1000x magnification. A representative field is shown. (E) Colocalization of mCherry-VP40 and GP. Three fields of each type of VLP (stained as in (D)) were analyzed by ImageJ using the JACoP plugin. Mander's colocalization coefficients were generated and then averaged. In all panels, error bars represent standard deviation. Asterisks denote optimal VLP type chosen for use in all subsequent experiments.

**A**

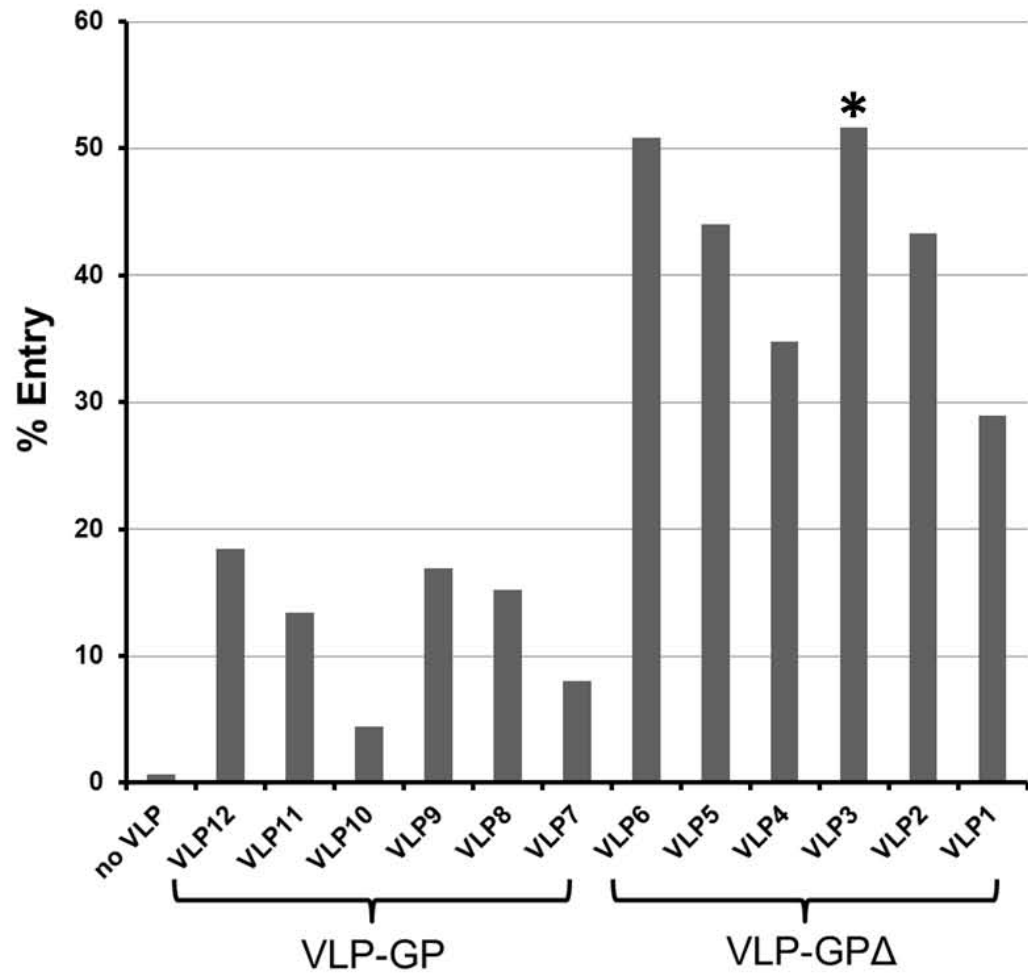
	Cherry- VP40	Blam- VP40	VP40	GP
VLP-12	4.0 µg	4.0 µg	2 µg	2 µg
VLP-11	4.0 µg	4.0 µg	1 µg	2 µg
VLP-10	4.0 µg	4.0 µg	0	2 µg
VLP-9	4.5 µg	4.5 µg	2 µg	3 µg
VLP-8	4.5 µg	4.5 µg	1 µg	3 µg
VLP-7	4.5 µg	4.5 µg	0 µg	3 µg

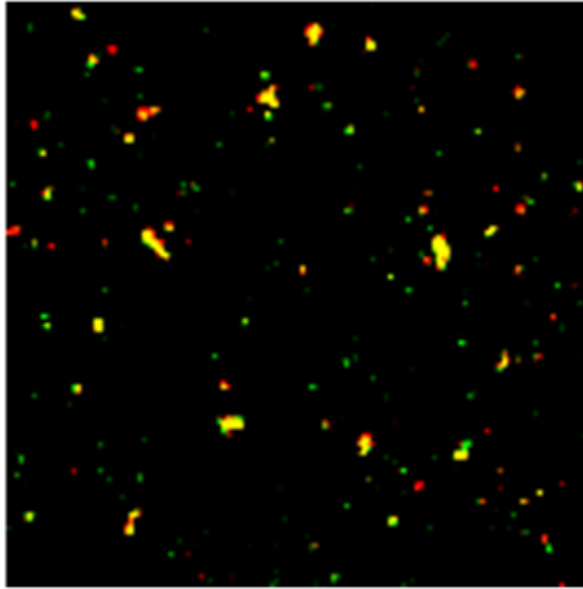
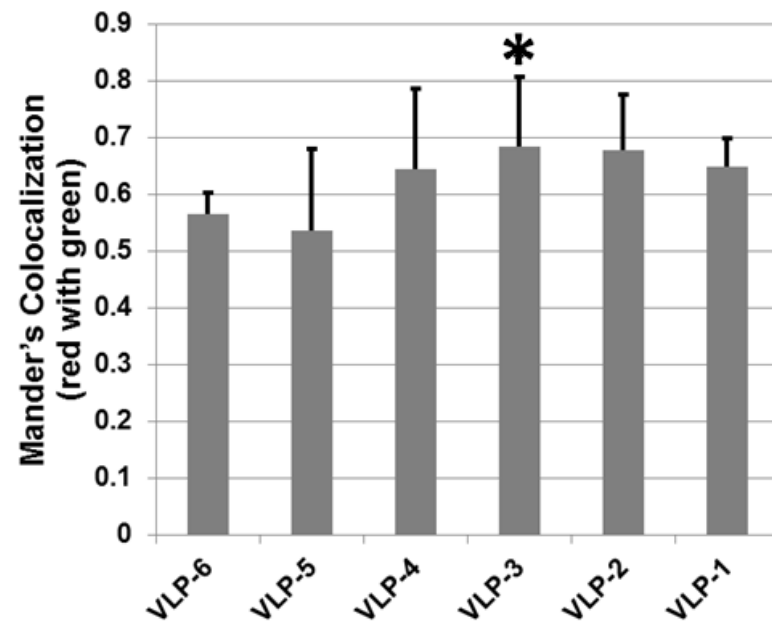
\*

	Cherry- VP40	Blam- VP40	VP40	GPΔ
VLP-6	4.0 µg	4.0 µg	2 µg	2 µg
VLP-5	4.0 µg	4.0 µg	1 µg	2 µg
VLP-4	4.0 µg	4.0 µg	0	2 µg
VLP-3	4.5 µg	4.5 µg	2 µg	3 µg
VLP-2	4.5 µg	4.5 µg	1 µg	3 µg
VLP-1	4.5 µg	4.5 µg	0 µg	3 µg

**B**

C



**D****E**

has been shown to be dispensable for EBOV-mediated infection in cell culture (40, 112, 227).

### **Response of VLPs to known inhibitors of EBOV internalization and/or**

**entry.** To test the utility of multi-purpose VLPs, I assessed the effects of chemical inhibitors (as well as a GP mutant) that are known to or are strongly predicted to impair either GP-mediated entry into the cytoplasm (Fig. 2.4A and B) or GP-mediated internalization from the cell surface (Fig. 2.4C and D). Priming of EBOV GP by endosomal cathepsins, a prerequisite for GP-mediated infection, is potentially inhibited by E64d, a membrane permeable cysteine protease inhibitor (40, 58, 117, 227). E64d should, therefore, block GP-mediated entry without affecting GP-mediated internalization. As seen in figure 2.4A, E64d had the predicted effect. Similarly, a well-characterized point mutation (F535R) in the fusion loop of EBOV GP (28, 110) should impede GP-mediated entry into the cytoplasm, but have no effect on GP-mediated internalization. As predicted, VLPs bearing F535R GP $\Delta$  were fully competent to mediate particle internalization, but were completely blocked for cytoplasmic entry (Fig. 2.4B). Treatment of cells with sodium azide/2-Deoxy-D-glucose (NaN<sub>3</sub>/2-DOG) blocks all modes of internalization from the cell surface (212). As expected, this treatment potentially blocked VLP internalization (Fig. 2.4C). The macropinocytosis inhibitor 5-(N-Ethyl-N-isopropyl) amiloride (EIPA) inhibits GP-mediated infection by blocking virus internalization (2, 107, 182, 183, 216). Consistently, EIPA blocked the internalization, and hence entry, of dually-tagged VLPs (Fig. 2.4D). My analysis revealed, however, that EIPA has a stronger effect on the entry, than

on the internalization, of VLPs (Fig. 2.4D). This finding, recapitulated with VLPs coated with full length GP (data not shown), indicates that EIPA not only inhibits GP-mediated internalization, but also likely inhibits a downstream post-internalization step of GP-mediated entry.

### **Time courses of internalization and entry mediated by EBOV GP $\Delta$ and 19**

**kDa GP.** We next analyzed the time courses of internalization and entry of VLPs bearing EBOV GP $\Delta$  and compared them with the equivalent time courses for VLPs bearing VSV-G. As seen in figure 2.5A VLPs bearing VSV-G are rapidly internalized from the cell surface and enter the cytoplasm soon thereafter. This rapid entry time course reflects the relatively high pH dependence for VSV-G mediated fusion (22, 274) and the consequent entry of the majority of VSV particles into the cytoplasm at the level of early endosomes (114, 175). As seen in figure 2.5B, VLPs bearing EBOV GP $\Delta$  are also internalized quickly from the cell surface. However, whereas VLPs bearing VSV-G enter soon after they are internalized (Fig. 2.5A), entry of VLPs bearing EBOV GP $\Delta$  lags approximately 60 min behind their internalization (Fig. 2.5B). Similar results were observed for VLPs coated with full length GP (data not shown). Although a time course for EBOV GP-mediated internalization has not been reported, the time course for GP $\Delta$  mediated entry that I observed here agrees well with findings using a luciferase reporter assay (217). Of note, the time course for entry of VLP-GP $\Delta$  lagged considerably behind (~30 min) that for VLPs coated with the LCMV GP (Fig. 2.5C), a GP that mediates entry through late endosomes (150, 207).

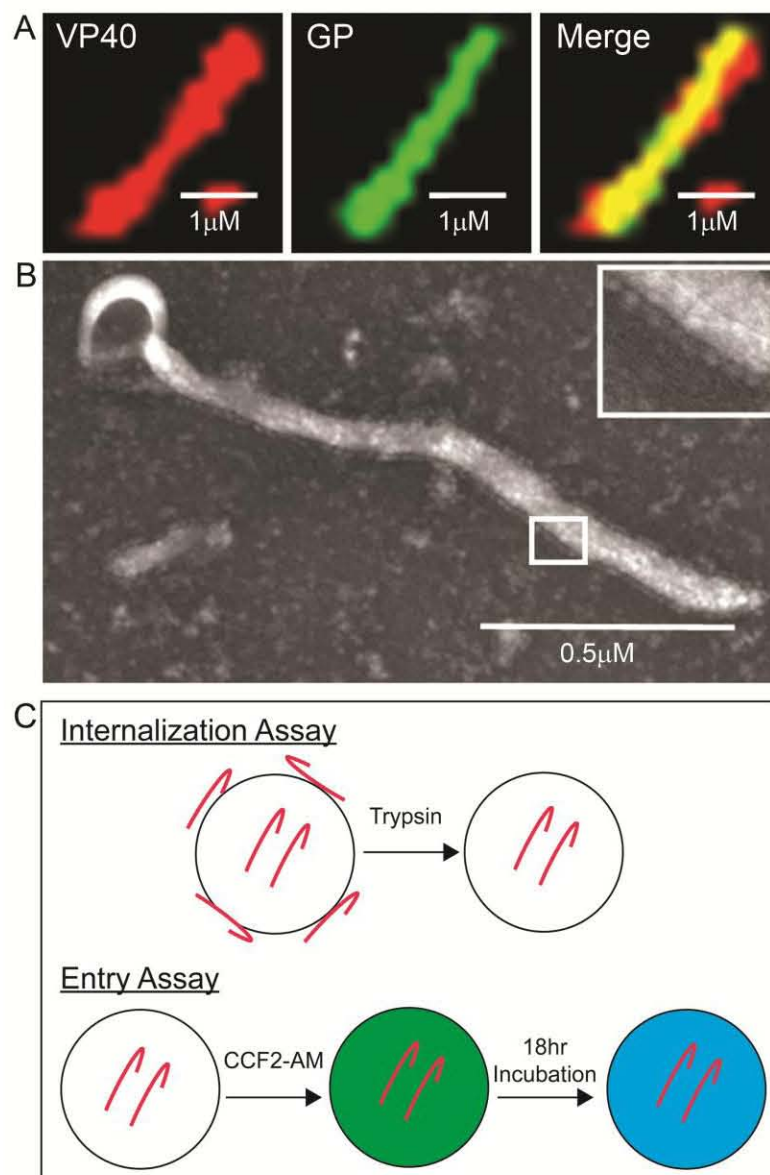
Since cathepsin priming of GP in LE/Lys is an essential step of EBOV entry, I next asked whether pre-priming of EBOV GP affects the rate of EBOV entry into the cell. To do this I compared the time courses of internalization and entry for VLPs coated with GP $\Delta$  or with GP $\Delta$  that had been primed *in vitro* to 19 kDa EBOV GP (Fig. 2.5B). Efficient pre-cleavage of GP on the particles (to 19 kDa) was confirmed by western blotting (data not shown). The two sets of particles showed virtually identical time courses for both internalization and entry. Importantly, as for uncleaved (mock) VLP-GP $\Delta$ , there was a considerable lag (~60 min) between the time at which VLPs-coated with 19 kDa EBOV GP are internalized and when they gain access to the cytoplasm. Therefore, priming of GP to the key 19 kDa species is not a rate limiting step in EBOV entry.

**NPC1-dependence of EBOV VLP internalization and entry.** We also tested the effect of NPC1 in target cells on the internalization and entry dynamics of EBOV VLPs. As predicted, the NPC1 status of the cell had no effect on the internalization kinetics of the particles (Fig. 2.6). Entry however, was totally dependent on NPC1; cells lacking functional NPC1 did not support entry. This agrees well with previously reported results with other EBOV surrogate particles indicating that NPC1 plays a key role at a late stage of EBOV entry (35).

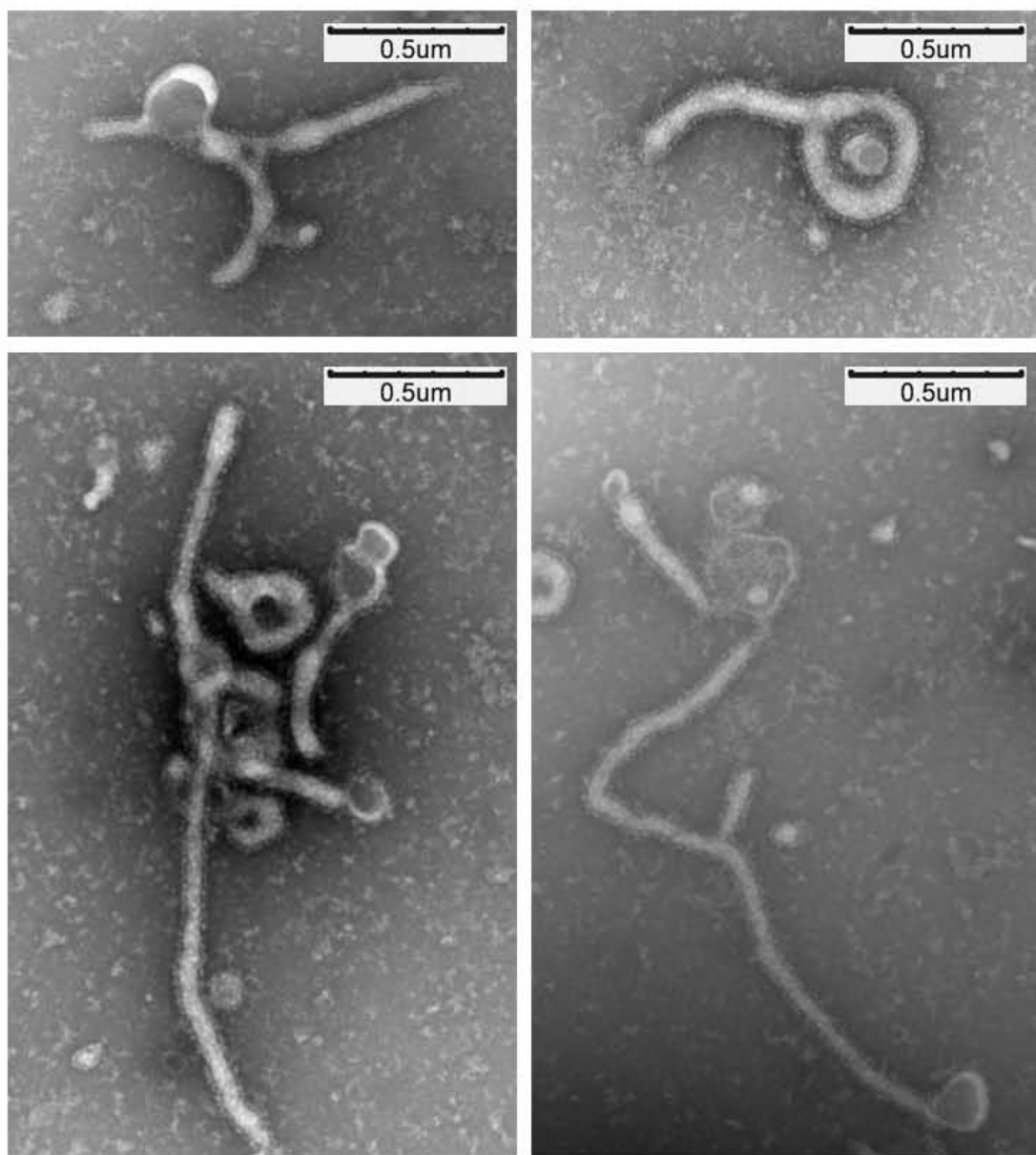
### Summary

In conclusion, I have developed a system of multi-purpose VLPs for studies of individual steps of EBOV entry into host cells. In particular, I have interrogated

**Figure 2.2. Multi-purpose VLPs for studies of EBOV internalization and entry.** (A) VLPs were fixed and stained with a mAb to EBOV GP, followed by anti-mouse AlexaFluor 488 IgG, and then imaged on a confocal laser microscope. (B) VLPs were imaged by negative stain electron microscopy at a magnification of 20,000 x. Inset shows surface glycoproteins in greater detail. (C) Schematics for using multi-purpose EBOV VLPs to monitor particle internalization and entry.

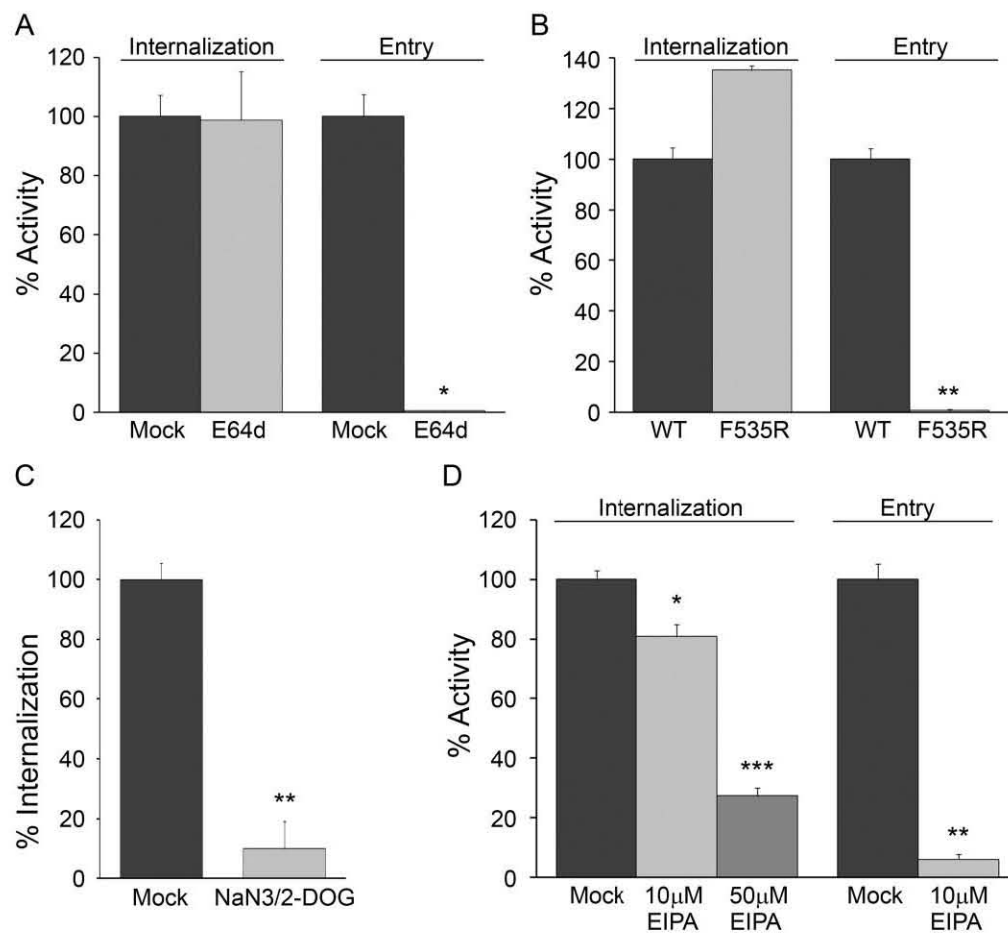


**Figure 2.3. Multi-purpose VLPs are uniform in diameter but pleomorphic in shape.** VLPs with GP $\Delta$  were imaged by negative stain transmission electron microscopy at a magnification of 20,000 x.



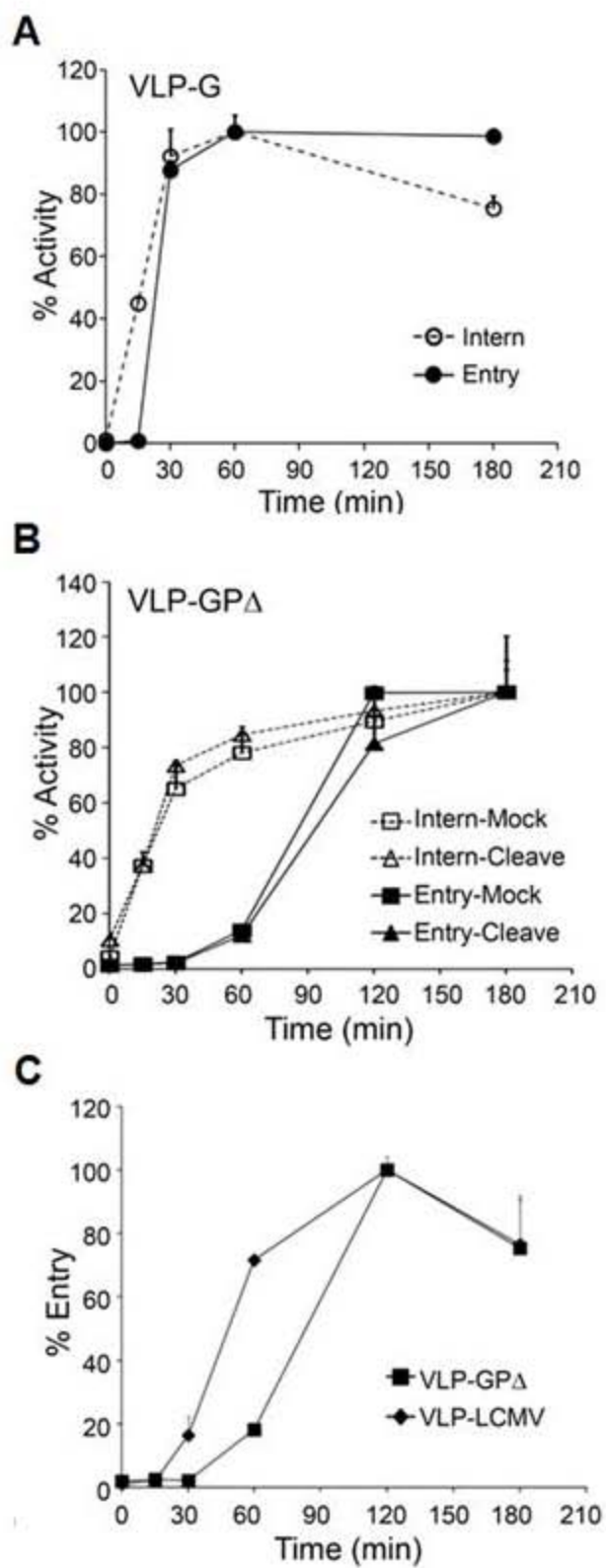
## **Figure 2.4. Validation of multi-purpose VLPs for studies of VLP**

**internalization and entry.** (A) SNB19 cells were pre-treated for 30 min with 10  $\mu$ M E64d, spinoculated with multi-purpose VLP-GP $\Delta$  particles, and then assayed for particle internalization and entry as described in Materials and Methods. (B) VLP-GP $\Delta$  with the fusion loop mutation F535R was assayed for internalization and entry. Data shown in A and B are from one experiment, each in with triplicate. (C) Effect of energy starvation by NaN<sub>3</sub>/2-DOG treatment on VLP-GP $\Delta$  internalization. Cells were pre-treated for 30 min, prior to addition of VLPs. 3 hr treatment with NaN<sub>3</sub>/2-DOG was toxic, and so entry was not measured. (D) Sensitivity of VLP-GP $\Delta$  internalization and entry to 10  $\mu$ M and 50  $\mu$ M EIPA . Cells were pre-treated for 1 hr prior to VLP addition. Effect of 50  $\mu$ M EIPA on entry could not be assessed due to background fluorescence. Inhibitors were present in all experiments from pre-treatment through 1 hr (internalization) or 3 hr (entry) 37°C incubations. Data in C and D are from one representative of two experiments (each performed in triplicate). Data represent percent cells displaying internalization and/or entry, normalized to mock-treated cells (A, C, D) or WT virus (B). Error bars represent standard deviation: \* (P<.01), \*\* (P<.001), or \*\*\* (P<.0001).

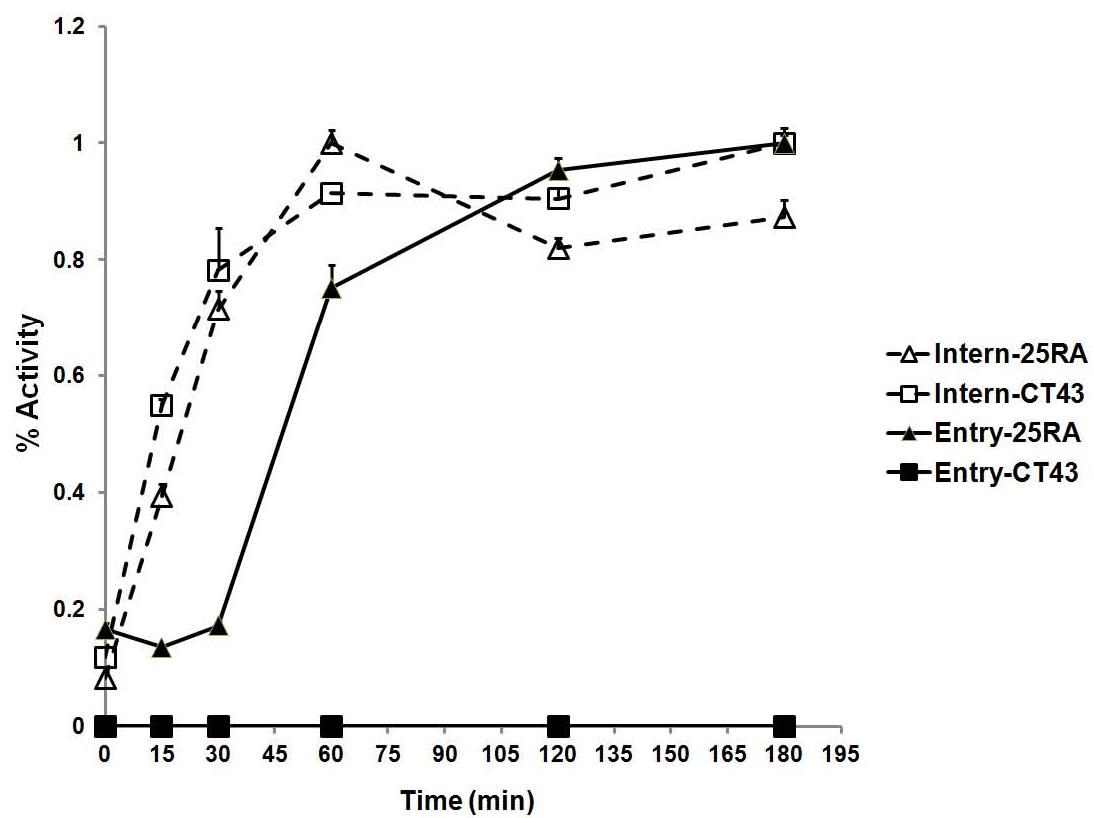


**Figure 2.5. Time courses of EBOV VLP internalization and entry.**

Internalization and entry into SNB19 cells were determined for (A) VLP-G (one representative of two experiments, each with duplicate samples) and (B) Mock or thermolysin-cleaved VLP-GPΔ (single experiment, triplicate samples). (C) Entry time course of VLP-GPΔ and VLP-LCMV (single experiment with duplicate samples). Time on x-axis is from time of release from cold block following spinfection. All data represents percent cells showing internalization or entry normalized to the maximal signal. Error bars represent standard deviation.



**Figure 2.6. Time courses of EBOV VLP internalization and entry in NPC1 +/- cells.** Internalization and entry into parental 25RA cells or NPC1 null CT43 cells were determined for VLP-GP $\Delta$  particles. Data are from a single experiment performed with duplicate samples. Error bars represent standard deviation.



the internalization and subsequent entry of VLPs bearing EBOV GP $\Delta$  into target cells. The particles were validated by showing that the internalization and entry characteristics behaved as expected, based on what is known to date about EBOV infection. We did, however, make two interesting observations concerning the timing of EBOV GP-mediated entry into host cells. Of particular note, we observed that VLPs bearing EBOV GP $\Delta$  are internalized fairly rapidly, but display delayed penetration into the cytoplasm. In addition, we observed that cathepsin priming of GP is not responsible for this slow entry. This lag between internalization and entry may be due to particle trafficking to the fusion compartment or, rather, it may suggest a requirement for additional cellular factors necessary for fusion.

In its current configuration, the internalization and cytoplasmic entry assays are conducted in parallel sets of cells. Theoretically, since the excitation/emission wavelengths used for both assays are widely separated, it should be possible to conduct them both on the same group of cells (i.e. by multi-color flow cytometry). This would further enhance the usefulness of these multi-purpose VLPs for studies of EBOV entry. Additional possible uses for these VLPs include measuring particle binding to the cell surface, which has been done by us and by other groups (171, 216) and direct membrane fusion assays, which our lab has conducted both at the cell surface and in an *in vitro* liposome model (White lab, unpublished data). In brief, this multi-purpose EBOV VLP system represents a powerful tool for future studies dissecting the multi-faceted steps of EBOV entry into the host cell.

## **Chapter III: FDA Approved Selective Estrogen Receptor Modulators Inhibit Ebola Infection**

Lisa M. Johansen, Jennifer M. Brannan, Sue E. Delos, Charles J. Shoemaker,  
Andrea Stossel, Calli Lear, Benjamin G. Hoffstrom, Kathryn L. Schornberg,  
Corinne Scully, Joseph Lehár, Lisa E. Hensley, Judith M. White, and Gene G.  
Olinger

- This chapter was modified from a manuscript in revision (115), and minor changes were made to integrate it into this dissertation

## Abstract

Ebolaviruses remain a significant threat to the both civilian and military populations as bioweapons, during sporadic outbreaks, and from the possibility of accidental importation from epidemic regions by infected individuals. Currently, no approved therapeutics exist to treat or prevent ebolavirus infection. Therefore, we performed a phenotypic high throughput screen of approved drugs and select molecular probes to identify drugs with antiviral activity against ebolavirus. From this screen, we identified a set of selective estrogen receptor modulators (SERMs) including clomiphene citrate and toremifene citrate that act as potent inhibitors of ebolavirus infection. Anti-ebolavirus activity was confirmed for both of these SERMs in an *in vivo* mouse infection model. This anti-ebolavirus activity occurs even in the absence of detectable estrogen receptor expression, and both SERMs inhibit virus entry after internalization, suggesting that clomiphene citrate and toremifene citrate are not working through classical pathways associated with the estrogen receptor. These data support the use of approved-drug screening to identify therapeutics for poorly understood diseases which, as a consequence of their origins, may readily be available for usage.

## Introduction

The filoviruses (Ebola and Marburg) are responsible for some of the most lethal viral hemorrhagic fevers (VHFs). The genera *Ebolavirus* comprises five distinct species with mortality rates up to 90% for Zaire ebolavirus (EBOV), while the single marburgvirus species (MARV) has different isolates with differing mortality rates (20–90%). Natural outbreaks of filoviruses in humans have been

reported in the Democratic Republic of the Congo, Republic of the Congo, Sudan, Uganda, Angola and Gabon. Filovirus illness is characterized by fever, myalgia, headache and gastrointestinal symptoms (81). Patients may also develop a maculopapular rash and alterations with coagulation. Fatal outcomes correlate with increasing viremia, convulsions and disseminated intravascular coagulation (81). Thus, EBOV and MARV are grave viral threats that continue to infect humans as well as non-human primates (155). The potential for accidental importation from epidemic regions by humans with asymptomatic infections is of great concern. Furthermore, there is a concern that filoviruses may be employed as a biological warfare agent by terrorist organizations (3).

Although effective drugs have been found to treat several other viral diseases, there are currently no approved therapeutics (small molecule or biologic) against filovirus infections. At the moment, supportive care is the primary clinical response (an option with little therapeutic benefit) for treating patients infected during natural or intentional disease outbreaks. Therefore, it is important to develop therapeutics that can be used for treating a filovirus infection.

Recently, the production of a genetically engineered EBOV expressing the green fluorescent protein (EBOV-eGFP) has led to the development of a novel high-throughput assay for drug discovery efforts (256). The genetically engineered virus has the unique property of making infected cells glow fluorescent green and this green signal can be detected and measured by flow cytometry or fluorimeters. Importantly, the GFP expressing EBOV-eGFP virus

retains the infection and replication characteristics of the parent virus (256) so that screening efforts using this virus target the complete virus lifecycle. Such a phenotypic cell-based assay may be used to identify inhibitors that target both viral and host pathways relevant to viral replication. As such, the identification of active compounds from this type of screen may be helpful in identifying the critical pathways or targets that are essential for viral replication.

In this study, we conducted a cell-based, high-throughput screen of approved drugs and molecular probes to identify novel inhibitors of ebolavirus using the aforementioned EBOV-eGFP assay. We identified many approved drugs and probes with previously undocumented anti-ebolavirus activity, including the selective estrogen receptor modulators (SERM) clomiphene citrate and toremifene citrate. SERM activity involves binding of the ligand SERM to the estrogen receptor (ER), a member of the nuclear receptor superfamily, causing conformational changes which facilitate interactions with coactivator or corepressor proteins, and subsequently initiate or suppress transcription of target genes. SERM activity is intrinsic to each ER ligand, which accomplishes its unique profile by specific interactions in the target cell, leading to tissue selective actions (reviewed in(233) and (193). Clomiphene citrate (brand names Clomid™ and Serophene™) is used to treat female infertility due to anovulation. Toremifene citrate (brand name Fareston™) is approved for the treatment of advanced metastatic breast cancer.

We confirmed the anti-EBOV activity of clomiphene citrate and toremifene citrate in mouse infection models. Importantly, we demonstrated that expression

of the ER was not required for clomiphene citrate inhibition of EBOV infection, suggesting that these drugs are likely not acting through their known targets. Follow-up work with EBOV virus-like particle (VLP) entry assays indicated that these drugs are acting as entry inhibitors after binding and internalization. Taken together, these findings suggest that clomiphene citrate and toremifene citrate inhibit EBOV infection through pathways unrelated to the classical estrogen pathway.

## **Materials and Methods**

**Ethics statement.** Research was conducted under an IACUC approved protocol at USAMRIID (USDA Registration Number 51-F-0021/728 & OLAW Assurance number A3473-01) in compliance with the Animal Welfare Act and other Federal statutes and regulations relating to animals and experiments involving animals and adheres to principles stated in the Guide for the Care and Use of Laboratory Animals, National Research Council, 1996. The facility where this research was conducted is fully accredited by the Association for Assessment and Accreditation of Laboratory Animal Care International. All efforts were made to minimize pain and suffering during the design and execution of these studies.

**Reagents.** Clomiphene citrate (CAS # 50-41-9), tamoxifen citrate (CAS # 54965-29-1), raloxifene hydrochloride (CAS # 82640-04-8), diethylstilbestrol (CAS # 56-53-1), Quinestrol (CAS # 152-43-2) were purchased from Sigma Aldrich (St. Louis, MO). Toremifene citrate (CAS # 89778-27-8) was purchased from Sequoia Research Chemicals (Reading, UK). Equilin (CAS # 474-86-2) was purchased from ICN Biomedicals Inc (Irving, CA). Hydroxyprogesterone caproate

(CAS # 630-56-8) was purchased from Professional Compounding Centers of America (Houston, TX). Dimethylsulfoxide was used as solvent for the high-throughput screening assay described below. PBS was used as a solvent for the mouse infection studies described below. Estrogen receptor alpha antibody was purchased from Millipore (Billerica, MA; Catalog # 04-820). Antibody against estrogen receptor beta and beta-actin was purchased from Cell Signaling Technology (Danvers, MA; Cat. #s 5513 and 3700, respectively). The Alexa fluor 488 goat anti-mouse antibody was purchased from Invitrogen (Carlsbad, CA; Catalog number A-11001). The 9G4 antibody(100, 101) was a gift of Dr. Michael Hevey, USAMRIID.

**Cells and viruses.** Vero E6 cells (ATCC: CRL-1586) and HepG2 cells (ATCC: HB-8065) were maintained in Eagle's Minimum Essential medium (EMEM, Gibco Invitrogen) supplemented with 10% fetal bovine serum (FBS, Gibco Invitrogen). The breast cancer cell lines ZR-75-1, MDA-MB-231, MCF-7 and SK-BR-3 cells were purchased from the ATCC and maintained as above. The non-small cell lung cancer cell lines A549, H460, H322 and H1650 cells were a kind gift from Dr. Faye M. Johnson (M.D. Anderson Cancer Center, Houston, TX), and were maintained as above. SNB19 cells were maintained in Opti-MEM medium (Gibco Invitrogen), 293T cells were maintained in Dulbecco's Modified Eagle's medium (DMEM, Gibco Invitrogen) supplemented with 10% FBS (Gibco Invitrogen) and 1% penicillin/streptomycin (Gibco Invitrogen).

The filoviral species Zaire ebolavirus (EBOV, Mayinga strain) and Sudan ebolavirus (SUDV, Boniface strain), or Lake Victoria marburgvirus (MARV,

Angola strain) were replicated in Vero E6 cells (ATCC: CRL-1586) at 90-100% confluency. Cells were inoculated with an approximate multiplicity of infection of 0.1 from historical stocks, and the medium was replaced 72 h after inoculation. Cells were monitored for cytopathic effects, and the supernatant was collected once 95-100% of the cells had detached from the surface). The cell supernatant was clarified by centrifugation at 1200 RPM for 10 min at 4°C, and aliquots were placed at -80°C storage until further use.

**High-throughput screening assays.** The high-throughput screening assay for EBOV utilized a genetically engineered EBOV expressing the green fluorescent protein (GFP), EBOV-eGFP, described in (256) and was kindly provided by Dr. Johathan Towner of the CDC. The Angola strain was used for all MARV experiments. For all high-throughput experiments, Vero E6 or HepG2 cells were plated on 96-well plates at a density of 40,000 cells/well in a total volume of 100 µL/well and incubated overnight at 37°C, 5% CO<sub>2</sub>. Next, 50 µl of pre-diluted compounds were added at a 4X concentration to each well to achieve the desired final concentration. Finally, 50 µl of the indicated virus (corresponding to an approximate multiplicity of infection of 0.01) was added to cells. These assay plates were centrifuged at 2,000 RPM for 5 min and were incubated for 48 h at 37°C, 5% CO<sub>2</sub>. After this incubation, the amount of GFP in each well of the EBOV-eGFP infected plates was determined using a spectrofluorometer from Molecular Devices (excitation: 485 nm, emission: 515 nm, cutoff: 495 nm). Antiviral activity was calculated by the inhibition of GFP compared to untreated control cells. For MARV-infected cells in plates, after the incubation, cells were

fixed in formalin and kept in solution for 3 days at 4<sup>0</sup>C. Plates were then washed with PBS and blocked with 3% bovine serum albumin diluted in PBS for 1 h at room temperature. Plates were subsequently incubated with a 1:1000 dilution of 9G4 antibody for 2 h at room temperature. After incubation, plates were washed with PBS and incubated with Alexa fluor 488 goat anti-mouse antibody at a 1:1000 dilution for 1 h at room temperature in the dark. Plates were washed with PBS and the level of fluorescence measured using a Spectromax M5 from Molecular Devices (excitation: 494 nm, emission: 517 nm).

The compound responses for SERM compounds were tested at three concentrations in the preliminary screen for both EBOV-eGFP and MARV. The *in vitro* anti-EBOV activity was confirmed by testing clomiphene citrate and toremifene citrate compounds at seven serially diluted doses in both Vero E6 and HepG2 cells.

To confirm that a decrease in fluorescence correlated with the inhibition of viral replication and not an increase in cell death, a counter screen was run in tandem using uninfected Vero E6 or HepG2 cells. Cells were seeded on 96-well plates as described above and incubated overnight at 37°C, 5% CO<sub>2</sub>. The following day, cells were treated with compounds and mock infected with medium. After a 48 hr incubation, cell viability was assessed using the Promega Cell Titer-Glo luminescent Cell viability kit. This assay provided a quantitative measure of the levels of ATP in the cell cultures in each well, with higher levels of ATP correlating with greater cellular viability. Thus, a compound with antiviral

activity is expected to inhibit the levels of fluorescence measured with minimal effect on the ATP levels measured by the Cell Titer-Glo assay.

**Quantitative real-time PCR.** Quantitative real-time PCR (qRT-PCR) to detect the nucleoprotein (NP) of EBOV and, SUDV was performed as previously published (268). Viral RNA was purified with the Qiagen Viral RNA Mini kit per manufacturer's directions. Plaque-forming units (PFU) equivalents (PFUe) were determined using a known virus concentration (as determined by filovirus plaque assay). Clomiphene citrate, toremifene citrate, and tamoxifen citrate were evaluated across the viral strains using six serially three-fold dilutions of the compounds starting at 50  $\mu$ M.

**Western blotting.** After the indicated treatment and time, adherent cells were washed with ice-cold PBS and collected in RIPA buffer (Sigma-Aldrich, St. Louis, MO) with 10  $\mu$ g/ml HALT protease and phosphatase inhibitor cocktail (Thermo-Fisher, Rockford, IL). Lysates were held on ice for 10 min, then clarified at maximum speed in a tabletop centrifuge for 10 min. Protein concentration was determined using the Quick-Start Bradford protein assay (BioRad, Hercules, CA) and equal protein aliquots were resolved using Mini-Protein TGX gels (BioRad), then transferred to nitrocellulose using the iBlot system (Invitrogen, Carlsbad, CA). After transfer, membranes were immunoblotted with primary antibody, and detected with horseradish peroxidase-conjugated secondary antibody (Cell Signaling Technology, Danvers, MA) and ECL reagent (Thermo-Fisher, Waltham, MA). Immunoblots were imaged using the ChemiDoc XRS+ (BioRad).

**Murine EBOV infection model.** The murine Ebola infection model has been described previously (27). Mouse-adapted EBOV (Mayinga), was obtained from Dr. Mike Bray, Virology Division, USAMRIID. C57BL/6 mice (5 – 8 weeks old) were obtained from the National Cancer Institute (Frederick, MD) and housed under specific pathogen-free conditions. C57BL/6 mice were challenged with 1000 PFU of the mouse-adapted EBOV (maEBOV) by intraperitoneal injection in a biosafety level 4 (BSL-4) laboratory. One hour after challenge, the animals were treated with the single agents in Table II at the indicated dose and frequency for a total of 10 days. Animals were monitored for survival for a total of 28 days after infection; survival rates were compared. The p-value was calculated using Fisher's exact test (with step-down Bonferroni adjustment where necessary) to compare the mean times-to death between the compound treated and vehicle treated control groups. A p-value of <0.05 means a significant difference between experimental groups.

These studies were conducted in compliance with the Animal Welfare Act and other federal statutes and regulations relating to animals and experiments involving animals, and adhere to principles stated in the *Guide for the Care and Use of Laboratory Animals*, National Research council, 1996. The facility where these studies were conducted is fully accredited by the Association for the Assessment and Accreditation of Laboratory Animal Care International.

**Virus-like particle (VLP) preparation.** For VLP entry assays, EBOV VLPs were prepared by transfecting 293T cells using polyethylenimine (25) with three plasmids: one encoding VP40 with  $\beta$ -lactamase fused to its N-terminus (Blam-

VP40), one encoding untagged VP40, and a third encoding codon-optimized full-length EBOV GP, VSV-G, or LCMV GP. The plasmids were transfected at a ratio 8:2:3, respectively. Four hr later, cells were treated with 10 mM sodium butyrate to boost expression. A first harvest was collected at 24 hrs postransfection (hpt), cleared of cellular debris, and concentrated. VLPs in the concentrated medium were then pelleted through 20% sucrose-VRB, re-suspended overnight in 10% sucrose (in VRB, see Chap. II Materials and Methods), aliquoted, and stored at -80°C. Fresh medium containing 10 mM sodium butyrate was added to the cells, cells were returned to the incubator, a second harvest was collected 48 hpt, and VLPs were pelleted and stored as described above. For internalization assays, VLPs were prepared as described in chapter II. All VLPs were checked by western blot for incorporation of proteins encoded by all plasmids.

**Ebolavirus entry and internalization assays.** The  $\beta$ -lactamase (Blam) entry assay (36) was adapted for assessing the effect of candidate inhibitor compounds on EBOV VLP entry as follows. In the afternoon before each experiment 100,000 SNB19 cells were plated in each well of a 48-well dish. The next day, compounds were diluted in DMSO so that equal volumes of inhibitor (DMSO only for controls) were added to all buffers to achieve the indicated concentration. Cells were then pretreated for 30 min with Opti-mem I (OMEM) medium (Gibco Invitrogen) to which the appropriate concentration of inhibitor had been added; they were maintained in the same concentration of inhibitor for all steps of the experiment. After the preincubation period, the cells were cooled on ice, washed once with OMEM (+/- inhibitor), and VLPs (in OMEM +/- inhibitor)

were added. VLPs were concentrated at the cell surface by spinfection at 4°C at 250 x g for 60 min, and placed in a 37°C incubator for 3-4 h to allow entry to occur. Cells were then loaded with CCF2/AM dye (Gene Blazer loading kit, Catalog number: K1095, Invitrogen) in loading medium (DMEM containing 25 mM HEPES, 10% FBS, 2.5 mM probenecid, and 2 mM L-glutamine) for 1 h in the dark at room temperature. After loading, the plates were washed with fresh medium (as above, but lacking CCF2/AM) and incubated overnight in the dark at room temperature. Cells were fixed, and then analyzed (on the same day as fixation) by flow cytometry using a CyAn LX 9 Color flow cytometer (DakoCytomation). If CCF2/AM is cleaved by Blam-VP40 its fluorescence shifts from green to blue (286). Data were analyzed using FloJo software. The percent of cells showing VLP entry was calculated as the ratio of the number of blue cells to the total number of cells gated (those containing CCF2/AM dye) subtracting off backgrounds in samples without VLPs. Two to three independent experiments were performed for each compound, each condition (concentration of compound) analyzed in triplicate. Activities were expressed as an inhibition as described below.

EBOV VLP internalization was assessed using VLPs containing a fluorescent mCherry-tagged VP40 (Shoemaker et al., manuscript in preparation). In brief, after spinfection and a 1 h warm-up period, cells were treated with protease to remove VLPs remaining on the cell surface. Samples were then analyzed by flow cytometry to determine the percentage of cells with fluorescent VP40 signal, representing internalized VLPs.

**Cathepsin activity and endosome acidification assays.** Cathepsin B activity in cell lysates was assayed using the cathepsin B substrate Z-Arg-Arg-7-AMC (Calbiochem), as described in (62). Cathepsin L was assayed the same as cathepsin B but using the cathepsin L substrate Z-Phe-Arg-7-AMC (Calbiochem) in the presence of 1  $\mu$ M CA074, a cathepsin B inhibitor (Calbiochem). Combined activity of cathepsins B plus L was assayed as above using the cathepsin L substrate in the absence of any inhibitor. Endosomal acidification was assessed using LysoTracker Red (Molecular Probes) as a probe for low pH organelles. Cells were pre-treated with or without inhibitor (as indicated) for 1h at 37°C, and then incubated with 50 nM LysoTracker Red for an additional 30 min (+/- inhibitor). Cells were fixed and analyzed by fluorescence microscopy.

**In-vitro compound activity calculations.** Raw phenotype measurements **T** from each treated well were converted to normalized fractional inhibition  $I = 1 - T/V$  relative to the median **V** of vehicle-treated wells arranged around the plate. After normalization, average activity values were calculated between replicate measurements at the same treatment doses along with the accompanying standard error estimates. Drug response curves were represented by a logistic sigmoidal function with a maximal effect level ( $A_{max}$ ), the concentration at half-maximal activity of the compound ( $EC_{50}$ ), and a Hill coefficient representing the sigmoidal transition. We used the fitted curve parameters to calculate the concentration ( $IC_{50}$ ) at which the drug response reached an absolute inhibition of 50%, limited to the maximum tested concentration for inactive compounds.

## Results

### Identification of approved clomiphene citrate and toremifene citrate in vitro

**anti-ebolavirus activity.** We assembled a library of 2,599 biologically active small molecules comprised of approved drugs and common mechanistic probes to identify novel inhibitors of EBOV infection using an EBOV variant engineered with a green fluorescent protein (GFP) reporter gene. For the preliminary screen, compounds were screened at three dose points around 10  $\mu$ M, 4  $\mu$ M and 1  $\mu$ M. Compounds were considered active if they inhibited the GFP signal by >40% and the parallel anti-proliferation screen in uninfected host cells showed no or minimal effects on cell viability. From this preliminary screen, a set of approximately ~130 active compounds was identified, including a set of compounds that are known to modulate the estrogen receptor (ER). Some of the strongest antiviral activity was observed with the ER antagonists, including clomiphene citrate, toremifene citrate, tamoxifen citrate and raloxifene hydrochloride (Fig. 3.1). The ER antagonist diethylstilbestrol also inhibited ebolavirus infection but to a lesser extent (data not shown). Additionally, we observed antiviral activity with ER agonists: hydroxyprogesterone caproate, equillin and quonestrol (data not shown). A subset of the active compounds identified in this primary screen, including clomiphene citrate and toremifene citrate, were selected for confirmatory studies using an 8-point dose response in Vero E6 cells where the active drug concentrations could be refined and an accurate inhibitory concentration of 50% (IC<sub>50</sub>) determined (Fig. 3.2). Further, we evaluated the antiviral activity in human HepG2 cells to rule out mechanisms

that may be unique to the Vero E6 cell line, which is a monkey-derived cell line (Fig. 3.2). The antiviral activities of both clomiphene citrate and toremifene citrate were confirmed in both the Vero E6 and HepG2 cell lines. While toremifene citrate showed no impact on cell proliferation in both Vero E6 cells and HepG2 cells, we did observe that clomiphene citrate inhibited HepG2 cell proliferation at the higher concentrations evaluated.

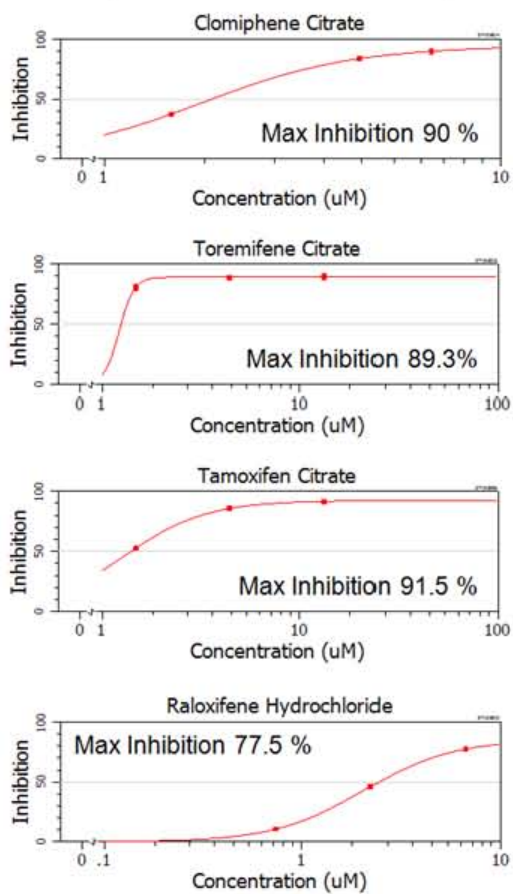
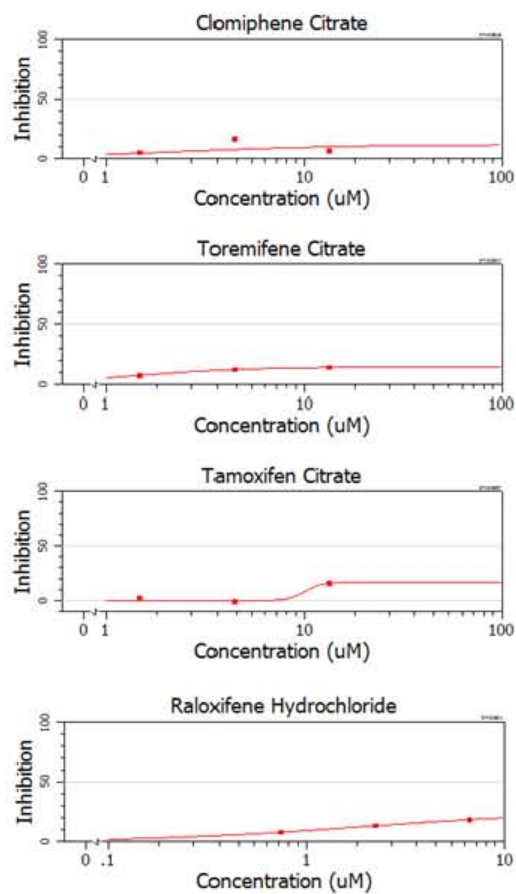
To rule out the possibility that antiviral activity observed with clomiphene citrate and toremifene citrate was specific to the engineered EBOV-eGFP strain, we tested the antiviral activity of clomiphene citrate and tamoxifen citrate against native ebolavirus strains including EBOV (Mayinga) and SUDV (Boniface). These viral isolates were used to infect Vero E6 cells in the presence of vehicle, clomiphene citrate or toremifene citrate (concentration ranges of 0.2  $\mu$ M to 50  $\mu$ M) and the virus PFU determined by PCR. Results indicate that both clomiphene citrate and tamoxifen citrate were active against the native ebolavirus strains (Fig 3.3).

The spectrum of antiviral activity for clomiphene citrate and toremifene citrate were further evaluated for MARV infection using native virus to infect Vero E6 cells in an 8-point dose response. Results indicated that clomiphene citrate inhibited MARV infection with a similar potency and maximal inhibition as EBOV (Fig. 3.3). Similarly, toremifene citrate showed strong antiviral activity against MARV in the concentration range tested.

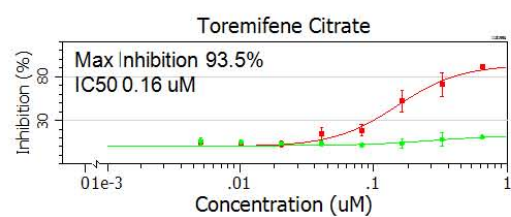
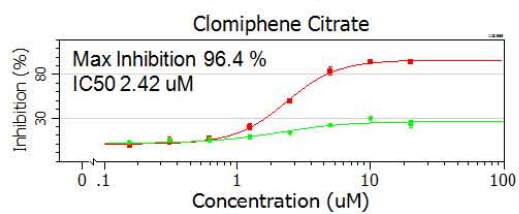
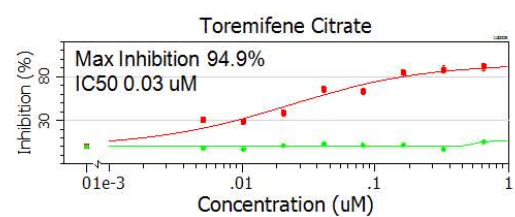
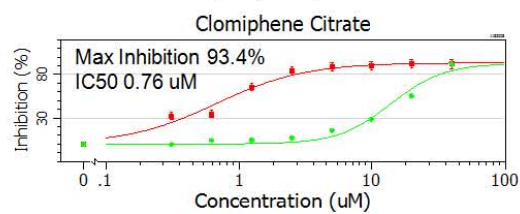
**Inhibition of EBOV infection by clomiphene and toremifene in a mouse model of infection.** To confirm that the antiviral activity observed with

**Figure 3.1. Selective estrogen receptor (ER) modulators inhibit EBOV**

**infection *in vitro*.** ER antagonists inhibit ebolavirus infection identified from the high-throughput screen using EBOV-eGFP engineered ebolavirus. Panels on the left show the 3-point dose response curve for the indicated compounds for Vero E6 cells infected with EBOV-eGFP. Indicated is the maximum % EBOV inhibition observed for the compounds. The panels on the right show the effect of the compound on cell viability in uninfected Vero E6 cells.

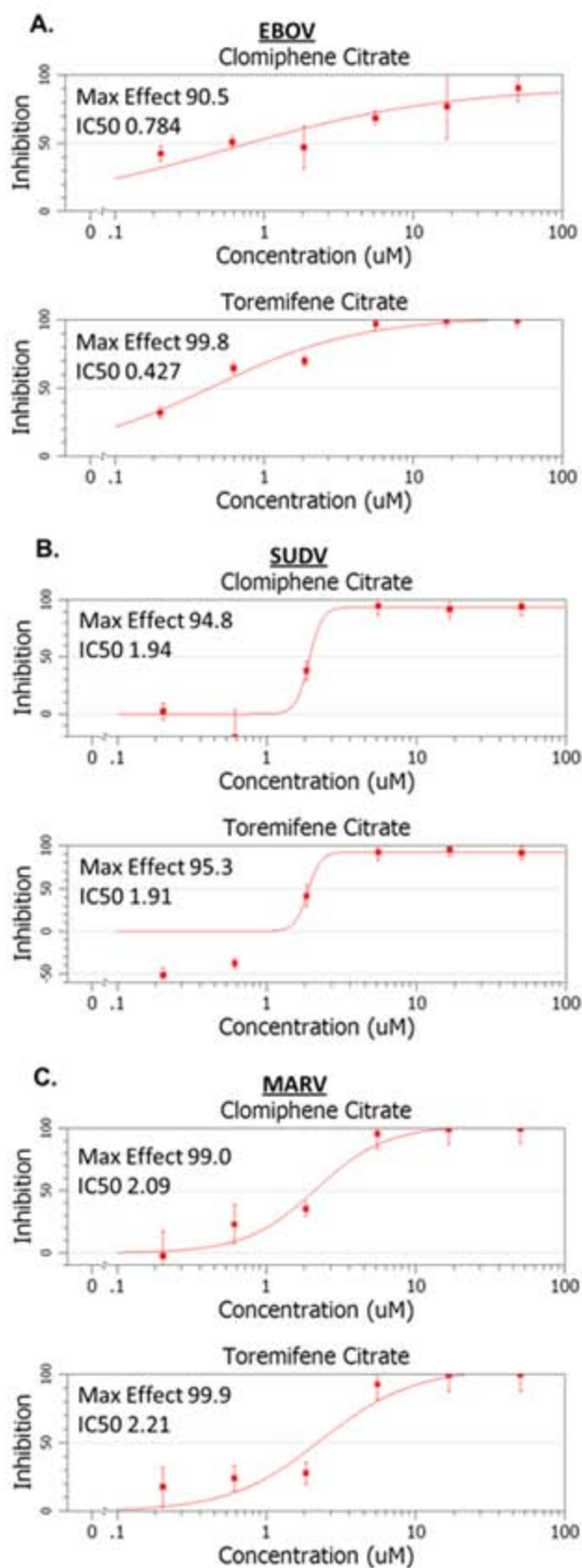
**EBOV-eGFP****Viability**

**Figure 3.2. *In vitro* 8-point dose response curves for clomiphene and toremifene.** Compounds were evaluated in both the Vero E6 and HepG2 cell lines. The activity of the compound in the EBOV infection assay is shown in red and the activity in the host cell viability is shown in green. The maximal % inhibition and IC<sub>50</sub> are indicated.

Vero E6HepG2

■ EBOV ■ Host Proliferation

**Figure 3.3. The activity of clomiphene and toremifene with native strains of filoviruses.** Native isolates of **A)** EBOV, **B)** SUDV and **C)** MARV were used to infect Vero E6 cells and the number of PFUs determined by qRT-PCR. Results indicate that both clomiphene citrate and toremifene citrate strongly inhibit infection by these native isolates. Shown for each dose response is the Max Effect of the compound in % Inhibition (Max Effect) and the IC<sub>50</sub> concentration in  $\mu\text{M}$  (IC<sub>50</sub>).



clomiphene citrate and toremifene citrate translated to *in vivo* ebolavirus infection, these compounds were evaluated in a murine EBOV infection model using a mouse-adapted viral strain (27). The intraperitoneal inoculation of mouse-adapted virus results in the acute onset of severe illness 3 – 4 days after infection, with high-level viral replication observed in the liver and spleen, multifocal hepatic necrosis, and a rapid increase in viremia to titers  $>10^8$  PFU/ml (27).

For these studies, female mice (n=10 unless otherwise noted) were challenged intraperitoneally with 1000 PFU of maEBOV. One hour after infection, the animals were treated with clomiphene citrate, toremifene citrate or vehicle for 10 days at the doses and treatment regimen outlined in table 3.1. Survival was monitored out to 28 days following infection. The half-life of these ESR1 antagonists has been shown to be greater than 24 hours (170, 180, 251). Thus, these compounds were evaluated with dosing every other day (QID) or as once daily dosing (SID). For both clomiphene citrate and toremifene citrate, treatment of infected mice resulted in significant survival benefit as well as an increase in mean time to death (MTD). Additional experiments evaluating treatment response in male mice did not show any difference in response; however, these data should be confirmed with larger studies (data not shown). Representative survival plots are shown in figure 3.4. For clomiphene citrate, up to 90% of the treated animals survived, depending on the dose and treatment schedule (p-value  $<0.0001$ ). For toremifene citrate, 50% (p-value 0.0441) of the treated animals survived the maEBOV challenge. In summary, the antiviral activity

**Table 3.1. Summary of clomiphene and toremifene evaluation in the mouse EBOV infection model.** QID – dosing every other day; SID – once daily dosing; BID – twice daily dosing; MTD – mean time to death; the p-value was determined using a standard T test to compare the mean times-to death between the compound treated and vehicle treated control groups. \*Seven vehicle-treated mice were used for this experiment.

Compound	Study No.	N=	Dose (mg/kg)	Regimen	Survival day 28	p-value
Clomiphene citrate	1	10	60	SID	90%	<0.0001
	2*	10	35	SID	70%	.0491-
	2	5	60	QID	60%	0.1818
Toremifene citrate	1		60	QID	50%	.0441

**Figure 3.4. Representative survival plots for clomiphene and toremifene in**

**a mouse model of EBOV infection.** (A) A representative survival plot for

clomiphene citrate shows 90% of treated animals survived ebolavirus infection.

All animals in the PBS vehicle control group succumbed to disease by day 7. (B)

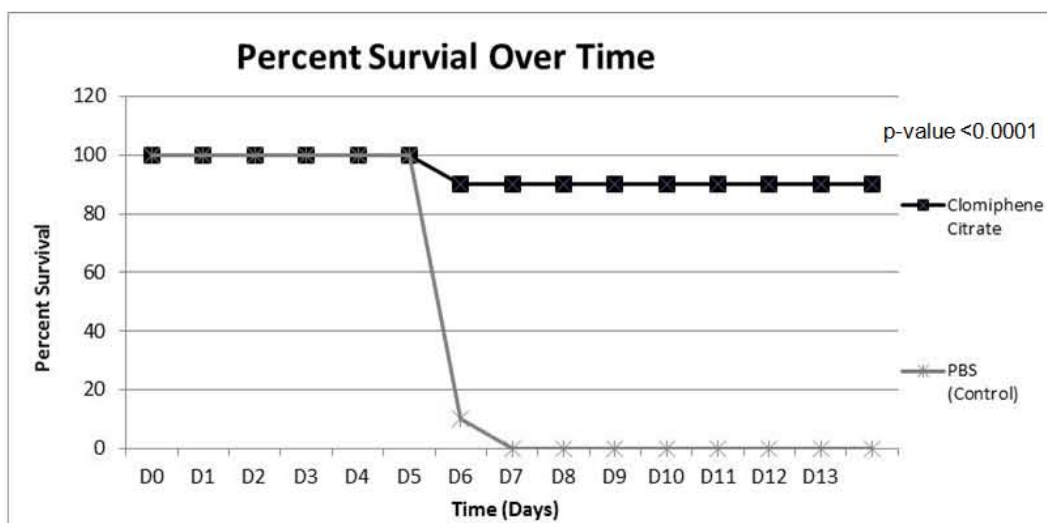
A representative survival plot for toremifene citrate indicating that 50% of the

treated animals survived infection by EBOV. Animals in the PBS vehicle control

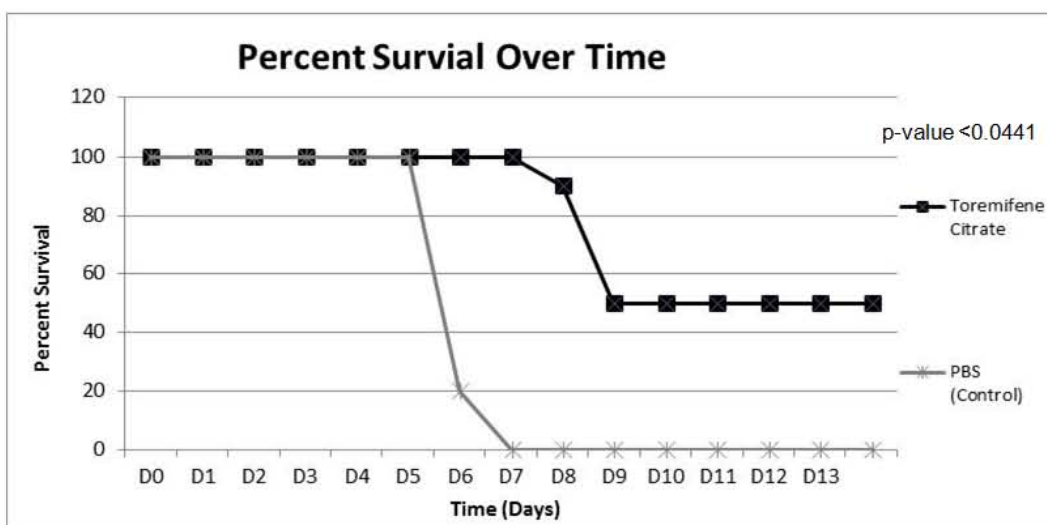
group succumbed to disease by day 7. The P-value for each study is indicated

and was determined by a Fisher's exact test.

A.



B.



observed for clomiphene citrate and toremifene citrate translated to a significant survival benefit for mice in a murine ebolavirus infection model.

**Clomiphene inhibition of EBOV infection is not dependent on estrogen receptor expression.** Given that ER signaling has not been reported to play a role in filovirus infection, and that we observed no differences in response to clomiphene citrate in infected male and female mice, we sought to determine if the classical estrogen signaling pathway was involved in ebolavirus infection, we first determined if either subtype of ER, alpha or beta, was expressed in Vero E6 or HepG2 cells before or after clomiphene treatment. Cells were either untreated, or treated with clomiphene citrate or treated with vehicle for 1 h, and then probed for ER expression by western blotting. We observed no expression of ER- $\alpha$  in untreated or clomiphene-treated Vero E6 or HepG2 cells, whereas ER- $\beta$  expression was observed in both cell lines (Fig. 3.5A). Treatment with clomiphene citrate did not affect levels of ER expression.

To further explore the possible role of ER signaling in filovirus infection, we established a panel of cell lines with varying combinations of ER expression (Table 3.2). Cell lines were infected with EBOV-eGFP and GFP expression was measured using a fluorometer. Two cell lines, the breast cancer cell line ZR-75-1 and the non-small cell lung cancer cell line H322, were not readily infected with EBOV. Further, two other breast cancer cell lines in the panel, MDA-MB-231 and SK-BR-3 only produced low levels of infection at the multiplicity of infection used for this study. No pattern was observed relating ER expression to infectibility of the cell lines. After clomiphene citrate treatment of cell lines susceptible to

**Table 3.2. Estrogen receptor expression and infection status in cell lines.**

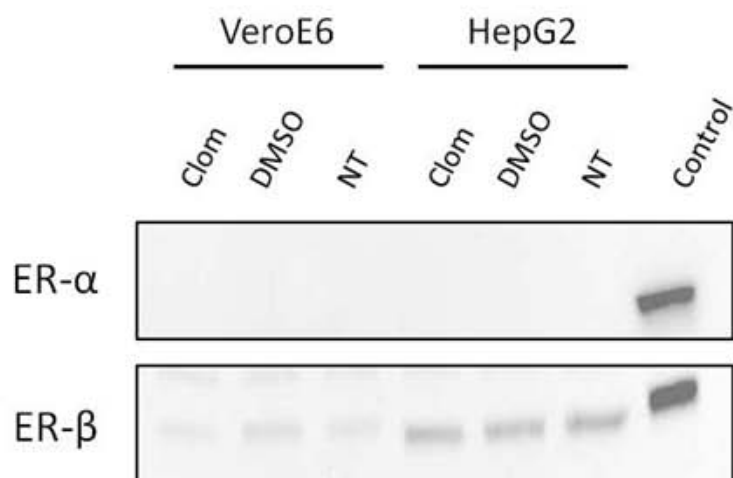
“-“ indicates no expression and “+” indicates positive expression based on analysis by western blotting; “Y” indicates cells that could be infected with EBOV-eGFP, “N” indicates cells resistant to infection with EBOV-eGFP, and “Low” indicates a low level of EBOV-eGFP infection noted.

Cell Line	ER-a	ER-b	Infection
Vero E6	-	+	Y
HepG2	-	+	Y
ZR-75-1	+	+	N
MDA-MB-231	-	+	Low
MCF-7	+	+	Y
SK-BR-3	-	+	Low
A549	-	+	Y
H460	-	-	Y
H322	-	+	N
H1650	-	-	Y

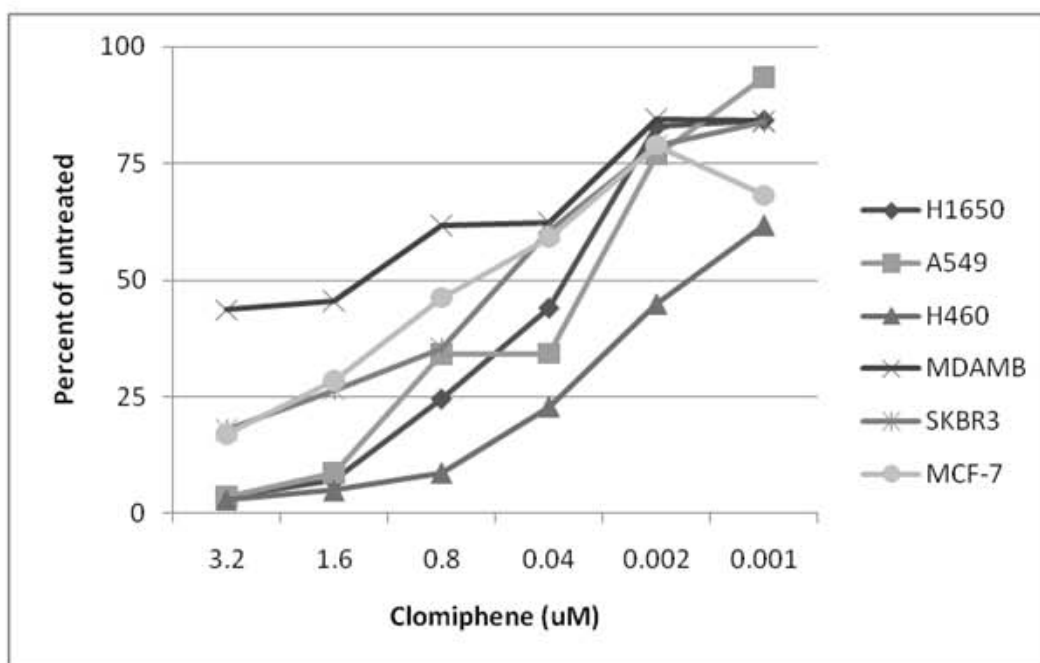
**Figure 3.5. Clomiphene inhibition of EBOV infection is not dependent on**

**ER expression.** (A) Western blot analysis of Vero E6 and HepG2 cells treated with clomiphene citrate, DMSO (vehicle control) and no treatment (NT) and probed for either ER a (ER- $\alpha$ ) or ER-b (ER- $\beta$ ) expression. MCF-7 and SK-BR-3 cell lysates were used as controls for ER- $\alpha$  and ER- $\beta$ , respectively. (B) EBOV-eGFP was used to infect cell lines both positive and negative for ER- $\alpha$  and ER- $\beta$  expression (as shown in Table II) that were treated with clomiphene citrate.

A.



B.



EBOV infection, we observed a dose-dependent inhibition of EBOV-eGFP infection similar to that seen in Vero E6 and HepG2 cells (Fig 3.5B). Greater than 50% inhibition was observed in all cell lines at the highest dose (3.2  $\mu$ M), and a dose response was present in all cell lines, including two (H1650 and H460) that do not express detectable levels of either ER. Taken together, these data suggest that clomiphene citrate is acting through a pathway independent of the classical estrogen signaling pathway.

**SERMs inhibit EBOV entry at a step after binding.** Following the observation that the antiviral effects of clomiphene citrate and toremifene citrate were independent of the classical estrogen signaling pathway, we sought to determine the mechanism of the antiviral activity of these compounds.

Recent progress has been made on characterizing the EBOV lifecycle and interactions with the host cell (56). As a first step to evaluate how clomiphene and toremifene impact the EBOV lifecycle, we evaluated if the compounds could be impacting viral entry, a process mediated exclusively by the ebolavirus glycoprotein (GP). After GP-mediated binding to the cell surface, EBOV enters the host cell through an endocytic pathway. Once in a proper endosomal compartment cathepsins B and L prime GP for subsequent fusion, by generating an 18-19 kDa form of the GP1 (29, 40, 222, 227). Next, an additional factor (or factors) triggers GP to mediate fusion with the endosomal membrane in a process that requires low pH (58, 227, 266). After fusion, the EBOV nucleocapsids are released into the cell cytoplasm where synthesis of new viral components ensues.

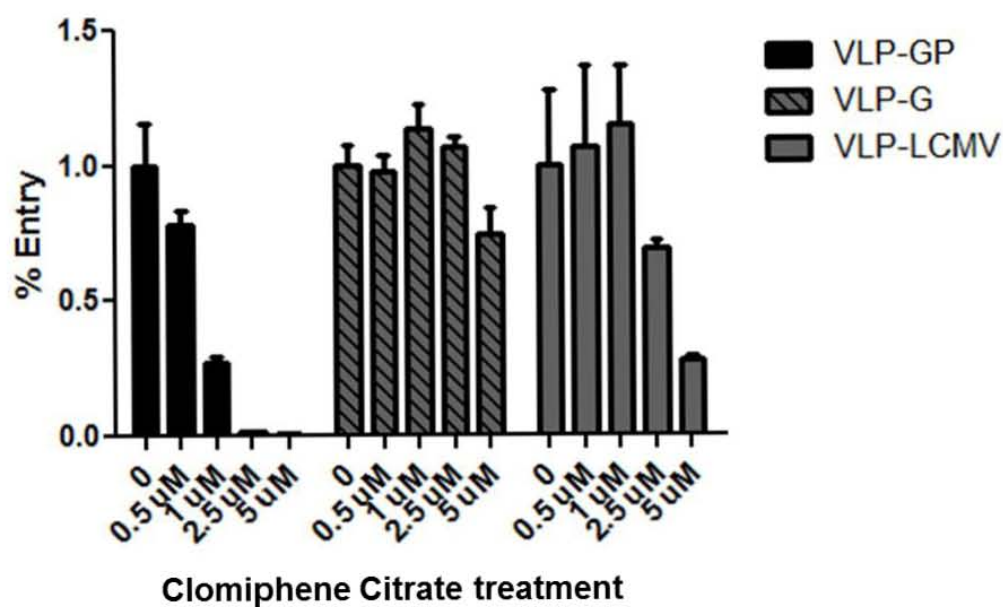
EBOV entry was examined using virus-like particles (VLPs) expressing the EBOV glycoprotein and containing a beta-lactamase reporter (Blam) (59, 227). For these experiments SNB19 cells were pretreated with clomiphene citrate, toremifene citrate or vehicle for 30 min and subsequently cooled on ice. VLPs were then added to the cells in the presence of the inhibitors. After allowing for binding at 4°C, the cells were placed at 37 °C to allow for VLP entry and then loaded with a Blam-cleavable fluorescent substrate. With this system, compounds that inhibit viral entry will result in low or no Blam signal. The results of the VLP entry assay in SNB19 cells show that both clomiphene citrate and toremifene citrate inhibit entry of EBOV VLPs (VLP-GP) (Figure 3.6A and B). Both compounds were evaluated with 4-point, two-fold dose titrations. For both clomiphene citrate and toremifene citrate, we observed a dose-response where higher concentrations resulted in higher levels of entry inhibition. Similar results were observed with Vero E6 cells (data not shown); however, the raw signal values were lower resulting in a lower signal to noise ratio for the assay.

To evaluate if the entry inhibition observed was specific to VLPs with EBOV GP, VLPs containing the vesicular stomatitis virus (VSV) glycoprotein G (VLP-G) and VLPs containing the lymphocytic choriomeningitis virus glycoprotein (VLP-LCMV) were evaluated in parallel (Figure 3.6 A and B). VSV viral entry is mediated largely in early endosomes soon after internalization whereas LCMV entry is mediated in late endosomes similar to EBOV entry (134, 211). Both clomiphene citrate and toremifene citrate inhibited the VLP-GPs with greater potency as compared to the VLP-Gs and VLP-LCMVs. Treatment with

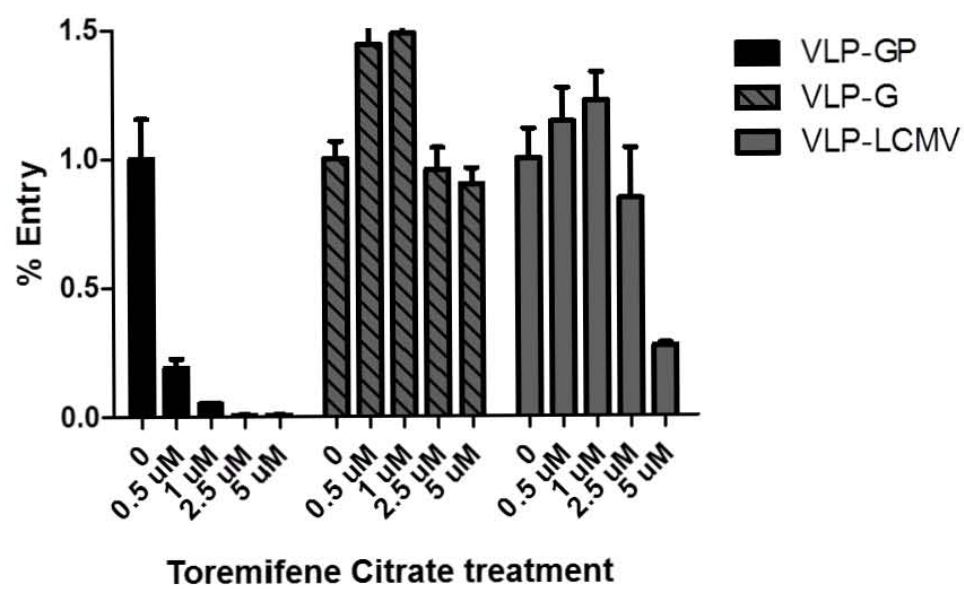
**Figure 3.6. Effects of clomiphene and toremifene in EBOV VLP entry assay.**

**A)** Clomiphene citrate and **B)** toremifene citrate were tested for their ability to inhibit VLPs with the EBOV GP (VLP-GP), the VSV G glycoprotein (VLP-G) and LCMV GP (VLP-LCMV). Results indicate that both clomiphene citrate and toremifene citrate exhibit greater specificity to VLPs bearing the EBOV GP as compared to VLPs bearing VSV-G or the LCMV GP. For each compound, assays with the different VLPs were performed in parallel. Error bars represent the standard error.

A.



B.



clomiphene citrate resulted in 93% inhibition of VLP-GP at 5  $\mu$ M compared to 25% inhibition of VLP-G entry and 73% inhibition of VLP-LCMV. Similar results were observed with toremifene citrate. Treatment with 5  $\mu$ M of toremifene citrate resulted in 95% VLP-GP entry inhibition compared to 10% inhibition of VLP-G and 70% of VLP-LCMV. Lower concentrations of the compounds, 1  $\mu$ M for clomiphene citrate and 0.5  $\mu$ M for toremifene citrate, still strongly inhibited the entry of VLPs containing the EBOV GP. In contrast these concentrations did not impact the entry of the VLPs containing the VSV or the LCMV glycoproteins.

We next asked if the compounds inhibit EBOV entry because they inhibit particle internalization. To do this we used VLPs that contained a fluorescent-tagged VP40 marker. After incubations for VLP binding (at 4°C) and internalization (at 37°C), SNB19 cells were treated with protease to remove VLPs remaining on the cell surface. Cells that retained fluorescently-tagged VP40 were therefore scored as positive for VLP internalization. For these experiments SNB19 cells were treated with clomiphene citrate (5  $\mu$ M), toremifene citrate (0.8  $\mu$ M), vehicle, or 50  $\mu$ M 5-N-ethyl-N-Isopropyl-amiloride (EIPA), which is a known inhibitor of EBOV VLP internalization (183, 216). As shown in figure 3.7A, neither clomiphene citrate nor toremifene citrate inhibited VLP internalization. In contrast, treatment of cells with EIPA resulted in a greater than threefold reduction in VLP internalization. The fact that neither clomiphene citrate nor toremifene citrate inhibit VLP internalization implies that neither inhibits VLP binding to the cell surface. The lack of effect of clomiphene citrate and toremifene citrate on VLP binding is consistent with a preliminary experiment showing that neither

compound inhibits binding of a protein construct containing the receptor binding region of EBOV GP (58) to the cell surface (data not shown).

Next we tested whether either clomiphene citrate or toremifene citrate affects the activity of cathepsin B or cathepsin L, endosomal proteases that are needed to prime EBOV GP for cellular entry (40, 227). Clomiphene citrate and toremifene citrate were added to cells for 3 hr at 5  $\mu$ M and 0.8  $\mu$ M respectively. Epoxysuccinylleucylamido-3-methylbutane ethyl ester (EST, a cysteine protease inhibitor) was used as a positive control for cathepsin inhibition (227). The cells were then lysed and assayed for enzyme activity as described in the Methods section. We found that neither clomiphene citrate nor toremifene citrate inhibited the activity of either cathepsin B or cathepsin L (Fig. 3.7B). Thus, these compounds are not inhibiting the cathepsin enzymes that prime ebola GP.

We also evaluated if clomiphene citrate or toremifene citrate affect endosome acidification, which is needed for ebolavirus entry. Endosome acidification was assessed in SNB19 cells using LysoTracker Red, which is a probe for low pH organelles. Cells were treated with vehicle, clomiphene citrate (5  $\mu$ M), toremifene citrate (0.8  $\mu$ M), or  $\text{NH}_4\text{Cl}$  (10 mM), the latter as a positive control for inhibition of acidification. While we observed strong inhibition of acidification with  $\text{NH}_4\text{Cl}$ , we observed no inhibition with clomiphene citrate or toremifene citrate (Fig. 3.8). Similar results were observed in Vero cells (not shown).

Taken together, our results show that clomiphene citrate and toremifene citrate specifically inhibit EBOV GP-mediated entry. This inhibition occurred after

particle binding and internalization and was not due to effects on either endosomal cathepsins or endosomal acidification. Instead, we believe these compounds could be inhibiting either viral trafficking to the fusion site or viral fusion itself.

## Discussion

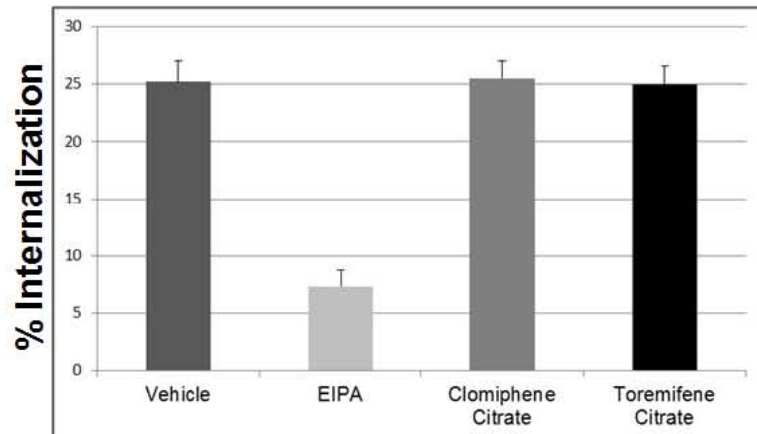
A set of SERM compounds were identified as novel and specific inhibitors of ebolavirus infection from a phenotypic high-throughput screen of approved drugs and mechanistic probes. Both ER agonists (hydroxyprogesterone caproate, equilin and quinestrol) and antagonists (clomiphene citrate, toremifene citrate, tamoxifen citrate and raloxifene hydrochloride) were observed to mediate antiviral effects. The ER antagonists are approved drugs with oral availability, good safety and tolerability profiles, and a long history of use. Moreover, these ER antagonist drugs have good plasma exposure and bioavailability making them excellent candidates for repurposing efforts for use with EBOV infection (170, 180). Therefore, we focused our efforts on confirming and understanding how these antagonist drugs inhibit EBOV infection.

The ER antagonist drugs stem from seven chemical structural classes (233). Our high-throughput screen contained antagonists from four of these classes including: the triphenylethylenes (tamoxifen citrate and toremifene citrate); chloroethylene (clomiphene citrate); the benzothiophenes (raloxifene hydrochloride); and the steroidal (fulvestrant). In contrast to the other ER antagonists evaluated in our screen, fulvestrant did not inhibit EBOV infection (data not shown). It is not clear if this is due to differences in its chemical

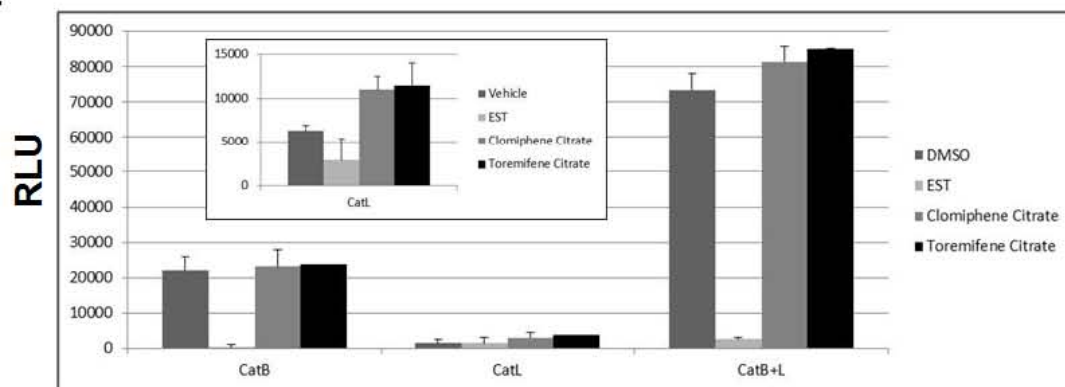
**Figure 3.7. Evaluation of clomiphene and toremifene on EBOV VLP-GP**

**internalization and cathepsin processing.** (A) Clomiphene citrate and toremifene citrate were evaluated at 5 mM and 0.8 mM, respectively. EIPA is a known inhibitor of ebolavirus internalization. Results indicate that neither clomiphene citrate nor toremifene citrate inhibit ebolavirus internalization. (B) Clomiphene citrate (5 mM) and toremifene citrate (0.8 mM) were evaluated, as described in the Methods section, for their effects on cathepsin B (CatB) and cathepsin L (CatL) activity (singly and combined) in SNB19 cells. EST is a cysteine protease inhibitor that was included as a positive control for the assay. Data in the main plot are from the 1.5 h time point. The inset graph notes the results for CatL at 18 hr. This was done because the raw signal values for cathepsin L were low at the 1.5 hr time point. Similar results were observed in Vero cells (not shown).

A.

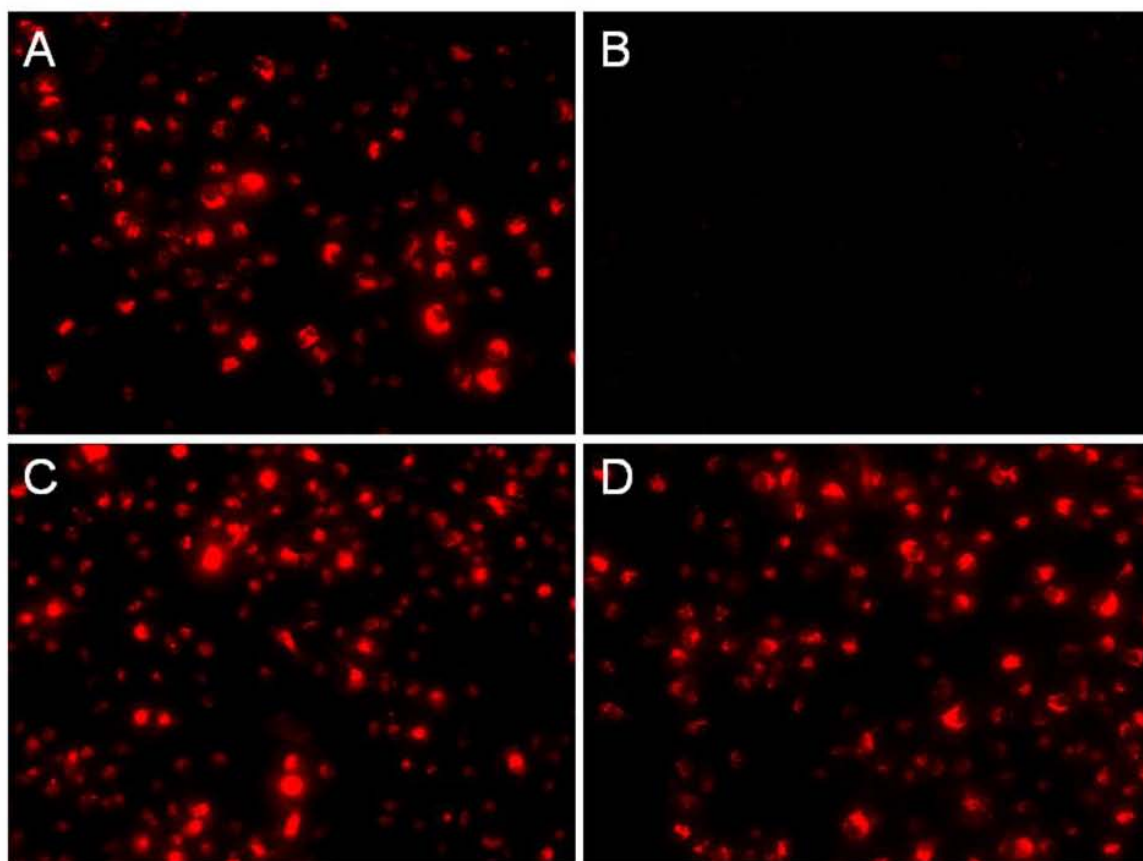


B.



**Figure 3.8. Clomiphene and toremifene do not affect the pH of endosomes.**

SNB19 cells were pre-incubated in the presence of: (A) DMSO vehicle (B) 10 mM  $\text{NH}_4\text{Cl}$  as a positive control for inhibition of endosomal acidification (C) 5 mM of clomiphene citrate or (D) 0.8 mM of toremifene citrate for 1 h at 37°C. At this time, LysoTracker Red (+/- inhibitor, as indicated) was added and the cells were incubated for an additional 30 min at 37°C. At this time the cells were fixed, viewed and photographed with an inverted fluorescence microscope. Images are representative of 10 fields observed per condition.



structure or its subset of targets. Toremifene citrate, tamoxifen citrate, clomiphene citrate and raloxifene hydrochloride are structurally similar with the compounds containing a tertiary amine group as well as a hydrophobic backbone (233). Toremifene citrate, tamoxifen citrate, and raloxifene hydrochloride have been shown to be effective at treating or preventing invasive breast cancer (233). However, raloxifene hydrochloride also has skeletal antiresorption activities rendering it an effective anti-osteoporosis treatment (180, 233). Clomiphene citrate, on the other hand, antagonizes a significant ER in the central nervous system (CNS), which is how it mediates follicular development and induction of ovulation (233). We selected clomiphene citrate for follow-up efforts because of its different ER target and structural classification. While both tamoxifen citrate and toremifene citrate are classified structurally as triphenylethylenes, toremifene citrate was selected for follow-up work due to a slightly more potent inhibitory effect in preliminary screens (Fig. 3.1).

As confirmation of their anti-EBOV activity, both clomiphene citrate and toremifene citrate showed a significant *in vitro* inhibition in infection assays using wild-type ebolavirus strains. While both of these ER antagonists inhibited both MARV and EBOV in *in vitro* infection assays (Fig. 3.3), tamoxifen citrate was unable to inhibit MARV infection in the high-throughput assay (data not shown). Further evaluation of the differences between ER antagonist structural classes is warranted and may provide insight to subtle differences in EBOV and MARV entry. Both clomiphene citrate and toremifene citrate demonstrated survival benefit in a mouse infection model of EBOV. Interestingly, our results indicate

that these compounds are mediating their antiviral effects through cell-based mechanisms unrelated to the classical estrogen signaling pathway. Various cell lines were susceptible to EBOV infection regardless of their expression (or lack of expression) of ERs. Additionally, the lack of ER expression did not impede the ability of clomiphene citrate to mediate its antiviral effects.

While we initially identified the ER antagonist compounds based on their collective known mechanism of action, our data with filamentous VLPs further demonstrate these drugs inhibit viral infection through an ER-independent mechanism. The compounds inhibit viral entry of the VLPs bearing EBOV GP in a dose dependent manner in both SNB19 and Vero E6 cells. The observed entry inhibition occurs after viral binding and internalization and does not involve inhibition of endosome acidification. Finally, based on our studies, the entry inhibition is not due to inhibition of cathepsin activity necessary for viral entry. Given this knowledge, we hypothesize that the activity is inhibiting either virus trafficking after internalization or a fusion triggering step. Because neither compound impacts entry/infection by influenza virus (data not shown) or VLPs bearing VSV-G, which also rely on trafficking through the endosomal system, these compounds are likely impacting viral fusion triggering.

The biological actions of the ER antagonist have been shown to be more complex than simple binding to ERs, and the impact of SERMs can vary in cells and tissues. Several ER interactive mechanisms have been proposed (193), including gene activation via non-estrogen response elements. In addition to the proposed gene activation through non-ER response elements, tamoxifen has

been shown to exert nongenomic effects by binding to microsomal anti-estrogen binding sites (AEBS). Clomiphene and other ER antagonists have been shown to impact sterols and fatty acids in bacteria, yeast and humans (10, 52, 93, 195, 223).

Interestingly, inhibition of the sterol biosynthesis pathway through host-mediated mechanisms or pharmacological manipulation has been implicated as a defense mechanism against viral infection for several viruses (45, 88, 118, 146, 177, 192, 204, 214, 284). Therefore, clomiphene citrate and toremifene citrate could be mediating their anti-EBOV activity through inhibition of the sterol biosynthesis pathway. It is possible that the resultant decrease in cholesterol results in modification of the membrane composition in the late endosome preventing viral fusion. Clomiphene citrate is a squalene epoxidase inhibitor which targets the sterol pathway downstream of HMG CoA reductase, the branch point for the protein prenylation pathway and squalene synthase (192). To further understand if inhibition of sterol biosynthesis pathway could play a role in ebolavirus entry, we tested U18666A which is an oxidosqualene cyclase (OSC) inhibitor that inhibits sterol synthesis downstream of clomiphene citrate (192), in the EBOV VLP entry assay. Our results indicate that U18666A does inhibit VLP entry (Shoemaker, submitted manuscript). In addition to inhibiting OSC and sterol biosynthesis, U18666A inhibits the trafficking of cholesterol including trafficking from the late endosomes (reviewed in(37)). The inhibition of cholesterol trafficking by U18666A mimics the loss of functional Niemann-Pick type C protein which is responsible for Niemann-Pick disease. It is possible that

the inhibition of cholesterol trafficking by U18666A could be contributing to its ability to block EBOV VLP entry. Definitive studies using native EBOV and EBOV VLPs, coupled with pharmaceutical manipulation of additional targets along the sterol pathway are required to explore the relevance of cholesterol synthesis and/or trafficking to EBOV entry.

These studies highlight the benefits of phenotypic high-throughput screening that utilizes assays that capture the full viral lifecycle. By screening with an approved drug library, we identified off-target host-cell mediated mechanisms for the ER antagonists clomiphene citrate and toremifene citrate. The approved drug status of the clomiphene citrate and toremifene citrate may allow them to be rapidly developed for use with filovirus disease. The oral availability of these drugs offers great utility in the resource-constrained geographical regions filovirus infection outbreaks frequently occur. Further studies are necessary to understand the antiviral impact of these compounds and their usefulness as treatments for filovirus infections. Current efforts are focused on the development of these drugs as a medical countermeasure alone or through synergistic combinations with other antiviral drugs identified in the drug screen.

### **Acknowledgements**

The authors thank Jonathan Towner for the eGFP expressing EBOV variant. We also thank Debbie Julias for assistance with the animal infection studies; James Pettitt for running the MARV assays; Jill Grenier for assistance with compound plate generation and for the evaluation of active compounds on MARV infection;

Mary Beth Kasda for technical assistance; and Elizabeth Nelson for technical assistance.

This work is funded by DTRA project 4.10007\_08\_RD\_B awarded to G.G.O and subcontract (W81XWH-08-0051) awarded to L.M.J. from USAMRIID as well a National Institute of Health grant U54 AI057168 awarded to J. W. Opinions, interpretations, conclusions, and recommendations are those of the author and are not necessarily endorsed by the U.S. Army.

**Chapter IV: Multiple Cationic Amphiphiles that  
Induce a Niemann-Pick C Phenotype Inhibit Ebola  
Virus Entry and Infection**

Charles J. Shoemaker, Kathryn L. Schornberg, Sue E. Delos, Corinne Scully,  
Hassan Pajouhesh, Gene G. Olinger, Lisa M. Johansen,  
and Judith M. White

- Submitted Manuscript (236)

**Abstract**

Ebola virus (EBOV) is an enveloped RNA virus that causes hemorrhagic fever in humans and non-human primates (NHPs). Infection requires internalization from the cell surface and trafficking to a late endocytic compartment, where viral fusion occurs, providing a conduit for the viral genome to enter the cytoplasm and initiate replication. In a concurrent study, we identified clomiphene as a potent inhibitor of EBOV entry. Here, we screened eleven inhibitors that target the same biosynthetic pathway as clomiphene. From this screen we identified six compounds, including U18666A, that block EBOV infection ( $IC_{50}$  1.6 to 8.0  $\mu$ M) at a late stage of entry. Intriguingly, all six are cationic amphiphiles that share additional chemical features. U18666A induces phenotypes, including cholesterol accumulation in endosomes, associated with defects in Niemann–Pick C1 protein (NPC1), a late endosomal and lysosomal protein required for EBOV entry. We tested and found that all six EBOV entry inhibitors from our screen induced cholesterol accumulation. We further showed that higher concentrations of cationic amphiphiles are required to inhibit EBOV entry into cells that overexpress NPC1 than parental cells, supporting the contention that they inhibit EBOV entry in an NPC1-dependent manner. A previously reported inhibitor, compound 3.47, inhibits EBOV entry by blocking binding of the EBOV glycoprotein to NPC1. None of the cationic amphiphiles tested had this effect. Hence, multiple cationic amphiphiles (including several FDA approved agents) inhibit EBOV entry in an NPC1-dependent fashion, but by a mechanism distinct from that of compound 3.47. Our findings suggest that

there are minimally two ways of perturbing NPC1-dependent pathways that can block EBOV entry, increasing NPC1's attractiveness as an anti-filoviral therapeutic target.

## **Introduction**

Ebolaviruses are members of the family Filoviridae. Infections by these viruses can produce acute hemorrhagic fever in humans and NHPs, with species dependent lethality ranging from ~50 to 90% (71, 104). However, there are currently no approved vaccines or anti-viral therapeutics with which to combat ebolavirus infections (71, 246). The virions are enveloped and contain a non-segmented negative-sense RNA genome. Morphologically, ebolaviruses are filamentous with a uniform diameter of ~80 nm and lengths ranging from several hundred nanometers to several micrometers (17, 83). The matrix protein VP40, the most abundant viral protein, drives virion formation (96, 188). The surrounding viral membrane is densely studded with a trimeric glycoprotein (GP) whose first function is to attach viral particles to the cell surface. The virions are then internalized into the cell by a macropinocytic-like process, (2, 107, 182, 183, 216) and trafficked to late endosomes and perhaps lysosomes, where the cysteine proteases, cathepsin B and cathepsin L, proteolytically prime GP to a 19 kDa fusogenic form (28, 40, 58, 159, 227). Fusion results in entry of the nucleocapsid into the cytoplasm, leading to genome replication and production of new virions (103).

Several cellular proteins required for the function and maturation of late endosomes (LE) and lysosomes (Lys) have recently emerged as ebolavirus entry

factors. These include subunits of the HOPS complex and NPC1 (35, 46, 94), a multi-membrane spanning protein found in the limiting membrane of late endosomes/ lysosomes (LE/Lys). When NPC1 is absent or dysfunctional, cholesterol and other substances accumulate in LE/Lys (145, 148). Interestingly, the ability of NPC1 to facilitate cholesterol egress from LE/Lys is not required for NPC1 to promote ebolavirus entry (35, 46). Although NPC1 can bind primed GP (171), its exact role(s) in ebolavirus entry has yet to be elucidated (276). Nonetheless, NPC1 appears to be a good target for anti-filovirus intervention (35, 46). For example, a novel inhibitor, compound 3.47, blocks binding of cathepsin-primed GP from Zaire ebolavirus (EBOV) to NPC1, and therefore blocks EBOV entry and infection (46).

The goal of this study was to identify additional small molecule EBOV entry inhibitors, and to probe their mechanisms of action. As a result, we identified six structurally related cationic amphiphiles that specifically blocked a late stage of EBOV entry. All of the inhibitors induced cholesterol accumulation in LE/Lys and those tested showed shifted dose-response curves in NPC1-overexpressing cells. However, none blocked the interaction of primed GP with NPC1. These results suggest that there are at least two ways of interfering with NPC1-dependent mechanisms that block EBOV entry into the cytoplasm, and that structurally-related cationic amphiphiles may prove clinically useful in combating EBOV infection.

## Materials and Methods

**Cells and plasmids.** HEK 293T cells (ATCC: CRL-11268) were maintained in high glucose Dulbecco's Modified Eagle Medium (DMEM, Gibco Invitrogen) supplemented with 10% supplemented calf serum (Hyclone), 1% antibiotic/antimycotic, 1% L-Glutamine, and 1% Sodium Pyruvate. SNB19 human glioblastoma cells (ATCC: CRL-2219) were maintained in DMEM supplemented with 10% FBS, 1% antibiotic/ antimycotic, 1% L-Glutamine, and 1% Sodium Pyruvate. Vero E6 cells (ATCC: CRL-1586) were maintained in Eagle's Minimum Essential medium (Gibco Invitrogen) supplemented with 10% FBS. JP17 parental Chinese Hamster Ovary cells (CHO) and JP17 cells overexpressing human NPC1 with a FLAG tag (CHO NPC1) were a gift of Frances Sharom and were maintained as previously described (145). mCherry-VP40 was generated by sub-cloning the VP40 gene from pCAGGS VP40 (gift of Yoshihiro Kawaoka), and inserting it, in-frame, to the C-terminus of mCherry in the pmCherry-C1 vector (Clontech).

**Chemical reagents.** Chemicals were obtained from the following sources: 5-(N-Ethyl-N-isopropyl) amiloride (EIPA; CAS 1154-25-2), clomiphene citrate (CAS 50-41-9), triparanol (CAS 78-41-1), BM 15766 (CAS 86621-94-5), SR 12813 (CAS 126411-39-0), and Filipin (CAS 480-49-9) (Sigma-Aldrich); bafilomycin A1 (CAS 88899-55-2) (LC Laboratories); U18666A (CAS 3039-71-2) and E64d (CAS 88321-09-9) (EMD Biosciences; Ro 48-8071 (CAS 161582-11-2) (BIOMOL); AY-9944 (CAS 366-93-8) (TOCRIS); alendronate sodium (CAS 129318-43-0) (ABATRA); terconazole (CAS 67915-31-5) (LEIRAS); amorolfine hydrochloride

(CAS 106614-68-0) (LKT); colestolone (CAS 50673-97-7)(Fisher Scientific).

Compound 3.47 was synthesized as previously described (46).

**Virus-like particle (VLP) production.** Using Polyethylenimine (PolySciences Inc), 293T cells were co-transfected with plasmids encoding EBOV GP (Zaire-Mayinga) deleted for the mucin domain (GP $\Delta$ ) along with three forms of the EBOV matrix protein: untagged VP40, VP40 tagged with  $\beta$ -lactamase, and VP40 tagged with mCherry (116, 157, 188). The plasmids were transfected at a ratio of 6:4:9:9 respectively. The mucin domain of GP has been shown to be dispensible for infection in tissue culture studies (112). Control VLPs were prepared by replacing the plasmid encoding EBOV GP $\Delta$  with plasmids encoding VSV-G (gift of Michael Whitt) or LCMV GP (gift of Jack Nunberg). Media were harvested at 24 and 48 hr post-transfection, and cleared of debris twice by centrifugation at 1,500 x g for 10 min at 4°C. VLPs were then pelleted through 20% sucrose in virus resuspension buffer (VRB; 130 mM NaCl, 20 mM HEPES, pH 7.4) by centrifugation for 2 hr at 112,398 x g (25,000 rpm) in an SW28 rotor at 4°C. VLPs were resuspended overnight in 10% sucrose-VRB at 4°C, and then frozen at -80°C for long-term storage. VLPs were examined by immunofluorescence microscopy, which showed a high incorporation of GP into mCherry labeled VLPs. Analysis by negative stain electron microscopy showed that the VLPs were densely studded with GP spikes (235).

**VLP internalization and cytoplasmic entry assays.** The day before each experiment, 100,000 SNB19 cells were seeded into each well of a 48-well plate. All internalization and cytoplasmic entry assays were conducted in serum-free

Optimem I media (Gibco Invitrogen). For inhibitor studies, SNB19 cells were pretreated with either DMSO (mock) or the indicated concentration of inhibitor for 1 hr at 37°C, and inhibitors were maintained in all following steps. Cells were then pre-chilled to 4°C for 15 min, and VLPs were bound to cells by spinfection at 250 x g for 1 hr at 4°C. Following 2 washes with inhibitor (where appropriate), cells were warmed to 37°C for 1 hr or 3 hr in a 5% CO<sub>2</sub> incubator for the internalization and cytoplasmic entry assays, respectively. Cells were then processed as indicated below.

For the internalization assay, samples were treated with 0.5% Trypsin-EDTA (Gibco Invitrogen) for 30 min at 4°C to strip surface associated particles. Cells were then lifted by gentle pipeting, washed, fixed, and analyzed on an LSR Fortessa flow cytometer (Becton Dickinson). Gating in the mCherry channel was determined from samples that were not exposed to VLPs, and data are presented as percent of cells with mCherry fluorescent signal. Cells exposed to VLPs, but maintained at 4°C throughout the experiment, served as a control confirming the efficiency of protease stripping of non- internalized VLPs. For the cytoplasmic entry assay, samples were washed once with loading buffer (phenol red free DMEM supplemented with 2 mM L-glutamine, 2.5  $\mu$ M probenecid, 25 mM HEPES, and 200 nM Bafilomycin) post-incubation. Cells were then incubated in the dark for 1 hr at RT in loading buffer supplemented with 1  $\mu$ M CCF2-AM (Invitrogen), a  $\beta$ -lactamase substrate. Cells were washed with loading buffer and then incubated overnight in the dark at RT with 10% FBS-loading buffer. Cells were lifted with trypsin, fixed, and analyzed on a FACSCaliber flow

cytometer. Cytoplasmic entry was assessed by the degree of positive shift by cells in the blue channel (447 nm emission) relative to cells that did not receive any VLPs. All flow cytometric data were analyzed with FlowJo software.

We validated the multi-purpose EBOV VLPs using chemical inhibitors and mutant GP proteins. For example, we showed that the cathepsin inhibitor, E64d, as well as the F535R fusion loop mutation in GP, potentially block EBOV-GP-VLP entry into the cytoplasm while having no effect on VLP internalization. We further characterized the kinetics of VLP internalization and cytoplasmic entry and, interestingly, found that cathepsin priming to 19 kDa GP is not a rate-limiting step for cytoplasmic entry (235).

**Live virus infections.** Infections were conducted with EBOV engineered to express the green fluorescent protein (EBOV-eGFP) (256). Vero E6 cells were infected as described in Johansen, et al. (115). All infections were performed in bio-safety level 4 (BSL-4) facilities at USAMRIID: personnel wear positive-pressure protective suits (ILC Dover, Frederica, DE) fitted with HEPA filters and umbilical-fed air. USAMRIID is registered with the Centers for Disease Control (CDC) Select Agent Program for the possession and use of biological select agents and toxins and has implemented a biological surety program in accordance with U.S. Army regulation AR 50-1 "Biological Surety". All procedures were conducted as previously described (240).

**Pseudovirion infection.** GFP encoding VSV-GP $\Delta$  was produced as described previously (227). The day before each experiment, 20,000 parental CHO or NPC1 overexpressing CHO NPC1 cells were seeded in each well of a 96 well

micro-titer plate. On the day of the experiment, cells were pre-treated with the indicated concentration of inhibitor for 1 hr at 37°C in a 5% CO<sub>2</sub> incubator. Cells were then infected in the presence or absence of inhibitor with VSV-GPΔ at a multiplicity of infection of ~0.5. Infections were allowed to proceed for 18 hr at which time samples were fixed and analyzed by flow cytometry for GFP expression (227).

**NPC1-19 kDa GP coimmunoprecipitation.** A fraction enriched for LE/Lys was prepared from CHO NPC1 cells essentially as described (46), except that the cells were first sheared with a cell cracker (11) with a cylinder bore of 0.25 inches and an 0.2496 inch diameter ball bearing. Briefly, CHO NPC1 cells were lifted and resuspended at a density of  $1.5 \times 10^6$  to  $2.5 \times 10^6$  cells/mL in HMB buffer (250 mM sucrose, 1 mM EDTA, 10 mM HEPES, pH 7.0) with protease inhibitors. After allowing cells to swell for 10 min on ice, cells were passed through the cell cracker 7 times. The cell homogenate was examined by microscope to confirm that plasma membranes (but not nuclear membranes) had been disrupted. Nuclei were then pelleted, and the post-nuclear supernatant was then centrifuged at  $15,000 \times g$  (9,400 rpm) in an SW41 rotor for 32 minutes at 4°C. Membrane pellets were then resuspended in HMB buffer, and the protein concentration was determined by BCA and adjusted to ~2 mg/mL. After disrupting the membranes with 20 mM methionine methyl-ester for 1 hr at RT, ~150 μg of disrupted NPC1-enriched membranes were pre-incubated with the indicated concentration of inhibitor for 30 min at RT. Next, 3 μg of soluble EBOV GP trimeric ectodomain (gift of Lianying Yan and Chris Broder), either full length (negative control) or

cleaved to the 19 kDa form were added. Cleavage to 19 kDa GP was accomplished by treating the full length ectodomain (0.5 mg/mL in 20 mM Mes, 20 mM HEPES, 130 mM NaCl) with 0.2 mg/mL of thermolysin (containing 2 mM  $\text{Ca}^{+2}$ ) for 1 hr at 37°C (28). Reactions were quenched with 500  $\mu\text{M}$  phosphoramidon and the GP proteins were frozen at -80°C until use. Cleavage of GP to 19 kDa was confirmed by western blot (data not shown). After incubating with ectodomain proteins for 1 hr at RT, the membranes were disrupted with 10 mM CHAPSO (EMD Biosciences) in TNE buffer (10 mM Tris, 150 mM NaCl, 1 mM EDTA, pH 7.4). After clearing debris at 21,100 x g (14,800 rpm) for 10 min at 4°C, supernatants were incubated with anti-FLAG coated magnetic beads (Sigma) overnight at 4°C with end-over-end rotation. The magnetic beads were then collected, washed 2 times with bead wash buffer (10 mM CHAPSO in TNE (pH 7.4) w/ protease inhibitors), and exposed to 0.1M glycine, pH 3.0 for 5 min at RT to elute bound GP and NPC1-FLAG from the anti-FLAG beads. The eluted proteins were then denatured in SDS sample buffer with DTT at a final conc. of 9 mM, and run on an Any KD® SDS-PAGE gel (Biorad). Proteins were transferred to nitrocellulose, and blotted with polyclonal antibodies against EBOV GP (gift of Paul Bates) and NPC1 (ThermoFischer Scientific: PA1-16817). Protein blots were imaged on an Odyssey® Infrared Imaging System (LI-COR Biosciences), and band intensities were quantified using Odyssey application software (version 3.0.16) and reported as the band intensity of GP or GP<sub>19 kDa</sub> divided by the band intensity of NPC1-FLAG.

**Cholesterol accumulation assay.** Cholesterol accumulation was monitored by staining SNB19 cells with filipin, as described in Kobayashi, et al. (124). The day before an experiment, 50,000 cells were plated on glass coverslips in a 24 well plate. The next day, cells were treated with inhibitors at the indicated concentrations for 21 hr. After fixation with 4% paraformaldehyde, cells were washed twice with PBS, incubated in 50  $\mu\text{g/mL}$  filipin (Sigma-Aldrich) in PBS for 1 hr at RT, and washed 3 times with PBS, after which the coverslips were mounted and imaged on a Zeiss Axio Observer fluorescence microscope. Samples were scored for cholesterol accumulation in LE/Lys by a blind observer in a minimum of 3 separate experiments. Representative images were inverted for clarity, and are shown with uniform adjustments to brightness and contrast across all images.

**Endosomal acidification and cathepsin activity assays.** Effects of inhibitors on endosomal pH and cathepsin B and L activity in SNB19 cells were assessed as described previously (115).

**Analyses of chemical structures.** The  $pK_a$  values were determined using the ACD/  $pK_a$  program, which quickly and accurately predicts the acid–base ionization constant of a wide range of organic compounds. It uses Hammett equations derived from a library of highly curated compounds to predict an aqueous  $pK_a$  value. In addition, two reference databases are available that offer quick look-ups of published data: one contains > 31,000 experimental  $pK_a$  values for approximately 16,000 compounds in aqueous solutions; the other provides experimental data for more than 2,000 molecules in non-aqueous solvents. This

software is used by the majority of pharmaceutical companies worldwide, and has been tested on a wide variety of chemical classes (68, 209, 239). The  $\text{clogP}$  is the log of the octanol-water partition coefficient,  $P$ , and is related to the hydrophobic character of the molecule. It is useful in predicting solubility, drug-likeness, and permeability. The values were determined using the ChemDraw program, which calculates the octanol-water coefficient for a wide range of neutral compounds under standard conditions, at 25°C. The calculations are provided with 95% confidence intervals (86, 263).

## Results and Discussion

**A subset of sterol synthesis inhibitors block EBOV entry and infection.** We recently found that clomiphene, an FDA-approved drug, blocks EBOV infection of Vero cells ( $\text{IC}_{50} = 2.42 \mu\text{M}$ ) (115). Clomiphene also inhibits EBOV in a mouse model of infection, providing 90% survival at day 28 post-infection. Although best known as an estrogen receptor antagonist, clomiphene inhibits EBOV infection whether or not target cells express estrogen receptors. Clomiphene is also known as an inhibitor of squalene epoxidase, a key enzyme in the pathway of sterol synthesis (192), a pathway necessary for infection by several viruses including hepatitis C virus (HCV) (20). We therefore tested eleven sterol synthesis pathway inhibitors, previously shown to affect replication of HCV, for their effects on EBOV infection (192). Seven of the eleven compounds tested inhibited infection by replication competent EBOV; the other four had no significant effect (Fig. 4.1). Since some, but not all, of the sterol synthesis

inhibitors blocked EBOV infection, it appears that, unlike for HCV (192), inhibition of sterol synthesis *per se* is not the mechanism by which these drugs block EBOV infection.

We next tested the panel of eleven compounds for their effects on EBOV GP $\Delta$ -mediated entry into the cytoplasm of host cells. We did this using VLPs containing EBOV VP40 fused with  $\beta$ -lactamase (157, 238) as well as EBOV GP $\Delta$  on their surface (235). When the VLPs fuse with the limiting membrane of a LE/Lys, VP40  $\beta$ -lactamase reaches the cytoplasm, where it can cleave a loaded substrate, causing a fluorescent color shift that can be read by flow cytometry (286). As seen in figure 4.2, eight of the compounds inhibited VLP entry. Six of them (clomiphene, Ro 48-8071, U18666A, terconazole, AY- 9944, and triparanol) inhibited entry  $\geq 91\%$  at the concentration tested (dashed line in Fig. 4.2), an apparent threshold (in this single cycle assay) for a corresponding inhibition of multiple cycles of replication with authentic virus (Fig. 4.1).

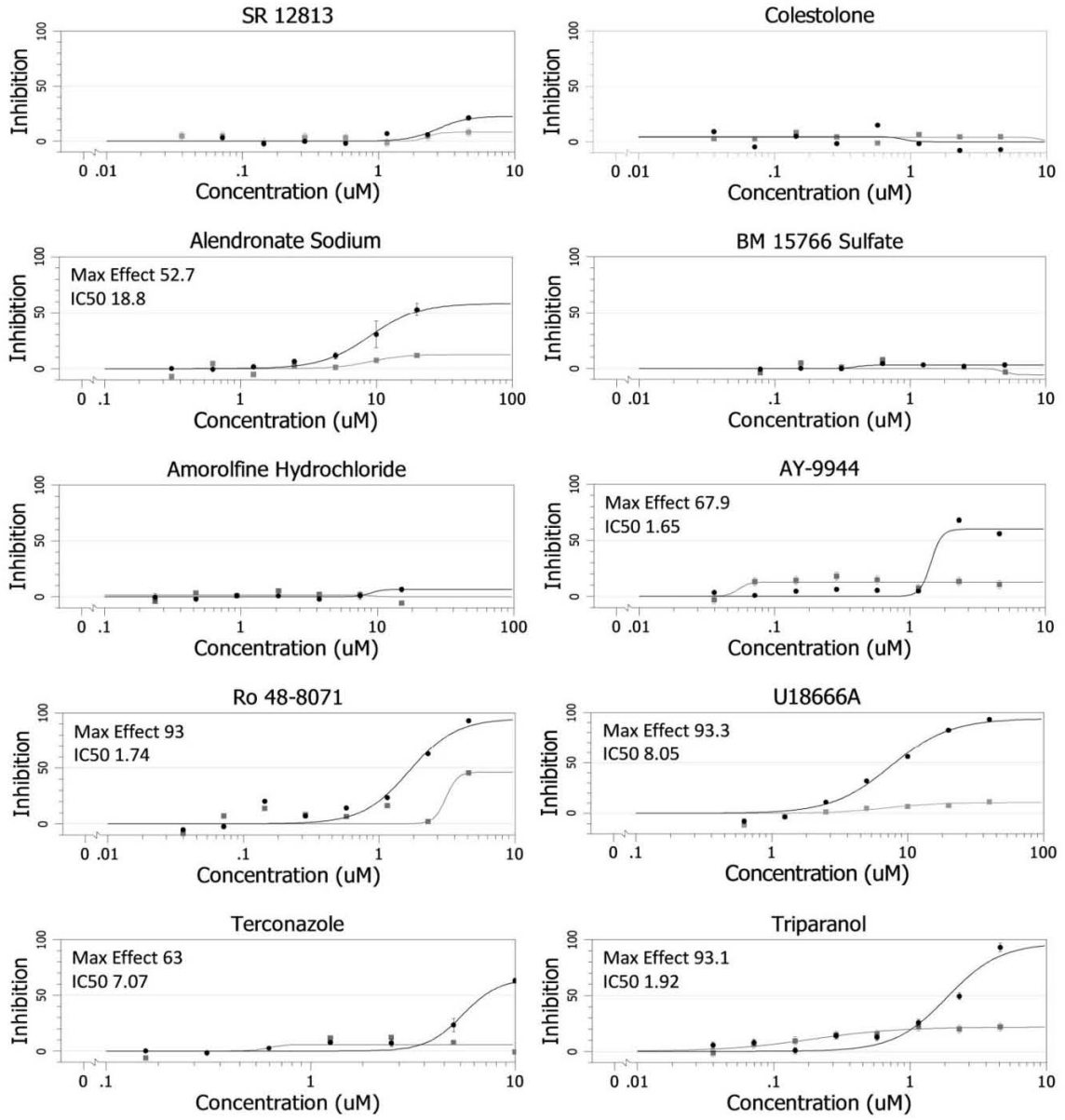
**Newly-identified strong EBOV entry inhibitors are cationic amphiphilic drugs.** Structures for the eleven compounds analyzed in this study are given in figure 4.9. Among them, eight are amphiphiles and three are not (Table 4.1). Among the three non-amphiphiles (blue in Fig. 4.2), two (SR12813 and colestolone) had no effect on EBOV infection (Fig. 4.1). The third, alendronate, inhibited infection (Fig. 4.1), but did not inhibit entry (Fig. 4.2), indicating that it blocks a post-entry step in the EBOV life cycle.

Among the eight amphiphiles, six strongly inhibited EBOV entry ( $\geq 91\%$ ) and infection. The six strong inhibitors are all cationic amphiphilic drugs (CADs),

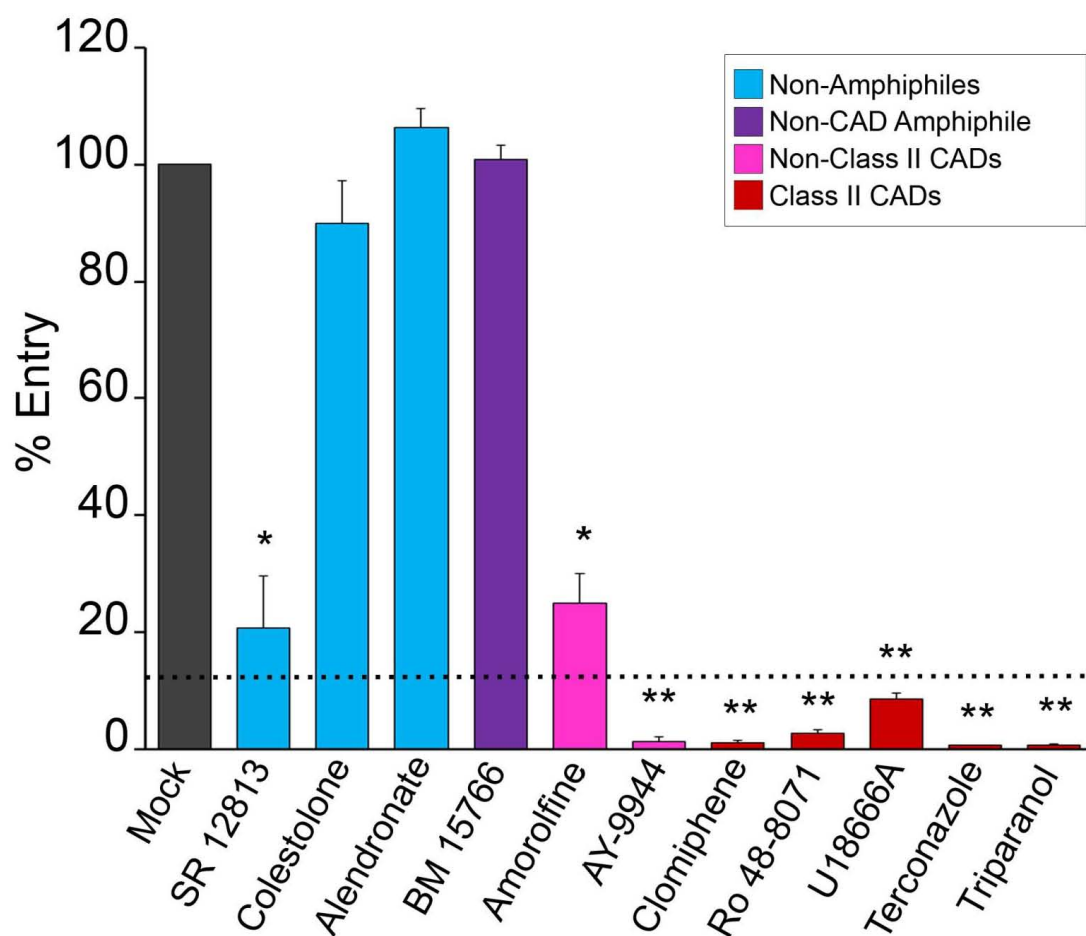
and five of the six are class II CADs (clomiphene, Ro 48-8071, U18666A, terconazole, and triparanol; red in Fig. 4.2); a class II CAD is an amphiphilic amine with clearly segregated hydrophobic and hydrophilic segments (Fig. 4.9, Table 4.1). The other three amphiphiles tested were BM 15766 (a zwitterionic amphiphile), AY-9944 and amorolfine. The zwitterionic amphiphile, BM 15766 (purple in Fig. 4.2), did not inhibit EBOV GP-mediated entry or infection, suggesting the importance of positive molecular charge for this entry inhibition mechanism. Interestingly, among the two non-class II CADs (pink in Fig. 4.2), AY-9944 strongly inhibited EBOV GP-mediated entry and infection, while amorolfine had only a modest effect on entry and no effect on infection. The  $pK_a$  of AY-9944, an EBOV inhibitor, is 9.1, whereas that of amorolfine, a non-inhibitor, is 7.1. All of the other strong EBOV entry inhibitors identified in this screen have  $pK_a$  values  $> 8.8$ . The relatively low  $pK_a$  of amorolfine might result in lower sequestration in LE/Lys (61), which could, in turn, account for its limited effect on EBOV entry, despite being a CAD.

Thus, the common features of the six strong EBOV entry inhibitors identified in this analysis (last six compounds in Fig. 4.2) are that they are all CADs (five of the six being class II CADs) containing one or more secondary or tertiary amines protonatable at physiological pH (Fig. 4.9; Table 4.1). Furthermore, all six strong CAD inhibitors have molecular weights in the range of 388 to 532, clogP values between 4.8 and 7.2, and  $pK_a$  values between 8.8 and 9.7. All six also cause cholesterol accumulation in endosomes (see below).

**Figure 4.1. Effects of sterol pathway inhibitors on EBOV infection.** Dose response curves for the indicated sterol pathway inhibitors are shown. The compounds were evaluated, in parallel at the indicated concentrations, for their ability to inhibit EBOV infection (black) and for inhibition of cell proliferation (gray). The maximal % inhibition and the IC<sub>50</sub> (μM) for their effects on EBOV infection are indicated. Data for clomiphene are presented in Johansen et al. (28).



**Figure 4.2. Effects of sterol pathway inhibitors on EBOV VLP entry.** SNB19 cells were pretreated with inhibitor for 1 hr, and EBOV VLP-GPΔ was then bound by spinfection at 4°C for 1 hr. Cells were then washed in media with inhibitor, incubated at 37°C for 3 hr (in inhibitor), and then processed for VLP entry as described in the Materials and Methods section. Compounds were tested in multiple (n) experiments (each in triplicate) at either the highest concentration under which no toxicity was observed (for compounds that did not inhibit infection), or at the concentration that resulted in maximum inhibition of EBOV infection (Fig. 1) with minimal toxicity: SR 12813 (5 μM), (n=4), colestolone (10 μM), (n=5), alendronate (20 μM), (n=3), BM 15766 (2 μM), (n=4), amorolfine (6 μM), (n=4), AY-9944 (5 μM), (n=3), clomiphene (5 μM), (n=9), Ro 48-8071 (5 μM, (n=6), U18666A (5 μM), (n=7), terconazole (10 μM), (n=4), and triparanol (5 μM), (n=3). Error bars represent standard error: \* ( $P < 2.96 \times 10^{-3}$ ) or \*\* ( $P < 6.14 \times 10^{-5}$ ). Dashed line represents the observed threshold for entry inhibition needed to observe corresponding inhibition of live EBOV infection (Fig 1). As indicated in the key, colors denote classes of molecules. Note that three of the nine experiments averaged to generate the values for clomiphene are from Johansen et al. (28).



**CADs inhibit a late stage of EBOV entry.** We characterized the mode of action of two of the CADs, Ro 48-8071 and U18666A, in more detail. As seen in figures 4.3A and B, Ro 48-8071 strongly inhibited entry of VLP-GP $\Delta$  into the cytoplasm, while having only small effects on the cytoplasmic entry of VLPs coated with either VSV G (Fig. 4.3A) or LCMV GP (Fig. 4.3B), indicating specificity for EBOV GP-mediated entry rather than a general impairment in function of early or late endosomes. Moreover, Ro 48-8071 did not inhibit VLP-GP $\Delta$  internalization from the cell surface (Fig. 4.3C), endosomal acidification (Fig. 4.3D), or cathepsin activity levels (Fig. 4.3E). U18666A (Fig. 4.4) and clomiphen (115) behaved similarly to Ro 48-8071 in all of these respects. Hence, these CADs most likely impede EBOV entry by blocking events closely associated with EBOV fusion with the limiting membrane of a LE/Lys.

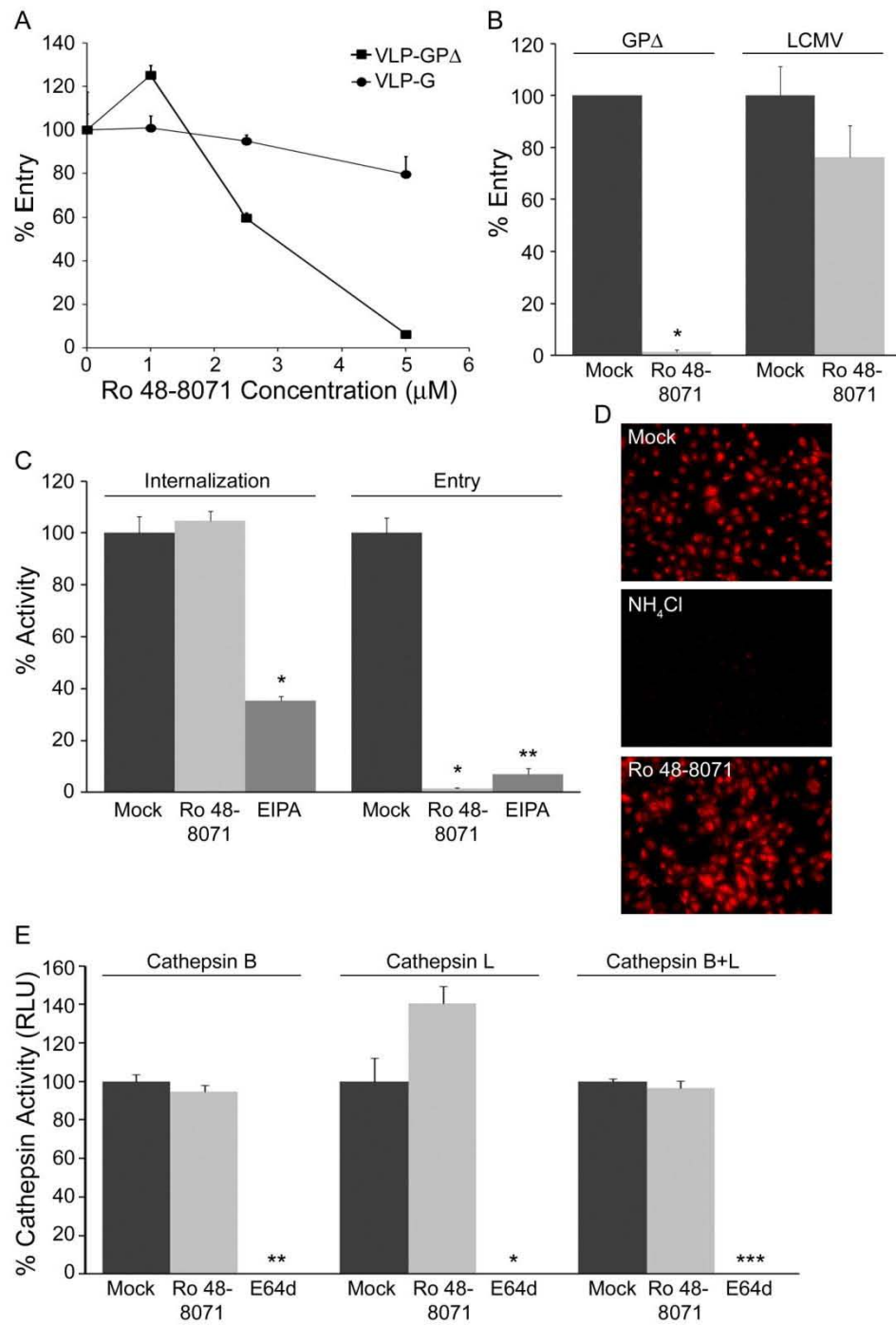
**CADs inhibit EBOV entry through an NPC1-dependent pathway.** U18666A, one of the inhibitors identified in our set, as well as by Carette, et al. (35), is known to induce many of the defects seen in NPC1-deficient cells, notably cholesterol accumulation in LE/Lys (124). We therefore tested our panel of compounds for their effects on cholesterol accumulation (242). As seen in figure 4.5, the six CADs that potently inhibited VLP-GP $\Delta$  entry ( $\geq 91\%$ ) and EBOV infection all induced cholesterol accumulation in LE/Lys (bottom two rows, Fig. 4.5). In contrast, the compounds that did not strongly inhibit VLP-GP $\Delta$  entry did not cause detectable cholesterol accumulation (top two rows, Fig. 4.5). Two other CADs, which are not sterol synthesis pathway inhibitors, also block a late stage of EBOV GP-mediated entry, inhibit EBOV infection, and cause the cholesterol

accumulation phenotype ((115), and data not shown). Hence, among the CADs tested, there is a strict correlation between inhibition of EBOV entry and induction of cholesterol accumulation.

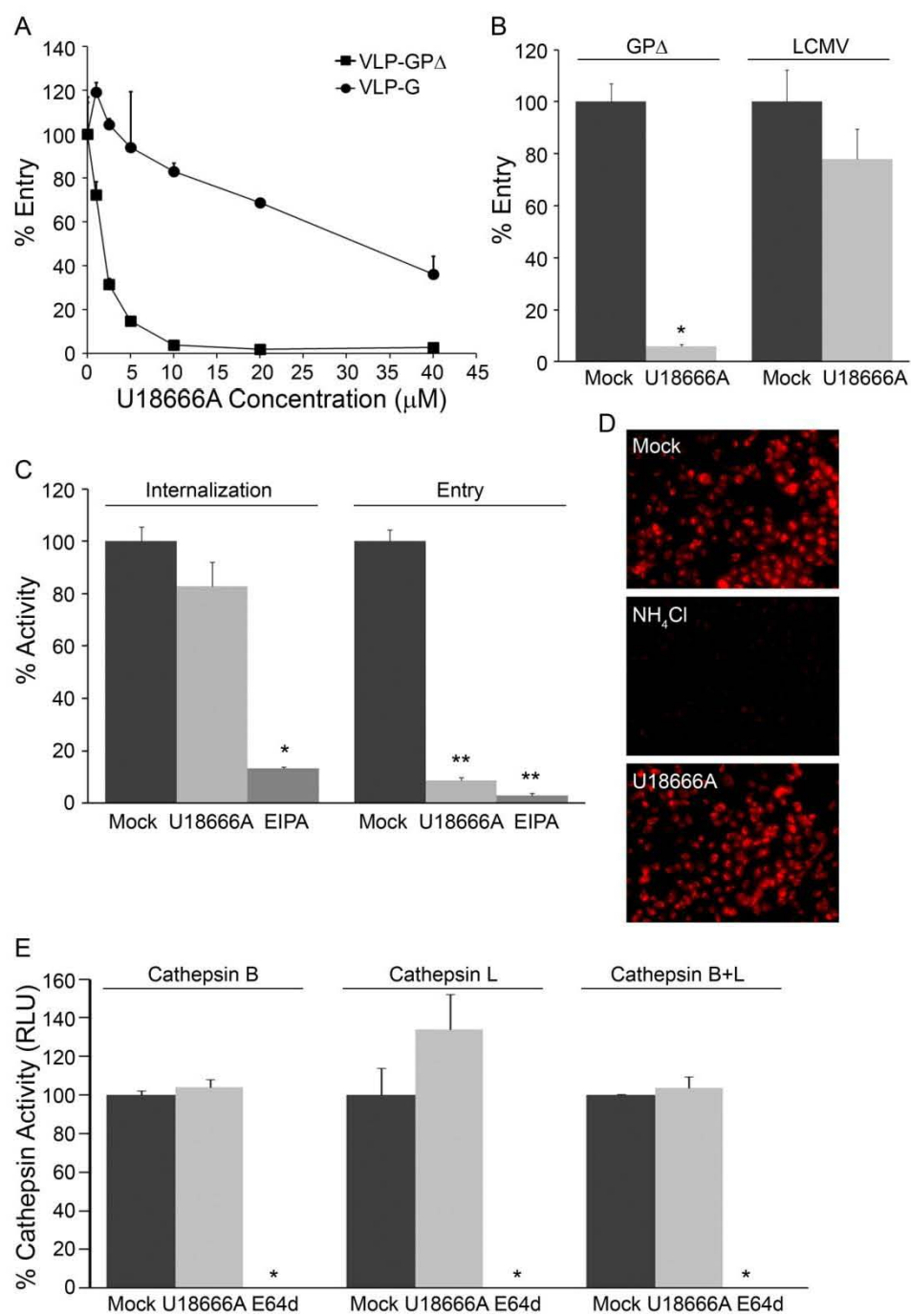
The results shown in figure 4.5 suggested that the six CADs that inhibit EBOV entry exert their effects through an NPC1-dependent pathway. To test this hypothesis, we compared the effects of three of them, clomiphene, Ro 48-8071, and U18666A, on EBOV GP-mediated pseudovirion infection in CHO cells expressing basal or heightened levels of NPC1. (The VLP cytoplasmic entry assay could not be performed in the NPC1 overexpressing cells due to beta lactamase activity from the ampicillin resistant plasmid used to create the cell line (102)). As a negative control, we tested the effects of the cysteine protease inhibitor E64d, which blocks EBOV entry by inhibiting cathepsins B and L (i.e. functions independent of NPC1). As predicted, E64d inhibited EBOV GP-mediated infection with the same dose-dependence in parental and NPC1 overexpressing cells (Fig. 4.6A). As shown previously, higher concentrations of compound 3.47, a piperazine that inhibits EBOV infection by blocking GP binding to NPC1 (46), were required to inhibit EBOV GP-mediated infection in NPC1 overexpressing vs. parental cells (Fig. 4.6B). Similar to compound 3.47, higher concentrations of each of the three CADs tested were required to inhibit EBOV GP-mediated infection of the NPC1-overexpressing cells relative to parental cells (Fig. 4.6C-E). Our findings for U18666A in the two cell lines (Fig. 4.6E) are consistent with the observation that higher concentrations of U18666A are required to induce cholesterol accumulation in cells that overexpress NPC1(123).

**Figure 4.3. Ro 48-8071 inhibits EBOV entry at a post internalization step and does not inhibit endosome acidification or cathepsin activity levels.**

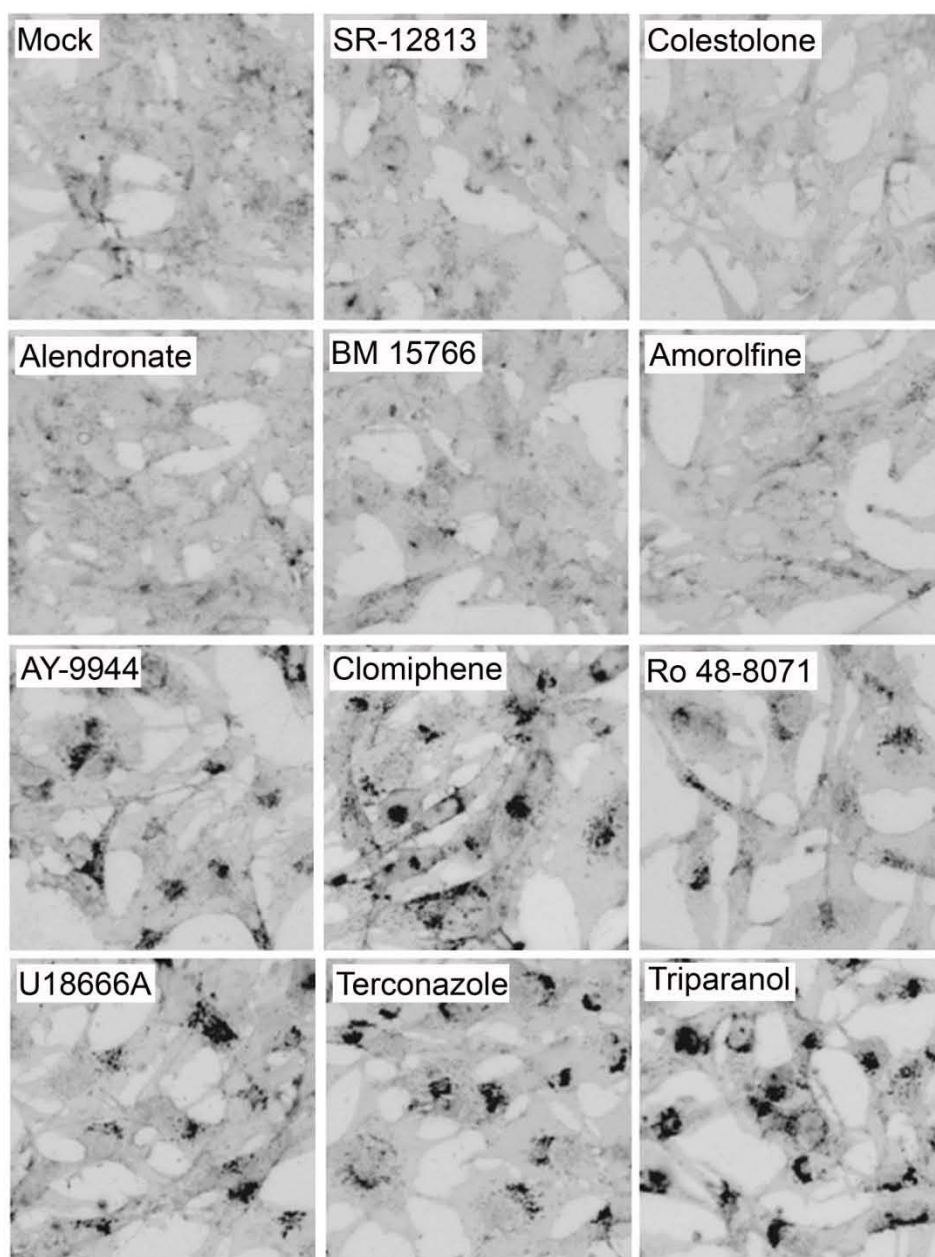
Effects of Ro 48-8071 (indicated concentration in A, 5  $\mu$ M in B-E) on: (A) VLP-GP $\Delta$  and VLP-G entry; one representative of two experiments (done in triplicate). (B) VLP-GP $\Delta$  and VLP-LCMV entry; one representative of three experiments (done in duplicate). (C) VLP-GP $\Delta$  internalization and entry; 50  $\mu$ M EIPA was used as the positive control for an inhibitor of EBOV internalization (49); 10  $\mu$ M EIPA was used as the control for the entry assay (50  $\mu$ M EIPA caused high background fluorescence in the entry assay); one representative of two experiments (done in triplicate). (D) Low endosomal pH was detected by incubating cells with LysoTracker Red; 10 mM NH<sub>4</sub>Cl was used as the control for pH neutralization; representative images from multiple coverslips from a single experiment. (E) Cathepsin B, L, and combined B/L activity; 10  $\mu$ M E64d was used as the positive control for inhibition of cysteine protease activity; results from a single experiment performed in duplicate. In all assays, SNB19 cells were pre-treated with the indicated concentration of inhibitor for 1 hr at 37°C, and inhibitors were maintained throughout the assays. Error bars represent standard deviation from the mean of mock-treated samples: \* (P<.01), \*\* (P<.001), or \*\*\* (P<.0001).



**Figure 4.4. U18666A inhibits EBOV entry at a post internalization step and does not inhibit endosome acidification or cathepsin activity levels.** Effects of U18666A (indicated concentration in A, 5  $\mu$ M in B-E) on: (A) VLP-GP $\Delta$  and VLP-G entry; one representative of two experiments (done in triplicate). (B) VLP-GP $\Delta$  and VLP-LCMV entry; one representative of three experiments (done in duplicate). (C) VLP-GP $\Delta$  internalization and entry (controls as in Fig. 3C); one representative of two experiments (done in triplicate). (D) Endosomal pH detected by LysoTracker Red; 10 mM NH<sub>4</sub>Cl was used as the control for pH neutralization; representative images from multiple coverslips from a single experiment (E) Cathepsin B, L, and combined B/L activity; E64d was used as the positive control as in Fig. 3E; results from a single experiment performed in duplicate. In all assays, SNB19 cells were pre-treated with the indicated concentration of inhibitor for 1 hr at 37°C, and inhibitors were maintained throughout the assays. Error bars represent standard deviation from the mean of mock-treated samples: \* (P<.01), \*\* (P<.001), or \*\*\* (P<.0001).



**Figure 4.5. CADs that strongly inhibit EBOV entry and infection cause cholesterol accumulation in LE/Lys.** SNB19 cells were treated for 21 hr with either DMSO or inhibitor (concentrations as in Fig. 2). Cells were then fixed, stained with filipin, and imaged on a fluorescence microscope. Images were inverted and uniformly adjusted for contrast and brightness. Representative images are shown. Each compound was tested at least 3 times, and scored (+/-) by a blind observer (Table 4.1).



Collectively, the results in figures 4.5 and 4.6 support our proposal that the CADs that block EBOV entry do so through an NPC1-dependent pathway.

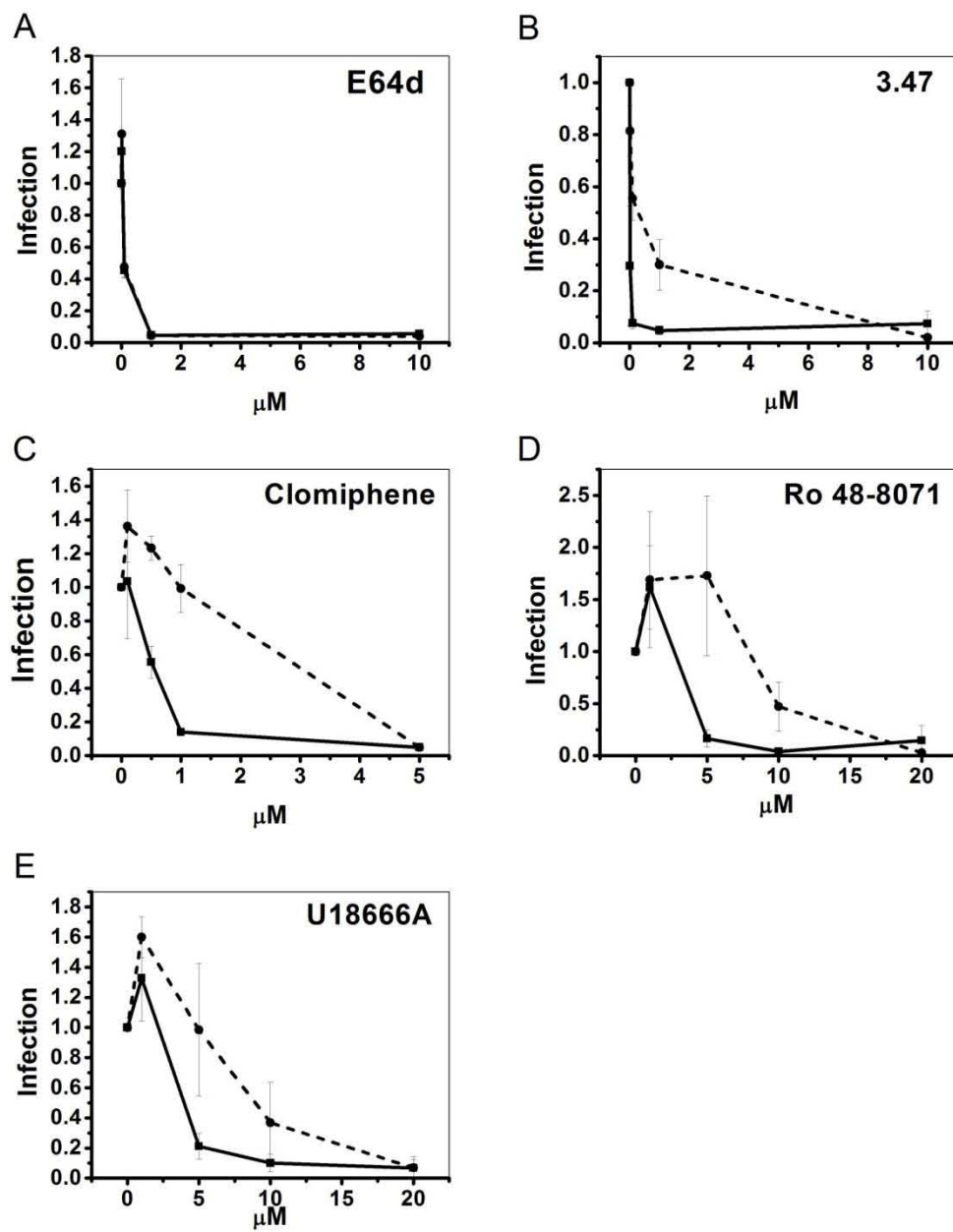
We note, however, that as for the requirement of NPC1 for EBOV entry (35, 46), the inhibitory effect of the CADs on EBOV entry is not likely a direct consequence of their induction of cholesterol accumulation. Our reasoning is that clomiphene, Ro 48-8071, and U18666A all inhibit EBOV entry well before they cause detectable cholesterol accumulation. For the entry experiments, cells are pretreated with inhibitors for 1 hr and then maintained in inhibitor during a 3 hr entry period. Furthermore, the CADs can be added at the initiation of VLP-GP $\Delta$  internalization and still strongly block entry (data not shown), whereas a minimum of ~8 hrs is required to see detectable cholesterol accumulation (147). Since EBOV GP-mediated entry begins within 1 hr following binding ((235), see Chap. II, Fig. 2.5) the CADs appear to act rapidly on a cellular target that is critical for EBOV entry.

**CADs do not disrupt the *in vitro* interaction of primed EBOV GP with NPC1.**

Compound 3.47, the piperazine EBOV entry inhibitor, blocks binding of cathepsin-primed EBOV GP to NPC1 *in vitro* (46). Curiously, it also causes cholesterol accumulation in LE/Lys ((46), and data not shown). We therefore asked whether clomiphene, Ro 48-8071, or U18666A act similarly. In contrast to compound 3.47, however, none of the CADs tested inhibited primed GP binding to NPC1 (nor, as expected, did the cathepsin inhibitor E64d) (Fig. 4.7).

Collectively, the results in figures 5, 6, and 7 suggest that the CADs that block EBOV entry do so by perturbing an NPC1-dependent pathway without, however,

**Figure 4.6. CADs inhibit EBOV GP-mediated infection in an NPC1-dependent manner.** Parental CHO cells (—■—) and stably overexpressing CHO NPC1 cells (-●-) were pre-treated with the indicated concentration of inhibitor for 1 hr at 37°C, and then infected with VSV-GPΔ for 18 hr in the continued presence of inhibitor. Each concentration of inhibitor was tested (in duplicate) in the following number of experiments: E64d (n=2), compound 3.47 (n=2), clomiphene (n=3), Ro 48-8071 (n=3), and U18666A (n=4). Infection values were normalized to DMSO treated samples and averaged across experiments. Error bars represent standard error.



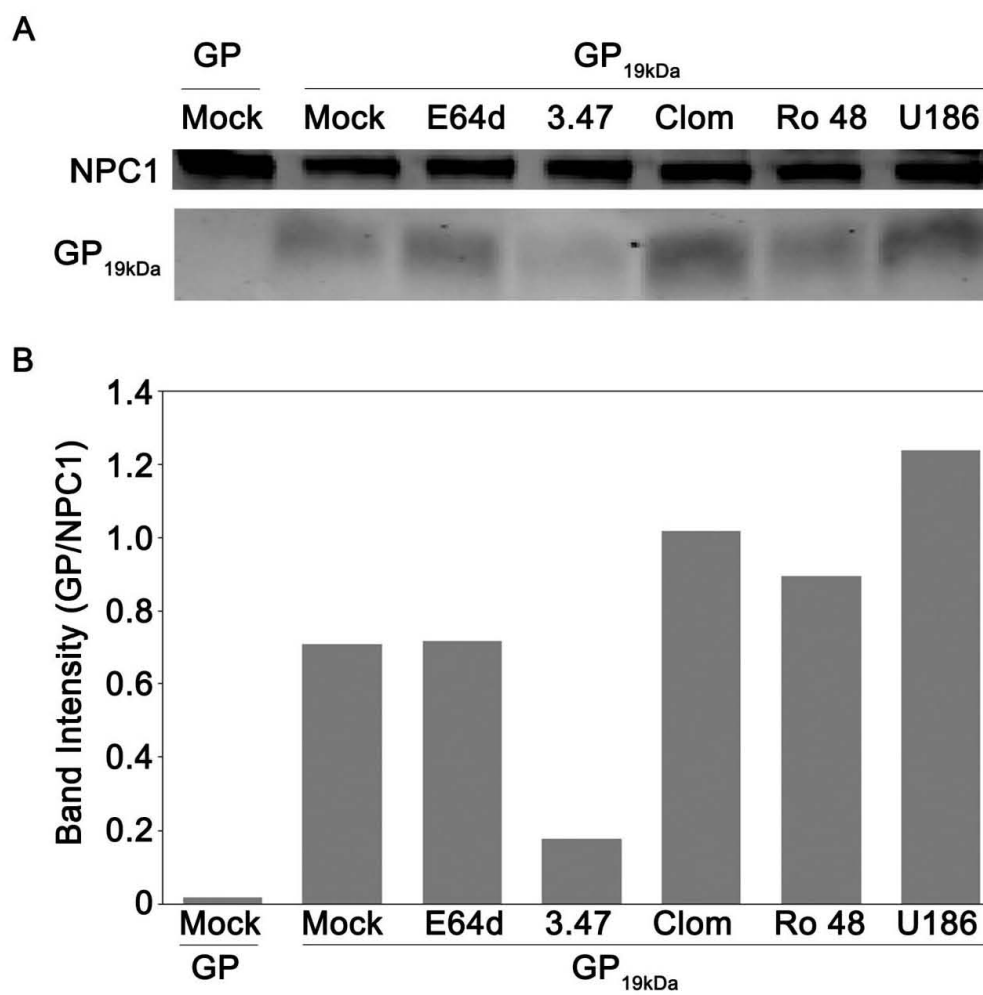
disrupting the direct interaction between NPC1 and primed EBOV GP.

**Three possible modes by which CADs inhibit EBOV entry.** Here, we have shown that six CADs inhibit EBOV infection by blocking GP-mediated entry: AY-9944, clomiphene, Ro 48-8071, U18666A, terconazole, and triparanol (Fig. 4.1 and 4.2, Table 4.1). Moreover, there are at least four other CADs that inhibit EBOV infection, likely by blocking entry (35, 115, 172). For the three CADs that we characterized in detail (clomiphene, Ro 48-8071, U18666A), we found that they all (a) block a late stage of entry (i.e., at or close to the step of membrane fusion) and (b) exert their effect through an NPC1-dependent pathway, but (c) do not impede the interaction between primed EBOV GP and NPC1. How then do these CADs inhibit EBOV entry, and in what way is NPC1 involved?

We envision three ways in which CADs might perturb EBOV entry in an NPC1-dependent manner (Fig. 4.8). In the first model (Fig. 4.8A), NPC1 is the direct target of the CADs, but they bind to a site distinct from the C-loop of NPC1, the binding site for primed GP (171). Support for this possibility is provided by fluorescence spectroscopy experiments showing an interaction between U18666A and purified NPC1 (145). According to model A, CAD binding to NPC1 compromises a second function of NPC1 in EBOV entry (i.e., in addition to binding primed GP). This function could be an NPC1-dependent modulation of the membrane or luminal composition of the LE/Lys (149, 241, 287) that renders the LE/Lys supportive of primed-GP mediated fusion (276). However, as previously described (35, 46), this purported second NPC1 function is not

**Figure 4.7. CADs do not disrupt the interaction of 19 kDa GP and NPC1.** (A)

NPC1-FLAG-enriched LE/Lys membranes from CHO NPC1 cells were disrupted and then incubated with inhibitors for 30 min at RT: mock (4% DMSO), E64d (10  $\mu$ M), compound 3.47 (13  $\mu$ M), clomiphene (242  $\mu$ M), Ro 48-8071 (174  $\mu$ M), and U18666A (800  $\mu$ M); each inhibitor was used at a concentration 100 fold over its  $IC_{50}$  for inhibition of infection. The samples were then incubated with 3  $\mu$ g uncleaved (GP) or cleaved (GP<sub>19 kDa</sub>) EBOV GP ectodomains for 1 hr at RT. Samples were then lysed, and incubated overnight with anti-FLAG beads. Bound NPC1 and GP were then eluted from beads, and run on an SDS-PAGE gel. The gel was then transferred, blotted for both NPC1 and EBOV GP, and imaged for fluorescent signal. As predicted, uncleaved GP (~130 kDa) did not co-precipitate with NPC1 (12, 41). (B) The intensities of the GP, GP<sub>19 kDa</sub>, and NPC1 bands from each sample of the blot shown in Fig. 7A were quantified and GP or GP<sub>19 kDa</sub> was normalized to its respective NPC1 band signal. The experiment was conducted four times with similar results, and a representative experiment is shown.



cholesterol egress from LE/Lys.

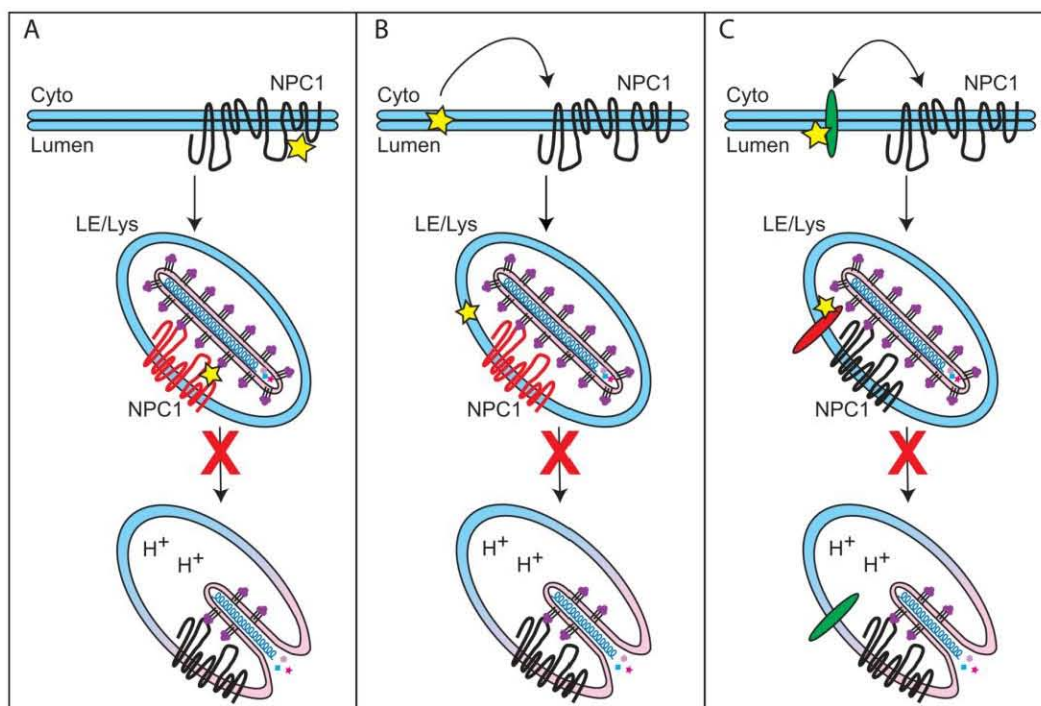
A second possible mechanism of action for the CADs (Fig. 4.8B) stems from their propensity to intercalate into membranes (37, 38). Such intercalation can disrupt membrane order and affect the function of integral membrane proteins. A precedent for such a scenario has been reported for two membrane proteins, P-glycoprotein (129) and a potassium ion channel (203). Similarly, by intercalating into the LE/Lys membrane, the CADs may indirectly affect a purported second function of NPC1 necessary for EBOV entry.

A third means by which CADs could block EBOV entry is by interacting (directly or indirectly) with a distinct (i.e., not NPC1) target (protein or membrane) in LE/Lys whose function is not only required for EBOV entry, but is also regulated by NPC1 (Fig. 4.8C). For example, a potential target could be acid sphingomyelinase (ASMase), a positively charged enzyme that interacts with negatively charged phospholipids in LE/Lys (126). According to several reports, in response to (positively charged) CADs, ASMase dissociates from LE/Lys membranes and is then degraded by acid hydrolases in the lumen of the LE/Lys (1, 8, 127). A similar set of events has been reported for another lysosomal enzyme in response to CADs (64). Deficiencies in ASMase cause cholesterol accumulation in LE/Lys and the genetic diseases Niemann Pick Types A and B (230). Moreover, there is evidence for cross-regulation of NPC1 and ASMase; it has been reported that ASMase activity is reduced ~50% in NPC1-deficient cells, and addition of exogenous ASMase to NPC1-deficient cells largely rescues their defect in cholesterol egress (54). Interestingly, a recent study has implicated

ASMase as a critical factor for EBOV entry (172). In this respect, it is further interesting that while low pH, cathepsins, and NPC1 are essential for EBOV entry, collectively these three endosomal factors are not sufficient to trigger EBOV fusion ((171, 276) and White lab, unpublished data). This suggests that at least one additional endosomal factor, perhaps ASMase, might be required to support EBOV fusion.

**Summary.** In this study we have presented two major findings. The first is that among eleven small molecules, there was a strict correlation between (a) their chemical structures and their abilities to: (b) induce cholesterol accumulation in LE/Lys, (c) potentially (>91%) block a late stage of EBOV VLP entry, and (d) block infection by replication competent EBOV. All of the potent inhibitors are CADs with similar MW, clogP, and  $pK_a$  values, and most are class II CADs with at least one tertiary amine group (Table 4.1, Fig 4.9). The second major result is that the CADs tested inhibit EBOV entry through an NPC1-dependent pathway, but by a mechanism that differs from the primary mode of action of compound 3.47, a piperazine that blocks binding of primed GP to NPC1 (46). Our findings have two implications. The first is that there are at least two ways to interfere with an NPC1-dependent pathway that can block EBOV entry. Speculatively, this suggests to us that NPC1 may play more than one role in EBOV entry (276). The second implication deals with further drug screening efforts. Collectively we and others have now identified ten CADs that inhibit EBOV, and six of these are FDA approved (35, 115, 172). As there are many other FDA-approved CADs, a data mining effort (for CADs with the chemical properties described above) may yield

**Figure 4.8. Models for how CADs may block EBOV entry.** (A) In the first model, the CADs (yellow star) interact directly with NPC1, but at a site distinct from the C loop of NPC1 (which binds GP<sub>19 kDa</sub>). Binding to NPC1 inhibits a second function of NPC1 (i.e. in addition to its role in binding GP<sub>19 kDa</sub>) that is critical for EBOV entry. (B) In the second model, the CADs intercalate into the LE/Lys membrane, indirectly inhibiting a second function of NPC1 that promotes EBOV entry. (C) In a final model, the CADs disrupt a target distinct from NPC1 that is critical for EBOV fusion with LE/Lys) and is regulated by NPC1. The target may be another LE/Lys protein (e.g. ASMase) or a lipid of the LE/Lys membrane system. (See text for details.) Alternatively, the CADs may interfere with NPC1-dependent membrane trafficking (30, 56) such that the virus is never found in an NPC1-containing compartment. In all of the models, the yellow star denotes a CAD and red in each middle image denotes the target molecule.



additional compounds to assess for potential repurposing to combat ebolavirus infections.

### **Acknowledgements**

The authors thank Dr. Jennifer Brannan (National Research Council Fellow), Jill Grenier, Calli Lear, James A. Simmons, Elizabeth Nelson, and James Pettit for excellent assistance.

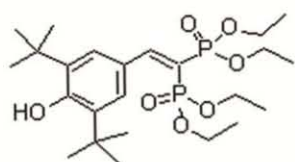
The work was funded by DTRA project 4.10007\_08\_RD\_B (G.G.O) and subcontract W81XWH-08-0051 (L.M.J) as well as a grant from the NIH: U54 AI057168 (J.M.W)

**Table 4.1. Properties and effects of sterol synthesis pathway inhibitors on EBOV entry and infection and on cholesterol accumulation in LE/Lys.** (a)

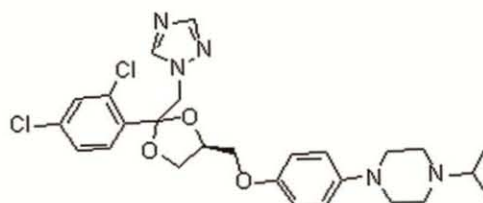
abbreviations of target enzymes in cholesterol synthesis pathway: HMGCR, HMG CoA Reductase; FPPS, Farnesyl pyrophosphate synthase; d7R, Sterol delta-7 reductase; c14d8, Lanosterol C14-demethylase/sterol delta; d7/d14R, Sterol delta-7 and delta-14 reductase; SQLE, Squalene epoxidase; OSC, 2,3 Oxidosqualene cyclase; c14dM, Lanosterol C14-demethylase; d24R, Sterol delta-24 reductase. (b) data for clomiphen are from Johansen et al., in revision; all other data are from Fig. 1. (c) data from Fig. 2. (d) data from Fig. 5; CHOL, cholesterol. (e) Ro 48-8071 appeared to induce less CHOL accumulation than the other inhibitors scored 'yes' for this phenotype. (f) CAD, Cationic amphiphilic drug. (g)  $pK_a$  and cLogP were calculated as described in the Methods section. All compounds highlighted in gray were shown to robustly block EBOV GP-mediated VLP entry ( $\geq 90\%$  inhibition) and infection by authentic EBOV.

Compound	Target Enzyme <sup>a</sup>	Inhibit EBOV Infection (IC <sub>50</sub> ) <sup>b</sup>	Inhibit VLP Entry <sup>c</sup> (% +/- SD)	Increase CHOL in LE/Lys <sup>d</sup>	Chemical Structure	MW	pK <sub>a</sub> <sup>g</sup>	clogP <sup>g</sup>
SR 12813	HMGCR	No	79.3 +/- 8.9	No	Not amphiphile	504.5	9.5	6.6
Colestolone	HMGCR	No	10.0 +/- 7.3	No	Not amphiphile	400.6	15.1	7.2
Alendronate	FPPS	Yes (18.8 $\mu$ M)	-6.3 +/- 3.3	No	Not amphiphile	248.1	14.4	-5.6
BM 15766	d7R	No	-7 +/- 2.5	No	Zwitterionic amphiphile	384.0	8.4	1.9
Amorolfine	c14d8	No	75.0 +/- 5.0	No	CAD <sup>f</sup>	317.0	7.1	6.4
AY 9944	d7/d14R	Yes (1.65 $\mu$ M)	98.7 +/- 0.8	Yes	CAD	391.4	9.1	6.4
Clomiphene	SQLE	Yes (2.42 $\mu$ M)	98.8 +/- .4	Yes	Class II CAD	405.9	9.6	7.2
Ro 48-8071	OSC	Yes (1.74 $\mu$ M)	97.2 +/- .6	Yes*	Class II CAD	434.3	8.8	5.7
U18666A	OSC	Yes (8.00 $\mu$ M)	91.4 +/- 1.1	Yes	Class II CAD	387.6	9.7	5.1
Terconazole	c14dM	Yes (7.07 $\mu$ M)	99.3 +/- 0	Yes	Class II CAD	532.5	8.8	4.8
Triparanol	d24R	Yes (1.92 $\mu$ M)	99.3 +/- 0.3	Yes	Class II CAD	438.0	9.6	6.7

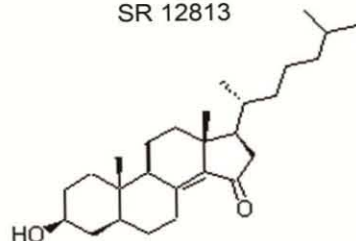
**Figure 4.9. Structures of the eleven compounds analyzed in this study.**



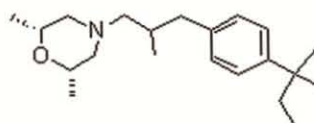
SR 12813



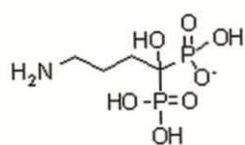
Terconazole



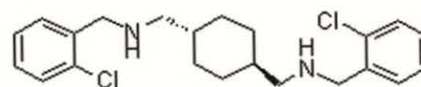
Colestolone



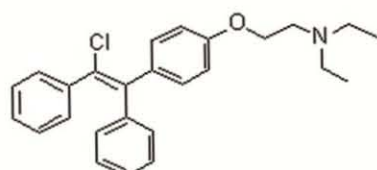
Amorolfine



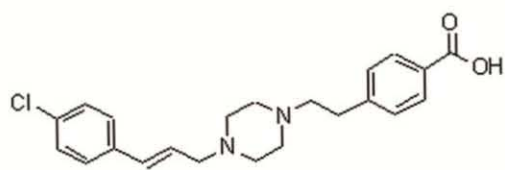
Alendronate



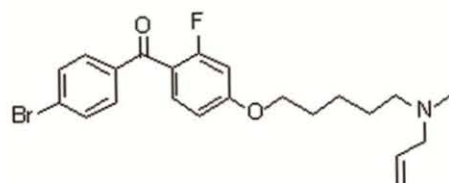
AY 9944



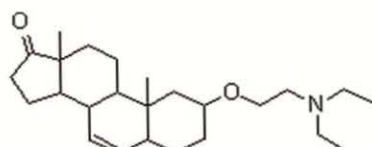
Clomiphene



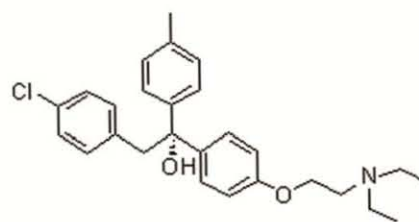
BM 15766



RO 48-8071



U18666A



Triparanol

## **Chapter V: Summary and Future Directions**

## **Development of a Multi-Purpose VLP System for Studying EBOV Entry**

In this dissertation, I first endeavored to elucidate unresolved aspects of EBOV entry. To this end, I developed a novel VLP reagent to use as a surrogate for studying the pathway and requirements of EBOV entry. This VLP system enables us to dissect discrete steps of EBOV internalization and cytoplasmic entry. Using this versatile VLP reagent, I confirmed findings in the literature (183, 216) that identified macropinocytosis as a major route of EBOV internalization (Chap. II). It should be noted, however, that my preliminary findings (Chap. I) along with other publications (19, 107, 182), suggest that EBOV either uses multiple endocytic pathways or a novel form of macropinocytosis that incorporates factors normally associated with clathrin and/or dynamin-dependent endocytosis. In addition, I used our multi-purpose EBOV VLP system to assess the internalization and cytoplasmic entry kinetics of EBOV into cells. I found that while these particles are rapidly internalized from the cell surface (~50% by 30 min), they are slow to enter the cytoplasm (~50% by 90 min) (Chap. II, Fig. 2.5B), and that this entry was considerably slower than that mediated by other viral glycoproteins including LCMV GP, which directs entry through LE (207)(Chap. II, Fig. 2.5B and C). Also, I found that neither the internalization kinetics nor the slow entry kinetics were altered if EBOV GP was proteolytically primed *in vitro* suggesting, importantly, that cathepsin-priming to the fusion-ready 19 kDa form is not a rate-limiting step for fusion in LE/Lys (Chap. II, Fig. 2.5B). Whether slow entry of VLPs coated with EBOV GP is a consequence of viral trafficking or some

other fusion-related requirement of GP (e.g. activation by a fusion trigger) remains to be determined.

### **CADs Inhibit a Late Stage of EBOV Entry**

With my novel multi-purpose VLP system, I next interrogated the mechanism by which prospective small molecule inhibitors disrupt EBOV infection. Collectively, we identified ~20 compounds (all data not shown) that block EBOV infection at the level of entry. We showed that two of these, clomiphene and toremiphene, block EBOV entry downstream of particle internalization (Chap. III). We further showed that inhibition of entry was specific for EBOV GP, and was not due to interference with endosomal pH or cathepsin activity, two known requirements for EBOV entry. While clomiphene and toremiphene are both primarily known as SERMs, their inhibitory effects against EBOV infection were shown to be independent of the estrogen receptor status of the host cell (Chap. III). (115).

In a subsequent study, we further probed the mechanism of action of clomiphene (Chap. IV). Having ruled out SERM functionality as the basis for inhibition of EBOV entry, we pursued the fact that clomiphene is also known as an inhibitor of squalene epoxidase, a key enzyme in the pathway of sterol biosynthesis. We therefore screened a set of compounds that inhibit distinct enzymes involved in sterol biosynthesis, and that had previously all been shown to inhibit replication of HCV (192). Interestingly, and in contrast to the experience with HCV, we found that only a subset of these compounds blocked EBOV entry and infection. This strongly suggested that clomiphene and the other five newly

identified inhibitors were not blocking EBOV entry by interfering with sterol biosynthesis.

The next cue we followed in pursuing the mechanism of action of clomiphen, toremiphen, and the other five EBOV inhibitory compounds was our observation that they are all cationic amphiphiles; more specifically all but one (AY-9944) are class II cationic amphiphiles. To begin our analysis, we further characterized two more additional compounds in our set, Ro48-8071 and U18666A. We found that, like clomiphen and toremiphen, their ability to inhibit EBOV entry is specific for EBOV GP and not due to inhibition of endosomal acidification or cathepsin activity.

### **CADs Inhibit EBOV Entry in an NPC1-Dependent Manner**

One of the inhibitory compounds, U18666A, has been used extensively to simulate the lysosomal storage disease Niemann Pick Type C, which is caused by dysfunction of the NPC1 protein (148). Since NPC1 has recently been shown to be a crucial factor for EBOV entry (35, 46, 94, 171), I assessed if the cationic amphiphilic inhibitors perturb EBOV entry through an NPC1-dependent pathway. U18666A likely mimics NPC1 deficiency by disrupting NPC1 function (37, 123). Since the hallmark feature of both U18666A treatment and NPC1 deficiency is cholesterol accumulation in LE/Lys, I tested whether the CADs that I identified as robust inhibitors of EBOV entry and infection cause cholesterol accumulation in LE/Lys. They all did, suggesting that NPC1 is involved in the inhibitory mechanism of these drugs.

To further investigate the involvement of NPC1, I tested the effects of NPC1 overexpression on the inhibitory efficacy of clomiphene, Ro48-8071, and U18666A. I found that each of these CADs displayed an apparent NPC1-dependence in their ability to inhibit EBOV GP-mediated infection (more inhibitor was needed to block infection in NPC1-overexpressing vs. parental cells). Lastly, I showed that the CADs tested do not inhibit the binding of primed GP to NPC1, the only known function currently ascribed to NPC1 in EBOV entry (and which is blocked by compound 3.47 (46)). Taken together, these results suggest that cationic amphiphiles block a novel function of NPC1, one that is required in addition to its already described role in binding 19 kDa GP.

### **Potential Roles of NPC1 in EBOV Entry**

I have described various direct and indirect strategies (Chap. IV, Fig. 4.8) by which cationic amphiphiles might block EBOV entry. Two of the proposed mechanisms (Fig. 4.8A and B) rely on a function of NPC1 in supporting EBOV entry that extends beyond its ability to bind 19 kDa GP. The precise nature of this novel additional role of NPC1 in EBOV entry is unknown, and unraveling this proposed second role is complicated by the fact that there are still considerable questions regarding the normal role of NPC1 in cell physiology. NPC1 is best known for the role it plays in cholesterol homeostasis, a function that is, however, dispensable for EBOV entry (35, 46). Despite its clear role in cholesterol egress from LE/Lys, it has not been conclusively determined if NPC1 directly transports cholesterol (109, 135), or if it has a more indirect function. Additionally, NPC1 may directly or indirectly transport sphingosine and other

amine cargoes out of LE/Lys (147). Sphingosine has been shown to accumulate in the LE/Lys of both NPC1-deficient cells and cells treated with the CAD U18666A (147). This sphingosine accumulation was, in turn, linked to subsequent disruptions in lysosomal calcium homeostasis, followed by eventual accumulation of different endosomal lipids (sphingomyelin, cholesterol, etc.) (148). Evidence for sphingosine transport by NPC1 is currently controversial, with the aforementioned studies proposing sphingosine as the most proximal “offending metabolite” of the NPC1 phenotype (147) and a more recent study suggesting that sphingosine transport from the LE/Lys is independent of NPC1 (21). Therefore, while inhibition of sphingosine egress from LE/Lys remains a potential mechanism of action for CADs against EBOV infection, the uncertainty over this aspect of NPC1 function it leaves open the possibility of other novel NPC1 roles in EBOV entry.

#### *Facilitation of Fusion Triggering*

It was originally proposed (46), and still contended (171), that NPC1 plays a role in fusion triggering of EBOV GP. Preliminary evidence collected by our group (White lab, unpublished data), along with data not shown in a publication from another group (171), suggests that NPC1 (in conjunction with low pH) is not sufficient to trigger the fusion activity of 19 kDa GP. While not sufficient to trigger EBOV GP fusion, it is possible that NPC1 nevertheless helps the fusion process, perhaps in a manner analogous to how CD4 potentiates HIV Env for binding to its co-receptor (46). Regardless of whether it participates directly or indirectly in facilitating EBOV fusion, additional roles for NPC1 in EBOV entry should be

considered, especially in light of our evidence in chapter IV suggesting that NPC1 may play more than one role in EBOV entry.

#### *NPC1 as a Proteolytic Shield*

Another possible role could be to act as a shield preventing inactivating proteolysis of GP. Our lab has previously shown that continued *in vitro* digestion by cathepsin L (after 19 kDa formation) results in a loss of ectodomain binding to target liposomes ((28), and White lab, unpublished data) and, consistent with another study (281), a severe reduction in infection by EBOV GP pseudovirions (White lab, unpublished data). As such, NPC1 may serve as an *in vivo* shield guarding GP from proteolytic inactivation which could occur in LE/Lys, since they are replete with proteolytic enzymes.

#### *NPC1 as a Targeting Molecule to the Limiting Membrane of the LE/Lys*

Alternatively, NPC1 could be acting as an anchor molecule, which by binding to proteolytically primed EBOV virions, brings them into intimate contact with the limiting membrane of LE/Lys (where NPC1 resides). This targeting to the limiting membrane could enable EBOV particles to fuse more efficiently than in a diffusion-limited model, where the particles would encounter numerous internal vesicles. Fusion with the internal vesicles would likely be non-productive (i.e. no cytoplasmic delivery) or less efficient (137).

#### *NPC1 as a Promoter of Endosomal Reduction*

Preliminary evidence from our lab suggests that reducing conditions (similar to those reported in late endosomes) combined with low pH are capable of triggering EBOV GP for fusion (28). To date, we have examined this effect on

both soluble GP in a liposome binding assay (28) as well as membrane bound GP on VLPs that were “force fused” at the plasma membrane of target cells (White lab, unpublished data). In both assays, the combination of low pH and mild sulfhydryl reduction causes primed 19 kDa GP, but not unprimed GP, to fuse. Our lab is currently expanding on these studies to determine if endosomal redox potential plays a role in EBOV entry. Reducing potential in LE/Lys is maintained by cysteine and cystine transporters that normally pump cysteine in, while pumping cystine out (199). Since the thiol group of cysteine is nucleophilic, it can reduce disulfide bonds present on proteins (e.g. EBOV GP) in LE/Lys, yielding cystine in the process. If cystine is not removed, it accumulates and crystallizes, as is the case in LE/Lys from patients with cystinosis (201). A precedent for NPC1 involvement in endosomal cysteine/cystine homeostasis in LE/Lys was reported in studies on NPC1 null mice. Specifically, cystine levels in LE/Lys from NPC1 null mice were reported to be ~70-fold higher than those in LE/Lys from WT mice (30). Therefore, LE/Lys in NPC1 null cells may be less reducing than those in NPC1 positive cells. It should be noted that 19 kDa GP retains five disulfide bonds, one linking GP1 and GP2 and two intra-subunit bonds apiece in GP1 and GP2; four of these are critical for EBOV GP-mediated infection (112), and could be targets for endosomal reduction. If LE/Lys redox potential does prove to be required for EBOV entry, cationic amphiphiles may be blocking EBOV infection by disrupting NPC1-mediated maintenance of endosomal reduction.

*NPC1 as a Regulator of ASMase and LBPA*

While it is certainly possible that CADs inhibit (directly or indirectly) a function of NPC1 that is necessary for EBOV entry, an alternate mode of inhibition (Chap. IV, Fig. 4.8C) is that CADs could act on another target in LE/Lys that is critical for EBOV entry, and which is regulated in some manner by NPC1. The well characterized inhibition of acid sphingomyelinase (ASMase) by CADs (1, 8, 127), combined with the recent report of the importance of ASMase for EBOV infection (172), suggest that CADs may target ASMase (and/or related LE/Lys factors such as acid ceramidase). Interestingly, ASMase activity levels have been shown to be significantly reduced in NPC1-deficient cells (54). Furthermore, the other two forms of Niemann Pick disease (types A and B) are both caused by defects in ASMase (rather than NPC1) (87, 148), and yet all three forms of NPC disease (A, B, and C) have similar cellular phenotypes (i.e. lipid accumulation) in LE/Lys. If further inquiries indicate a role of ASMase at a late stage of EBOV entry, as is the case for NPC1 (35, 171), it would be of interest to characterize the precise contribution that this endosomal housekeeping enzyme makes to EBOV entry.

In another scenario, NPC1 could also modulate lipids in LE/Lys membranes, specifically the phospholipid LBPA (also known as BMP), which is enriched in the inner membranes of LE/Lys (75, 176, 200). CADs are thought to compete with ASMase for binding to LBPA within LE/Lys (127). A possible connection exists between NPC1, ASMase, and LBPA in that NPC1 defective cells have deficient ASMase activity and accumulate both LBPA and cholesterol

(Table 5.1) (42, 54). Interestingly, cholesterol accumulation in LE/Lys seen in NPC1 diseased cells can be significantly restored by addition of either LBPA or ASMase (42, 54). Similarly, LBPA accumulation in NPC1-defective cells can be ameliorated by addition of ASMase (54). Taken together, these results suggest that NPC1 may be responsible for modulating both ASMase and LBPA in a way that is conducive for cholesterol transport and somehow supportive of EBOV entry. Perhaps this optimally permissive endosomal environment (for EBOV fusion) is disrupted by CADs. Speculatively, NPC1 could help maintain a level of LBPA in LE/Lys (via ASMase) that is crucial for EBOV fusion. Fusion of Dengue virus is optimal with membranes containing LBPA, but to our knowledge no one has yet tested whether Dengue virus entry requires NPC1 or ASMase (287). Further work on the role of NPC1, ASMase, and LBPA in relation to EBOV entry should be undertaken to unravel this intriguing story.

It is important to note that all of the potential direct and indirect roles for NPC1 in EBOV entry detailed above would theoretically result in an inability of the virus to fuse and enter the cytoplasm in the absence of NPC1. At present, while we cannot discern which (if any) of these theoretical NPC1-mediated mechanisms is at play, we can say with confidence that the role of NPC1 in EBOV entry is more complex than as first proposed (35, 46).

### **Future Directions for Assessing the Role of NPC1 in EBOV Entry**

The additional NPC1-dependent function that my pharmacological studies suggest as being important for EBOV entry remains to be fully elucidated. A first step in this process would be a determination of whether cationic amphiphiles

**Table 5.1. Observations made by other groups studying interplay of**

**ASMase and LBPA in NPC1-defective cells.** This table summarizes the known effects of NPC1 deficiency and rescue by ASMase or LBPA on levels of ASMase, sphingomyelin (SM), cholesterol (Chol), and LBPA. Symbols are as follows: —, non-detectable levels; +, lower than wildtype levels; ++, wildtype levels; +++, higher than wildtype levels; ND, not determined. References to relevant publications are indicated.

	<b>WT NPC1</b>	<b>NPC1 Null</b>	<b>NPC1 Null+ASMase</b>	<b>NPC1 Null+LBPA</b>
<b>NPC1</b>	<b>++</b>	<b>-</b>	<b>-</b>	<b>-</b>
<b>ASMase</b>	<b>++</b>	<b>+</b> <b>(54)</b>	<b>++</b> <b>(54)</b>	<b>ND</b>
<b>SM</b>	<b>++</b>	<b>+++</b> <b>(148)</b>	<b>ND</b>	<b>ND</b>
<b>Endosomal Chol.</b>	<b>++</b>	<b>+++</b> <b>(147)</b>	<b>++</b> <b>(54)</b>	<b>++</b> <b>(42)</b>
<b>LBPA</b>	<b>++</b>	<b>+++</b> <b>(54)</b>	<b>++</b> <b>(54)</b>	<b>ND</b>

interact directly with NPC1. This would best be resolved via biochemical assessment of CAD binding to NPC1. This could potentially be done using a probe conjugation and immunoprecipitation scheme similar to that employed by Cote, et al. (46), in which a photoactivatable CAD would be exposed to a membrane containing NPC1, crosslinked with biotin (after being exposed to a specific wavelength of light), immunoprecipitated (by NPC1 pull-down, see Chap. IV, Fig. 4.7), and the sample then blotted with streptavidin. Alternatively, a mass spectroscopic analysis of purified NPC1 incubated with these compounds (130, 247, 262) could be done, potentially providing the actual NPC1 residues involved in CAD binding. Moreover, a tandem surface plasmon resonance (Biacore)-mass spectrometric approach could give both CAD-NPC1 binding kinetics as well as structural information on the binding site (184). A useful comparison in all of these approaches would be to analyze compound 3.47 binding to NPC1. Additionally, it would be interesting to observe whether CADs inhibit EBOV GP-mediated fusion in a VLP-liposome fusion assay, with liposomes that are reconstituted both with and without NPC1.

In order to assess the connection (if any) between NPC1, ASMase and LBPA in EBOV entry, it would be prudent to investigate EBOV entry in either mutant or siRNA treated cells mimicking ASMase or LBPA deficiencies. Relatedly, it would be beneficial to see if addition of exogenous ASMase and/or LBPA (by DNA transfection or direct addition) to NPC1-deficient cells, or wildtype cells treated with CADs, rescues EBOV entry in a manner similar to how they rescue cholesterol egress in NPC1 null cells (42, 54).

## **CADs as Potential Anti-Ebolavirus Therapeutics**

Beyond the suggestion of an additional role for NPC1 in EBOV entry, we have uncovered several new compounds that hold potential as new tools for treating EBOV infection. At present, there are no effective therapeutic treatments against EBOV infection. The mouse studies detailed in chapter III (performed at USAMRIID), which showed protection against EBOV challenge by clomiphene and toremiphene (both class II CADs), suggest that these compounds hold therapeutic promise, at least if administered shortly after an exposure or prophylactically (Chap. III, Fig. 3.4). These results certainly need to be expanded into non-human primates. If successful, human trials will, eventually, have to be conducted, presumably during a future natural EBOV outbreak. Since these compounds are already FDA-approved, their potential development for human treatment should be dramatically streamlined. Although not yet tested in animal models of infection, we have also described two additional FDA-approved CADs, tamoxifen and terconazole, which inhibit EBOV infection, EBOV VLP entry, and induce an NPC1-like cholesterol accumulation defect (Chap. III and IV; entry and cholesterol data not shown for tamoxifen). Other groups have reported three additional FDA-approved CADs: imipramine, desipramine, and chlorpromazine that also inhibit EBOV infection (19, 35, 172, 219). Interestingly, chlorpromazine's identity as a class II CAD may account for my previous observations detailing its robust inhibitory effects on EBOV GP-mediated infection (Chap. I, Fig. 1.8), and may therefore argue against its effects having anything to do with inhibition of clathrin-mediated endocytosis as suggested by other groups (19, 219).

Collectively, seven FDA-approved CADs have already been shown to block EBOV infection (Table 5.2). All of these compounds most likely inhibit cytoplasmic entry of viral particles at a step proximal to fusion. Since CADs are a well-represented chemical class of drugs approved for human use (208), they represent a potentially large resource for repurposing efforts against EBOV infection.

All but one of the CADs tested in these studies robustly inhibited EBOV GP mediated VLP entry (and consequently live EBOV infection), and caused endosomal cholesterol accumulation. Interestingly, the exception to this was the compound amorolfine, which has a notably lower pKa (7.1) than any of the other CADs tested. In fact, all of the EBOV inhibitory CADs we tested have a pKa in the range of 8.0 (toremifene) to 9.6 (Clomiphene/Triparanol). This fact likely gives further support for the probable cellular site of action for these drugs, namely the low pH environment of LE/Lys. This is due to the fact that higher pKas are associated with higher degrees of lysosomal sequestration (61). An additional common element shared by all of the EBOV inhibitory CADs was their ability to induce a similar cholesterol phenotype to that seen with NPC1 deficiency. Future EBOV drug design efforts would be well advised to screen for CADs (in particular class II CADs), with pKas above 8.0, that also induce cholesterol accumulation in LE/Lys. The fact that both clomiphene and toremifene displayed efficacy against SUDV as well as EBOV (Chap. III, Fig. 3.3) indicates that CADs likely hold treatment potential against multiple ebolavirus strains. Interestingly, both clomiphene and toremifene were also active against MARV (Fig. 3.3), while

**Table 5.2. Summary: FDA-approved CADs that block EBOV entry and infection.** This is a summation of data collected by both our lab and other groups that identifies all known FDA-approved CADs that block EBOV infection. All are class II CADs. Abbreviations: CPZ, Chlorpromazine; ND, not determined; CHOL, cholesterol; DNS, data not shown. Note that molecular weights (MW) are reported for non-salt forms of compounds. References to relevant publications and chapters of this thesis are indicated.

Compound	Approved Clinical Use	Inhibit EBOV Infection (IC <sub>50</sub> )	Inhibit VLP Entry	Inhibit MARV Infection	Increase CHOL in LE/Lys	pK <sub>a</sub>	MW
CPZ	antipsychotic	Yes (IC <sub>50</sub> ND) (19, 219)	ND	Yes (219)	Yes (208)	9.2	318.9
Clomiphene	female infertility	Yes (2.42 μM) (Chap. III)	Yes (Chap. III, IV)	Yes (Chap. III)	Yes (Chap. IV)	9.6	405.9
Desipramine	antidepressant	Yes (IC <sub>50</sub> ND) (172)	ND	ND	Yes (122)	10.2	266.4
Imipramine	antidepressant	Yes (IC <sub>50</sub> ND) (35, 172)	Yes (172)	ND	Yes (208)	9.4	280.4
Tamoxifen	anti-estrogen therapy (cancer)	Yes (IC <sub>50</sub> ND) (Chap. III)	Yes (DNS)	ND	Yes (DNS)	8.8	371.5
Terconazole	anti-fungal	Yes (7.07 μM) (Chap. IV)	Yes (Chap. IV)	ND	Yes (Chap. IV)	8.8	532.5
Toremifene	anti-estrogen therapy (cancer)	Yes (0.162 μM) (Chap. III)	Yes (Chap. III)	No (Chap. III)	Yes (DNS)	8.0	406

tamoxifen was not (data not shown). Additional work remains to be done to determine the structural differences between different CADs that account for their relative activity or inactivity against different filoviruses.

### **Final Conclusions**

In summary, I have developed a novel multi-purpose VLP system capable of assessing multiple steps of the EBOV entry cycle (binding, internalization, trafficking , and fusion), all with the same set of particles. Our lab is currently using these VLPs tool to elucidate the requirements of EBOV GP triggering and the relative contributions of NPC1 and endosomal reduction to the promotion of EBOV fusion in LE/Lys.

In the studies conducted for this thesis, I have primarily used pharmacological inhibitors as tools for dissecting the role played by NPC1 in EBOV entry into the host cell. The evidence collected suggests at least two roles for NPC1. The first is the previously described direct biochemical interaction with 19 kDa GP, which provides an unknown contribution to EBOV egress into the cytoplasm. The second is an apparently novel contribution, which appears to be independent of an interaction with 19 kDa GP, and may involve other endosomal factors (e.g. ASMase). Future studies should focus on elucidating what this role is, and whether the drug-induced effects detailed here are the result of direct binding to NPC1, indirect effects on NPC1, or effects on another LE/Lys factor that is regulated by NPC1. Lastly, an important consequence of this study has been the identification of cationic amphiphiles as a promising new class of drugs, with a number already FDA-approved, for combating ebolavirus infection.

## Literature Cited

1. **Albouz, S., F. Le Saux, D. Wenger, J. J. Hauw, and N. Baumann.** 1986. Modifications of sphingomyelin and phosphatidylcholine metabolism by tricyclic antidepressants and phenothiazines. *Life sciences* **38**:357-363.
2. **Aleksandrowicz, P., A. Marzi, N. Biedenkopf, N. Beimforde, S. Becker, T. Hoenen, H. Feldmann, and H. J. Schnittler.** 2011. Ebola virus enters host cells by macropinocytosis and clathrin-mediated endocytosis. *J Infect Dis* **204 Suppl 3**:S957-967.
3. **Alibek, K.** 1999. The Soviet Union's anti-agricultural biological weapons. *Ann N Y Acad Sci* **894**:18-19.
4. **Alvarez, C. P., F. Lasala, J. Carrillo, O. Muniz, A. L. Corbi, and R. Delgado.** 2002. C-type lectins DC-SIGN and L-SIGN mediate cellular entry by Ebola virus in cis and in trans. *J Virol* **76**:6841-6844.
5. **Amman, B. R., S. A. Carroll, Z. D. Reed, T. K. Sealy, S. Balinandi, R. Swanepoel, A. Kemp, B. R. Erickson, J. A. Comer, S. Campbell, D. L. Cannon, M. L. Khristova, P. Atimnedi, C. D. Paddock, R. J. Kent Crockett, T. D. Flietstra, K. L. Warfield, R. Unfer, E. Katongole-Mbidde, R. Downing, J. W. Tappero, S. R. Zaki, P. E. Rollin, T. G. Ksiazek, S. T. Nichol, and J. S. Towner.** 2012. Seasonal Pulses of Marburg Virus Circulation in Juvenile *Rousettus aegyptiacus* Bats Coincide with Periods of Increased Risk of Human Infection. *PLoS Pathog* **8**:e1002877.
6. **Amstutz, B., M. Gastaldelli, S. Kalin, N. Imelli, K. Boucke, E. Wandeler, J. Mercer, S. Hemmi, and U. F. Greber.** 2008. Subversion of CtBP1-controlled macropinocytosis by human adenovirus serotype 3. *The EMBO journal* **27**:956-969.
7. **Anderson, R. G., M. S. Brown, and J. L. Goldstein.** 1977. Role of the coated endocytic vesicle in the uptake of receptor-bound low density lipoprotein in human fibroblasts. *Cell* **10**:351-364.
8. **Arenz, C.** 2010. Small molecule inhibitors of acid sphingomyelinase. *Cellular physiology and biochemistry : international journal of experimental cellular physiology, biochemistry, and pharmacology* **26**:1-8.
9. **Arunachalam, B., U. T. Phan, H. J. Geuze, and P. Cresswell.** 2000. Enzymatic reduction of disulfide bonds in lysosomes: Characterization of a Gamma-interferon-inducible lysosomal thiol reductase (GILT). *Proc. Natl. Acad. Sci. USA* **97**:745-750.
10. **Asem, E. K., and F. Hertelendy.** 1986. Clomiphene and tamoxifen inhibit the cholesterol side-chain cleavage enzyme activity in hen granulosa cells. *Journal of reproduction and fertility* **77**:153-158.
11. **Balch, W. E., and J. E. Rothman.** 1985. Characterization of protein transport between successive compartments of the Golgi apparatus: asymmetric properties of donor and acceptor activities in a cell-free system. *Archives of biochemistry and biophysics* **240**:413-425.
12. **Baribaud, F., S. Pohlmann, and R. W. Doms.** 2001. The role of DC-SIGN and DC-SIGNR in HIV and SIV attachment, infection, and transmission. *Virology* **286**:1-6.
13. **Barth, H., C. Schafer, M. I. Adah, F. Zhang, R. J. Linhardt, H. Toyoda, A. Kinoshita-Toyoda, T. Toida, T. H. Van Kuppevelt, E. Depla, F. Von Weizsacker, H. E. Blum, and T. F. Baumert.** 2003. Cellular binding of hepatitis C virus envelope glycoprotein E2 requires cell surface heparan sulfate. *J Biol Chem* **278**:41003-41012.

14. **Barton, E. S., J. C. Forrest, J. L. Connolly, J. D. Chappell, Y. Liu, F. J. Schnell, A. Nusrat, C. A. Parkos, and T. S. Dermody.** 2001. Junction adhesion molecule is a receptor for reovirus. *Cell* **104**:441-451.
15. **Basler, C. F., and G. K. Amarasinghe.** 2009. Evasion of interferon responses by Ebola and Marburg viruses. *Journal of interferon & cytokine research : the official journal of the International Society for Interferon and Cytokine Research* **29**:511-520.
16. **Bavari, S., C. M. Bosio, E. Wiegand, G. Ruthel, A. B. Will, T. W. Geisbert, M. Hevey, C. Schmaljohn, A. Schmaljohn, and M. J. Aman.** 2002. Lipid raft microdomains: a gateway for compartmentalized trafficking of Ebola and Marburg viruses. *J Exp Med* **195**:593-602.
17. **Beniac, D. R., P. L. Melito, S. L. Devareennes, S. L. Hiebert, M. J. Rabb, L. L. Lamboo, S. M. Jones, and T. F. Booth.** 2012. The organisation of Ebola virus reveals a capacity for extensive, modular polyploidy. *PloS one* **7**:e29608.
18. **Bergelson, J. M., J. A. Cunningham, G. Droguett, E. A. Kurt-Jones, A. Krithivas, J. S. Hong, M. S. Horwitz, R. L. Crowell, and R. W. Finberg.** 1997. Isolation of a common receptor for Coxsackie B viruses and adenoviruses 2 and 5. *Science* **275**:1320-1323.
19. **Bhattacharyya, S., K. L. Warfield, G. Ruthel, S. Bavari, M. J. Aman, and T. J. Hope.** 2010. Ebola virus uses clathrin-mediated endocytosis as an entry pathway. *Virology* **401**:18-28.
20. **Blanc, M., W. Y. Hsieh, K. A. Robertson, S. Watterson, G. Shui, P. Lacaze, M. Khondoker, P. Dickinson, G. Sing, S. Rodriguez-Martin, P. Phelan, T. Forster, B. Strobl, M. Muller, R. Riemersma, T. Osborne, M. R. Wenk, A. Angulo, and P. Ghazal.** 2011. Host defense against viral infection involves interferon mediated down-regulation of sterol biosynthesis. *PLoS biology* **9**:e1000598.
21. **Blom, T., Z. Li, R. Bittman, P. Somerharju, and E. Ikonen.** 2012. Tracking sphingosine metabolism and transport in sphingolipidoses: NPC1 deficiency as a test case. *Traffic* **13**:1234-1243.
22. **Blumenthal, R., A. Bali-Puri, A. Walter, D. Covell, and O. Eidelman.** 1987. pH-dependent fusion of vesicular stomatitis virus with Vero cells. Measurement by dequenching of octadecyl rhodamine fluorescence. *J Biol Chem* **262**:13614-13619.
23. **Bonifacino, J. S., and A. M. Weissman.** 1998. Ubiquitin and the control of protein fate in the secretory and endocytic pathways. *Annual review of cell and developmental biology* **14**:19-57.
24. **Bosch, B. J., W. Bartelink, and P. J. M. Rottier.** 2008. Cathepsin L functionally cleaves the severe acute respiratory syndrome coronavirus class I fusion protein upstream of rather than adjacent to the fusion peptide. *J. Virol.* **82**:8887-8890.
25. **Boussif, O., F. Lezoualc'h, M. A. Zanta, M. D. Mergny, D. Scherman, B. Demeneix, and J. P. Behr.** 1995. A versatile vector for gene and oligonucleotide transfer into cells in culture and in vivo: polyethylenimine. *Proc Natl Acad Sci U S A* **92**:7297-7301.
26. **Bradfute, S. B., P. E. Swanson, M. A. Smith, E. Watanabe, J. E. McDunn, R. S. Hotchkiss, and S. Bavari.** 2010. Mechanisms and consequences of ebolavirus-induced lymphocyte apoptosis. *Journal of immunology* **184**:327-335.
27. **Bray, M., K. Davis, T. Geisbert, C. Schmaljohn, and J. Huggins.** 1998. A mouse model for evaluation of prophylaxis and therapy of Ebola hemorrhagic fever. *J Infect Dis* **178**:651-661.
28. **Brecher, M., K. L. Schornberg, S. E. Delos, M. L. Fusco, E. O. Saphire, and J. M. White.** 2011. Cathepsin cleavage potentiates the ebola virus glycoprotein to undergo a subsequent fusion-relevant conformational change. *J Virol* **86**:364-372.

29. **Brindley, M. A., L. Hughes, A. Ruiz, P. B. McCray, Jr., A. Sanchez, D. A. Sanders, and W. Maury.** 2007. Ebola virus glycoprotein 1: identification of residues important for binding and postbinding events. *J Virol* **81**:7702-7709.
30. **Butler, J. D., M. T. Vanier, and P. G. Pentchev.** 1993. Niemann-Pick C disease: cystine and lipids accumulate in the murine model of this lysosomal cholesterol lipidosis. *Biochemical and biophysical research communications* **196**:154-159.
31. **Bwaka, M. A., M. J. Bonnet, P. Calain, R. Colebunders, A. De Roo, Y. Guimard, K. R. Katwiki, K. Kibadi, M. A. Kipasa, K. J. Kuvula, B. B. Mapanda, M. Massamba, K. D. Mupapa, J. J. Muyembe-Tamfum, E. Ndaberey, C. J. Peters, P. E. Rollin, and E. Van den Enden.** 1999. Ebola hemorrhagic fever in Kikwit, Democratic Republic of the Congo: clinical observations in 103 patients. *J Infect Dis* **179 Suppl 1**:S1-7.
32. **Cao, W., M. D. Henry, P. Borrow, H. Yamada, J. H. Elder, E. V. Ravkov, S. T. Nichol, R. W. Compans, K. P. Campbell, and M. B. Oldstone.** 1998. Identification of alpha-dystroglycan as a receptor for lymphocytic choriomeningitis virus and Lassa fever virus. *Science* **282**:2079-2081.
33. **Cao, Z., K. Huang, and A. F. Horwitz.** 1998. Identification of a domain on the integrin  $\alpha 5$  subunit implicated in cell spreading and signaling. *J. Biol. Chem.* **273**:31670-31679.
34. **Cardone, G., M. Brecher, J. Fontana, D. C. Winkler, C. Butan, J. M. White, and A. C. Steven.** 2012. Visualization of the Two-Step Fusion Process of the Retrovirus Avian Sarcoma/Leukosis Virus by Cryo-Electron Tomography. *J Virol*.
35. **Carette, J. E., M. Raaben, A. C. Wong, A. S. Herbert, G. Obernosterer, N. Mulherkar, A. I. Kuehne, P. J. Kranzusch, A. M. Griffin, G. Ruthel, P. D. Cin, J. M. Dye, S. P. Whelan, K. Chandran, and T. R. Brummelkamp.** 2011. Ebola virus entry requires the cholesterol transporter Niemann-Pick C1. *Nature*.
36. **Cavrois, M., C. De Noronha, and W. C. Greene.** 2002. A sensitive and specific enzyme-based assay detecting HIV-1 virion fusion in primary T lymphocytes. *Nat Biotechnol* **20**:1151-1154.
37. **Cenedella, R. J.** 2009. Cholesterol synthesis inhibitor U18666A and the role of sterol metabolism and trafficking in numerous pathophysiological processes. *Lipids* **44**:477-487.
38. **Cenedella, R. J., R. Jacob, D. Borchman, D. Tang, A. R. Neely, A. Samadi, R. P. Mason, and P. Sexton.** 2004. Direct perturbation of lens membrane structure may contribute to cataracts caused by U18666A, an oxidosqualene cyclase inhibitor. *Journal of lipid research* **45**:1232-1241.
39. **Chan, S. Y., R. F. Speck, M. C. Ma, and M. A. Goldsmith.** 2000. Distinct mechanisms of entry by envelope glycoproteins of Marburg and Ebola (Zaire) viruses. *J Virol* **74**:4933-4937.
40. **Chandran, K., N. J. Sullivan, U. Felbor, S. P. Whelan, and J. M. Cunningham.** 2005. Endosomal proteolysis of the Ebola virus glycoprotein is necessary for infection. *Science* **308**:1643-1645.
41. **Chemello, M. E., O. C. Aristimuno, F. Michelangeli, and M. C. Ruiz.** 2002. Requirement for vacuolar H<sup>+</sup>-ATPase activity and Ca<sup>2+</sup> gradient during entry of rotavirus into MA104 cells. *J Virol* **76**:13083-13087.
42. **Chevallier, J., Z. Chamoun, G. Jiang, G. Prestwich, N. Sakai, S. Matile, R. G. Parton, and J. Gruenberg.** 2008. Lysobisphosphatidic acid controls endosomal cholesterol levels. *J Biol Chem* **283**:27871-27880.

43. **Choe, H., M. Farzan, Y. Sun, N. Sullivan, B. Rollins, P. D. Ponath, L. Wu, C. R. Mackay, G. LaRosa, W. Newman, N. Gerard, C. Gerard, and J. Sodroski.** 1996. The beta-chemokine receptors CCR3 and CCR5 facilitate infection by primary HIV-1 isolates. *Cell* **85**:1135-1148.
44. **Clement, C., V. Tiwari, P. M. Scanlan, T. Valyi-Nagy, B. Y. Yue, and D. Shukla.** 2006. A novel role for phagocytosis-like uptake in herpes simplex virus entry. *J Cell Biol* **174**:1009-1021.
45. **Cohen, J. I.** 2005. HMG CoA reductase inhibitors (statins) to treat Epstein-Barr virus-driven lymphoma. *British journal of cancer* **92**:1593-1598.
46. **Cote, M., J. Misasi, T. Ren, A. Bruchez, K. Lee, C. M. Filone, L. Hensley, Q. Li, D. Ory, K. Chandran, and J. Cunningham.** 2011. Small molecule inhibitors reveal Niemann-Pick C1 is essential for Ebola virus infection. *Nature* **477**:344-348.
47. **Cruz, J. C., S. Sugii, C. Yu, and T. Y. Chang.** 2000. Role of Niemann-Pick type C1 protein in intracellular trafficking of low density lipoprotein-derived cholesterol. *J Biol Chem* **275**:4013-4021.
48. **Cureton, D. K., R. H. Massol, S. Saffarian, T. L. Kirchhausen, and S. P. Whelan.** 2009. Vesicular stomatitis virus enters cells through vesicles incompletely coated with clathrin that depend upon actin for internalization. *PLoS Pathog* **5**:e1000394.
49. **Dalglish, A. G., P. C. Beverley, P. R. Clapham, D. H. Crawford, M. F. Greaves, and R. A. Weiss.** 1984. The CD4 (T4) antigen is an essential component of the receptor for the AIDS retrovirus. *Nature* **312**:763-767.
50. **Damke, H., T. Baba, D. E. Warnock, and S. L. Schmid.** 1994. Induction of mutant dynamin specifically blocks endocytic coated vesicle formation. *J Cell Biol* **127**:915-934.
51. **De Kruif, P.** 1926. *Microbe hunters*. Harcourt, New York,.
52. **de Medina, P., B. Payre, N. Boubekour, J. Bertrand-Michel, F. Terce, S. Silvente-Poirot, and M. Poirot.** 2009. Ligands of the antiestrogen-binding site induce active cell death and autophagy in human breast cancer cells through the modulation of cholesterol metabolism. *Cell death and differentiation* **16**:1372-1384.
53. **Deng, H., R. Liu, W. Ellmeier, S. Choe, D. Unutmaz, M. Burkhart, P. Di Marzio, S. Marmon, R. E. Sutton, C. M. Hill, C. B. Davis, S. C. Peiper, T. J. Schall, D. R. Littman, and N. R. Landau.** 1996. Identification of a major co-receptor for primary isolates of HIV-1. *Nature* **381**:661-666.
54. **Devlin, C., N. H. Pipalia, X. Liao, E. H. Schuchman, F. R. Maxfield, and I. Tabas.** 2010. Improvement in lipid and protein trafficking in Niemann-Pick C1 cells by correction of a secondary enzyme defect. *Traffic* **11**:601-615.
55. **Diederich, S., L. Thiel, and A. Maisner.** 2008. Role of endocytosis and cathepsin-mediated activation in Nipah virus entry. *Virology* **375**:391-400.
56. **Dolnik, O., L. Kolesnikova, and S. Becker.** 2008. Filoviruses: Interactions with the host cell. *Cell Mol. Life Sci.* **65**:756-776.
57. **Dragic, T., V. Litwin, G. P. Allaway, S. R. Martin, Y. Huang, K. A. Nagashima, C. Cayanan, P. J. Maddon, R. A. Koup, J. P. Moore, and W. A. Paxton.** 1996. HIV-1 entry into CD4+ cells is mediated by the chemokine receptor CC-CKR-5. *Nature* **381**:667-673.
58. **Dube, D., M. B. Brecher, S. E. Delos, S. C. Rose, E. W. Park, K. L. Schornberg, J. H. Kuhn, and J. M. White.** 2009. The primed ebolavirus glycoprotein (19-kilodalton GP1,2): sequence and residues critical for host cell binding. *J Virol* **83**:2883-2891.
59. **Dube, D., K. L. Schornberg, C. J. Shoemaker, S. E. Delos, T. S. Stantchev, K. A. Clouse, C. C. Broder, and J. M. White.** 2010. Cell adhesion-dependent membrane trafficking of a

- binding partner for the ebolavirus glycoprotein is a determinant of viral entry. *Proc Natl Acad Sci U S A* **107**:16637-16642.
60. **Dube, D., K. L. Schornberg, T. S. Stantchev, M. I. Bonaparte, S. E. Delos, A. H. Bouton, C. C. Broder, and J. M. White.** 2008. Cell adhesion promotes Ebola virus envelope glycoprotein-mediated binding and infection. *J Virol* **82**:7238-7242.
  61. **Duvvuri, M., S. Konkar, R. S. Funk, J. M. Krise, and J. P. Krise.** 2005. A chemical strategy to manipulate the intracellular localization of drugs in resistant cancer cells. *Biochemistry* **44**:15743-15749.
  62. **Ebert, D. H., J. Deussing, C. Peters, and T. S. Dermody.** 2002. Cathepsin L and cathepsin B mediate reovirus disassembly in murine fibroblast cells. *J. Biol. Chem.* **277**:24609-24617.
  63. **Ebert, D. H., S. A. Kopecky-Bromberg, and T. S. Dermody.** 2004. Cathepsin B is inhibited in mutant cells selected during persistent reovirus infection. *J. Biol. Chem.* **279**:3837-3851.
  64. **Elojeimy, S., D. H. Holman, X. Liu, A. El-Zawahry, M. Villani, J. C. Cheng, A. Mahdy, Y. Zeidan, A. Bielwaska, Y. A. Hannun, and J. S. Norris.** 2006. New insights on the use of desipramine as an inhibitor for acid ceramidase. *FEBS letters* **580**:4751-4756.
  65. **Empig, C. J., and M. A. Goldsmith.** 2002. Association of the caveola vesicular system with cellular entry by filoviruses. *J Virol* **76**:5266-5270.
  66. **Engelman, A., and P. Cherepanov.** 2012. The structural biology of HIV-1: mechanistic and therapeutic insights. *Nat Rev Microbiol* **10**:279-290.
  67. **Erik H.J. Danen, K. M. Y.** 2001. Fibronectin, integrins, and growth control. *Journal of Cellular Physiology* **189**:1-13.
  68. **Ertl, P.** 1997. Simple Quantum Chemical Parameters as an Alternative to the Hammett Sigma Constants in QSAR Studies. *Quantitative Structure-Activity Relationships* **16**:377-382.
  69. **Evans, M. J., T. von Hahn, D. M. Tscherne, A. J. Syder, M. Panis, B. Wolk, T. Hatziioannou, J. A. McKeating, P. D. Bieniasz, and C. M. Rice.** 2007. Claudin-1 is a hepatitis C virus co-receptor required for a late step in entry. *Nature* **446**:801-805.
  70. **Falzarano, D., F. Feldmann, A. Grolla, A. Leung, H. Ebihara, J. E. Strong, A. Marzi, A. Takada, S. Jones, J. Gren, J. Geisbert, S. M. Jones, T. W. Geisbert, and H. Feldmann.** 2011. Single immunization with a monovalent vesicular stomatitis virus-based vaccine protects nonhuman primates against heterologous challenge with Bundibugyo ebolavirus. *J Infect Dis* **204 Suppl 3**:S1082-1089.
  71. **Feldmann, H., and T. W. Geisbert.** 2011. Ebola haemorrhagic fever. *Lancet* **377**:849-862.
  72. **Feldmann, H., S. Jones, H. D. Klenk, and H. J. Schnittler.** 2003. Ebola virus: from discovery to vaccine. *Nature reviews. Immunology* **3**:677-685.
  73. **Feldmann, H., V. E. Volchkov, V. A. Volchkova, and H. D. Klenk.** 1999. The glycoproteins of Marburg and Ebola virus and their potential roles in pathogenesis. *Archives of virology. Supplementum* **15**:159-169.
  74. **Feng, Y., C. C. Broder, P. E. Kennedy, and E. A. Berger.** 1996. HIV-1 entry cofactor: functional cDNA cloning of a seven-transmembrane, G protein-coupled receptor. *Science* **272**:872-877.
  75. **Gallala, H. D., and K. Sandhoff.** 2011. Biological function of the cellular lipid BMP-BMP as a key activator for cholesterol sorting and membrane digestion. *Neurochemical research* **36**:1594-1600.

76. **Garcia, M., A. Cooper, W. Shi, W. Bornmann, R. Carrion, D. Kalman, and G. J. Nabel.** 2012. Productive replication of Ebola virus is regulated by the c-Abl1 tyrosine kinase. *Science translational medicine* **4**:123ra124.
77. **Gardner, J. P., R. J. Durso, R. R. Arrigale, G. P. Donovan, P. J. Maddon, T. Dragic, and W. C. Olson.** 2003. L-SIGN (CD 209L) is a liver-specific capture receptor for hepatitis C virus. *Proc Natl Acad Sci U S A* **100**:4498-4503.
78. **Geisbert, T. W., D. G. Bausch, and H. Feldmann.** 2010. Prospects for immunisation against Marburg and Ebola viruses. *Reviews in medical virology* **20**:344-357.
79. **Geisbert, T. W., K. M. Daddario-Dicaprio, J. B. Geisbert, D. S. Reed, F. Feldmann, A. Grolla, U. Stroher, E. A. Fritz, L. E. Hensley, S. M. Jones, and H. Feldmann.** 2008. Vesicular stomatitis virus-based vaccines protect nonhuman primates against aerosol challenge with Ebola and Marburg viruses. *Vaccine* **26**:6894-6900.
80. **Geisbert, T. W., K. M. Daddario-DiCaprio, K. J. Williams, J. B. Geisbert, A. Leung, F. Feldmann, L. E. Hensley, H. Feldmann, and S. M. Jones.** 2008. Recombinant vesicular stomatitis virus vector mediates postexposure protection against Sudan Ebola hemorrhagic fever in nonhuman primates. *J Virol* **82**:5664-5668.
81. **Geisbert, T. W., and L. E. Hensley.** 2004. Ebola virus: new insights into disease aetiopathology and possible therapeutic interventions. *Expert Rev Mol Med* **6**:1-24.
82. **Geisbert, T. W., L. E. Hensley, T. Larsen, H. A. Young, D. S. Reed, J. B. Geisbert, D. P. Scott, E. Kagan, P. B. Jahrling, and K. J. Davis.** 2003. Pathogenesis of Ebola Hemorrhagic Fever in Cynomolgus Macaques: Evidence that Dendritic Cells Are Early and Sustained Targets of Infection. *The American journal of pathology* **163**:2347-2370.
83. **Geisbert, T. W., and P. B. Jahrling.** 1995. Differentiation of filoviruses by electron microscopy. *Virus Res* **39**:129-150.
84. **Geraghty, R. J., C. Krummenacher, G. H. Cohen, R. J. Eisenberg, and P. G. Spear.** 1998. Entry of alphaherpesviruses mediated by poliovirus receptor-related protein 1 and poliovirus receptor. *Science* **280**:1618-1620.
85. **Ghigo, E., J. Kartenbeck, P. Lien, L. Pelkmans, C. Capo, J. L. Mege, and D. Raoult.** 2008. Ameobal pathogen mimivirus infects macrophages through phagocytosis. *PLoS Pathog* **4**:e1000087.
86. **Ghose, A. K., and G. M. Crippen.** 1987. Atomic physicochemical parameters for three-dimensional-structure-directed quantitative structure-activity relationships. 2. Modeling dispersive and hydrophobic interactions. *J Chem Inf Comput Sci* **27**:21-35.
87. **Ginzburg, L., and A. H. Futerman.** 2005. Defective calcium homeostasis in the cerebellum in a mouse model of Niemann-Pick A disease. *Journal of neurochemistry* **95**:1619-1628.
88. **Gower, T. L., and B. S. Graham.** 2001. Antiviral activity of lovastatin against respiratory syncytial virus in vivo and in vitro. *Antimicrobial agents and chemotherapy* **45**:1231-1237.
89. **Groseth, A., H. Feldmann, and J. E. Strong.** 2007. The ecology of Ebola virus. *Trends in Microbiology* **15**:408-416.
90. **Groseth, A., T. Hoenen, M. Eickmann, and S. Becker.** 2011. *Filoviruses: Ebola, Marburg and Disease*, eLS. John Wiley & Sons, Ltd.
91. **Grove, J., and M. Marsh.** 2011. The cell biology of receptor-mediated virus entry. *J Cell Biol* **195**:1071-1082.
92. **Gruenberg, J., and F. G. van der Goot.** 2006. Mechanisms of pathogen entry through the endosomal compartments. *Nat Rev Mol Cell Biol* **7**:495-504.

93. **Gylling, H., S. Pyrhonen, E. Mantyla, H. Maenpaa, L. Kangas, and T. A. Miettinen.** 1995. Tamoxifen and toremifene lower serum cholesterol by inhibition of delta 8-cholesterol conversion to lathosterol in women with breast cancer. *Journal of clinical oncology : official journal of the American Society of Clinical Oncology* **13**:2900-2905.
94. **Haines, K. M., N. H. Vande Burgt, J. R. Francica, R. L. Kaletsky, and P. Bates.** 2012. Chinese hamster ovary cell lines selected for resistance to ebolavirus glycoprotein mediated infection are defective for NPC1 expression. *Virology* **432**:20-28.
95. **Harty, R. N.** 2009. No exit: targeting the budding process to inhibit filovirus replication. *Antiviral research* **81**:189-197.
96. **Harty, R. N., M. E. Brown, G. Wang, J. Huibregtse, and F. P. Hayes.** 2000. A PPxY motif within the VP40 protein of Ebola virus interacts physically and functionally with a ubiquitin ligase: implications for filovirus budding. *Proc Natl Acad Sci U S A* **97**:13871-13876.
97. **Haspot, F., A. Lavault, C. Sinzger, K. Laib Sampaio, Y. D. Stierhof, P. Pilet, C. Bressolette-Bodin, and F. Halary.** 2012. Human cytomegalovirus entry into dendritic cells occurs via a macropinocytosis-like pathway in a pH-independent and cholesterol-dependent manner. *PloS one* **7**:e34795.
98. **Helenius, A., J. Kartenbeck, K. Simons, and E. Fries.** 1980. On the entry of Semliki forest virus into BHK-21 cells. *J Cell Biol* **84**:404-420.
99. **Herskovits, J. S., C. C. Burgess, R. A. Obar, and R. B. Vallee.** 1993. Effects of mutant rat dynamin on endocytosis. *J Cell Biol* **122**:565-578.
100. **Hevey, M., D. Negley, J. Geisbert, P. Jahrling, and A. Schmaljohn.** 1997. Antigenicity and vaccine potential of Marburg virus glycoprotein expressed by baculovirus recombinants. *Virology* **239**:206-216.
101. **Hevey, M., D. Negley, and A. Schmaljohn.** 2003. Characterization of monoclonal antibodies to Marburg virus (strain Musoke) glycoprotein and identification of two protective epitopes. *Virology* **314**:350-357.
102. **Higgins, M. E., J. P. Davies, F. W. Chen, and Y. A. Ioannou.** 1999. Niemann-Pick C1 is a late endosome-resident protein that transiently associates with lysosomes and the trans-Golgi network. *Molecular genetics and metabolism* **68**:1-13.
103. **Hoenen, T., N. Biedenkopf, F. Zielecki, S. Jung, A. Groseth, H. Feldmann, and S. Becker.** 2010. Oligomerization of Ebola virus VP40 is essential for particle morphogenesis and regulation of viral transcription. *J Virol* **84**:7053-7063.
104. **Hoenen, T., A. Groseth, D. Falzarano, and H. Feldmann.** 2006. Ebola virus: unravelling pathogenesis to combat a deadly disease. *Trends Mol Med* **12**:206-215.
105. **Hoffman, T. L., C. C. LaBranche, W. Zhang, G. Canziani, J. Robinson, I. Chaiken, J. A. Hoxie, and R. W. Doms.** 1999. Stable exposure of the coreceptor-binding site in a CD4-independent HIV-1 envelope protein. *Proc Natl Acad Sci U S A* **96**:6359-6364.
106. **Huang, J., L. C. Bridges, and J. M. White.** 2005. Selective modulation of integrin-mediated cell migration by distinct ADAM family members. *Mol. Biol. Cell* **16**:4982-4991.
107. **Hunt, C. L., A. A. Kolokoltsov, R. A. Davey, and W. Maury.** 2010. The Tyro3 receptor kinase Axl enhances macropinocytosis of Zaire ebolavirus. *J Virol* **85**:334-347.
108. **Hynes, R. O.** 2002. Integrins: Bidirectional, allosteric signaling machines. *Cell* **110**:673-687.
109. **Infante, R. E., M. L. Wang, A. Radhakrishnan, H. J. Kwon, M. S. Brown, and J. L. Goldstein.** 2008. NPC2 facilitates bidirectional transfer of cholesterol between NPC1 and

- lipid bilayers, a step in cholesterol egress from lysosomes. *Proc Natl Acad Sci U S A* **105**:15287-15292.
110. **Ito, H., S. Watanabe, A. Sanchez, M. A. Whitt, and Y. Kawaoka.** 1999. Mutational analysis of the putative fusion domain of Ebola virus glycoprotein. *J Virol* **73**:8907-8912.
  111. **Ito, H., S. Watanabe, A. Takada, and Y. Kawaoka.** 2001. Ebola Virus Glycoprotein: Proteolytic Processing, Acylation, Cell Tropism, and Detection of Neutralizing Antibodies. *J. Virol.* **75**:1576-1580.
  112. **Jeffers, S. A., D. A. Sanders, and A. Sanchez.** 2002. Covalent modifications of the ebola virus glycoprotein. *J Virol* **76**:12463-12472.
  113. **Jeffs, B.** 2006. A clinical guide to viral haemorrhagic fevers: Ebola, Marburg and Lassa. *Tropical doctor* **36**:1-4.
  114. **Johannsdottir, H. K., R. Mancini, J. Kartenbeck, L. Amato, and A. Helenius.** 2009. Host cell factors and functions involved in vesicular stomatitis virus entry. *J Virol* **83**:440-453.
  115. **Johansen, L. M., Brannan, J.M., Delos, S.E., Shoemaker, C.J., Stossel, A., Lear, C., Hoffstrom, B.G., Schornberg, K.L., Scully, C., Lehar, J., Hensley, L.E., White, J.M., Olinger, G.O.** 2012. FDA Approved Selective Estrogen Receptor Modulators Inhibit Ebola Infection. In revision.
  116. **Johnson, R. F., P. Bell, and R. N. Harty.** 2006. Effect of Ebola virus proteins GP, NP and VP35 on VP40 VLP morphology. *Virol J* **3**:31.
  117. **Kaletsky, R. L., G. Simmons, and P. Bates.** 2007. Proteolysis of the Ebola virus glycoproteins enhances virus binding and infectivity. *J Virol* **81**:13378-13384.
  118. **Kapadia, S. B., H. Barth, T. Baumert, J. A. McKeating, and F. V. Chisari.** 2007. Initiation of hepatitis C virus infection is dependent on cholesterol and cooperativity between CD81 and scavenger receptor B type I. *J Virol* **81**:374-383.
  119. **Kaplan, G., A. Totsuka, P. Thompson, T. Akatsuka, Y. Moritsugu, and S. M. Feinstone.** 1996. Identification of a surface glycoprotein on African green monkey kidney cells as a receptor for hepatitis A virus. *The EMBO journal* **15**:4282-4296.
  120. **Kharas, M. G., and D. A. Fruman.** 2005. ABL oncogenes and phosphoinositide 3-kinase: mechanism of activation and downstream effectors. *Cancer Res* **65**:2047-2053.
  121. **Klatzmann, D., E. Champagne, S. Chamaret, J. Gruet, D. Guetard, T. Hercend, J. C. Gluckman, and L. Montagnier.** 1984. T-lymphocyte T4 molecule behaves as the receptor for human retrovirus LAV. *Nature* **312**:767-768.
  122. **Klingenstein, R., S. Lober, P. Kujala, S. Godsave, S. R. Leliveld, P. Gmeiner, P. J. Peters, and C. Korth.** 2006. Tricyclic antidepressants, quinacrine and a novel, synthetic chimera thereof clear prions by destabilizing detergent-resistant membrane compartments. *Journal of neurochemistry* **98**:748-759.
  123. **Ko, D. C., M. D. Gordon, J. Y. Jin, and M. P. Scott.** 2001. Dynamic movements of organelles containing Niemann-Pick C1 protein: NPC1 involvement in late endocytic events. *Mol Biol Cell* **12**:601-614.
  124. **Kobayashi, T., M. H. Beuchat, M. Lindsay, S. Frias, R. D. Palmiter, H. Sakuraba, R. G. Parton, and J. Gruenberg.** 1999. Late endosomal membranes rich in lysobisphosphatidic acid regulate cholesterol transport. *Nat Cell Biol* **1**:113-118.
  125. **Kolokoltsov, A. A., S. Adhikary, J. Garver, L. Johnson, R. A. Davey, and E. M. Vela.** 2012. Inhibition of Lassa virus and Ebola virus infection in host cells treated with the kinase inhibitors genistein and tyrphostin. *Archives of virology* **157**:121-127.
  126. **Kolter, T., and K. Sandhoff.** 2010. Lysosomal degradation of membrane lipids. *FEBS letters* **584**:1700-1712.

127. **Kolzer, M., N. Werth, and K. Sandhoff.** 2004. Interactions of acid sphingomyelinase and lipid bilayers in the presence of the tricyclic antidepressant desipramine. *FEBS letters* **559**:96-98.
128. **Kondratowicz, A. S., N. J. Lennemann, P. L. Sinn, R. A. Davey, C. L. Hunt, S. Moller-Tank, D. K. Meyerholz, P. Rennert, R. F. Mullins, M. Brindley, L. M. Sandersfeld, K. Quinn, M. Weller, P. B. McCray, Jr., J. Chiorini, and W. Maury.** 2011. T-cell immunoglobulin and mucin domain 1 (TIM-1) is a receptor for Zaire Ebolavirus and Lake Victoria Marburgvirus. *Proc Natl Acad Sci U S A* **108**:8426-8431.
129. **König, G., P. Chiba, and G. F. Ecker.** 2008. Hydrophobic moments as physicochemical descriptors in structure-activity relationship studies of P-glycoprotein inhibitors. *Monatshefte für Chemie / Chemical Monthly* **139**:401-405.
130. **Kool, J., N. Jonker, H. Irth, and W. M. Niessen.** 2011. Studying protein-protein affinity and immobilized ligand-protein affinity interactions using MS-based methods. *Analytical and bioanalytical chemistry* **401**:1109-1125.
131. **Krummenacher, C., A. V. Nicola, J. C. Whitbeck, H. Lou, W. Hou, J. D. Lambris, R. J. Geraghty, P. G. Spear, G. H. Cohen, and R. J. Eisenberg.** 1998. Herpes simplex virus glycoprotein D can bind to poliovirus receptor-related protein 1 or herpesvirus entry mediator, two structurally unrelated mediators of virus entry. *J Virol* **72**:7064-7074.
132. **Kuhn, J. H., S. Becker, H. Ebihara, T. W. Geisbert, K. M. Johnson, Y. Kawaoka, W. I. Lipkin, A. I. Negredo, S. V. Netesov, S. T. Nichol, G. Palacios, C. J. Peters, A. Tenorio, V. E. Volchkov, and P. B. Jahrling.** 2010. Proposal for a revised taxonomy of the family Filoviridae: classification, names of taxa and viruses, and virus abbreviations. *Archives of virology* **155**:2083-2103.
133. **Kuhn, J. H., S. R. Radoshitzky, A. C. Guth, K. L. Warfield, W. Li, M. J. Vincent, J. S. Towner, S. T. Nichol, S. Bavari, H. Choe, M. J. Aman, and M. Farzan.** 2006. Conserved receptor-binding domains of Lake Victoria marburgvirus and Zaire ebolavirus bind a common receptor. *J Biol Chem* **281**:15951-15958.
134. **Kunz, S.** 2009. Receptor binding and cell entry of Old World arenaviruses reveal novel aspects of virus-host interaction. *Virology* **387**:245-249.
135. **Kwon, H. J., L. Abi-Mosleh, M. L. Wang, J. Deisenhofer, J. L. Goldstein, M. S. Brown, and R. E. Infante.** 2009. Structure of N-terminal domain of NPC1 reveals distinct subdomains for binding and transfer of cholesterol. *Cell* **137**:1213-1224.
136. **Lakadamyali, M., M. J. Rust, H. P. Babcock, and X. Zhuang.** 2003. Visualizing infection of individual influenza viruses. *Proc Natl Acad Sci U S A* **100**:9280-9285.
137. **Le Blanc, I., P. P. Luyet, V. Pons, C. Ferguson, N. Emans, A. Petiot, N. Mayran, N. Demaurex, J. Faure, R. Sadoul, R. G. Parton, and J. Gruenberg.** 2005. Endosome-to-cytosol transport of viral nucleocapsids. *Nat Cell Biol* **7**:653-664.
138. **Lechner, A. M., I. Assfalg-Machleidt, S. Zahler, M. Stoeckelhuber, W. Machleidt, M. Jochum, and D. K. Nagler.** 2006. RGD-dependent binding of procathepsin X to integrin  $\alpha\beta 3$  mediates cell-adhesive properties. *J. Biol. Chem.* **281**:39588-39597.
139. **Leroy, E. M., B. Kumulungui, X. Pourrut, P. Rouquet, A. Hassanin, P. Yaba, A. Delicat, J. T. Paweska, J. P. Gonzalez, and R. Swanepoel.** 2005. Fruit bats as reservoirs of Ebola virus. *Nature* **438**:575-576.
140. **Lewis, J. M., R. Baskaran, S. Taagepera, M. A. Schwartz, and J. Y. Wang.** 1996. Integrin regulation of c-Abl tyrosine kinase activity and cytoplasmic-nuclear transport. *Proc Natl Acad Sci U S A* **93**:15174-15179.

141. **Li, W., M. J. Moore, N. Vasilieva, J. Sui, S. K. Wong, M. A. Berne, M. Somasundaran, J. L. Sullivan, K. Luzuriaga, T. C. Greenough, H. Choe, and M. Farzan.** 2003. Angiotensin-converting enzyme 2 is a functional receptor for the SARS coronavirus. *Nature* **426**:450-454.
142. **Liberali, P., E. Kakkonen, G. Turacchio, C. Valente, A. Spaar, G. Perinetti, R. A. Bockmann, D. Corda, A. Colanzi, V. Marjomaki, and A. Luini.** 2008. The closure of Pak1-dependent macropinosomes requires the phosphorylation of CtBP1/BARS. *The EMBO journal* **27**:970-981.
143. **Liebl, D., F. Difato, L. Hornikova, P. Mannova, J. Stokrova, and J. Forstova.** 2006. Mouse polyomavirus enters early endosomes, requires their acidic pH for productive infection, and meets transferrin cargo in Rab11-positive endosomes. *J Virol* **80**:4610-4622.
144. **Liu, J., A. Bartesaghi, M. J. Borgnia, G. Sapiro, and S. Subramaniam.** 2008. Molecular architecture of native HIV-1 gp120 trimers. *Nature* **455**:109-113.
145. **Liu, R., P. Lu, J. W. Chu, and F. J. Sharom.** 2009. Characterization of fluorescent sterol binding to purified human NPC1. *J Biol Chem* **284**:1840-1852.
146. **Liu, S., A. V. Rodriguez, and M. T. Tosteson.** 2006. Role of simvastatin and methyl-beta-cyclodextrin [corrected] on inhibition of poliovirus infection. *Biochemical and biophysical research communications* **347**:51-59.
147. **Lloyd-Evans, E., A. J. Morgan, X. He, D. A. Smith, E. Elliot-Smith, D. J. Sillence, G. C. Churchill, E. H. Schuchman, A. Galione, and F. M. Platt.** 2008. Niemann-Pick disease type C1 is a sphingosine storage disease that causes deregulation of lysosomal calcium. *Nat Med* **14**:1247-1255.
148. **Lloyd-Evans, E., and F. M. Platt.** 2010. Lipids on trial: the search for the offending metabolite in Niemann-Pick type C disease. *Traffic* **11**:419-428.
149. **Lorizate, M., and H. G. Krausslich.** 2011. Role of lipids in virus replication. *Cold Spring Harbor perspectives in biology* **3**:a004820.
150. **Lozach, P.-Y., J. Huotari, and A. Helenius.** 2011. Late-penetrating viruses. *Current Opinion in Virology* **1**:35-43.
151. **Lozach, P. Y., A. Kuhbacher, R. Meier, R. Mancini, D. Bitto, M. Bouloy, and A. Helenius.** 2011. DC-SIGN as a receptor for phleboviruses. *Cell host & microbe* **10**:75-88.
152. **Luque, D., G. Rivas, C. Alfonso, J. L. Carrascosa, J. F. Rodriguez, and J. R. Caston.** 2009. Infectious bursal disease virus is an icosahedral polypliod dsRNA virus. *Proc Natl Acad Sci U S A* **106**:2148-2152.
153. **Maginnis, M. S., J. C. Forrest, S. A. Kopecky-Bromberg, S. K. Dickeson, S. A. Santoro, M. M. Zutter, G. R. Nemerow, J. M. Bergelson, and T. S. Dermody.** 2006.  $\beta$ 1 integrin mediates internalization of mammalian reovirus. *J. Virol.* **80**:2760-2770.
154. **Maginnis, M. S., B. A. Mainou, A. Derdowski, E. M. Johnson, R. Zent, and T. S. Dermody.** 2008. NPXY motifs in the  $\beta$ 1 Integrin cytoplasmic tail are required for functional reovirus entry. *J. Virol.* **82**:3181-3191.
155. **Mahanty, S., and M. Bray.** 2004. Pathogenesis of filoviral haemorrhagic fevers. *Lancet Infect Dis* **4**:487-498.
156. **Malashkevich, V. N., B. J. Schneider, M. L. McNally, M. A. Milhollen, J. X. Pang, and P. S. Kim.** 1999. Core structure of the envelope glycoprotein GP2 from Ebola virus at 1.9-A resolution. *Proc Natl Acad Sci U S A* **96**:2662-2667.
157. **Manicassamy, B., and L. Rong.** 2009. Expression of Ebolavirus glycoprotein on the target cells enhances viral entry. *Virol J* **6**:75.

158. **Manicassamy, B., J. Wang, H. Jiang, and L. Rong.** 2005. Comprehensive analysis of ebola virus GP1 in viral entry. *J Virol* **79**:4793-4805.
159. **Martinez, O., J. Johnson, B. Manicassamy, L. Rong, G. G. Olinger, L. E. Hensley, and C. F. Basler.** 2010. Zaire Ebola virus entry into human dendritic cells is insensitive to cathepsin L inhibition. *Cellular microbiology* **12**:148-157.
160. **Maruyama, T., P. W. Parren, A. Sanchez, I. Rensink, L. L. Rodriguez, A. S. Khan, C. J. Peters, and D. R. Burton.** 1999. Recombinant human monoclonal antibodies to Ebola virus. *J Infect Dis* **179 Suppl 1**:S235-239.
161. **Masuyama, N., T. Kuronita, R. Tanaka, T. Muto, Y. Hirota, A. Takigawa, H. Fujita, Y. Aso, J. Amano, and Y. Tanaka.** 2009. HM1.24 is internalized from lipid rafts by clathrin-mediated endocytosis through interaction with alpha-adaptin. *J Biol Chem* **284**:15927-15941.
162. **Matlin, K. S., H. Reggio, A. Helenius, and K. Simons.** 1981. Infectious entry pathway of influenza virus in a canine kidney cell line. *J Cell Biol* **91**:601-613.
163. **Matlin, K. S., H. Reggio, A. Helenius, and K. Simons.** 1982. Pathway of vesicular stomatitis virus entry leading to infection. *J Mol Biol* **156**:609-631.
164. **Mayor, S., and R. E. Pagano.** 2007. Pathways of clathrin-independent endocytosis. *Nat Rev Mol Cell Biol* **8**:603-612.
165. **Meertens, L., C. Bertaux, and T. Dragic.** 2006. Hepatitis C virus entry requires a critical postinternalization step and delivery to early endosomes via clathrin-coated vesicles. *J Virol* **80**:11571-11578.
166. **Mercer, J., and A. Helenius.** 2012. Gulping rather than sipping: macropinocytosis as a way of virus entry. *Current opinion in microbiology*.
167. **Mercer, J., and A. Helenius.** 2008. Vaccinia virus uses macropinocytosis and apoptotic mimicry to enter host cells. *Science* **320**:531-535.
168. **Mercer, J., and A. Helenius.** 2009. Virus entry by macropinocytosis. *Nat Cell Biol* **11**:510-520.
169. **Mercer, J., M. Schelhaas, and A. Helenius.** 2010. Virus entry by endocytosis. *Annual review of biochemistry* **79**:803-833.
170. **Mikkelsen, T. J., P. D. Kroboth, W. J. Cameron, L. W. Dittert, V. Chungi, and P. J. Manberg.** 1986. Single-dose pharmacokinetics of clomiphene citrate in normal volunteers. *Fertil Steril* **46**:392-396.
171. **Miller, E. H., G. Obernosterer, M. Raaben, A. S. Herbert, M. S. Deffieu, A. Krishnan, E. Ndungo, R. G. Sandesara, J. E. Carette, A. I. Kuehne, G. Ruthel, S. R. Pfeffer, J. M. Dye, S. P. Whelan, T. R. Brummelkamp, and K. Chandran.** 2012. Ebola virus entry requires the host-programmed recognition of an intracellular receptor. *The EMBO journal* **31**:1947-1960.
172. **Miller, M. E., S. Adhikary, A. A. Kolokoltsov, and R. A. Davey.** 2012. Ebolavirus requires acid sphingomyelinase activity and plasma membrane sphingomyelin for infection. *J Virol* **86**:7473-7483.
173. **Miranda, M. E., T. G. Ksiazek, T. J. Retuya, A. S. Khan, A. Sanchez, C. F. Fulhorst, P. E. Rollin, A. B. Calaor, D. L. Manalo, M. C. Roces, M. M. Dayrit, and C. J. Peters.** 1999. Epidemiology of Ebola (subtype Reston) virus in the Philippines, 1996. *J Infect Dis* **179 Suppl 1**:S115-119.
174. **Miranda, M. E., and N. L. Miranda.** 2011. Reston ebolavirus in humans and animals in the Philippines: a review. *J Infect Dis* **204 Suppl 3**:S757-760.

175. **Mire, C. E., J. M. White, and M. A. Whitt.** 2010. A spatio-temporal analysis of matrix protein and nucleocapsid trafficking during vesicular stomatitis virus uncoating. *PLoS Pathog* **6**:e1000994.
176. **Mobius, W., E. van Donselaar, Y. Ohno-Iwashita, Y. Shimada, H. F. Heijnen, J. W. Slot, and H. J. Geuze.** 2003. Recycling compartments and the internal vesicles of multivesicular bodies harbor most of the cholesterol found in the endocytic pathway. *Traffic* **4**:222-231.
177. **Mohan, K. V., J. Muller, and C. D. Atreya.** 2008. Defective rotavirus particle assembly in lovastatin-treated MA104 cells. *Archives of virology* **153**:2283-2290.
178. **Mondor, I., S. Ugolini, and Q. J. Sattentau.** 1998. Human immunodeficiency virus type 1 attachment to HeLa CD4 cells is CD4 independent and gp120 dependent and requires cell surface heparans. *J Virol* **72**:3623-3634.
179. **Montgomery, R. I., M. S. Warner, B. J. Lum, and P. G. Spear.** 1996. Herpes simplex virus-1 entry into cells mediated by a novel member of the TNF/NGF receptor family. *Cell* **87**:427-436.
180. **Morello, K. C., G. T. Wurz, and M. W. DeGregorio.** 2003. Pharmacokinetics of selective estrogen receptor modulators. *Clin Pharmacokinet* **42**:361-372.
181. **Muhlberger, E., M. Weik, V. E. Volchkov, H. D. Klenk, and S. Becker.** 1999. Comparison of the transcription and replication strategies of marburg virus and Ebola virus by using artificial replication systems. *J Virol* **73**:2333-2342.
182. **Mulherkar, N., M. Raaben, J. C. de la Torre, S. P. Whelan, and K. Chandran.** 2011. The Ebola virus glycoprotein mediates entry via a non-classical dynamin-dependent macropinocytic pathway. *Virology* **419**:72-83.
183. **Nanbo, A., M. Imai, S. Watanabe, T. Noda, K. Takahashi, G. Neumann, P. Halfmann, and Y. Kawaoka.** 2010. Ebolavirus is internalized into host cells via macropinocytosis in a viral glycoprotein-dependent manner. *PLoS Pathog* **6**:e1001121.
184. **Nedelkov, D., and R. W. Nelson.** 2006. Surface plasmon resonance mass spectrometry for protein analysis. *Methods in molecular biology* **328**:131-139.
185. **Negredo, A., G. Palacios, S. Vazquez-Moron, F. Gonzalez, H. Dopazo, F. Molero, J. Juste, J. Quetglas, N. Savji, M. de la Cruz Martinez, J. E. Herrera, M. Pizarro, S. K. Hutchison, J. E. Echevarria, W. I. Lipkin, and A. Tenorio.** 2011. Discovery of an ebolavirus-like filovirus in europe. *PLoS Pathog* **7**:e1002304.
186. **Negrete, O. A., E. L. Levrony, H. C. Aguilar, A. Bertolotti-Ciarlet, R. Nazarian, S. Tajyar, and B. Lee.** 2005. EphrinB2 is the entry receptor for Nipah virus, an emergent deadly paramyxovirus. *Nature* **436**:401-405.
187. **Neumann, G., K. Shinya, and Y. Kawaoka.** 2007. Molecular pathogenesis of H5N1 influenza virus infections. *Antiviral therapy* **12**:617-626.
188. **Noda, T., H. Sagara, E. Suzuki, A. Takada, H. Kida, and Y. Kawaoka.** 2002. Ebola virus VP40 drives the formation of virus-like filamentous particles along with GP. *J Virol* **76**:4855-4865.
189. **Noyce, R. S., D. G. Bondre, M. N. Ha, L. T. Lin, G. Sisson, M. S. Tsao, and C. D. Richardson.** 2011. Tumor cell marker PVRL4 (nectin 4) is an epithelial cell receptor for measles virus. *PLoS Pathog* **7**:e1002240.
190. **Okumura, A., P. M. Pitha, and R. N. Harty.** 2008. ISG15 inhibits Ebola VP40 VLP budding in an L-domain-dependent manner by blocking Nedd4 ligase activity. *Proc Natl Acad Sci U S A* **105**:3974-3979.

191. **Ou, W., J. Delisle, K. Konduru, S. Bradfute, S. R. Radoshitzky, C. Retterer, K. Kota, S. Bavari, J. H. Kuhn, P. B. Jahrling, G. Kaplan, and C. A. Wilson.** 2011. Development and characterization of rabbit and mouse antibodies against ebolavirus envelope glycoproteins. *J Virol Methods* **174**:99-109.
192. **Owens, C. M., C. Mawhinney, J. M. Grenier, R. Altmeyer, M. S. Lee, A. A. Borisy, J. Lehar, and L. M. Johansen.** 2010. Chemical combinations elucidate pathway interactions and regulation relevant to Hepatitis C replication. *Molecular systems biology* **6**:375.
193. **Palacios, S.** 2007. The future of the new selective estrogen receptor modulators. *Menopause Int* **13**:27-34.
194. **Panchal, R. G., G. Ruthel, T. A. Kenny, G. H. Kallstrom, D. Lane, S. S. Badie, L. Li, S. Bavari, and M. J. Aman.** 2003. In vivo oligomerization and raft localization of Ebola virus protein VP40 during vesicular budding. *Proc Natl Acad Sci U S A* **100**:15936-15941.
195. **Payre, B., P. de Medina, N. Boubekeur, L. Mhamdi, J. Bertrand-Michel, F. Terce, I. Fourquaux, D. Goudouneche, M. Record, M. Poirot, and S. Silvente-Poirot.** 2008. Microsomal antiestrogen-binding site ligands induce growth control and differentiation of human breast cancer cells through the modulation of cholesterol metabolism. *Molecular cancer therapeutics* **7**:3707-3718.
196. **Pearse, B. M.** 1976. Clathrin: a unique protein associated with intracellular transfer of membrane by coated vesicles. *Proc Natl Acad Sci U S A* **73**:1255-1259.
197. **Pelkmans, L., J. Kartenbeck, and A. Helenius.** 2001. Caveolar endocytosis of simian virus 40 reveals a new two-step vesicular-transport pathway to the ER. *Nat Cell Biol* **3**:473-483.
198. **Pileri, P., Y. Uematsu, S. Campagnoli, G. Galli, F. Falugi, R. Petracca, A. J. Weiner, M. Houghton, D. Rosa, G. Grandi, and S. Abrignani.** 1998. Binding of hepatitis C virus to CD81. *Science* **282**:938-941.
199. **Pillay, C. S., E. Elliott, and C. Dennison.** 2002. Endolysosomal proteolysis and its regulation. *Biochem J* **363**:417-429.
200. **Piper, R. C., and D. J. Katzmann.** 2007. Biogenesis and function of multivesicular bodies. *Annual review of cell and developmental biology* **23**:519-547.
201. **Pisoni, R. L., and J. G. Thoene.** 1991. The transport systems of mammalian lysosomes. *Biochimica et biophysica acta* **1071**:351-373.
202. **Ploss, A., M. J. Evans, V. A. Gaysinskaya, M. Panis, H. You, Y. P. de Jong, and C. M. Rice.** 2009. Human occludin is a hepatitis C virus entry factor required for infection of mouse cells. *Nature* **457**:882-886.
203. **Ponce-Balbuena, D., A. Lopez-Izquierdo, T. Ferrer, A. A. Rodriguez-Menchaca, I. A. Arechiga-Figueroa, and J. A. Sanchez-Chapula.** 2009. Tamoxifen inhibits inward rectifier K<sup>+</sup> 2.x family of inward rectifier channels by interfering with phosphatidylinositol 4,5-bisphosphate-channel interactions. *The Journal of pharmacology and experimental therapeutics* **331**:563-573.
204. **Potena, L., G. Frascaroli, F. Grigioni, T. Lazzarotto, G. Magnani, L. Tomasi, F. Coccolo, L. Gabrielli, C. Magelli, M. P. Landini, and A. Branzi.** 2004. Hydroxymethyl-glutaryl coenzyme a reductase inhibition limits cytomegalovirus infection in human endothelial cells. *Circulation* **109**:532-536.
205. **Qiu, X., J. Audet, G. Wong, S. Pillet, A. Bello, T. Cabral, J. E. Strong, F. Plummer, C. R. Corbett, J. B. Alimonti, and G. P. Kobinger.** 2012. Successful treatment of ebola virus-infected cynomolgus macaques with monoclonal antibodies. *Science translational medicine* **4**:138ra181.

206. **Qiu, Z., S. T. Hingley, G. Simmons, C. Yu, J. Das Sarma, P. Bates, and S. R. Weiss.** 2006. Endosomal proteolysis by cathepsins is necessary for murine coronavirus mouse hepatitis virus type 2 spike-mediated entry. *J. Virol.* **80**:5768-5776.
207. **Quirin, K., B. Eschli, I. Scheu, L. Poort, J. Kartenbeck, and A. Helenius.** 2008. Lymphocytic choriomeningitis virus uses a novel endocytic pathway for infectious entry via late endosomes. *Virology* **378**:21-33.
208. **Reiners, J. J., Jr., M. Kleinman, D. Kessel, P. A. Mathieu, and J. A. Caruso.** 2011. Nonesterified cholesterol content of lysosomes modulates susceptibility to oxidant-induced permeabilization. *Free radical biology & medicine* **50**:281-294.
209. **Rekker, R. F., A. M. T. Laak, and R. Mannhold.** 1993. On the Reliability of Calculated Log P-values: Rekker, Hansch/Leo and Suzuki Approach. *Quantitative Structure-Activity Relationships* **12**:152-157.
210. **Roels, T. H., A. S. Bloom, J. Buffington, G. L. Muhungu, W. R. Mac Kenzie, A. S. Khan, R. Ndambi, D. L. Noah, H. R. Rolka, C. J. Peters, and T. G. Ksiazek.** 1999. Ebola hemorrhagic fever, Kikwit, Democratic Republic of the Congo, 1995: risk factors for patients without a reported exposure. *J Infect Dis* **179 Suppl 1**:S92-97.
211. **Rojek, J. M., M. Perez, and S. Kunz.** 2008. Cellular entry of lymphocytic choriomeningitis virus. *J Virol* **82**:1505-1517.
212. **Romer, W., L. Berland, V. Chambon, K. Gaus, B. Windschiegel, D. Tenza, M. R. Aly, V. Fraissier, J. C. Florent, D. Perrais, C. Lamaze, G. Raposo, C. Steinem, P. Sens, P. Bassereau, and L. Johannes.** 2007. Shiga toxin induces tubular membrane invaginations for its uptake into cells. *Nature* **450**:670-675.
213. **Roth, T. F., and K. R. Porter.** 1964. Yolk Protein Uptake in the Oocyte of the Mosquito *Aedes Aegypti*. *L. J Cell Biol* **20**:313-332.
214. **Rothwell, C., A. Lebreton, C. Young Ng, J. Y. Lim, W. Liu, S. Vasudevan, M. Labow, F. Gu, and L. A. Gaither.** 2009. Cholesterol biosynthesis modulation regulates dengue viral replication. *Virology* **389**:8-19.
215. **Ryabchikova, E. I., L. V. Kolesnikova, and S. V. Luchko.** 1999. An analysis of features of pathogenesis in two animal models of Ebola virus infection. *J Infect Dis* **179 Suppl 1**:S199-202.
216. **Saeed, M. F., A. A. Kolokoltsov, T. Albrecht, and R. A. Davey.** 2010. Cellular entry of ebola virus involves uptake by a macropinocytosis-like mechanism and subsequent trafficking through early and late endosomes. *PLoS Pathog* **6**:e1001110.
217. **Saeed, M. F., A. A. Kolokoltsov, A. N. Freiberg, M. R. Holbrook, and R. A. Davey.** 2008. Phosphoinositide-3 kinase-Akt pathway controls cellular entry of Ebola virus. *PLoS Pathog* **4**:e1000141.
218. **Saffarian, S., E. Cocucci, and T. Kirchhausen.** 2009. Distinct dynamics of endocytic clathrin-coated pits and coated plaques. *PLoS biology* **7**:e1000191.
219. **Sanchez, A.** 2007. Analysis of filovirus entry into vero e6 cells, using inhibitors of endocytosis, endosomal acidification, structural integrity, and cathepsin (B and L) activity. *J Infect Dis* **196 Suppl 2**:S251-258.
220. **Sanchez A, G. T. a. F. H.** 2007. *Filoviridae –Marburg and Ebola viruses.*, 5th ed. ed. Lippincott Williams & Wilkins., Philadelphia, PA.
221. **Sanchez, A., S. G. Trappier, B. W. Mahy, C. J. Peters, and S. T. Nichol.** 1996. The virion glycoproteins of Ebola viruses are encoded in two reading frames and are expressed through transcriptional editing. *Proc Natl Acad Sci U S A* **93**:3602-3607.

222. **Sanchez, A., K. E. Wagoner, and P. E. Rollin.** 2007. Sequence-based human leukocyte antigen-B typing of patients infected with Ebola virus in Uganda in 2000: identification of alleles associated with fatal and nonfatal disease outcomes. *J Infect Dis* **196 Suppl 2**:S329-336.
223. **Sawaki, M., A. Idota, H. Uchida, S. Noda, S. Sato, T. Kikumori, and T. Imai.** 2011. The effect of toremifene on lipid metabolism compared with that of tamoxifen in vitro. *Gynecologic and obstetric investigation* **71**:213-216.
224. **Scarselli, E., H. Ansuini, R. Cerino, R. M. Roccasecca, S. Acali, G. Filocamo, C. Traboni, A. Nicosia, R. Cortese, and A. Vitelli.** 2002. The human scavenger receptor class B type I is a novel candidate receptor for the hepatitis C virus. *The EMBO journal* **21**:5017-5025.
225. **Schiff, L. A., M. L. Nibert, and K. L. Tyler.** 2007. Orthoreoviruses and their replication, p. 1853-1915. *In* B. N. Fields, D. M. Knipe, and P. M. Howley (ed.), *Fields Virology*, 5th ed, vol. 1. Lippincott Williams & Wilkins, Philadelphia.
226. **Schornerberg, K.** 2008. *Ebolavirus Entry*. University of Virginia, Charlottesville, VA.
227. **Schornerberg, K., S. Matsuyama, K. Kabsch, S. Delos, A. Bouton, and J. White.** 2006. Role of endosomal cathepsins in entry mediated by the Ebola virus glycoprotein. *J Virol* **80**:4174-4178.
228. **Schornerberg, K. L., C. J. Shoemaker, D. Dube, M. Y. Abshire, S. E. Delos, A. H. Bouton, and J. M. White.** 2009. Alpha5beta1-integrin controls ebolavirus entry by regulating endosomal cathepsins. *Proc Natl Acad Sci U S A* **106**:8003-8008.
229. **Schreiner, C., J. Bauer, Y. Danilov, S. Hussein, M. Sczekan, and R. Juliano.** 1989. Isolation and characterization of Chinese hamster ovary cell variants deficient in the expression of fibronectin receptor. *J. Cell Biol.* **109**:3157-3167.
230. **Schuchman, E. H.** 2007. The pathogenesis and treatment of acid sphingomyelinase-deficient Niemann-Pick disease. *Journal of inherited metabolic disease* **30**:654-663.
231. **Scott, C., and Y. A. Ioannou.** 2004. The NPC1 protein: structure implies function. *Biochimica et biophysica acta* **1685**:8-13.
232. **Seo, N.-S., C. Q.-Y. Zeng, J. M. Hyser, B. Utama, S. E. Crawford, K. J. Kim, M. HÅÅk, and M. K. Estes.** 2008. Integrins  $\alpha 1\beta 1$  and  $\alpha 2\beta 1$  are receptors for the rotavirus enterotoxin. *Proc. Natl. Acad. Sci. USA* **105**:8811-8818.
233. **Shelly, W., M. W. Draper, V. Krishnan, M. Wong, and R. B. Jaffe.** 2008. Selective estrogen receptor modulators: an update on recent clinical findings. *Obstet Gynecol Surv* **63**:163-181.
234. **Shimojima, M., A. Takada, H. Ebihara, G. Neumann, K. Fujioka, T. Irimura, S. Jones, H. Feldmann, and Y. Kawaoka.** 2006. Tyro3 family-mediated cell entry of Ebola and Marburg viruses. *J Virol* **80**:10109-10116.
235. **Shoemaker, C. J.** 2012. *Mechanisms of Ebolavirus Entry*. University of Virginia, Charlottesville, VA.
236. **Shoemaker, C. J., Schornerberg, K.L., Delos, S.E., Scully, C., Pajouhesh, H., Olinger, G.G., Johansen, L.M., and White, J.M.** 2012. Multiple Cationic Amphiphiles that Induce a Niemann-Pick C Phenotype Inhibit Ebola Virus Entry and Infection. Submitted.
237. **Sieczkarski, S. B., and G. R. Whittaker.** 2003. Differential requirements of Rab5 and Rab7 for endocytosis of influenza and other enveloped viruses. *Traffic* **4**:333-343.
238. **Simmons, G., A. J. Rennekamp, N. Chai, L. H. Vandenberghe, J. L. Riley, and P. Bates.** 2003. Folate receptor alpha and caveolae are not required for Ebola virus glycoprotein-mediated viral infection. *J Virol* **77**:13433-13438.

239. **Slater, B., A. McCormack, A. Avdeef, and J. E. Comer.** 1994. pH-metric log P. 4. Comparison of partition coefficients determined by HPLC and potentiometric methods to literature values. *J Pharm Sci* **83**:1280-1283.
240. **Smith, D. R., S. McCarthy, A. Chrovian, G. Olinger, A. Stossel, T. W. Geisbert, L. E. Hensley, and J. H. Connor.** 2010. Inhibition of heat-shock protein 90 reduces Ebola virus replication. *Antiviral research* **87**:187-194.
241. **Sobo, K., I. Le Blanc, P. P. Luyet, M. Fivaz, C. Ferguson, R. G. Parton, J. Gruenberg, and F. G. van der Goot.** 2007. Late endosomal cholesterol accumulation leads to impaired intra-endosomal trafficking. *PLoS one* **2**:e851.
242. **Sokol, J., J. Blanchette-Mackie, H. S. Kruth, N. K. Dwyer, L. M. Amende, J. D. Butler, E. Robinson, S. Patel, R. O. Brady, M. E. Comly, and et al.** 1988. Type C Niemann-Pick disease. Lysosomal accumulation and defective intracellular mobilization of low density lipoprotein cholesterol. *J Biol Chem* **263**:3411-3417.
243. **Stewart, P. L., and G. R. Nemerow.** 2007. Cell integrins: commonly used receptors for diverse viral pathogens. *Trends Microbiol.* **15**:500-507.
244. **Stroher, U., and H. Feldmann.** 2006. Progress towards the treatment of Ebola haemorrhagic fever. *Expert opinion on investigational drugs* **15**:1523-1535.
245. **Sullivan, N., Z. Y. Yang, and G. J. Nabel.** 2003. Ebola virus pathogenesis: implications for vaccines and therapies. *J Virol* **77**:9733-9737.
246. **Sullivan, N. J., J. E. Martin, B. S. Graham, and G. J. Nabel.** 2009. Correlates of protective immunity for Ebola vaccines: implications for regulatory approval by the animal rule. *Nat Rev Microbiol* **7**:393-400.
247. **Swaminathan, K., and K. M. Downard.** 2012. Anti-viral inhibitor binding to influenza neuraminidase by MALDI mass spectrometry. *Analytical chemistry* **84**:3725-3730.
248. **Swanepoel, R., P. A. Leman, F. J. Burt, N. A. Zachariades, L. E. Braack, T. G. Ksiazek, P. E. Rollin, S. R. Zaki, and C. J. Peters.** 1996. Experimental inoculation of plants and animals with Ebola virus. *Emerging infectious diseases* **2**:321-325.
249. **Takada, A., C. Robison, H. Goto, A. Sanchez, K. G. Murti, M. A. Whitt, and Y. Kawaoka.** 1997. A system for functional analysis of Ebola virus glycoprotein. *Proc Natl Acad Sci U S A* **94**:14764-14769.
250. **Takada, A., S. Watanabe, H. Ito, K. Okazaki, H. Kida, and Y. Kawaoka.** 2000. Downregulation of  $\beta$ 1 integrins by Ebola virus glycoprotein: Implication for virus entry. *Virology* **278**:20-26.
251. **Taras, T. L., G. T. Wurz, G. R. Linares, and M. W. DeGregorio.** 2000. Clinical pharmacokinetics of toremifene. *Clin Pharmacokinet* **39**:327-334.
252. **Tatsuo, H., N. Ono, K. Tanaka, and Y. Yanagi.** 2000. SLAM (CDw150) is a cellular receptor for measles virus. *Nature* **406**:893-897.
253. **Timmins, J., G. Schoehn, C. Kohlhaas, H. D. Klenk, R. W. Ruigrok, and W. Weissenhorn.** 2003. Oligomerization and polymerization of the filovirus matrix protein VP40. *Virology* **312**:359-368.
254. **Timmins, J., S. Scianimanico, G. Schoehn, and W. Weissenhorn.** 2001. Vesicular release of ebola virus matrix protein VP40. *Virology* **283**:1-6.
255. **Tomko, R. P., R. Xu, and L. Philipson.** 1997. HCAR and MCAR: the human and mouse cellular receptors for subgroup C adenoviruses and group B coxsackieviruses. *Proc Natl Acad Sci U S A* **94**:3352-3356.
256. **Towner, J. S., J. Paragas, J. E. Dover, M. Gupta, C. S. Goldsmith, J. W. Huggins, and S. T. Nichol.** 2005. Generation of eGFP expressing recombinant Zaire ebolavirus for analysis

- of early pathogenesis events and high-throughput antiviral drug screening. *Virology* **332**:20-27.
257. **Towner, J. S., P. E. Rollin, D. G. Bausch, A. Sanchez, S. M. Crary, M. Vincent, W. F. Lee, C. F. Spiropoulou, T. G. Ksiazek, M. Lukwiya, F. Kaducu, R. Downing, and S. T. Nichol.** 2004. Rapid diagnosis of Ebola hemorrhagic fever by reverse transcription-PCR in an outbreak setting and assessment of patient viral load as a predictor of outcome. *J Virol* **78**:4330-4341.
  258. **Tsai, B., J. M. Gilbert, T. Stehle, W. Lencer, T. L. Benjamin, and T. A. Rapoport.** 2003. Gangliosides are receptors for murine polyoma virus and SV40. *The EMBO journal* **22**:4346-4355.
  259. **Tscherne, D. M., B. Manicassamy, and A. Garcia-Sastre.** 2010. An enzymatic virus-like particle assay for sensitive detection of virus entry. *J Virol Methods* **163**:336-343.
  260. **Tuffs, A.** 2009. Experimental vaccine may have saved Hamburg scientist from Ebola fever. *BMJ* **338**:b1223.
  261. **van der Blik, A. M., T. E. Redelmeier, H. Damke, E. J. Tisdale, E. M. Meyerowitz, and S. L. Schmid.** 1993. Mutations in human dynamin block an intermediate stage in coated vesicle formation. *J Cell Biol* **122**:553-563.
  262. **Vaughan, R. A., M. L. Parnas, J. D. Gaffaney, M. J. Lowe, S. Wirtz, A. Pham, B. Reed, S. M. Dutta, K. K. Murray, and J. B. Justice.** 2005. Affinity labeling the dopamine transporter ligand binding site. *Journal of neuroscience methods* **143**:33-40.
  263. **Viswanadhan, V. N., A. K. Ghose, G. R. Revankar, and R. K. Robins.** 1989. Atomic physicochemical parameters for three dimensional structure directed quantitative structure-activity relationships. 4. Additional parameters for hydrophobic and dispersive interactions and their application for an automated superposition of certain naturally occurring nucleoside antibiotics. *Journal of Chemical Information and Computer Sciences* **29**:163-172.
  264. **Volchkov, V. E., S. Becker, V. A. Volchkova, V. A. Ternovoj, A. N. Kotov, S. V. Netesov, and H. D. Klenk.** 1995. GP mRNA of Ebola virus is edited by the Ebola virus polymerase and by T7 and vaccinia virus polymerases. *Virology* **214**:421-430.
  265. **Wahl-Jensen, V. M., T. A. Afanasieva, J. Seebach, U. Stroher, H. Feldmann, and H. J. Schnittler.** 2005. Effects of Ebola virus glycoproteins on endothelial cell activation and barrier function. *J Virol* **79**:10442-10450.
  266. **Wallin, M., M. Ekstrom, and H. Garoff.** 2004. Isomerization of the intersubunit disulphide-bond in Env controls retrovirus fusion. *EMBO J* **23**:54-65.
  267. **Watanabe, S., A. Takada, T. Watanabe, H. Ito, H. Kida, and Y. Kawaoka.** 2000. Functional importance of the coiled-coil of the Ebola virus glycoprotein. *J Virol* **74**:10194-10201.
  268. **Weidmann, M., E. Muhlberger, and F. T. Hufert.** 2004. Rapid detection protocol for filoviruses. *Journal of clinical virology : the official publication of the Pan American Society for Clinical Virology* **30**:94-99.
  269. **Weik, M., J. Modrof, H. D. Klenk, S. Becker, and E. Muhlberger.** 2002. Ebola virus VP30-mediated transcription is regulated by RNA secondary structure formation. *J Virol* **76**:8532-8539.
  270. **Wenigenrath, J., L. Kolesnikova, T. Hoenen, E. Mittler, and S. Becker.** 2010. Establishment and application of an infectious virus-like particle system for Marburg virus. *J Gen Virol* **91**:1325-1334.

271. **Wennerberg, K., L. Lohikangas, D. Gullberg, M. Pfaff, S. Johansson, and R. Fassler.** 1996.  $\beta$ 1 integrin-dependent and -independent polymerization of fibronectin. *J. Cell Biol.* **132**:227-238.
272. **White, J., and A. Helenius.** 1980. pH-dependent fusion between the Semliki Forest virus membrane and liposomes. *Proceedings of the National Academy of Sciences* **77**:3273-3277.
273. **White, J., J. Kartenbeck, and A. Helenius.** 1982. Membrane fusion activity of influenza virus. *The EMBO journal* **1**:217-222.
274. **White, J., K. Matlin, and A. Helenius.** 1981. Cell fusion by Semliki Forest, influenza, and vesicular stomatitis viruses. *J Cell Biol* **89**:674-679.
275. **White, J. M., S. E. Delos, M. Brecher, and K. Schornberg.** 2008. Structures and mechanisms of viral membrane fusion proteins: multiple variations on a common theme. *Critical reviews in biochemistry and molecular biology* **43**:189-219.
276. **White, J. M., and K. L. Schornberg.** 2012. A new player in the puzzle of filovirus entry. *Nat Rev Microbiol* **10**:317-322.
277. **WHO.** 1978. Ebola haemorrhagic fever in Zaire, 1976. *Bulletin of the World Health Organization.*
278. **Wickham, T. J., P. Mathias, D. A. Cheresch, and G. R. Nemerow.** 1993. Integrins alpha v beta 3 and alpha v beta 5 promote adenovirus internalization but not virus attachment. *Cell* **73**:309-319.
279. **Wilen, C. B., J. C. Tilton, and R. W. Doms.** 2012. Molecular mechanisms of HIV entry. *Advances in experimental medicine and biology* **726**:223-242.
280. **Wittmann, T. J., R. Biek, A. Hassanin, P. Rouquet, P. Reed, P. Yaba, X. Pourrut, L. A. Real, J. P. Gonzalez, and E. M. Leroy.** 2007. Isolates of Zaire ebolavirus from wild apes reveal genetic lineage and recombinants. *Proc Natl Acad Sci U S A* **104**:17123-17127.
281. **Wong, A. C., R. G. Sandesara, N. Mulherkar, S. P. Whelan, and K. Chandran.** 2010. A forward genetic strategy reveals destabilizing mutations in the Ebolavirus glycoprotein that alter its protease dependence during cell entry. *J Virol* **84**:163-175.
282. **Wool-Lewis, R. J., and P. Bates.** 1999. Endoproteolytic processing of the ebola virus envelope glycoprotein: cleavage is not required for function. *J Virol* **73**:1419-1426.
283. **Yang, Z., R. Delgado, L. Xu, R. F. Todd, E. G. Nabel, A. Sanchez, and G. J. Nabel.** 1998. Distinct cellular interactions of secreted and transmembrane Ebola virus glycoproteins. *Science* **279**:1034-1037.
284. **Ye, J., C. Wang, R. Sumpter, Jr., M. S. Brown, J. L. Goldstein, and M. Gale, Jr.** 2003. Disruption of hepatitis C virus RNA replication through inhibition of host protein geranylgeranylation. *Proc Natl Acad Sci U S A* **100**:15865-15870.
285. **Yogalingam, G., and A. M. Pendergast.** 2008. ABL kinases regulate autophagy by promoting the trafficking and function of lysosomal components. *J Biol Chem* **283**:35941-35953.
286. **Yonezawa, A., M. Cavrois, and W. C. Greene.** 2005. Studies of ebola virus glycoprotein-mediated entry and fusion by using pseudotyped human immunodeficiency virus type 1 virions: involvement of cytoskeletal proteins and enhancement by tumor necrosis factor alpha. *J Virol* **79**:918-926.
287. **Zaitseva, E., S. T. Yang, K. Melikov, S. Pourmal, and L. V. Chernomordik.** 2010. Dengue virus ensures its fusion in late endosomes using compartment-specific lipids. *PLoS Pathog* **6**:e1001131.

## Appendix

## **$\alpha 5 \beta 1$ Integrin Controls Ebolavirus Entry by Regulating Endosomal Cathepsins**

Kathryn L. Schornberg, Charles J. Shoemaker, Derek Dube, Michelle Y. Abshire,  
Sue E. Delos, Amy H. Bouton, and Judith M. White

- Adapted from Schornberg, et al. Proc Natl Acad Sci USA. 2009 May  
12;106(19):8003-8. (228)

**Abstract**

Integrins are involved in the binding and internalization of both enveloped and non-enveloped viruses. Using three distinct cell systems, CHO cells lacking expression of  $\alpha 5\beta 1$  integrin, Hela cells treated with siRNA to  $\alpha 5$  integrin, and mouse  $\beta 1$  integrin knockout fibroblasts, we show that  $\alpha 5\beta 1$  integrin is required for efficient infection by pseudovirions bearing the ebolavirus glycoprotein (GP). These integrins are necessary for viral entry, but not for binding or internalization. Given the need for endosomal cathepsins B and L (CatB and CatL) to prime GP for fusion, we investigated the status of CatB and CatL in integrin-positive and negative cell lines.  $\alpha 5\beta 1$  integrin-deficient cells lacked the double chain forms of CatB and CatL, and this correlated with decreased CatL activity in integrin-negative CHO cells. These data indicate that  $\alpha 5\beta 1$  integrin-negative cells may be refractory to infection by GP pseudovirions because they lack the necessary priming machinery (the double chain forms of CatB and CatL). In support of this model, we show that GP pseudovirions that have been pre-primed *in vitro* to generate the 19 kDa form of GP overcome the requirement for  $\alpha 5\beta 1$  integrin for infection. These results provide further support for the requirement for endosomal cathepsins for ebolavirus infection, identify the DC forms of these cathepsins as previously unrecognized factors that contribute to cell tropism of this virus, and reveal a novel role for integrins during viral entry as regulators of endosomal cathepsins, which are required to prime the entry proteins of ebolavirus and other pathogenic viruses.

## Introduction

Integrins are used by a variety of enveloped and non-enveloped viruses, as well as bacteria, to establish infection in host cells. Integrins are heterodimers composed of an  $\alpha$  and a  $\beta$  subunit. They play an important role in a number of cellular functions, including cell adhesion, migration, proliferation, differentiation, and apoptosis. Integrins are attractive targets for pathogens because they are expressed on a wide variety of different cell types, where they initiate a cascade of signaling events that can facilitate endocytosis and intracellular trafficking of the pathogen (108).

Integrins often serve as primary receptors, allowing viruses to bind to and infect host cells. This is the case with several picornaviruses and hantaviruses (243). For certain adenoviruses and reoviruses, the virus binds to a separate primary cell surface receptor, but interaction with an integrin co-receptor is necessary for internalization. Several herpesviruses have also been shown to bind to host cells via association with other receptors, but require interactions with integrins to initiate cell signaling cascades that promote virus endocytosis and trafficking. Finally, in addition to utilizing integrins for virus internalization, rotavirus encodes an enterotoxin which binds to integrins on intestinal epithelial cells and induces a diarrheal response in mice (232).

$\alpha 1$  integrins have been proposed to facilitate entry of the highly virulent filovirus, Ebola virus (EBOV). Kawaoka and colleagues (250) found that  $\beta 1$  integrin expression was downregulated in cells transfected with the EBOV glycoprotein (GP). They hypothesized that GP interacted directly with  $\beta 1$

integrins leading to its downregulation, as is the case for the HIV glycoprotein gp120 and its receptor CD4. In support of this hypothesis, they found that treatment of target cells with Abs to  $\beta 1$  integrin or with soluble  $\alpha 5\beta 1$  integrin complexes reduced GP-pseudotyped virus infection ~50%. Several other cell surface proteins have also been shown to influence GP-mediated entry, including C-type lectins and members of the Tyro3 family (56). So far no single cell surface protein has been found to be both necessary and sufficient for EBOV entry. Thus, it is possible that viral entry involves a combination of receptor molecules and could vary by cell type.

Here we confirmed a role for  $\alpha 5\beta 1$  integrin in EBOV infection. Surprisingly, we found that rather than being needed for virus binding or internalization,  $\alpha 5\beta 1$  integrin is required for steps leading to fusion. We further determined that this requirement is at the level of endosomal cathepsins, which have been previously implicated in EBOV entry (40, 227).

## Results

**Expression of  $\alpha 5\beta 1$  integrin enhances EBOV GP-mediated infection.** To examine the role of  $\alpha 5\beta 1$  integrin in EBOV infection, we took advantage of a series of CHO cells that differ in their  $\alpha 5\beta 1$  integrin expression. CHO K1 cells express endogenous hamster  $\alpha 5\beta 1$  integrin. CHO B2 cells are a clone of CHO K1 cells that was selected for very low cell surface expression of  $\alpha 5\beta 1$ . These cells still contain the  $\beta 1$  integrin chain as well as increased amounts of a pre-  $\beta 1$  integrin moiety, but lack detectable levels of  $\alpha 5$  integrin and therefore do not express  $\alpha 5\beta 1$  integrin on their surface (229). CHO B2-  $\alpha 5$  cells are a clone of

CHO B2 cells engineered to stably express human  $\alpha 5$  integrin, which can complex with hamster  $\beta 1$  integrin to promote surface expression of  $\alpha 5\beta 1$  (33). We confirmed expression of  $\alpha 5$  and  $\beta 1$  integrins in these cells by surface biotinylating the cells and immunoblotting either the whole cell lysate or avidin-precipitated lysate for  $\alpha 5$  and  $\beta 1$  integrins. As expected, only the CHO K1 and CHO B2-  $\alpha 5$  cells express  $\alpha 5$  integrin in whole cell lysates and on the surface (Fig. 1A, lanes 1 and 3, 4 and 6). All three cell lines are positive for  $\beta 1$  integrin in the whole cell lysates (lanes 1-3), but the CHO B2 cells have greatly reduced  $\beta 1$  integrin expression on their surface (lane 5).

Using VSV pseudotypes encoding GFP that express full-length or mucin domain-deleted EBOV GP or VSV G (VSV-GP, VSV-GP $\Delta$ , and VSV-G, respectively), we infected this panel of CHO cells and determined the percent of infected cells by flow cytometry. Although we observed consistently higher infection with VSV-GP $\Delta$  virus as compared to VSV-GP, in both cases there was an ~90% decrease in infection of the CHO B2 cells compared to CHO K1 cells (Fig. 1B). Re-expression of surface  $\alpha 5\beta 1$  integrin rescued infection by both VSV-GP and VSV-GP $\Delta$ . Infection by VSV-G was not significantly different across the three cell lines. These results support a previous report that indicated an important role for  $\alpha 5\beta 1$  integrin in EBOV GP-mediated infection (250).

To further confirm that  $\alpha 5\beta 1$  expression is important for EBOV GP-mediated infection, we used siRNA duplexes to knock down expression of  $\alpha 5$  and  $\beta 1$  integrin in Hela cells. Expression of  $\alpha 5$  integrin was reduced by 80% in whole cell lysates and 50% on the cell surface in  $\alpha 5$  siRNA-treated cells (Fig. 2A,

upper panels, lanes 2 and 5). This correlated well with a 50% decrease in infection by VSV-GPΔ (Fig. 2B). β1 integrin expression was not reduced, and in fact was increased, on the surface of the α5 siRNA-treated cells (middle panel, lane 5), suggesting that β1 is still present on the cell surface in complex with other α subunits. The residual infection in the α5 siRNA-treated HeLa cells could be due to these other α5x β1 complexes, and/or to the remaining 50% of α5β1 still present on the surface of these cells.

In β1 targeted siRNA-treated cells, expression of β1 integrin was reduced by 80% in whole cell lysates and by 60% on the cell surface (middle panel, lanes 3 and 6); however expression of α5 integrin was reduced by only 10% on the cell surface (top panel, lane 6). As α5 integrin is not known to form a complex with any other subunit besides β1, this result suggests that significant levels (~90%) of α5β1 integrin are still present on the surface of β1 siRNA-treated cells, likely explaining why VSV-GP infection of the β1 siRNA-treated cells was not reduced (Fig. 2B, left set, black bar). Infection by VSV-G was not significantly inhibited by either siRNA treatment.

**Integrin expression is not required for EBOV GP-mediated binding or internalization.** Integrins have been shown to be involved in infection by a wide range of viruses, most often at the stages of virus binding or internalization. The CHO cells lines described above were used to determine if α5β1 integrin is involved in EBOV GP-mediated binding or internalization using a biochemical assay (see Methods). As shown in Fig. 3A, neither virus binding (lanes 1-3) nor internalization (lanes 7-9) was dependent on α5β1 integrin expression. To

confirm these results, binding and internalization of VSV-GPΔ in CHO B2 and CHO B2-α5 cells was visualized by immunofluorescence. In agreement with the above results, we found that both cell lines bound and internalized equivalent amounts of virus (Fig. 3B and S1A). As a further test, we compared binding of increasing amounts of a recombinant EBOV receptor binding region (RBR) to CHO B2 and CHO B2- α5 cells. As shown previously (58, 60), this recombinant RBR protein binds specifically to cells that are susceptible to EBOV GP-mediated infection and not to cells that are refractory to EBOV infection (S1B). Consistent with the above data, there was no significant difference in RBR binding between the CHO B2 and CHO B2- α5 cells (Fig. 3C and S1B).

**α5β1 integrin expression is required at or before EBOV GP-mediated fusion.** Following binding and internalization, the virus must undergo fusion with a cellular membrane. To determine if surface expression of α5β1 integrin is required for events leading up to EBOV GP-mediated fusion, the three CHO cell lines were infected with HIV pseudotyped viruses containing β -lactamase (Blam) and bearing EboV GPΔ (HIV-GPΔ). Upon fusion, the Blam is released into the cytoplasm where it can cleave a fluorogenic substrate, resulting in a shift in fluorescence that can be measured by flow cytometry (36). This differs from the VSV pseudotype system used above in that neither transcription of viral mRNA nor translation of viral proteins is required to generate a positive signal. Our data with the HIV Blam-containing pseudotypes closely mirrored what was found with the VSV GFP-encoding pseudotypes; EBOV GP-mediated fusion was greatly reduced in the CHO B2 cells and was rescued by expression of α5β1 integrin

(Fig. 3D). There were no significant differences in fusion across the three cell lines when HIV Blam pseudotypes bearing VSV G (HIV-G) were used. Taken together, these data indicate that  $\alpha 5\beta 1$  integrin is not required for virus binding or internalization, but is required at or before virus fusion.

**Expression of  $\alpha 5\beta 1$  integrin correlates with CatL activity and the presence**

**of DC forms of CatB and CatL.** The endosomal cysteine proteases CatB and CatL are required for efficient EBOV GP-mediated infection (40, 227). We previously showed that CatB and CatL cleave GP into a 19 kDa primed form which is then triggered for fusion by an as yet unidentified mechanism. To examine if the block in viral fusion in the  $\alpha 5\beta 1$  integrin-negative CHO cells was at the stage of GP cleavage by cathepsins, we first looked at CatB and CatL activity in these cells. Using small fluorogenic peptide substrates for CatB and CatL, enzyme activity was measured in whole cell lysates of the three CHO cell lines. Surprisingly, CatL activity was reduced by over 90% in the CHO B2 cells as compared to the parental CHO K1 cells (Fig. 4A). This activity was significantly rescued by stable transfection of  $\alpha 5$  integrin. In contrast to CatL activity, CatB activity against the small peptide substrate was not significantly different across the panel of CHO cells (Fig. 4B).

Next, we asked if the decrease in CatL activity seen in the CHO B2 cells correlated with a loss of CatL protein. We found that the CHO B2 cells were missing an approximately 24 kDa protein that was detected by the CatL Ab (Fig. 4C, lane 2). The molecular weight of this missing band is consistent with it being the heavy chain of the mature DC form of hamster CatL (haDC), which is

generated by sequential processing of the pro- and single chain (SC) forms. The presence or absence of this putative DC form of CatL mirrored the CatL activity data (Fig. 4A), and coincided with the pattern seen for EBOV GP-mediated infection (Fig. 1B) and fusion (Fig. 3D) in these cells. To determine if overexpression of CatL could rescue infection and expression of the putative DC band in the CHO B2 cells, the CHO cell lines were transiently transfected with plasmids encoding human CatL and either infected with VSV-GP $\Delta$  or lysed for immunoblotting and activity assays. Neither infection nor CatL activity was rescued in the CHO B2 cells when CatL was ectopically expressed (data not shown). Strikingly, although these cells expressed high levels of the precursor (huPro) and SC (huSC) forms of CatL, they specifically lacked the presumptive DC form of the human enzyme (huDC) which runs at a slightly retarded electrophoretic mobility relative to the analogous hamster CatL species (Fig. 4C, lane 5).

We next examined CatB in the  $\alpha 5\beta 1$  integrin-negative cells. As was the case for CatL, the DC form of ectopically expressed CatB was also absent in the CHO B2 cells (Fig. 4D, lane 2). However, in contrast to CatL, the absence of the DC form of CatB did not correlate with a statistically significant decrease in CatB activity in these cells, as measured with a small peptide substrate (see Fig. 4B). This is in agreement with a study by Dermody and colleagues (63), who showed that CatB activity toward this peptide substrate correlated with expression of the SC, and not the DC, form of CatB.

To determine if the absence of the DC forms of these enzymes was due to increased secretion, supernatants from equivalent numbers of transfected cells were collected, concentrated, and analyzed by western blot. The levels of secreted CatB and CatL were not significantly different between the CHO B2 cells and the  $\alpha 5\beta 1$  integrin-positive cells (Fig. 4D and E, lanes 4-6). Moreover, the DC species were not trapped in high molecular weight or insoluble complexes following cell lysis, since these proteins were not present in the stacking gel or when transfected cells were lysed in low pH or boiling sample buffer (data not shown). Similarly, pre-treating the transfected cells for 24 hr with the cysteine protease inhibitor E64d (10-200 nM) did not result in detection of the DC species (data not shown), ruling out the possibility that the DC forms were being digested by a cysteine protease in the CHO B2 cells. The lack of the DC forms is also unlikely to be due to a defect in processing, as the pro- or SC forms of CatB and CatL did not significantly accumulate in the CHO B2 cells. Finally, bulk CatL protein is not grossly mislocalized in CHO B2 cells, as it colocalized predominantly with the late endosome and lysosome markers LBPA and LAMP1, as in the  $\alpha 5\beta 1$ -positive cells (S2 and S3).

**Expression of  $\alpha 5\beta 1$  integrin enhances infection and expression of the DC form of CatL in GD25 cells.** As the correlation between  $\alpha 5\beta 1$  integrin expression, EBOV GP-mediated fusion, and the presence of the DC form of CatL was highly unexpected, we utilized an additional cell line to confirm these findings. As shown in Fig. 5A, GD25 cells, which are fibroblastic cells derived from  $\beta 1$ -deficient mouse embryonic stem cells, do not express  $\alpha 5$  or  $\beta 1$  integrins

on their surface.  $\beta 1$ GD25, which have been stably transfected with the mouse  $\beta 1A$  subunit (271), express both  $\alpha 5$  and  $\beta 1$  integrins on their surface.  $\alpha 5\beta 1$  integrin expression again led to a significant increase in VSV-GP $\Delta$  but not VSV-G, infection, in this cell system (Fig. 5B). Although we were unable to visualize endogenous CatL (Fig. 5C, lanes 1-2) or CatB in these cells, the DC form of ectopically expressed human CatL was only detectable in the cells that express  $\alpha 5\beta 1$  (Fig. 5C, lanes 3-4). This supports what was seen in the CHO cells; surface expression of  $\alpha 5\beta 1$  integrin correlates with the presence of the DC form of CatL and leads to an enhancement of EBOV GP-mediated infection. However, in contrast to CHO cells, CatL activity against a small peptide substrate was not significantly different between the  $\alpha 5\beta 1$  expressing and non-expressing GD25 cells (data not shown). This suggests that the presence or absence of the DC forms of CatB and CatL may be a better indicator of EBOV susceptibility than is their activity against small peptide substrates. Nonetheless, there remains a basal level of infection of GD25 cells by VSV-GP $\Delta$  that is independent of  $\beta 1$  expression. This may be due to other integrins such as  $\alpha V\beta 3$  that contribute to cathepsin regulation and/or the presence of other proteases that can process GP at a low efficiency.

**Pre-priming of VSV-GP with thermolysin rescues infection in the  $\alpha 5\beta 1$ -negative CHO cells.** Previously, we found that *in vitro* treatment of VSV-GP with either a combination of CatB and CatL at low pH or thermolysin at neutral pH cleaves GP into a 20 kDa and subsequently a 19 kDa form. Virus bearing this cleaved form of GP (VSV-GP<sub>19k</sub>) has significantly overcome the block to infection

imposed by siRNAs targeting CatB or CatB + CatL (227). To determine if the block in infection of the  $\alpha 5\beta 1$ -negative CHO B2 cells was due to the reduction in CatL activity present in these cells, the panel of CHO cells was infected with VSV-GP $\Delta$  that had been pre-treated with thermolysin to generate VSV-GP<sub>19k</sub> (Fig. 6A). While infection with mock-treated VSV-GP $\Delta$  was again significantly decreased in CHO B2 cells relative to CHO K1 and CHO B2-  $\alpha 5$  cells (Fig. 6B, left), infection of CHO B2 cells by VSV-GP<sub>19k</sub> was significantly increased as compared to mock-treated virus and occurred at similar levels to those seen in each of the other cell lines (Fig. 6B, right). These results indicate that the primary block in infection in the  $\alpha 5\beta 1$ -negative CHO B2 cells is cleavage of GP to its primed 19 kDa form.

## Discussion

In this study, we show that expression of  $\alpha 5\beta 1$  integrin correlates with EBOV GP-pseudotyped virus infection post-binding and internalization, but prior to fusion. Expression of  $\alpha 5\beta 1$  integrin also correlates with expression of the DC forms of CatB and CatL. Cleavage of VSV-GP $\Delta$  to VSV-GP<sub>19k</sub> rescues infection in  $\alpha 5\beta 1$  integrin-negative CHO B2 cells, indicating that the primary defect in infection of these cells is cathepsin processing of GP. These studies provide further support for the requirement for active cathepsins for EBOV fusion with host cells and identify the DC forms of CatB and CatL as previously unrecognized factors that contribute to cell tropism of this virus. These findings also identify a novel role for integrins in virus entry: regulation of cathepsin expression and activity. This role for integrins in cathepsin regulation may not be restricted to  $\alpha 5\beta 1$  integrin, as a

partial rescue in EBOV GP-mediated infection and CatB and CatL DC expression was observed in CHO B2 cells engineered to express  $\alpha 4\beta 1$  integrin (data not shown).

In addition to EBOV, several other viruses have been shown to require endosomal cathepsin activity for cleavage of their fusion proteins. The F proteins of Hendra and Nipah viruses are cleaved by cathepsins prior to viral release, and this cleavage is required to prime the fusion protein (55). CatL cleavage of the spike proteins of MHV-2 and SARS following endocytosis has been shown to function as a trigger for fusion (24, 206). CatB and CatL are also required for productive infection by nonenveloped mammalian reoviruses (225). For reoviruses, it has been proposed that CatL or CatB cleavage promotes disassembly of virions to infectious subviral particles (ISVPs) within the endosome in cell culture and non-intestinal tissues, as is seen extracellularly with intestinal proteases (such as chymotrypsin) in natural enteric reovirus infections. Interestingly, reovirus also requires  $\beta 1$  integrins for efficient infection. Using the  $\beta 1$  integrin positive and negative GD25 cells described above, Dermody and colleagues (153) found that expression of  $\beta 1$  integrins significantly enhanced reovirus infection. Furthermore, they showed that pre-treating reovirus with chymotrypsin to generate ISVPs relieved the need for  $\beta 1$  integrin, similar to what we have shown here for thermolysin-generated VSV-GP<sub>19k</sub>. In contrast to what we found for EBOV pseudotypes, internalization of reovirus was also reduced in the  $\beta 1$  knockout cells. However, since the block in internalization of reovirus in GD25 cells was not complete and could not account for the full decrease in

infection of these cells (153), it is possible that loss of expression of the DC form of CatL may have also contributed to the reduction in reovirus infection.

The NPXY motifs within the  $\beta 1$  integrin cytoplasmic tail have been implicated in the process of reovirus trafficking (154). GD25 cells stably expressing  $\beta 1$  integrins containing mutations in these motifs ( $\beta 1$ GD25-NPXF) were able to internalize reovirus, but the virus was trafficked to organelles resembling secondary lysosomes and did not generate a productive infection. A similar phenomenon has recently been demonstrated for EBOV entry in the presence of inhibitors of the PI3K-Akt signaling pathway (217). PI3K is activated in response to integrin ligation in a wide range of cellular processes, as well as during the entry of several viruses (67, 243). Davey and colleagues showed that PI3K was activated during EBOV entry and that, while EBOV was still able to bind to cells and be internalized in the presence of PI3K inhibitors, the virus accumulated in cytosolic compartments and did not undergo fusion with the endosomal membrane. The observed defects in infection by reovirus in the NPXF-expressing cells and by EBOV in PI3K inhibitor-treated cells may have been due to defects in expression of the DC form of CatL in addition to the proposed defects in trafficking. Under these circumstances, uncleaved virus particles may be unable to escape the endosome and therefore may accumulate further down the endosomal pathway than in normally functioning cells.

One of the surprising outcomes of this study is that the DC form of CatL appears to be regulated by  $\alpha 5\beta 1$  integrin and, at least in the CHO cells, the DC form of CatB is similarly regulated. The absence of the DC forms of these

enzymes in the  $\alpha 5\beta 1$  integrin-negative cells does not appear to be due to a defect in processing, as there is no significant accumulation of the precursor forms of the cathepsins. The defect is also not due to a mutation in the CatB or CatL genes, as the DC forms of CatB and CatL are also missing when human cathepsins are ectopically expressed in these cells. Finally, secretion of these enzymes is not enhanced in the absence of  $\alpha 5\beta 1$  integrin. Instead, we suggest that surface expression of  $\alpha 5\beta 1$  integrin helps to stabilize the DC forms of CatB and CatL. For example, it is possible that the  $\alpha 5\beta 1$  integrin-negative cells have increased activity of an E64d-insensitive protease that degrades the DC forms of CatB and CatL. Alternatively,  $\alpha 5\beta 1$  integrin expression may be required for expression of a chaperone protein that can form a complex with the DC forms of the cathepsins and stabilize them. Finally, CatB and CatL may form a complex with  $\alpha 5\beta 1$  integrin itself, as has been shown for secreted cathepsin X (CatX) and  $\alpha v\beta 3$  integrin (138). While neither CatB nor CatL contains an RGD motif, as is found in CatX, it is possible that they can interact with  $\alpha 5\beta 1$  integrin through an RGD-independent mechanism, or via interactions with another molecule, and that this interaction either stabilizes or regulates trafficking of the DC form of the enzymes. Although the bulk of the CatL protein was found in late endosomes and lysosomes irrespective of  $\alpha 5\beta 1$  integrin surface expression, it is possible that the DC forms of the enzymes may be trafficked to a different location in the  $\alpha 5\beta 1$  integrin-negative cells. Such mislocalization could cause the enzymes to be rapidly degraded by bringing them into contact with a cellular protease that they

do not normally encounter or by preventing them from interacting with cellular factors that stabilize them.

It has recently been shown that miRNA targeting of the non-receptor tyrosine kinase Abl also results in specific loss of the DC form of CatL (285). As the activity and localization of Abl has been shown to be regulated by adhesion through  $\alpha 5$  integrins (140), it is possible that Abl may contribute to the regulation of CatL by  $\alpha 5\beta 1$  integrins. Abl can also activate the PI3K-Akt pathway (120), which is required for EBOV entry (217). It is therefore possible that PI3K, Akt, and Abl are all involved in the link between  $\alpha 5\beta 1$  integrin and the DC forms of cathepsins.

Based on our data and those of Dermody and colleagues, it appears that at least two different viruses have evolved similar entry mechanisms in which they take advantage of widely expressed integrins on the cell surface to promote virus penetration within an endocytic organelle containing active cathepsins. While integrins are well known to regulate binding and signaling activities at the cell surface that lead to viral entry, to our knowledge this is the first clear evidence that integrin expression can also regulate virus entry at subsequent steps within intracellular organelles, in this case by controlling endosomal cathepsins. These results raise the possibility that integrin expression may influence other organelle functions that could be important for infection by a variety of viruses.

## Materials and Methods

**Cells.** CHO K1, CHO B2, and CHO B2-  $\alpha 5$  cells (A. Rick Horwitz, UVa, Charlottesville) were maintained as described in (106). Hela cells were obtained from ATCC and maintained in the recommended growth media. GD25 and  $\beta 1$ GD25 cells (Deane Mosher, University of Wisconsin, Madison) were maintained as described in (271).

**Measuring integrin expression.** In Fig.1, cells were biotinylated, lysed, and avidin precipitated as described (106). Eluted proteins were analyzed under non-reducing conditions by immunoblotting with Abs specific for human  $\alpha 5$  (AB1928, Chemicon) or  $\beta 1$  (Doug DeSimone, UVa) integrins. In Fig. 5, cells were fixed and stained with Abs specific for mouse  $\alpha 5$  (BD biosciences) or  $\beta 1$  (19656, Santa Cruz) integrins.

**Viruses and infections.** VSV-GP, VSV-GP $\Delta$ , and VSV-G were made essentially as described in (227, 249) and infections were performed at approximate multiplicities of infection (m.o.i.) of 1-2 as described (227). HIV-GP $\Delta$  and HIV-G were produced and infections were performed essentially as described previously (286). The Blam-Vpr and HIV $\Delta$ Env plasmids were provided by Christopher Broder (Uniformed Services University, Bethesda, MD). Fusion was measured as the shift in fluorescence from green to blue using a CyAn™ ADP LX 9 Color flow cytometer (DakoCytomation).

**siRNA.** Hela cells were transfected with control non-targeting siRNA oligonucleotides or SMARTpool oligonucleotides consisting of four different siRNA oligonucleotides targeting  $\alpha 5$  or  $\beta 1$  integrin (Dharmacon) using

oligofectamine (Invitrogen). 48 hr post-transfection cells were infected with VSV-GPΔ or biotinylated and lysed for immunoblotting. Proteins were visualized using the Odyssey infrared imaging system and densitometry was performed using the Odyssey software (LiCor).

**Binding and internalization.** VSV-GPΔ was bound to cells at an approximate m.o.i. of 2 at 4°C. After 2 hr unbound virus was washed off and cells were either lysed to measure bound virus, or warmed to 37°C for 2 hr to allow internalization and then treated with 1 mg/ml proteinase K prior to lysing to remove uninternalized virus. Parallel wells were treated with proteinase K without the warm-up step to confirm that proteinase K effectively removed virus that was bound but not internalized. Lysates were analyzed by immunoblotting using an Ab specific for the matrix protein (M) of VSV (Michael Whitt, University of Tennessee, Memphis). For immunofluorescence, virus was bound and internalized as above at an approximate m.o.i. of 15. Cells were fixed in 2% PFA, permeabilized with 0.05% Saponin, and stained with a monoclonal Ab to GP (Lisa Hensley, U.S. Army Medical Research Institute of Infectious Diseases, Frederick, MD) followed by anti-mouse AlexaFluor 488. Texas-Red conjugated phalloidin was used to visualize actin. Images were collected with a Nikon C1 laser scanning confocal unit attached to a Nikon Eclipse TE2000-E microscope. Binding of the recombinant EBOV receptor binding region was performed as described in (58, 60).

**Cathepsin activity assays and immunoblotting.** Innozyme CatB and CatL activity assay kits (Calbiochem) were used to measure CatB and CatL enzyme

activities against small fluorogenic substrate peptides. To examine protein levels of CatB and CatL, cells were either left untransfected or transfected with plasmids encoding human CatL or CatB (Origene) using FuGENE 6 (Roche). 48 hr post-transfection the cells were lysed and equivalent amounts of protein, measured using the bicinchoninic acid assay (Pierce), were analyzed by immunoblotting with Abs specific for CatL or CatB (Athens Research and Technology). Alternatively, to visualize secreted CatB and CatL, transfection media was replaced with serum-free DMEM 24 hr post-transfection. After an additional 24 hr incubation, supernatants from equivalent cell numbers were collected and the cells were lysed for immunoblotting as above. Collected supernatants were centrifuged to remove cellular debris and proteins in the supernatant were precipitated using  $\text{CHCl}_3/\text{MeOH}$  containing salmon sperm DNA before analyzing by immunoblotting.

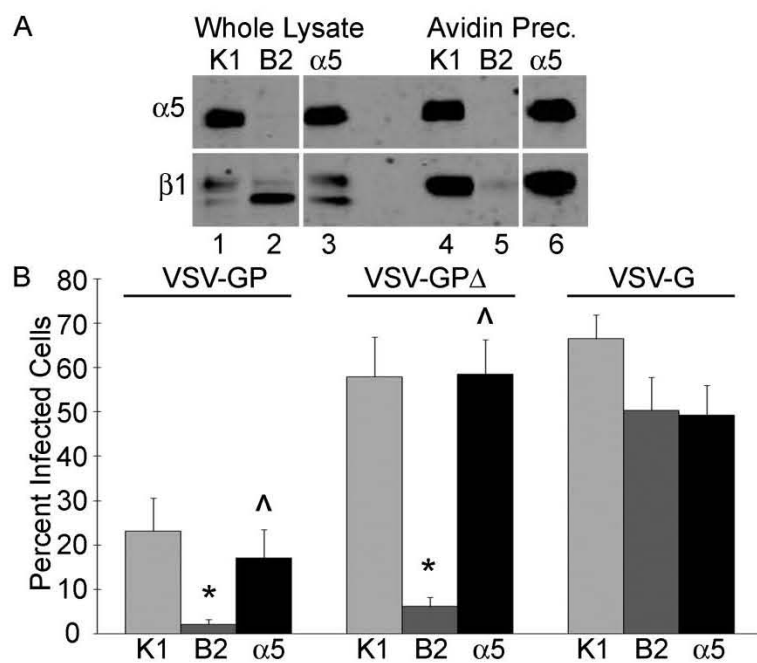
***In vitro* proteolysis of GP.** VSV-GP was mock-treated or treated with 0.5 mg/ml thermolysin (Sigma) for 30 min at 37°C as described (227). The reactions were neutralized by the addition of 10 mM EDTA. Virus samples were analyzed by immunoblotting with a polyclonal GP1 Ab raised against sGP-Fc (Paul Bates, University of Pennsylvania, Philadelphia) or used for infection.

### **Acknowledgements**

We thank our colleagues for generous gifts of reagents as indicated in Materials and Methods and Edward Park for excellent technical assistance. This work was supported by grants from the NIH (AI22470 and U54 AI7168 to JMW and in part

by AI050733 to AHB). KS, CS, and DD were supported in part by training grants 5T32 AI07046 and 5T32 AI055432 to UVa.

**Figure 1 - Expression of  $\alpha 5\beta 1$  integrin enhances EBOV GP-mediated infection of CHO cells.** (A) Total lysates and surface proteins of CHO K1 (K1), CHO B2 (B2), and CHO B2- $\alpha 5$  ( $\alpha 5$ ) cells were immunoblotted for  $\alpha 5$  (top) and  $\beta 1$  (bottom) integrin. Panels shown are from the same blot and same exposure; gaps indicate where lanes were removed. (B) The three CHO cell lines were infected with VSV-GP, VSV-GP $\Delta$ , or VSV-G and the percent of infected cells expressing GFP was measured by flow cytometry. Data shown are the averages from 10 experiments. Error bars indicate standard error from the mean (S.E.M.). \*,  $P \leq 0.02$  relative to CHO K1 cells. ^,  $P \leq 0.05$  relative to CHO B2 cells.



**Figure 2 - Knock down of  $\alpha 5$  integrin in Hela cells reduces EBOV GP-****mediated infection.** Hela cells transfected with a non-targeting control siRNAoligonucleotide (Con) or siRNA oligonucleotides targeting  $\alpha 5$  or  $\beta 1$  integrin werelysed for immunoblotting (A) or infected with VSV-GP $\Delta$  or VSV-G (B). (A)

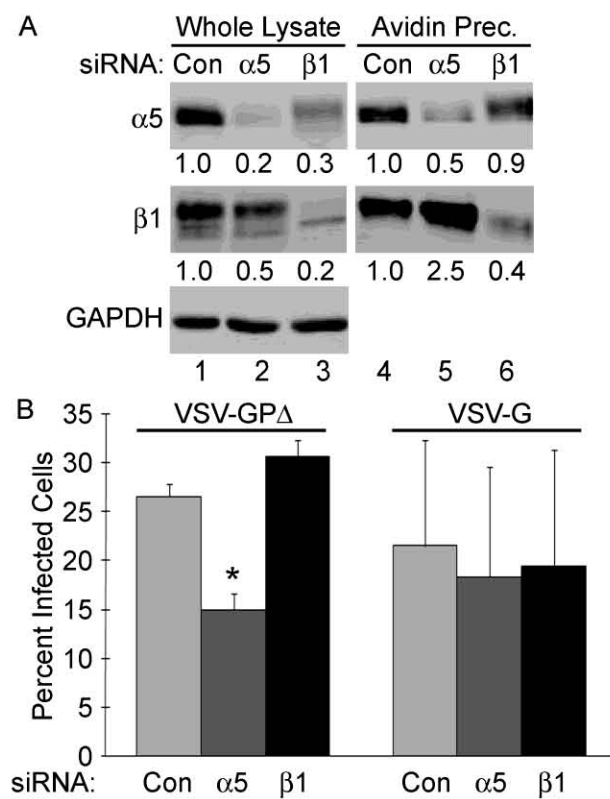
Representative immunoblots, presented as in Fig. 1, with densitometry values

presented below showing the amount of protein, normalized for GAPDH loading,

relative to the control siRNA treated cells. (B) Data shown are the averages from

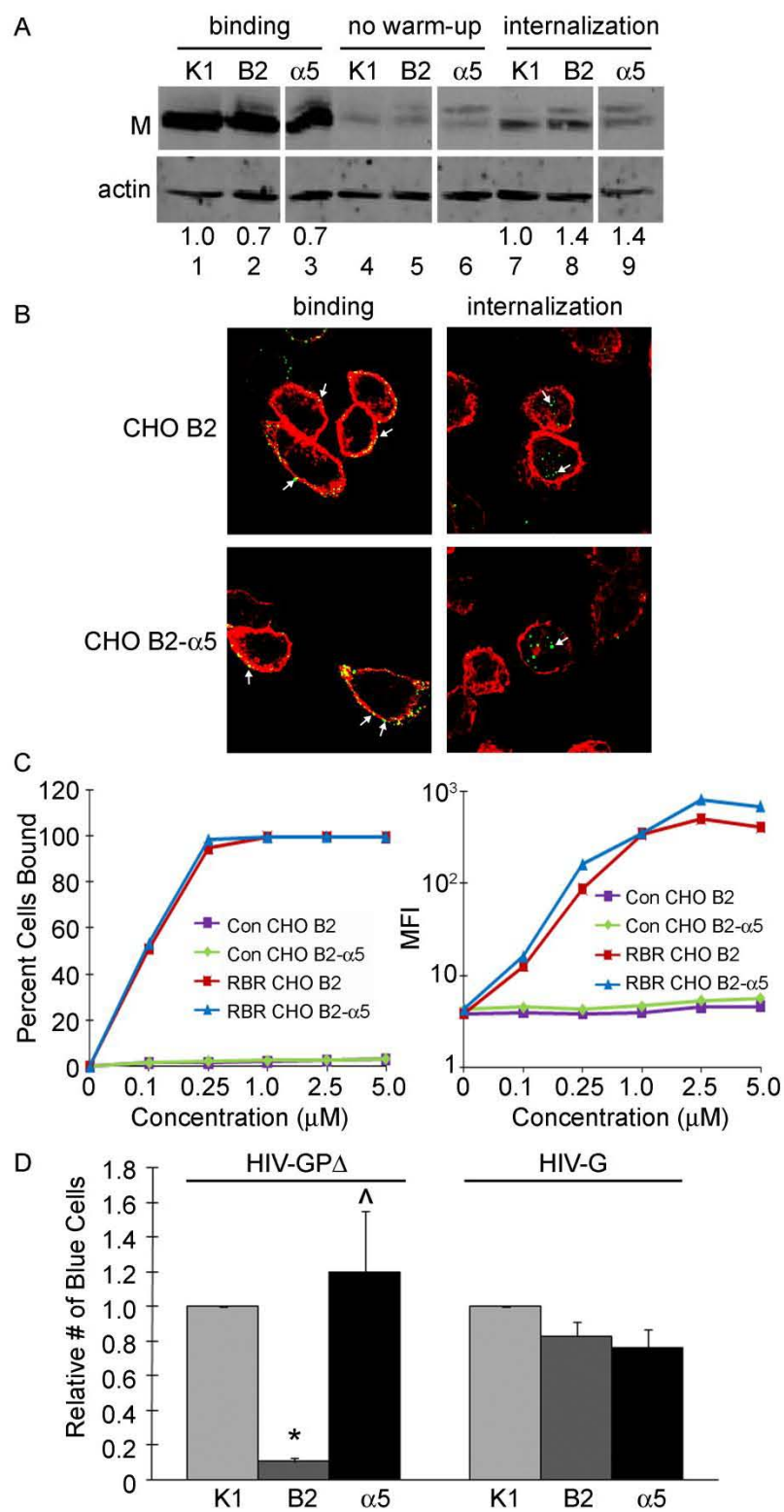
5 experiments. Error bars indicate S.E.M. \*,  $P \leq 0.0008$  relative to Control siRNA-

treated cells.

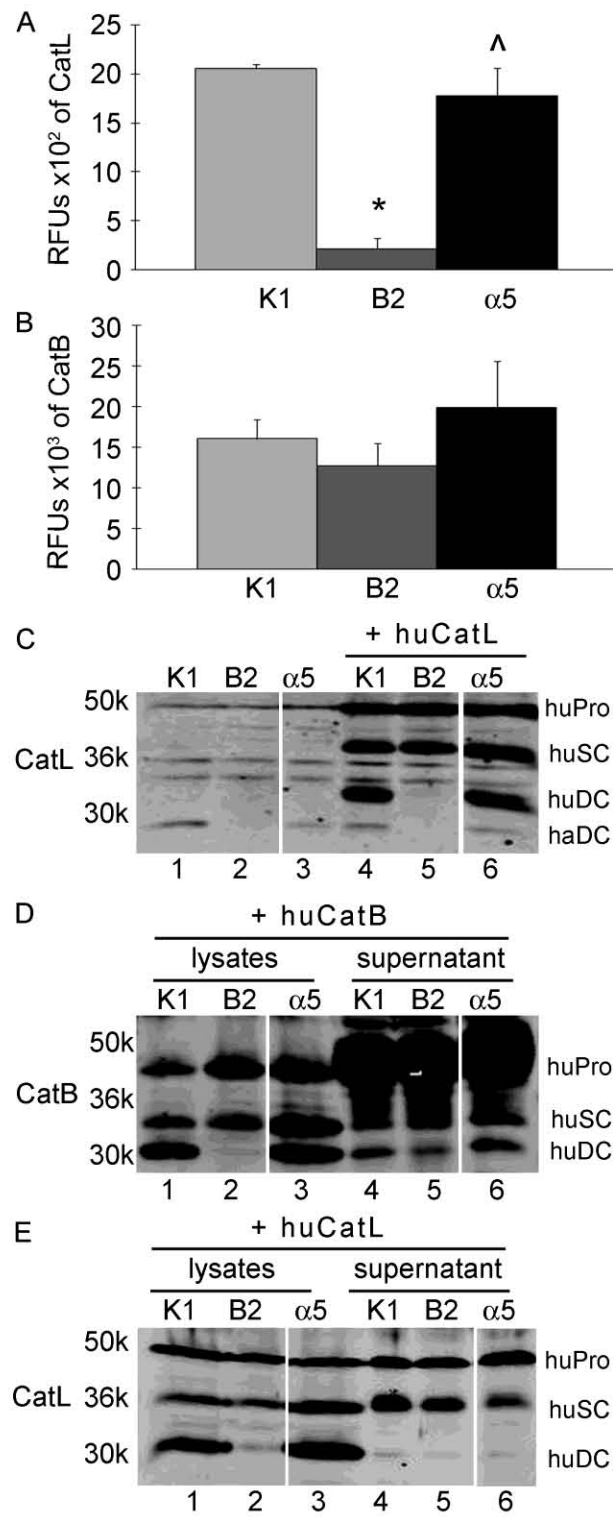


**Figure 3 -  $\alpha 5\beta 1$  integrin regulates EBOV GP-mediated entry post-binding**

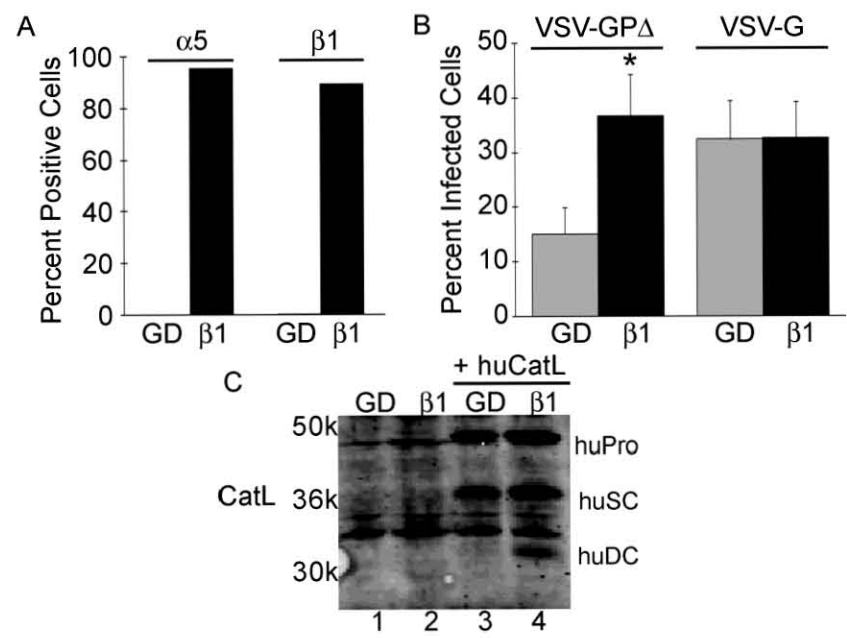
**and post-internalization.** (A) VSV-GP $\Delta$  was bound to the panel of CHO cells at 4°C, and the cells were either lysed directly (binding), treated with proteinase K to strip off bound virus and then lysed (no warm-up), or incubated at 37°C for 2 hr and then treated with proteinase K prior to lysing (internalization). Lysates were immunoblotted for the matrix protein of VSV (M). A representative blot from 8 separate experiments, presented as in Fig. 1, is shown with densitometry values representing the amount of M protein, normalized for actin loading, relative to the parental CHO K1 cells. (B) VSV-GP $\Delta$  was bound to cells and internalized as described in Methods. Cells were permeabilized and stained with anti-EBOV GP antibody (green) and phalloidin (red). Arrows indicate pseudovirions. (C) Increasing concentrations of recombinant EBOV RBR or control rabbit Fc (Con) was bound to cells, stained with AlexaFluor 488 conjugated Protein A, and analyzed by flow cytometry for the percent of cells bound (left) and for the mean fluorescence intensity (MFI) of cells (right). (D) HIV-GP $\Delta$  and HIV-G were added to the panel of CHO cells and fusion was measured as the percentage of blue cells. Results shown are the averages of normalized data from 8 experiments. The average percent infection in the CHO K1 cells was 26% for HIV-GP $\Delta$  and 64% for HIV-G. Error bars indicate S.E.M. \*,  $P \leq 6 \times 10^{-10}$  relative to CHO K1 cells. ^,  $P \leq 0.02$  relative to CHO B2 cells. Panels B and C represent experiments initiated or performed by Derek Dube.



**Figure 4 - CatL activity levels and expression of the DC forms of CatB and CatL are reduced in the  $\alpha 5\beta 1$ -negative CHO cells.** CatL (A) and CatB (B) activity in cell lysates was measured against a small fluorogenic peptide substrate. Results shown are the averages of 3 experiments. Error bars indicate S.E.M. \*,  $P \leq 0.001$  relative to CHO K1 cells. ^,  $P \leq 0.02$  relative to CHO B2 cells. (C) Untransfected CHO cells and CHO cells transfected with a plasmid encoding human CatL were analyzed by immunoblotting for CatL. (D and E) Cell lysates and supernatants from equivalent numbers of cells transfected with plasmids encoding human CatB (D) or CatL (E) were concentrated and analyzed by immunoblotting for CatB or CatL as indicated. haDC, DC form of endogenous hamster CatL; huPro, huSC, and huDC, proform, SC form, and DC form of over-expressed human CatB and CatL.



**Figure 5 - Expression of  $\alpha 5\beta 1$  integrin enhances EBOV GP-mediated infection of GD25 cells.** (A) GD25 (GD) and  $\beta 1$ GD25 ( $\beta 1$ ) cells were stained with Abs specific for  $\alpha 5$  and  $\beta 1$  integrins and the percent of positive cells was measured by flow cytometry. (B) GD25 and  $\beta 1$ GD25 cells were infected with VSV-GP $\Delta$  or VSV-G and the percent of infected cells was analyzed by flow cytometry. Data shown are the averages from 13 experiments. Error bars indicate S.E.M. \*,  $P \leq 0.03$  relative to GD25 cells. (C) GD25 and  $\beta 1$ GD25 cells were transfected with a plasmid encoding human CatL and lysates were analyzed by immunoblotting for CatL.



**Figure 6 - Pretreatment of VSV-GP $\Delta$  to form VSV-GP<sub>19K</sub> rescues infection in the  $\alpha 5\beta 1$  integrin-negative CHO cells.** VSV-GP $\Delta$  was either mock-treated (M; VSV-GP $\Delta_{\text{mock}}$ ) or pre-treated with thermolysin (T) to generate VSV-GP<sub>19K</sub> and analyzed by immunoblotting for GP1 (A) or used to infect the panel of CHO cells (B). Results shown in B are the averages from 9 experiments. Error bars indicate S.E.M. \*,  $P \leq 0.007$  relative to CHO K1 cells. ^,  $P \leq 0.01$  relative to CHO B2 cells. \*\*,  $P \leq 0.04$  relative to mock-treated VSV-GP $\Delta$  in the same cells.

